Newfoundland Labrador

Natural Resources

# GEOCHEMICAL QUANTIFICATION OF THE CLASTIC COMPONENT OF LABRADOR LAKE SEDIMENTS, AND APPLICATIONS TO EXPLORATION

**S.D. Amor**
**Geochemistry, Geophysics and Terrain Sciences**

**Open File LAB/1625**

**St. John's**
**Newfoundland and Labrador**
**June, 2014**

## NOTE

Open File reports and maps issued by the Geological Survey Division of the Newfoundland and Labrador Department of Natural Resources are made available for public use. They have not been formally edited or peer reviewed, and are based upon preliminary data and evaluation.

The purchaser agrees not to provide a digital reproduction or copy of this product to a third party. Derivative products should acknowledge the source of the data.

## DISCLAIMER

The Geological Survey, a division of the Department of Natural Resources (the "authors and publishers"), retains the sole right to the original data and information found in any product produced. The authors and publishers assume no legal liability or responsibility for any alterations, changes or misrepresentations made by third parties with respect to these products or the original data. Furthermore, the Geological Survey assumes no liability with respect to digital reproductions or copies of original products or for derivative products made by third parties. Please consult with the Geological Survey in order to ensure originality and correctness of data and/or products.

*Recommended citation:*

Amor, S.D.

2014: Geochemical Quantification of the clastic component of Labrador lake sediments, and applications to exploration. Government of Newfoundland and Labrador, Department of Natural Resources, Geological Survey, Open File LAB/1625, 187 pages.

Newfoundland Labrador

Natural Resources

# GEOCHEMICAL QUANTIFICATION OF THE CLASTIC COMPONENT OF LABRADOR LAKE SEDIMENTS, AND APPLICATIONS TO EXPLORATION

S.D. Amor

Open File LAB/1625

GEOLOGICAL SURVEY
NEWFOUNDLAND AND LABRADOR
Celebrating 150 years

St. John's
Newfoundland and Labrador
June, 2014

# CONTENTS

# CONTENTS

# FIGURES

# FIGURES

# FIGURES

# FIGURES

# FIGURES

# FIGURES

# FIGURES

# TABLES

# APPENDIX B

Page

**TABLE OF CONTENTS**



# FIGURES

# APPENDIX C: FIGURES

## ABSTRACT

*An association consisting primarily of the following elements: Al, Ba, Hf, K, Li, Mg, Na, Nb, Rb, Sc, Sr, and Ti is universal in the analyses of lake sediments from Labrador. It appears to be related to the amount of inorganic clastic material in the sediment, and is often more than sufficient to mask any responses of these elements (some of which are of potential economic significance) to local geology. It is not, however, directly complementary to the amount of organic material in the sediment, as represented by loss-on-ignition (LOI).*

*Modelling the clastic component numerically by regression analysis identifies departures from the model, in the form of regression residuals. The effectiveness of this method of removing the clastic contribution from the lake sediments' composition, thereby highlighting local areas of enrichment and depletion, is demonstrated by the emergence of a number of features whose geological significance is indisputable. Furthermore, the method has drawn attention to certain well-defined features whose source is unknown, but which may have economic significance: specifically, the Colville River and Bondurant Lake Ba anomalies, and the Thompson Lake / Michikamats Li anomaly.*

*This study shows that regression analysis offers a readily implementable method of isolating and compensating the effects of the clastic contribution to lake sediments in Labrador, with potential application in the analysis of lake-sediment geochemical data elsewhere in Canada.*

## INTRODUCTION

The National Geochemical Reconnaissance (NGR) program conducted by the Geological Survey of Canada (GSC) generated a regional geochemical database, comprising analyses of lake sediments and waters, covering a significant portion of the Canadian Shield. Analyses for more than 40 elements have been available for most of the NGR lake-sediment samples, including all the samples from Labrador, for two decades. With the recent release of ICP analyses of archived NGR samples from Labrador (McConnell and Finch, 2012), the resulting database provides a very large regional geochemical resource with great potential for understanding regional geochemical patterns and the relationships between individual elements.

The creation of misleading anomalies in various sample media, unrelated to mineralization, by Fe–Mn hydroxide scavenging is well documented (*e.g.,* Chao and Theobald, 1976). This paper describes another element association in lake-sediment data from Labrador that appears to be of comparable significance to the Fe–Mn association, interprets this association in terms of the physical composition of the sediment, and suggests a method of quantifying and compensating for its effects, to highlight local deviations from it. Features thus defined by two elements (Ba and Li) are examined in detail from the perspective of their possible relationships to bedrock composition and possible mineralization.

Several appendices provide additional information. These consist of box-and-whisker plots relating the chemical composition of the lake-sediment samples to various field observations made by the samplers (Appendix A); an explanation of the technique of factor analysis, upon which some of the initial assumptions in the investigation are based (Appendix B); and maps of Labrador showing measured and predicted values of certain elements that are not included in the report (Appendix C.

## DATABASE

The database consists of analyses of more than 18 000 lake-sediment samples, collected in Labrador in 1977 and 1978, and from 1982 to 1985, as part of the National Geochemical Reconnaissance (NGR) program of the Geological Survey of Canada (GSC). The samples were analyzed in three stages:

1. Initially, the samples were analyzed at the GSC by Atomic-Absorption Spectrophotometry (AAS), after *aqua-regia* digestion, for Ag, Cd (selected samples only), Co, Cu, Fe, Mn, Ni, Pb and Zn; by AAS after modified *aqua-regia* digestion, for Mo and V (selected samples only); for F by ion-specific electrode (ISE) after $Na_2CO_3$–$KNO_3$ fusion; for Hg by cold-vapour AAS (CVAAS) after *aqua-regia* digestion; for As by hydride AAS (HAAS) after *aqua-regia* digestion; for U by delayed neutron counting (DNC); and for loss-on-ignition (LOI) by gravimetry (Boyle *et al.*, 1981a, b; Hornbrook *et al*., 1977a, b; 1978a–c; 1979a–d; 1983a–d; 1984a–d).

2. The samples were analyzed by Instrumental Neutron Activation Analysis (INAA), under contract to the GSC, for As, Au, Ba, Br, Ce, Co, Cr, Cs, Eu, Fe, Hf, La, Lu, Mo, Na, Ni, Rb, Sb, Sc, Sm, Ta, Tb, Th, U, W, Yb and Zn (Friske *et al.*, 1992a, b; 1993a–j; 1994a–f).

3. Samples were analyzed by Induction-Coupled Plasma / Optical Emission Spectrometry (ICP-OES) after multi-acid ($HF/HCl/HClO_4/HNO_3$) digestion by the Geological Survey of Newfoundland and Labrador (GSNL) for Al, Ba, Be, Ca, Ce, Co, Cr, Cu, Dy, Fe, Ga (selected samples only), K, La, Li, Mg, Mn, Mo, Na, Nb, Ni, P, Pb, Sc, Sr, Ti, V, Y, Zn and Zr (McConnell and Finch, 2012).

In the descriptions that make up most of this report, the method by which each element was analyzed is denoted by a numeric suffix, employed as a general shorthand by the GSNL, as follows:

1: INAA
2: ICP-OES / multi-acid digestion
3: AAS / *aqua regia* digestion
5: AAS / modified *aqua regia* digestion
8: DNC
9: ISE
18: CVAAS
19: HAAS

Selection criteria comprised the following: at least 25% of values must be detectable (*i.e.*, exceed analytical detection limit); where the same element is analyzed by more than one method, the method with the fewest undetectable analyses is chosen; when analyses by all methods are detectable, Method 2 (multi-acid digestion, ICP-OES analysis) is chosen. Water samples were also collected at most sites, but their analyses are, for the most part, omitted from the current study.

## ELEMENT ASSOCIATIONS WITHIN THE DATASET

*Correlation*

The Spearman correlation matrix in Figure 1, whose input data constitute selected analytical variables from the original analyses, re-analyses by INAA and new ICP analyses, demonstrates strong correlations between many elements, suggesting that the processes responsible for concentrating these elements in the sediments are considerably less numerous than the elements themselves.

In particular, strong correlation exists between a large suite of elements: specifically, Al2, Ba2, Hf1, K2, Li2, Mg2, Na2, Nb2, Rb1, Sc2, S2r, Ti2 and Zr2, and to a lesser extent Be2, Ca2, Cr2, F9, Fe2, Mn2, Pb2, Th1 and V2. These elements are correlated inversely with LOI and to a lesser extent, Br1. This cluster of correlations is revealed in the upper part of Figure 1 by selective ordering of the elements according to their associations as revealed by factor analysis (see Appendix B).

The elements in this association have variable geological affinities; for example, they include Na and K, expected to be enriched in felsic igneous rocks, as well as Mg and Ti, whose enrichment is associated with their mafic or ultramafic counterparts. The association, although charac-

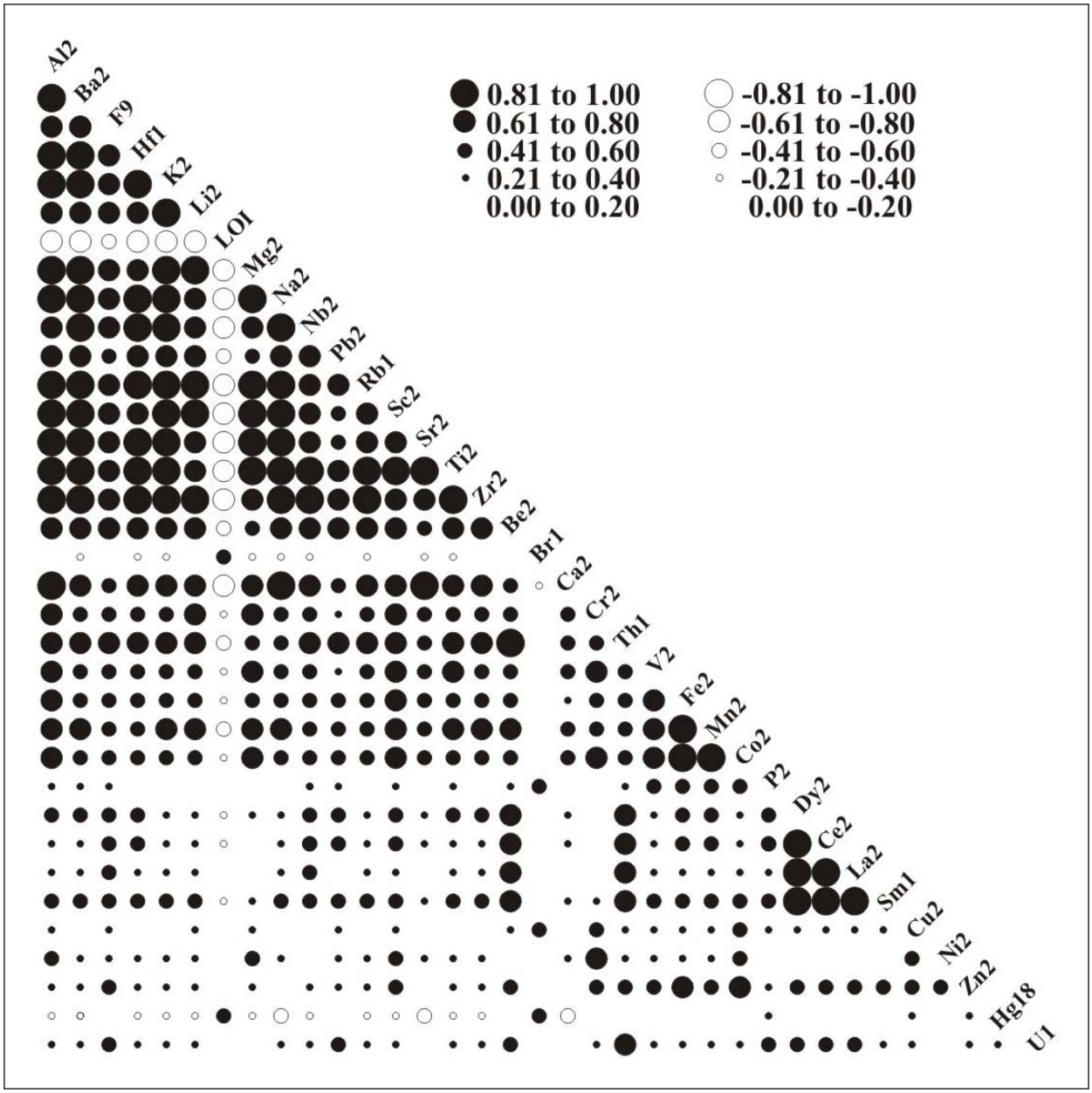


**Figure 1.** *Spearman Correlation Matrix of selected lake-sediment analyses, Labrador NGR data.*

terized by many other elements, will be referred to as the *K–Na–Ti–Mg association* pending investigation of its possible causes.

*R-Mode Factor Analysis*

The ubiquity of certain elements in the association throughout Labrador, as well as the variable affinities of certain others, is demonstrated by R-mode factor analysis of data from four regions of Labrador (Table 1). The underlying principles of this statistical method, as well as results of its application to the Labrador data, are described in Appendix B.

**Table 1:** NTS sheets comprising four subdivisions of Labrador dataset

| Area | NTS map areas covered | Number of Samples |
|---|---|---|
| Southeastern Labrador | 02M, 03D, 03E, 12P, 13A, 13B, 13G, 13H, 13I, 13J and 13O | 4170 |
| South-central Labrador | 13C, 13D, 13E, 13F, 13K and 13L | 5426 |
| Southwestern Labrador | 22P, 23A, 23B, 23G, 23 H, 23I, 23J, 23O | 4482 |
| Northern Labrador | 13M, 13N, 14C, 14D, 14E, 14F, 14L, 24A, 24H, 24I | 3997 |

**Table 2:** Elements in Factor 1 association in four areas of Labrador. Elements common to all three areas are printed in red. Elements in parentheses display negative factor loadings

| Area | Elements in Factor 1 with Varimax-rotated loadings (Davis, 1973) greater than \|0.5\|, in descending order of strength | Percentage of total variance accounted by this factor |
|---|---|---|
| SE Labrador | K2, Na2, Sr2, Zr2, Mg2, Hf1, Rb1, Ti2, Ba2, Ca2, Nb2, Al2, Li2, Sc2, F9, Pb2, Cr2, Be2 | 37.1 |
| S-C Labrador | Na2, Sr2, K2, Ti2, Ba2, Mg2, Hf1, Zr2, Ca2, Rb1, Nb2, Al2, Sc2, Li2, Pb2, F9, Cr2, Th1 (LOI) | 38.1 |
| SW Labrador | K2, Ti2, Rb1, Al2, Mg2, Nb2, Zr2, Na2, Hf1, Ba2, Sc2, F9, Be2, V2, Li2, Cr2, Th1, Sr2, Pb2, Fe2, Mn2 (LOI) | 42.6 |
| N Labrador | Na2, Sr2, K2, Ba2, Ti2, Al2, Ca2, Hf1, Rb1, Nb2, Zr2, Mg2, Sc2, Li2 (LOI, Hg18, Br1) | 33.2 |

R-mode factor analysis shows that the K–Na–Ti–Mg association (along with Al, Ba, Hf, Li, Nb, Rb, Sc, Sr and Zr) is present in all four areas (Table 2). Calcium is only absent from the association in southwestern Labrador, whereas Cr, F, and Pb are absent only from the association in northern Labrador, and LOI is only absent from the association in southeastern Labrador. Less-common elements in the association comprise Be2 (southeastern Labrador and southwestern Labrador only), Th1 (south-central Labrador and southwestern Labrador only), Fe2 and Mn2 (southwestern Labrador only), and Hg18 and Br1 (northern Labrador only).

## RELATION OF GEOCHEMICAL ANALYSES TO FIELD OBSERVATIONS

As an aid to interpreting the significance of the K–Na–Ti–Mg association, and discerning the physical factors that might control it, it is helpful to compare the concentration levels of the component elements in samples subdivided on the basis of various observations made by the samplers. For the NGR dataset, these observations comprise depth, lake area (in four categories), colour and relief.

**Table 3:** Sample totals in various observational categories

| COLOUR | |
|---|---|
| **Black** | **812** |
| *Includes* | |
| Black | 697 |
| Brown-black | 115 |
| **Brown** | **3,893** |
| **Yellow** | **124** |
| *Includes* | |
| Yellow | 61 |
| Yellow-brown | 2 |
| Yellow-green | 1 |
| Tan-yellow | 1 |
| Tan | 35 |
| Tan-brown | 16 |
| Tan-green | 2 |
| Tan-grey | 6 |
| **Grey** | **647** |
| *Includes* | |
| Grey | 510 |
| Grey-black | 9 |
| Grey-brown | 128 |
| **Green** | **1,135** |
| *Includes* | |
| Green | 938 |
| Green-black | 8 |
| Green-brown | 167 |
| Green-grey | 22 |
| **No Description** | **11,465** |

| AREA | |
|---|---|
| <0.25 $km^2$ | 4,422 |
| 0.25 to 1 $km^2$ | 8,237 |
| 1 to 5 $km^2$ | 3,519 |
| > 5 $km^2$ | 1,636 |

| DEPTH | |
|---|---|
| < 1 m | 24 |
| 1 m | 2,570 |
| 2 m | 2,983 |
| 3 to 4 m | 2,624 |
| 5 to 8 m | 4,311 |
| 9 to 16 m | 3,366 |
| > 16 m | 2,197 |

| COMPOSITION | |
|---|---|
| Clastic, fine grained | 213 |
| Clastic, coarse grained | 93 |
| Organic ooze | 4,482 |
| Organic, granular | 400 |
| Organic, peaty | 1,172 |

All the sampling data are incorporated into box plots in Appendix A. In these plots, the upper and lower bounds of the 'box' represent the quartiles of the data distribution (*i.e.*, the 25- and 75-percentile) whereas the limits of the 'whiskers' represent the bounds of the box, plus or minus 1.5 times the interquartile range, if this is not in excess of the maximum, or exceeded by the minimum. Values falling above or below the whisker limits are considered to be outliers and plotted as individual points.

Table 3 summarizes the sample totals in each class of field observation. All values are converted to percentiles of the entire dataset prior to compilation of the box plots; therefore, the Y-axis of the latter is always scaled between 0 and 100.

Box plots for K2 and Ti2, reproduced from Appendix A, are also displayed in Figures 2a to 2d, and 3a to 3d. Box plots for certain other elements (Ce2 and Fe2), that do not form significant components of the K–Na–Ti–Mg association, are also included in the body of the report (Figures 4a to 4d, and 5a to 5d) for the purposes of comparison.

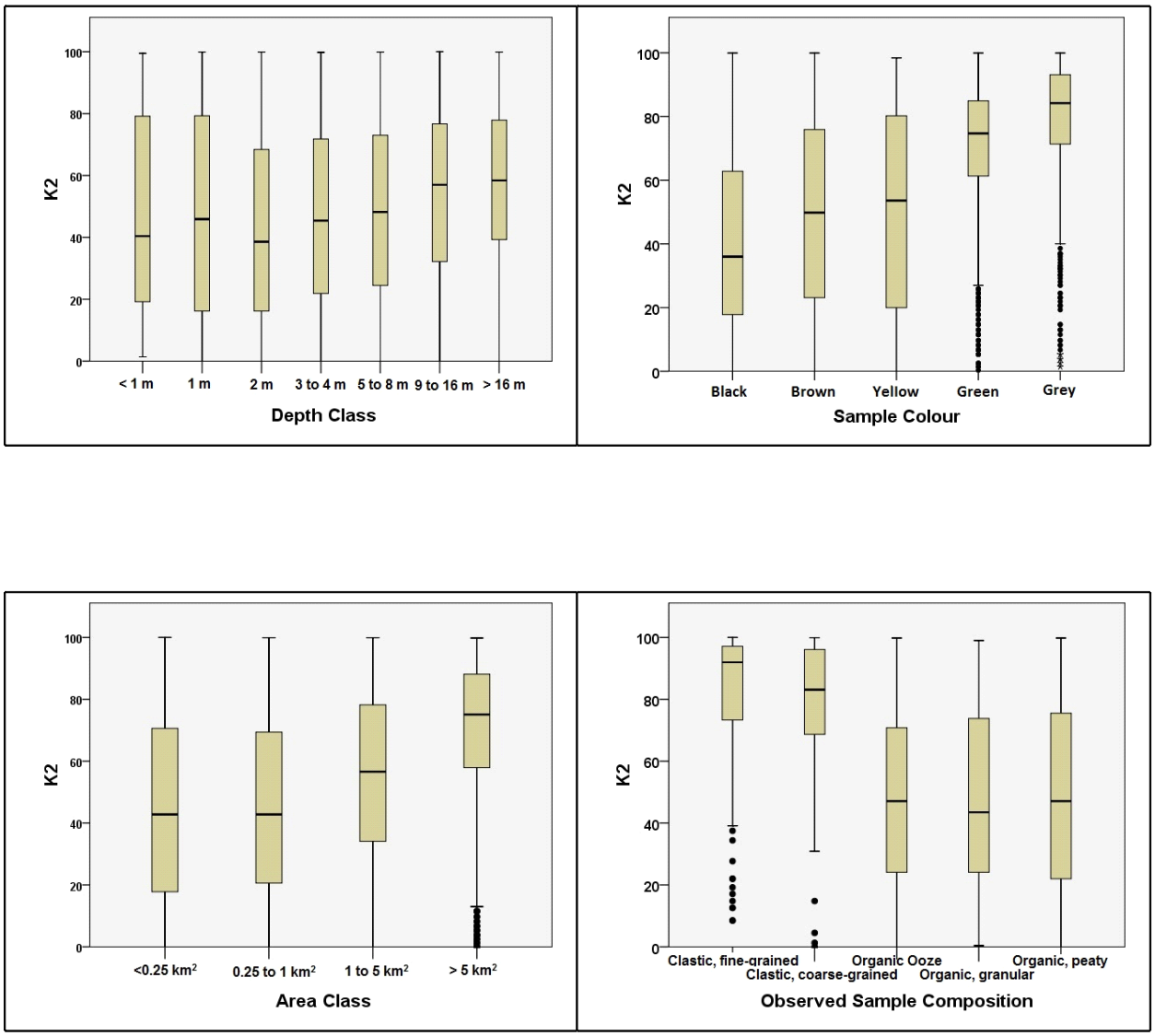


**Figure 2.** *a) Relationship between K2 concentration in lake sediment, and depth from which samples were collected; b) Relationship between K2 concentration in sediment and sample colour; c) Relationship between K2 concentration in lake sediment, and area of lake from which samples were collected; d) Relationship between K2 concentration in lake sediment, and observed sample composition.*

*Depth*

The relationship between K2 and depth suggests that overall concentrations of this element remain invariant to a depth of 2 m, below which there is a steady increase with depth; this pattern is also displayed by Ti2 (as well as Al2, Ca2, Li2, Mg2, Na2, Rb1, Sc2, Sr2 and Zr2), but also by Fe2 (as well as Be2, Mn2, P2, Pb2, and not by Hf1 or Nb2; *see* Appendix A), suggesting that the K–Na–Ti–Mg association is not uniquely associated with sample depth. There is a more systematic relationship between Ce2 and depth, with a steady increase from the shallowest samples to the deepest; this trend is also displayed by Br1, Co2, Cr2, Cu2, Dy2, F9, La2, Ni2, Sm1, Th1, U1 and Zn2.

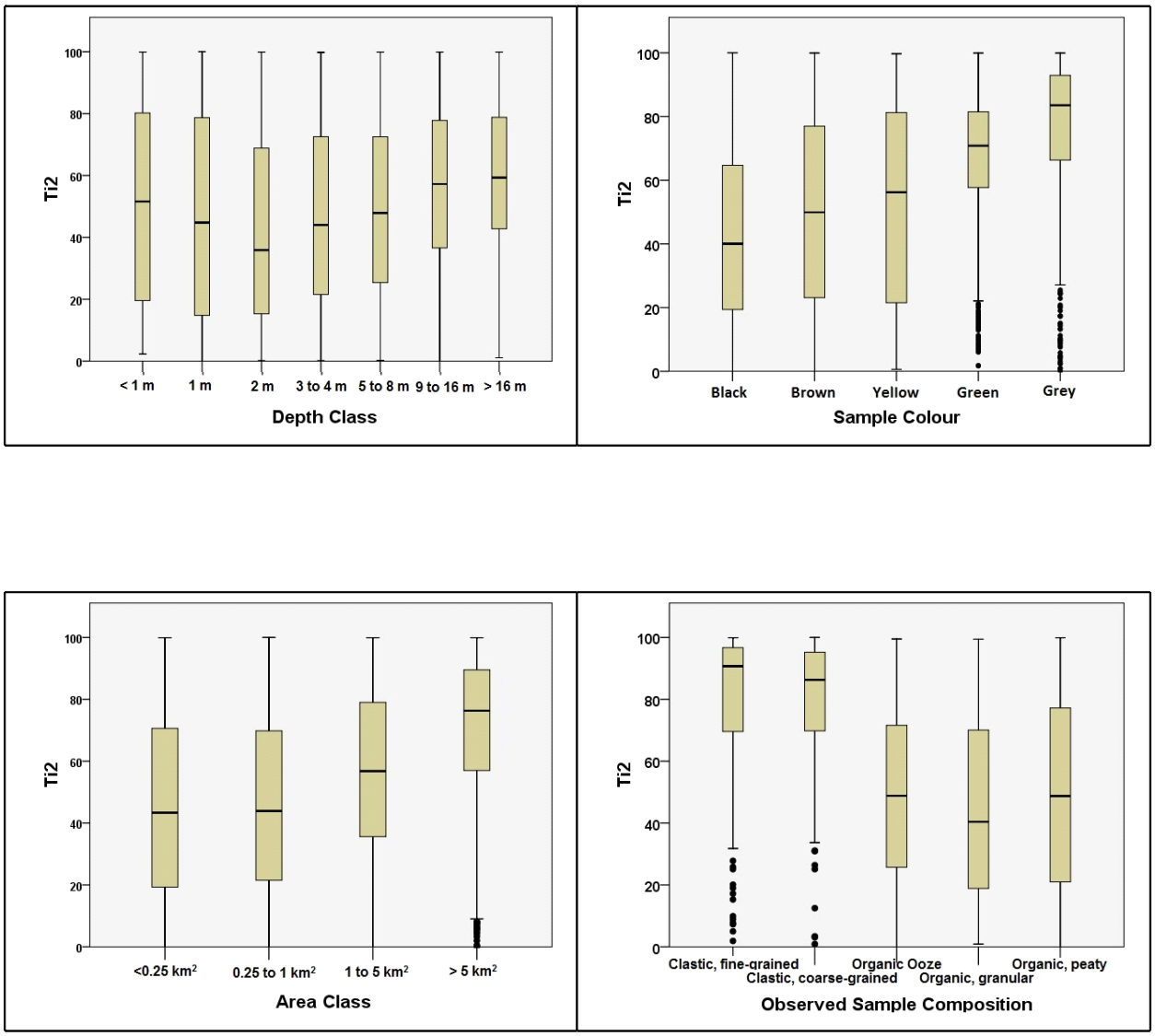


**Figure 3.** *a) Relationship between Ti2 concentration in lake sediment, and depth from which samples were collected; b) Relationship between Ti2 concentration in sediment and sample colour; c) Relationship between Ti2 concentration in lake sediment, and area of lake from which samples were collected; d) Relationship between Ti2 concentration in lake sediment, and observed sample composition.*

*Colour*

Samples described as 'green' and 'grey' (or similar colours; *see* Table 3), totalling 1782 out of the 6611 samples for which colour observations were made, are conspicuously higher in K2 and Ti2, as well as Al2, Ba2, Ca2, Hf1, Li2, Mg2, Na2, Rb1, Sc2 and Sr2. This characteristic is not very strong for Nb2 and Zr2, in green samples at least. In addition, F9 and Th1 (in particular), Ce2, Cu2, Dy2, La2 and Sm1 are also relatively enriched in such samples.

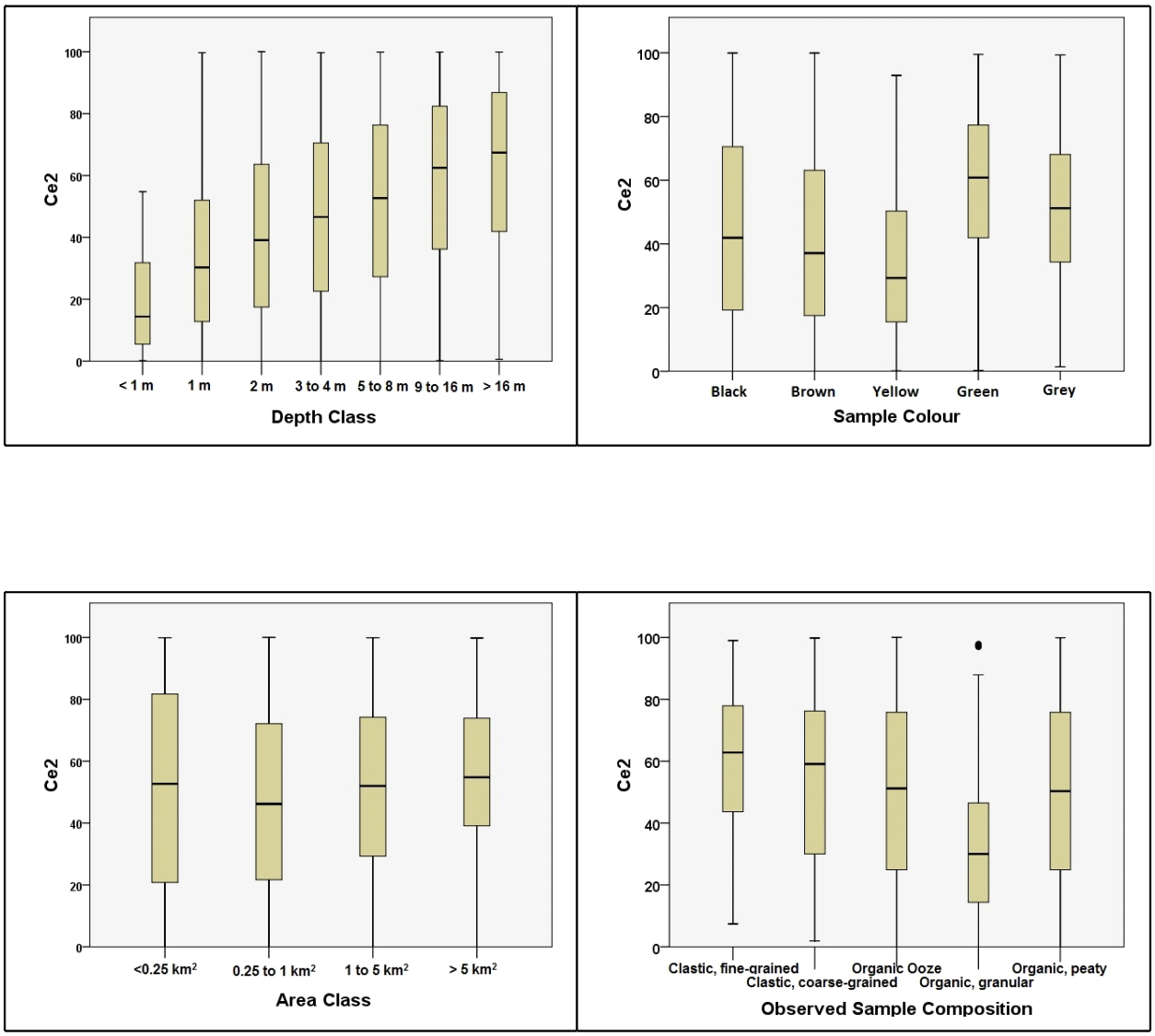


**Figure 4.** *a) Relationship between Ce2 concentration in lake sediment, and depth from which samples were collected; b) Relationship between Ce2 concentration in sediment and sample colour; c) Relationship between Ce2 concentration in lake sediment, and area of lake from which samples were collected; d) Relationship between Ce2 concentration in lake sediment, and observed sample composition.*

*Area*

Values of K2 are very similar in lakes of the two smaller area classes (< 0.25 km$^2$, and 0.25 to 1 km$^2$) but increase systematically in lakes of the two larger classes; this is also true of Ti2, as well as Al2, Ba2, Ca2, Hf1, Li2, Mg2, Na2, Nb2, Rb1, Sc2, Sr2 and Zr2 as well as Be2, F9, Mn2, P2, Pb2, Th1 and Zn2. An inverse relationship is apparent for LOI, with values decreasing systematically in the two larger lake classes. A more systematic increase in concentration levels from the smallest lakes to the largest is apparent for Co2, Cr2, Fe2, Ni2 and V2.

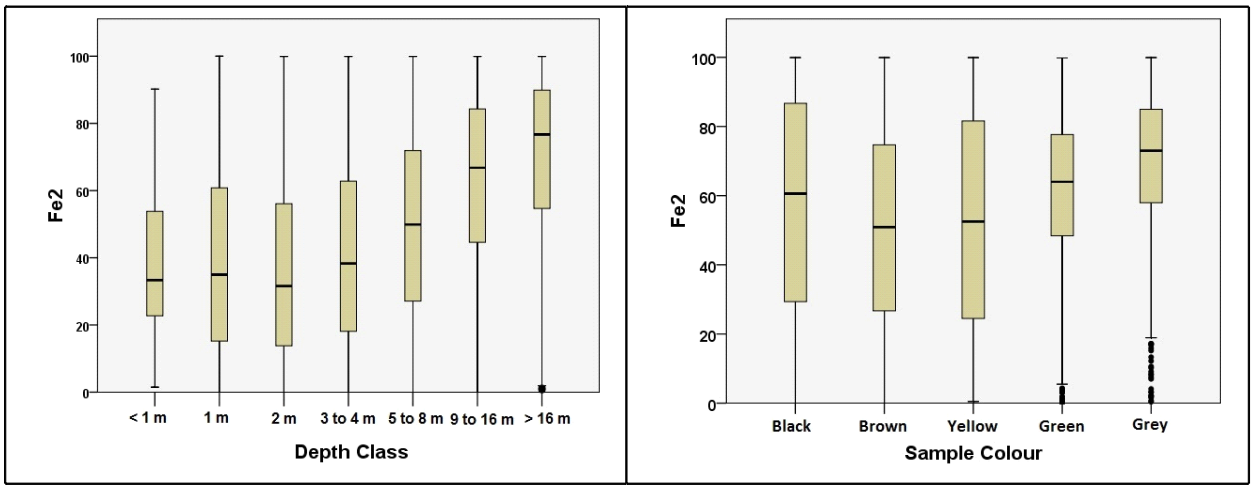


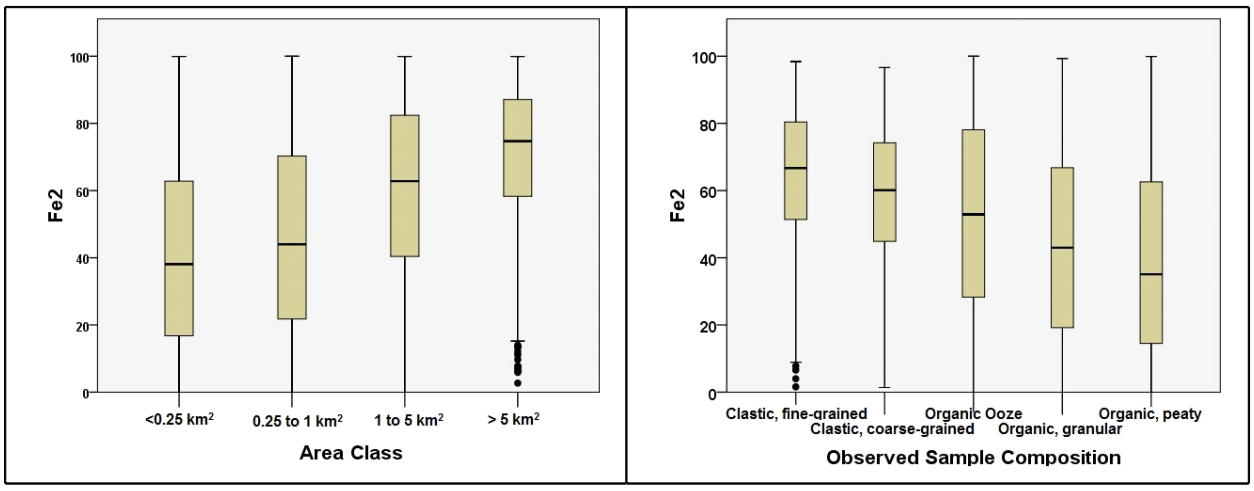


**Figure 5.** *a) Relationship between Fe2 concentration in lake sediment, and depth from which samples were collected; b) Relationship between Fe2 concentration in sediment and sample colour; c) Relationship between Fe2 concentration in lake sediment, and area of lake from which samples were collected; d) Relationship between Fe2 concentration in lake sediment, and observed sample composition.*

*Relief*

The chemical composition of the samples in relation to local relief is shown in Appendix A. No relation is apparent.

*Composition*

The field observations recorded during the original NGR sampling program do not include descriptions of the physical composition of the samples. This omission has, however, been addressed in the many detailed, focused lake-sampling programs carried out in Labrador by the

GSNL. Most of the results of these surveys have been compiled by McConnell (2010) and provide a convenient database in which to investigate the relationship between this parameter and the sediments' chemical composition. It is reasonable to assume that the areas covered by these surveys are representative of the limnological environments of Labrador, and that conclusions based upon their data apply equally to the larger regional (NGR) database.

Compositional descriptors comprise five categories, as follows: 'Clastic, fine-grained'; 'Clastic, coarse-grained'; 'Organic ooze'; 'Organic, granular' and 'Organic, peaty'. The assignment of a sample to one of these classes refers to the predominant material in the sediment, and does not imply that material from the other classes is absent; in particular, most samples assigned to the three organic classes also probably contain some inorganic clastic material.

Although they are not numerous (306 out of a total of 6360 observations), samples described as 'Clastic, fine grained' and 'Clastic, coarse grained' are associated with significantly higher values of both K2 and Ti2 (Figures 2d, 3d). The distinction between these two clastic classes and the three organic classes is stronger than any observed for colour, depth or area. It is equally evident in Al2, Ba2, Hf1, Li2, Mg2, Na2, Nb2, Sr2 and Zr2 (although less emphatic for Ca2 and Sc2), as well as Be2, F9 and Pb2, all of which feature in the Factor 1 association of at least one data subset (see Table 2). Both Br1 and LOI are, conversely, significantly lower in samples of the two inorganic classes. That LOI, representative for the most part of the organic content of the lake sediment, should decrease with increased inorganic, clastic content is to be expected; the less clear relationship of inorganic content with Br1 may be due to the much stronger control over this element's content by the depth at which the sample was collected (*see* Appendix A).

The relationship between observed and chemical composition of the lake sediments strongly suggests that the K–Na–Ti–Mg (Al–Ba–Hf–Li–Nb–Rb–Sc–Sr–Zr) association is related to the amount of clastic, detrital material in the samples and that these elements may be used to create a model of the amount of clastic material in the lake-sediment samples This is investigated in the next section.

## REGRESSION ANALYSIS

### *Prediction Efficiency*

The strong association between the elements K–Na–Ti–Mg, and its apparent ubiquity, suggest that with the aid of multiple linear regression, the clastic contribution to the sediment can be modelled numerically and that for a given sample, the value of any one element can thereby be predicted, with a reasonable degree of accuracy and precision, as a function of the values of all the others. This method can be used to remove the component of the samples' chemical composition that is largely related to the predominant inorganic clastic contribution, and better reveal contributions to the sediment from sources that are distinct and separate from it. Such contributions would be revealed by the differences between predicted and measured values, which are commonly termed *regression residuals*.

**Table 4:** Regression Summary: 'Clastic' Elements Regressed Against Each Other

| | Coefficients | | | | | | | | | | | | | | |
|---|---|---|---|---|---|---|---|---|---|---|---|---|---|---|---|
| | **Al2** | **Ba2** | **Hf1** | **K2** | **Li2** | **Mg2** | **Na2** | **Nb2** | **Rb1** | **Sc2** | **Sr2** | **Ti2** | **Zr2** | **Constant** | **$R^2$** |
| **Al2** | | -0.062 | -0.003 | -0.039 | -0.390 | 0.210 | -0.078 | 0.557 | 0.023 | 0.017 | 0.311 | 0.271 | 0.005 | 0.032 | 0.863 |
| **Ba2** | -0.001 | | -0.001 | 0.452 | -0.003 | -0.149 | -0.194 | 0.006 | 0.004 | 0.107 | 0.422 | 0.000 | 0.024 | 1.311 | 0.859 |
| **Hf1** | -0.027 | -0.003 | | 0.116 | -0.198 | -0.225 | 0.241 | 0.119 | 0.020 | 0.091 | 0.174 | 0.003 | 0.393 | -1.153 | 0.866 |
| **K2** | 0.272 | .031 | 0.056 | | 0.112 | 0.444 | 0.007 | 0.032 | -0.006 | -0.093 | 0.003 | 0.161 | 0.000 | -0.071 | 0.963 |
| **Li2** | 0.151 | -0.008 | -0.210 | 0.221 | | 0.690 | -0.007 | 0.093 | 0.017 | 0.056 | -0.425 | -0.008 | 0.349 | 1.203 | 0.824 |
| **Mg2** | -0.022 | -0.138 | -0.093 | 0.173 | 0.268 | | 0.088 | -0.134 | 0.013 | 0.121 | 0.299 | 0.008 | 0.002 | -1.243 | 0.909 |
| **Na2** | 0.133 | -0.154 | 0.084 | 0.585 | -0.002 | 0.075 | | -0.036 | -0.017 | -0.060 | 0.476 | 0.001 | 0.096 | -0.813 | 0.950 |
| **Nb2** | 0.050 | 0.045 | 0.387 | 0.083 | 0.288 | -1.060 | -0.336 | | 0.050 | -0.103 | 0.234 | 0.039 | 0.545 | -1.857 | 0.855 |
| **Rb1** | 0.462 | 0.344 | 0.785 | 4.757 | 0.638 | 1.214 | -1.925 | 0.607 | | -0.089 | -0.523 | -0.018 | -0.779 | 5.633 | 0.825 |
| **Sc2** | 0.596 | 0.225 | -0.055 | 0.131 | 0.725 | -0.424 | -0.078 | -0.006 | -0.513 | | 0.016 | -0.013 | 0.000 | 0.521 | 0.855 |
| **Sr2** | 0.068 | 0.349 | 0.064 | -0.128 | -0.148 | 0.267 | 0.497 | 0.026 | -0.005 | -0.076 | | 0.001 | -0.126 | 1.705 | 0.893 |
| **Ti2** | 2.30 | 0.18 | 2.06 | 6.18 | -4.73 | 12.40 | 1.95 | 7.40 | -0.29 | 4.05 | 1.43 | | -5.13 | 28.01 | 0.916 |
| **Zr2** | 0.014 | 0.035 | 0.253 | 0.389 | 0.212 | 0.004 | 0.175 | 0.108 | -0.013 | -0.003 | -0.220 | -0.005 | | 1.797 | 0.879 |

In this study, only those elements that displayed a varimax-rotated loading of greater than 0.5 in data from all four regions, when factor analysis was performed (see Appendix B), were included in the regression. This is a more rigorous way of identifying the core elements in the association, than the inevitably subjective examination of the correlation matrices.

Prior to performing the calculations, the data were subjected to square-root or logarithmic transformations to reduce skewness and simulate normal (Gaussian) distributions (as judged by the appearance of their histograms and probability plots), as follows:

Square-root transformation: Al2, Nb2, Rb1, Sc2, Ti2
Logarithmic transformation: Ba2, Hf1, K2, Li2, Mg2, Na2, Sr2, Zr2

Table 4 summarizes the results of regressing each of the 13 elements in the postulated clastic association (K2, Na2, Ti2 and Mg2, as well as Al2, Ba2, Hf1, Li2, Nb2, Rb1, Sc2, Sr2 and Zr2) against the other twelve, in terms of regression coefficients and multiple $R^2$ (a measure of the predicting power of the regression model).

It seems intuitive that because the elements under consideration are believed to model the amount of inorganic clastic material in the lake sediment, the content of LOI, as a representation of the sediment's organic component, is complementary. The results of the factor analysis described earlier suggest that this is an oversimplification; nevertheless, carrying out a simple regression, using LOI as the single independent variable, has certain advantages if it can be shown to achieve similar results to the multiple regressions described previously. Not least of these is the feasibility of

**Table 5:** Regression Summary: "Clastic" Elements Regressed against LOI

| | Coefficient | Constant | $R^2$ |
|---|---|---|---|
| **Al2** | -0.026 | 2.554 | 0.452 |
| **Ba2** | -0.013 | 2.886 | 0.391 |
| **Hf1** | -0.021 | 0.893 | 0.427 |
| **K2** | -0.022 | 0.292 | 0.476 |
| **Li2** | -0.017 | 1.115 | 0.341 |
| **Mg2** | -0.016 | -0.051 | 0.414 |
| **Na2** | -0.022 | 0.312 | 0.487 |
| **Nb2** | -0.035 | 3.071 | 0.384 |
| **Rb1** | -0.123 | 7.95 | 0.473 |
| **Sc2** | -0.031 | 3.438 | 0.388 |
| **Sr2** | -0.014 | 2.468 | 0.410 |
| **Ti2** | -0.692 | 60.766 | 0.456 |
| **Zr2** | -0.017 | 1.911 | 0.387 |

performing simple regression in a spreadsheet application, whereas multiple regression normally requires more sophisticated software. Table 5 summarizes the results of regressing each clastic element against LOI alone, in terms of regression coefficients and constants, and the quality of the regression fit as measured by $R^2$.

Figures 6a to 6m show X–Y plots of measured values versus values of these elements predicted by multiple regression, whereas Figures 7a to 7m show corresponding X–Y plots of measured values versus values predicted by simple regression with only one independent variable (LOI).

Values of $R^2$ for the multiple regression range from 0.824 for Li2 to 0.963 for K2 (Table 4). The lowest $R^2$ values are, significantly, for three elements for which the relationship between observed and predicted values is not rectilinear over the entire concentration range: Li2, Nb2 and Rb2. Nevertheless, it is apparent that the value of any of the elements in this group can be predicted

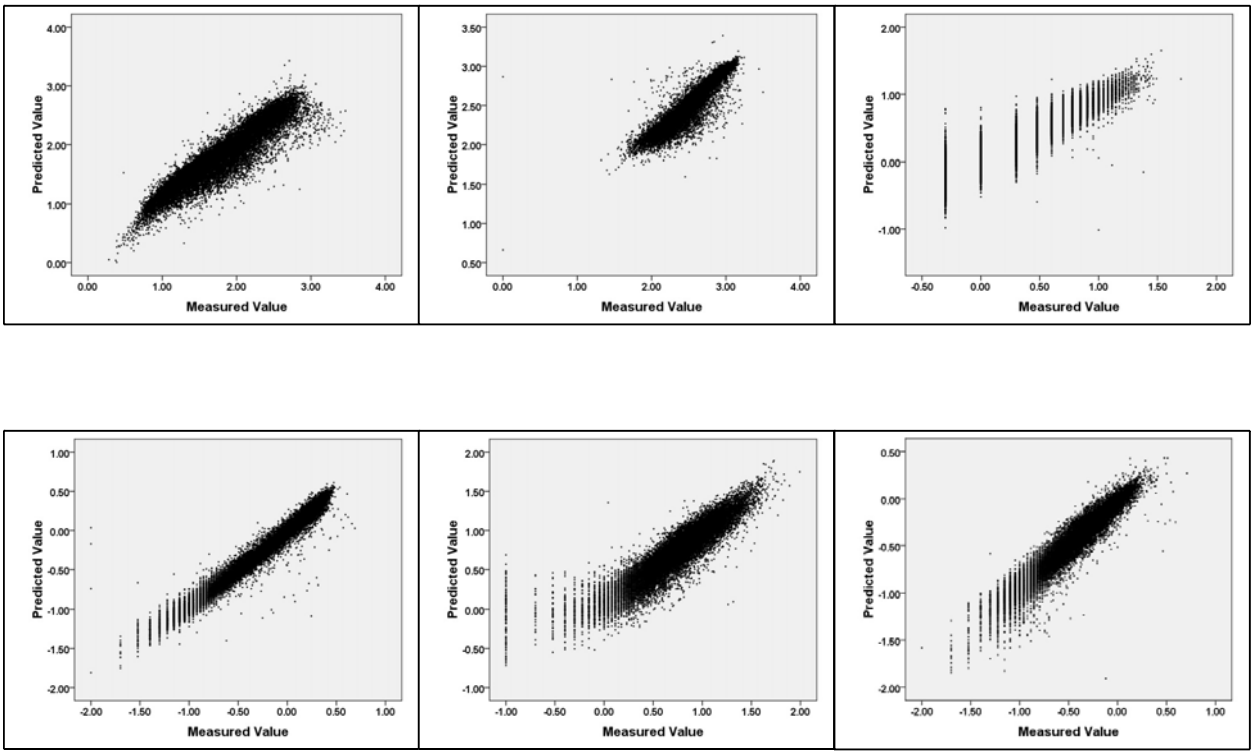


**Figure 6.** *a) Measured vs Predicted values of Al2; multiple regression; b) Measured vs Predicted values of Ba2; multiple regression; c) Measured vs Predicted values of Hf1; multiple regression; d) Measured vs Predicted values of K2; multiple regression; e) Measured vs Predicted values of Li2; multiple regression; f) Measured vs Predicted values of Mg2; multiple regression.*

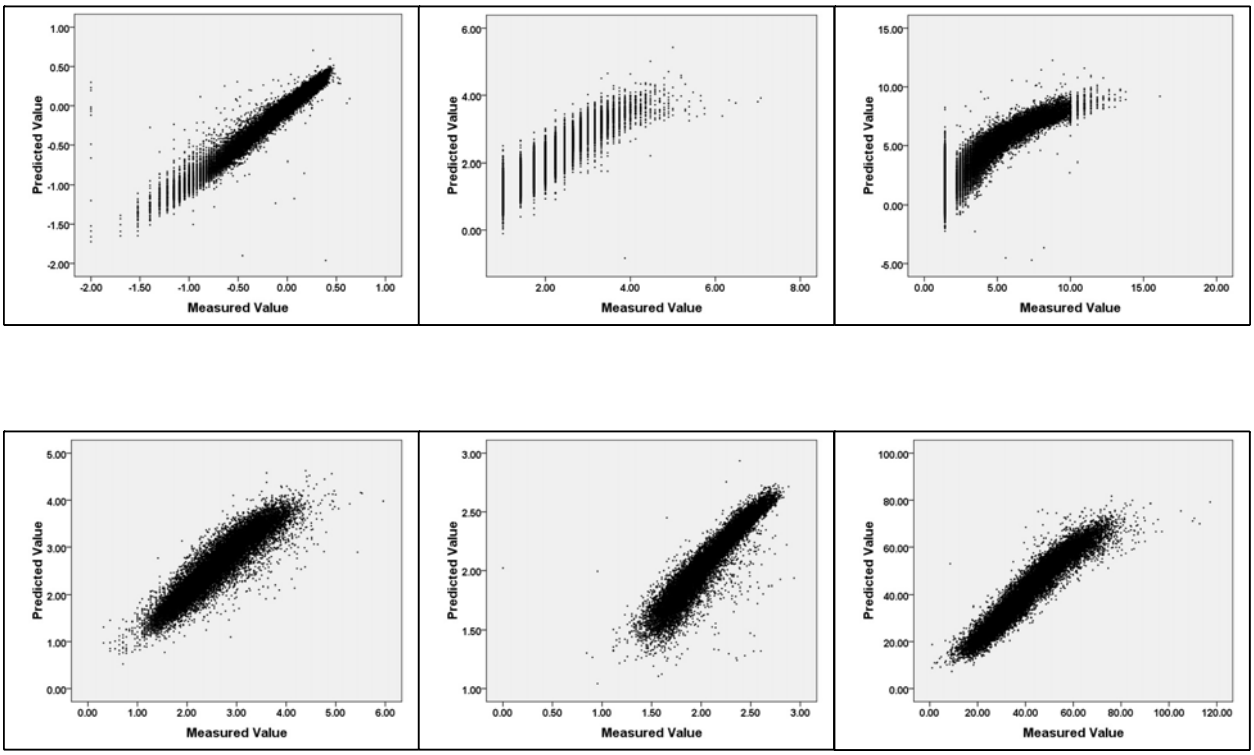


**Figure 6.** *g) Measured vs Predicted values of Na2; multiple regression; h) Measured vs Predicted values of Nb2; multiple regression; i) Measured vs Predicted values of Rb1; multiple regression; j) Measured vs Predicted values of Sc2; multiple regression; k) Measured vs Predicted values of Sr2; multiple regression; l) Measured vs Predicted values of Ti2; multiple regression.*

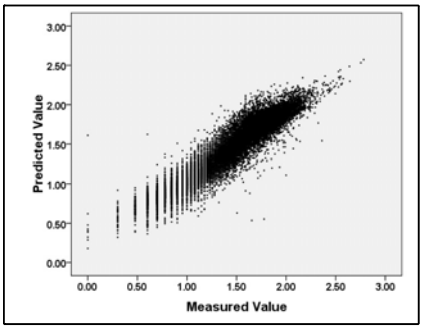


**Figure 6.** *m) Measured vs Predicted values of Zr2; multiple regression.*

from the values of the others with a fair degree of precision. For the simple regression (of the elements in the 'clastic' association against LOI), values of $R^2$ range from 0.341 for Li2 to 0.487 for K2 (Table 5). These values are much lower than the corresponding values when the clastic elements are regressed against each other. However, that the best fit is displayed by K, and the worst by Li, is a feature common to both regressions. The plots in Figures 6 and 7 provide a visual illustration of the better predictive results obtained from the multiple linear regression method.

The efficacy of the prediction is also demonstrable if the measured and predicted values are displayed in the form of colour-coded maps. Maps for Al2, Ba2, Li2, Ti2 and Zr2 are shown in Figures 8a–c to 12a–c. All remaining maps are included in Appendix C. Viewed at the scale of Labrador, the patterns defined by measured values of each element are, at least on cursory examination, essentially the same as those defined by corresponding values predicted by the other elements in the co-association using multiple regression analysis. If the maps are examined in more detail, certain differences become apparent on closer examination; *e.g.*, measured Al2 values are higher than predicted southwest of Hopedale (NTS map area 13N) , and measured Zr2 values in the Red Wine Mountains (NTS map areas13K and 13L) are conspicuously higher than their predicted counterparts.

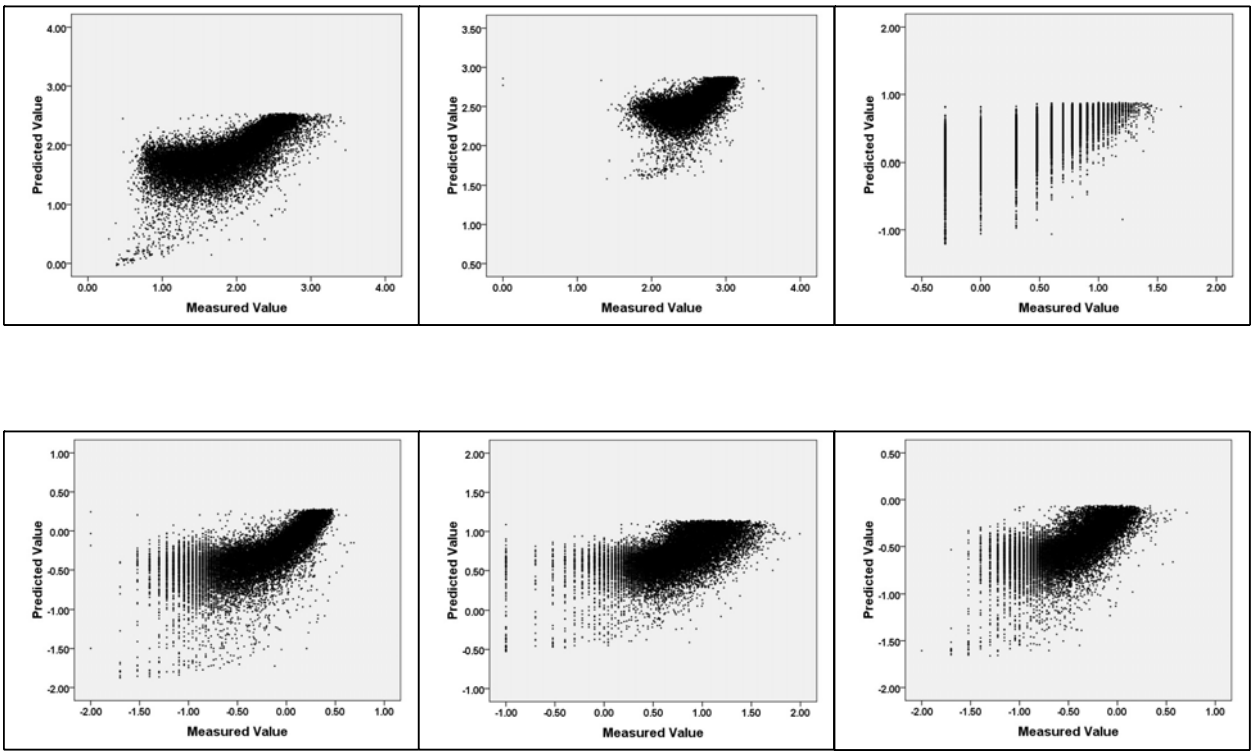


**Figure 7.** *a) Measured vs Predicted values of Al2; simple regression; b) Measured vs Predicted values of Ba2; simple regression; c) Measured vs Predicted values of Hf1; simple regression; d) Measured vs Predicted values of K2; simple regression; e) Measured vs Predicted values of Li2; simple regression; f) Measured vs Predicted values of Mg2; simple regression.*

Since the LOI-predicted value of each of the clastic elements is a linear function of a single variable, and since the coloured dots assigned to each sample point are based on percentiles, the maps of the LOI-predicted elements are essentially identical to maps of the distribution of LOI itself, although with increasingly 'warm' colours (grey, cyan, green, yellow, red) denoting decreasing instead of increasing values. Nevertheless, maps of the LOI-predicted values are also displayed for each element and it is clear that in most cases, at a regional scale, they also provide a reasonable match with those of the elements themselves.

A more systematic method exists to measure and plot the discrepancies between observed and predicted values of these elements – in other words, the component of each element's variation that is not explained simply by the amount of inorganic, clastic material in the sample, and which may reflect response to bedrock composition, including mineralization. These methods will be examined in detail in the next section.

*Residuals*

In the context of regression analysis a *residual* is defined as the difference between the predicted and observed value of the dependent value (Koch and Link, 1970, page 43). The most common application of residuals is in the specialized field of trend-surface analysis, but the method has been applied in a geochemical context by a number of workers, including Rose *et al.* (1970), Closs and Nichol (1973) and McConnell (1976). Residuals may be either positive or negative;

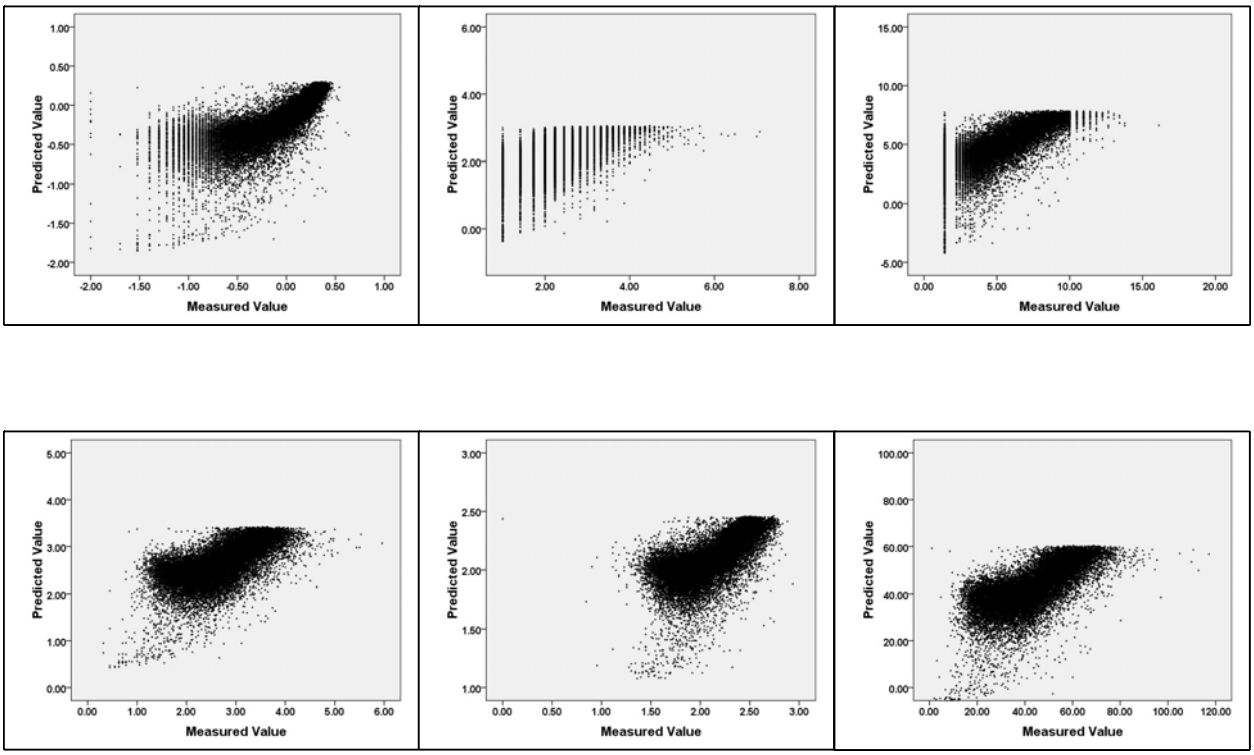


**Figure 7.** *g) Measured vs Predicted values of Na2; simple regression; h) Measured vs Predicted values of Nb2; simple regression; i) Measured vs Predicted values of Rb1; simple regression; j) Measured vs Predicted values of Sc2; simple regression; k) Measured vs Predicted values of Sr2; simple regression; l) Measured vs Predicted values of Ti2; simple regression.*

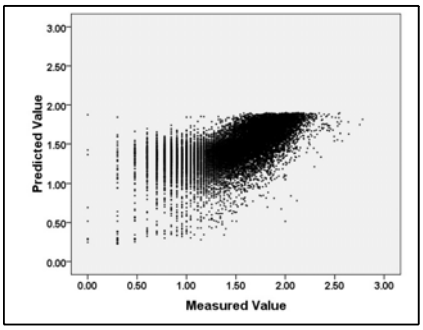


**Figure 7.** *m) Measured vs Predicted values of Zr2; simple regression.*

indeed, in a linear regression the residuals should be normally distributed with a mean of zero. In the context of the current study, a positive residual, therefore, indicates that the sample contains more of the dependent element than can be explained by the modelled clastic content, whereas a negative residual indicates that the dependent element is relatively depleted in the samples.

In the rest of this section, the residuals of the 13 elements that make up the clastic (K–Na–Ti–Mg) association, as calculated from the regression equations detailed in Table 4 (where each element is regressed against 12 others) and Table 5 (where each element is regressed against LOI), are displayed and described for the Labrador dataset. The former will be described as 'multiple-regression residuals' and the latter as 'LOI- regression residuals'. The patterns they delineate are also compared with those displayed by the elements' 'raw'(*i.e.*, unadjusted) values. For each element, the mapped symbols are assigned as follows:

- Red symbols indicate raw values or residuals that exceed the 97.5-percentile of the Labrador dataset; this category is termed 'anomalous'.
- Yellow symbols indicate values that exceed the corresponding 90-percentile of the

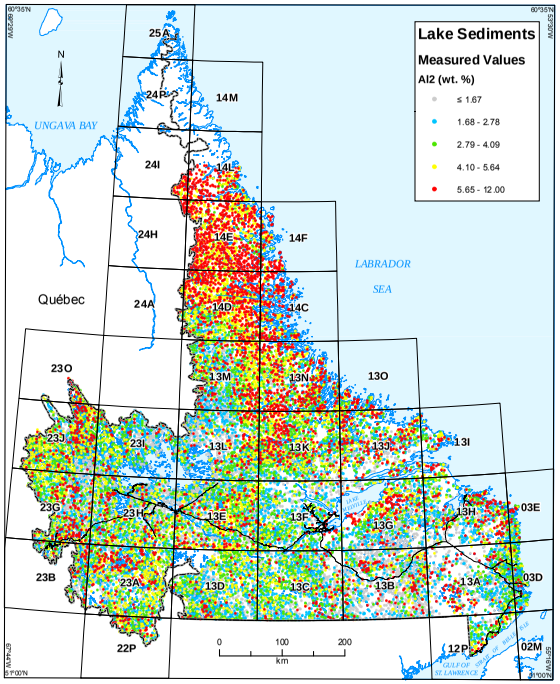


**Figure 8a.** *Measured values of Al2 in lake sediment, Labrador.*

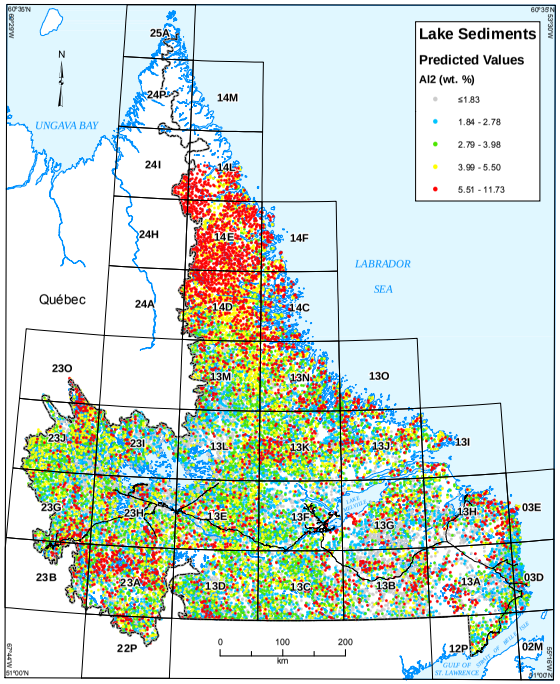


**Figure 8b.** *Multiple regression-predicted values of Al2 in lake sediment, Labrador.*

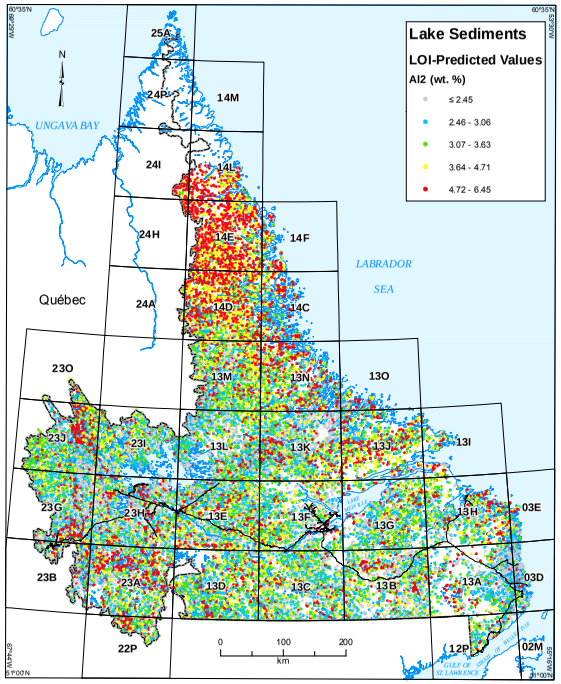


**Figure 8c.** *Simple regression-predicted values of Al2 in lake sediment, Labrador.*

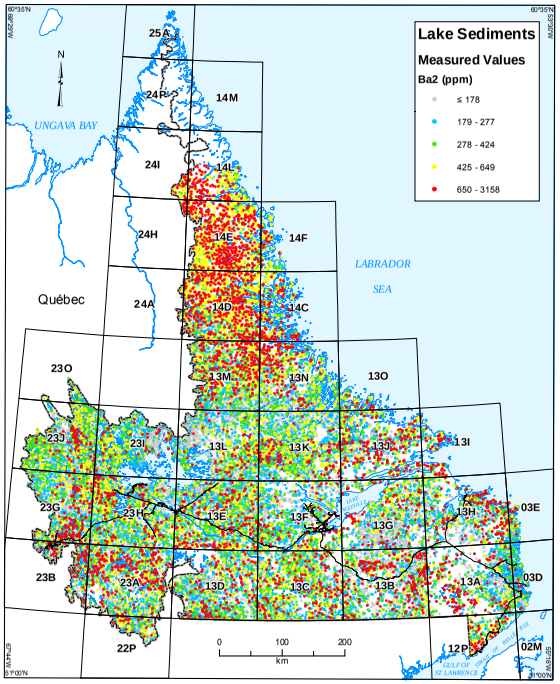


**Figure 9a.** *Measured values of Ba2 in lake sediment, Labrador.*

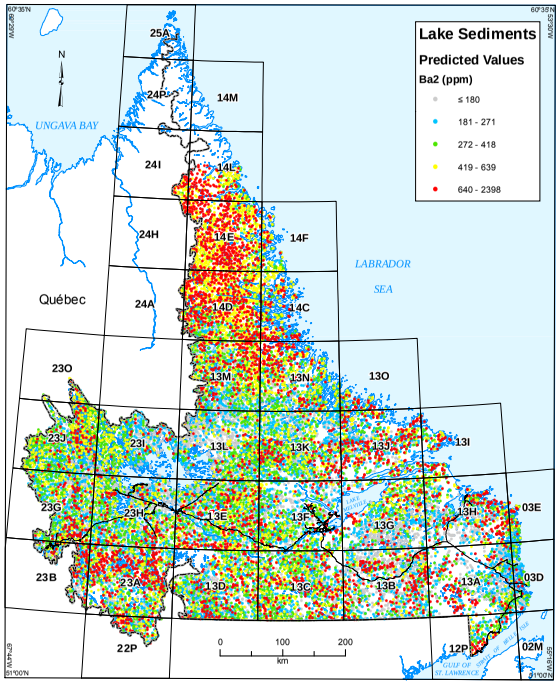


**Figure 9b.** *Multiple regression-predicted values of Ba2 in lake sediment, Labrador.*

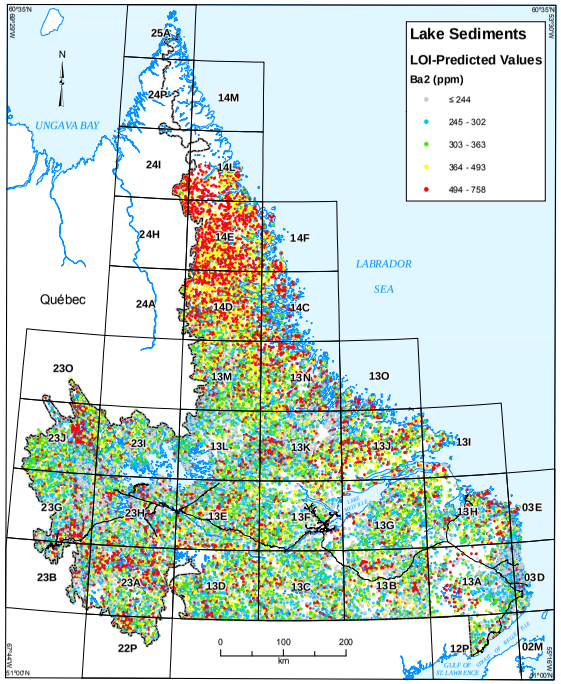


**Figure 9c.** *Simple regression-predicted values of Ba2 in lake sediment, Labrador.*

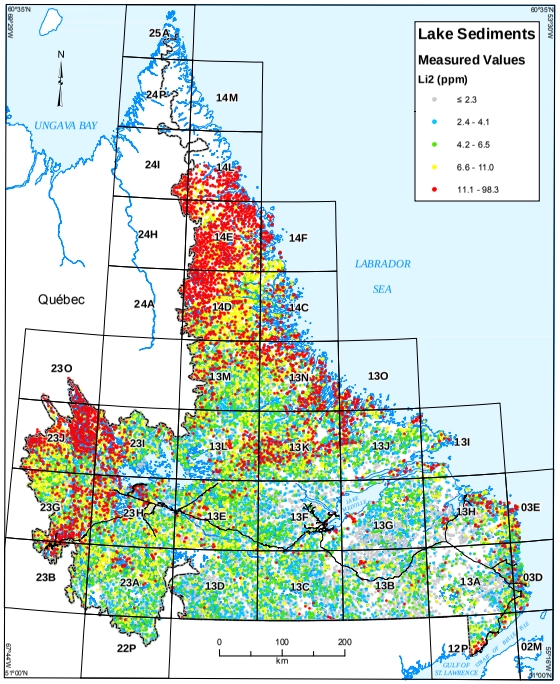


**Figure 10a.** *Measured values of Li2 in lake sediment, Labrador.*

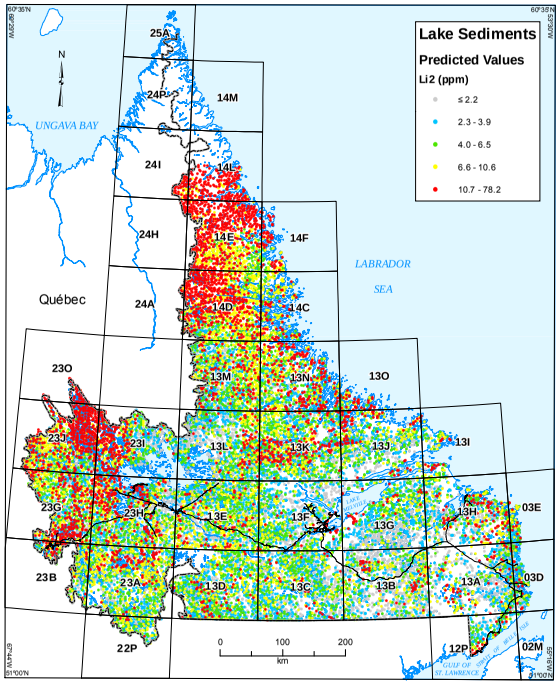


**Figure 10b.** *Multiple regression-predicted values of Li2 in lake sediment, Labrador.*

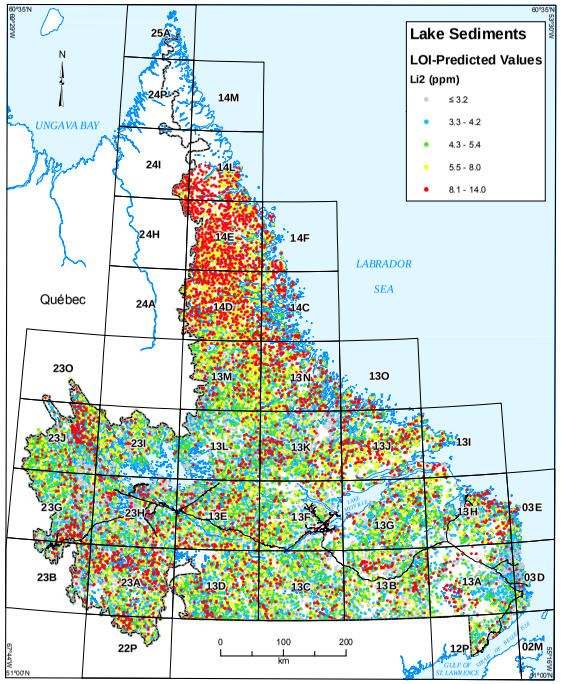


**Figure 10c.** *Simple regression-predicted values of Li2 in lake sediment, Labrador.*

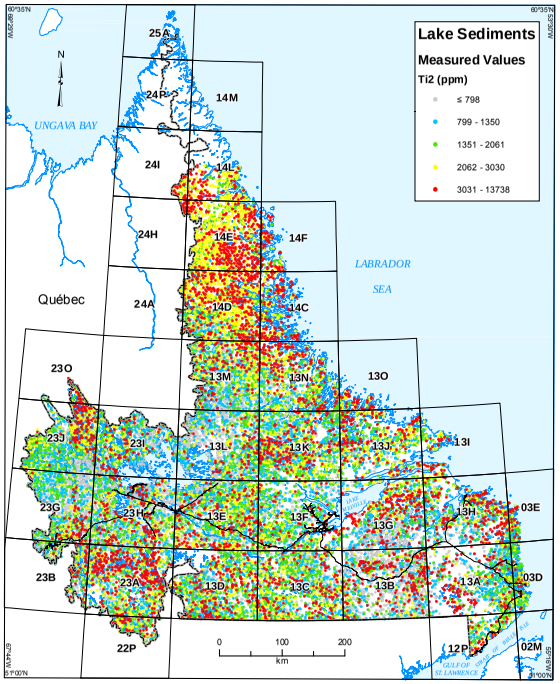


**Figure 11a.** *Measured values of Ti2 in lake sediment, Labrador.*

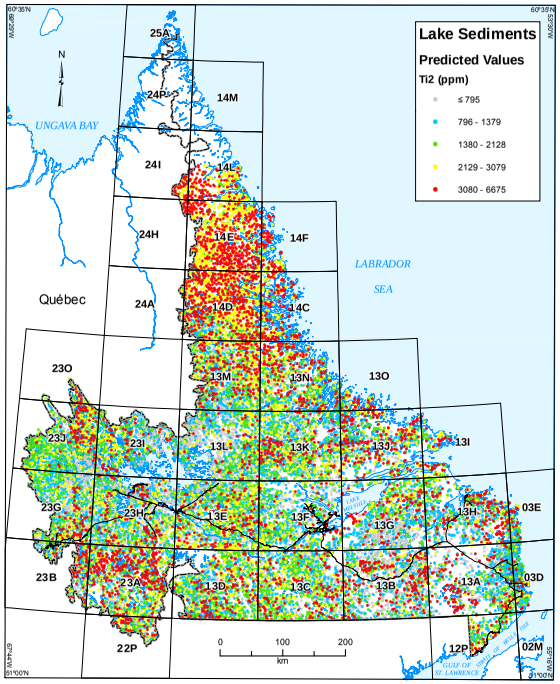


**Figure 11b.** *Multiple regression-predicted values of Ti2 in lake sediment, Labrador.*

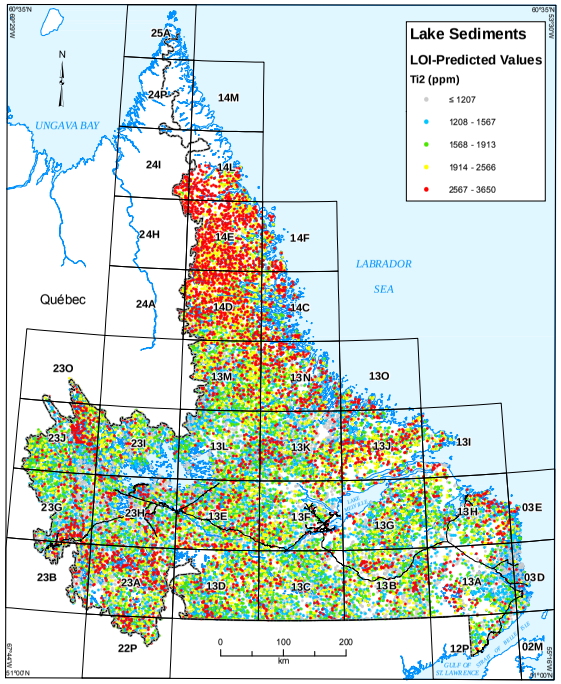


**Figure 11c.** *Simple regression-predicted values of Ti2 in lake sediment, Labrador.*

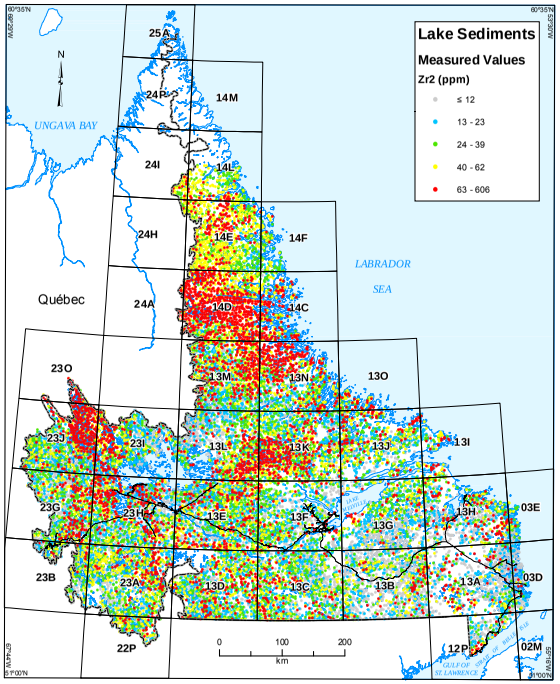


**Figure 12a.** *Measured values of Zr2 in lake sediment, Labrador.*

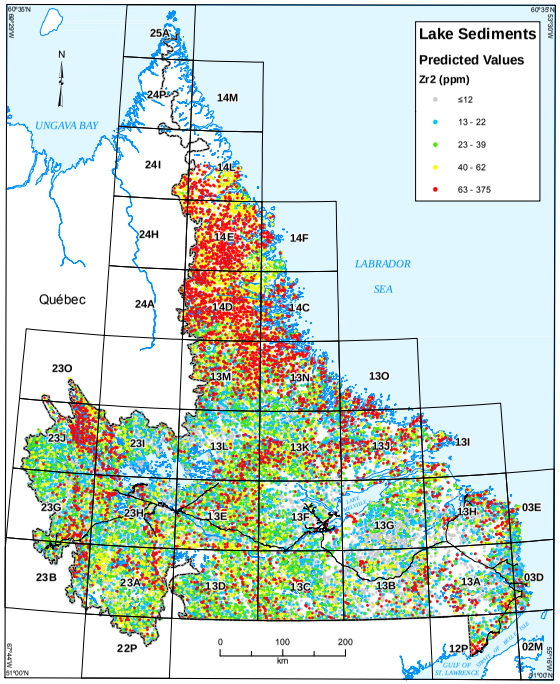


**Figure 12b.** *Multiple regression-predicted values of Zr2 in lake sediment, Labrador.*

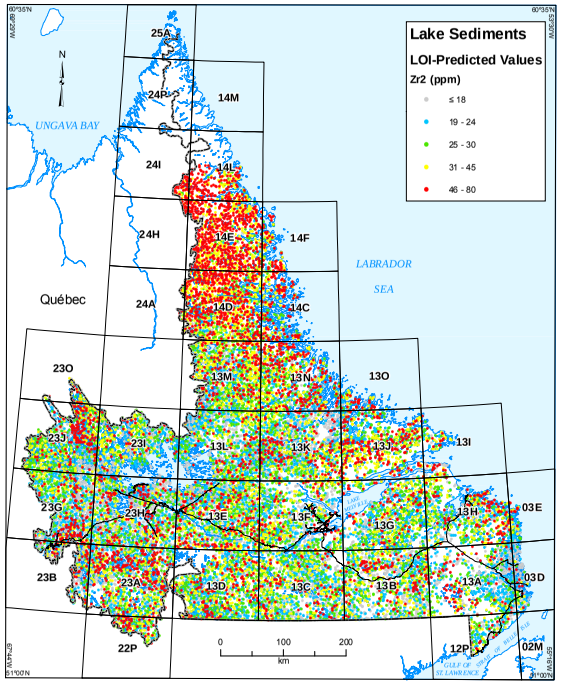


**Figure 12c.** *Simple regression-predicted values of Zr2 in lake sediment, Labrador.*

Labrador dataset; this category is termed ‘elevated’.
- Grey symbols indicate all other values.

Where low values are emphasized (Figures 13–25d and e, in each case), the following symbols are used:

- Dark-brown symbols indicate residual values lower than the 2.5-percentile of the Labrador dataset (termed ‘anomalously low’)
- Pale-brown symbols indicate values lower than the 10-percentile of the Labrador dataset (termed ‘depleted’)
- Yellow symbols indicate all other values.

*Aluminum (Al2)*

Figure 13a shows raw values of Al2 in sediment. Anomalous values (as defined above) are apparent over the Kiglapait Intrusion (NTS map areas 14C/13, 14F/03 and 14F04) and anorthositic Susie Brook slab (NTS 14D/15, 14D/16, 14E/01, 14E/02, 14E/07, 14E/08) in northern Labrador (Ryan, 1990), whereas lower values (grey symbols) characterize the gneisses that separate these two intrusions; the response may, therefore, be related to geology.

An area southwest of Hopedale underlain by the Harp Lake Intrusive Suite (NTS map areas 13K/13, 13L/16, 13M/01, 13M/08 and 13N/04; Emslie, 1980), and the granites and gneisses to the northeast of it (NTS map areas13N/02, 13N/03, 13N/06, 13N/07 and 13N/10), is also characterized by anomalous raw Al2 values, although the southern and western portions of the intrusion are not anomalous or elevated in this respect.

Standardized multiple- and simple (LOI)-regression residuals of Al2 (Figure 13b, 13c) confirm the anomaly over the Kiglapait Intrusion and Susie Brook slab in the north, although in both cases the values are mainly elevated, rather than anomalous. In the east of the Harp Lake Intrusive Suite, anomalous residuals of both types concentrate over the ‘anorthosite, leucotroctolite, leuconorite, minor leucogabbro’ phase (Unit *anol*, Emslie, 1980) and are conspicuously absent over the ‘anorthosite, leuconorite, less common leucogabbro’ phase (Unit *anln*), although this relationship does not hold in the west, where Al2 residuals are consistently low despite Unit *anol* being predominant. LOI-regressed residuals define a less-focused, more ‘noisy’ feature than their multiple-regression counterparts. The same relationship is exhibited by anomalous Mg2 residuals (multiple regression only; Figure 18b), and to some extent by depleted and anomalously low Sc2 residuals (multiple regression only; Figure 22d). The area overlying the gneisses to the northeast of the Harp Lake Intrusive Suite is characterized predominantly by elevated residual values of both types; this feature is not characteristic of the raw values. Like the raw values, residuals are not elevated or anomalous over the southern and western portions of the intrusion.

An anomaly southeast of Lake Melville (NTS map areas 13G/09, 13G/10, 13G/11 and 13G/15) is defined by anomalous and elevated Al2 multiple-regression residuals and rather precisely delineates the leucotroctolitic, leucogabbroic and anorthositic Etagaulet Bay and Kennemich massifs (Units $P_3$Clt and $P_3$Can; Gower, 2010a, personal communication, 2013); its expression in raw values is much less well defined. Once again, the feature defined by LOI-regres-

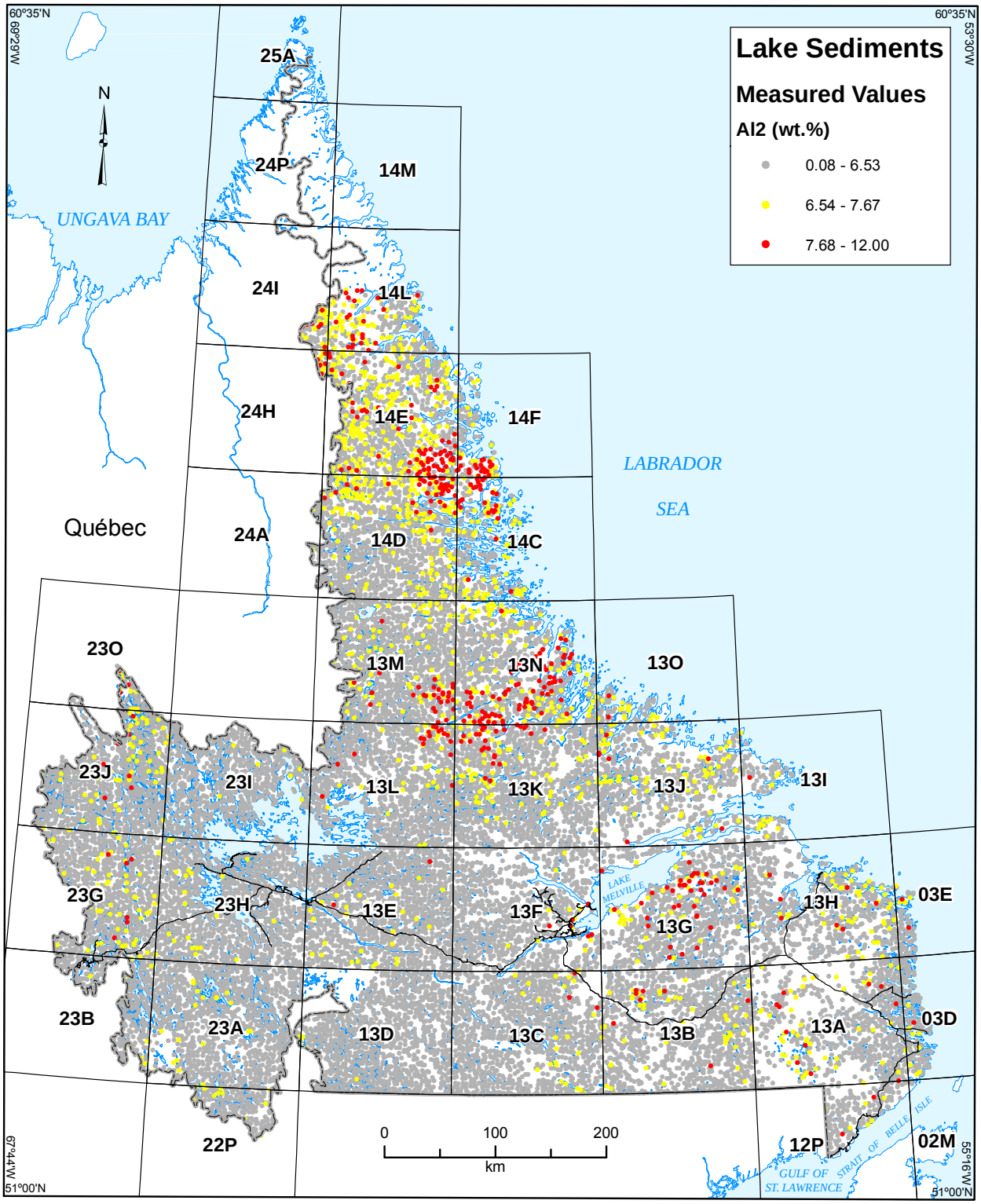


**Figure 13a.** *Measured values of Al2 in lake sediment, Labrador, with emphasis on highest values.*

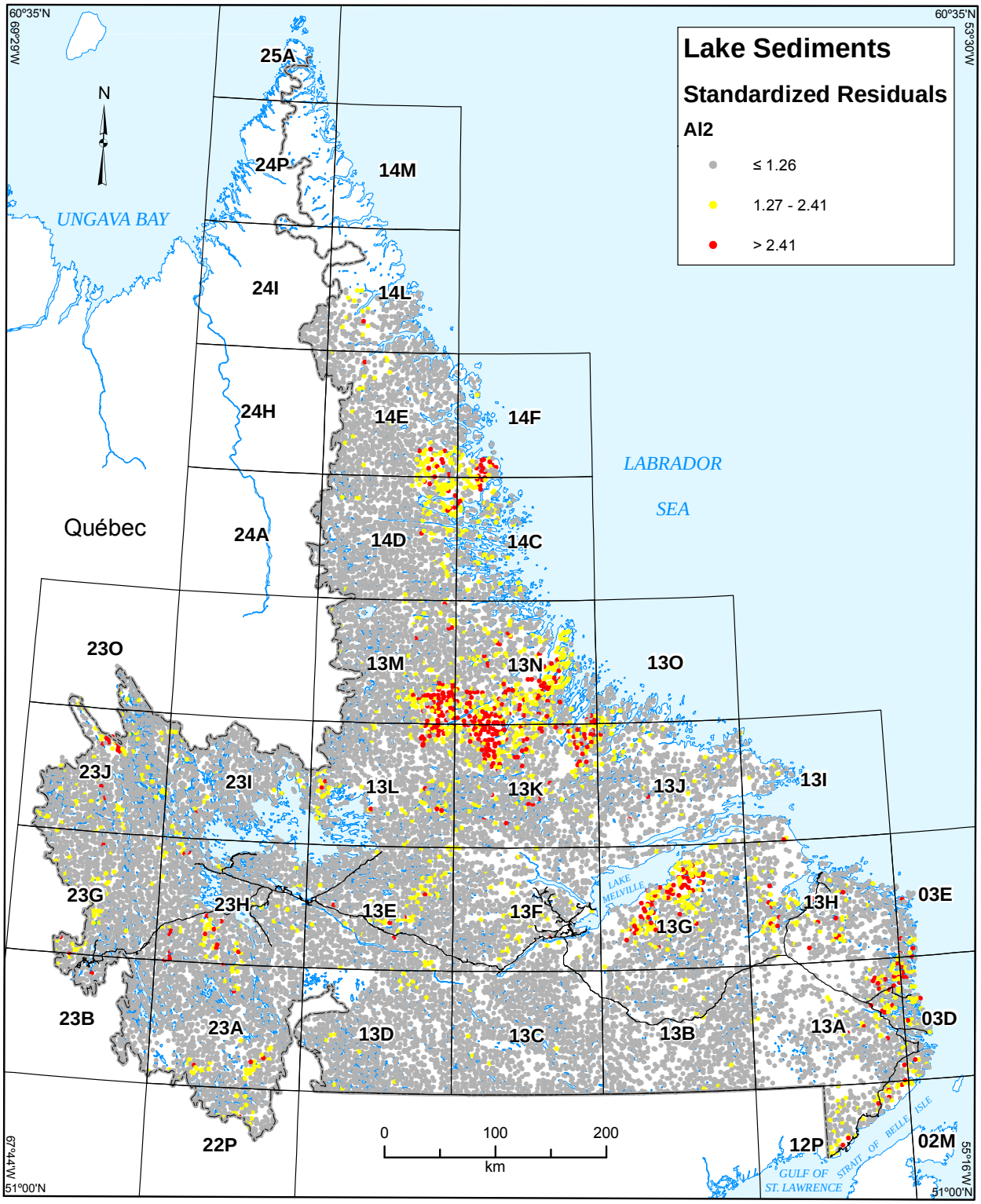


**Figure 13b.** *Standardized multiple-regression residuals of Al2 in lake sediment, Labrador, with emphasis on highest values.*

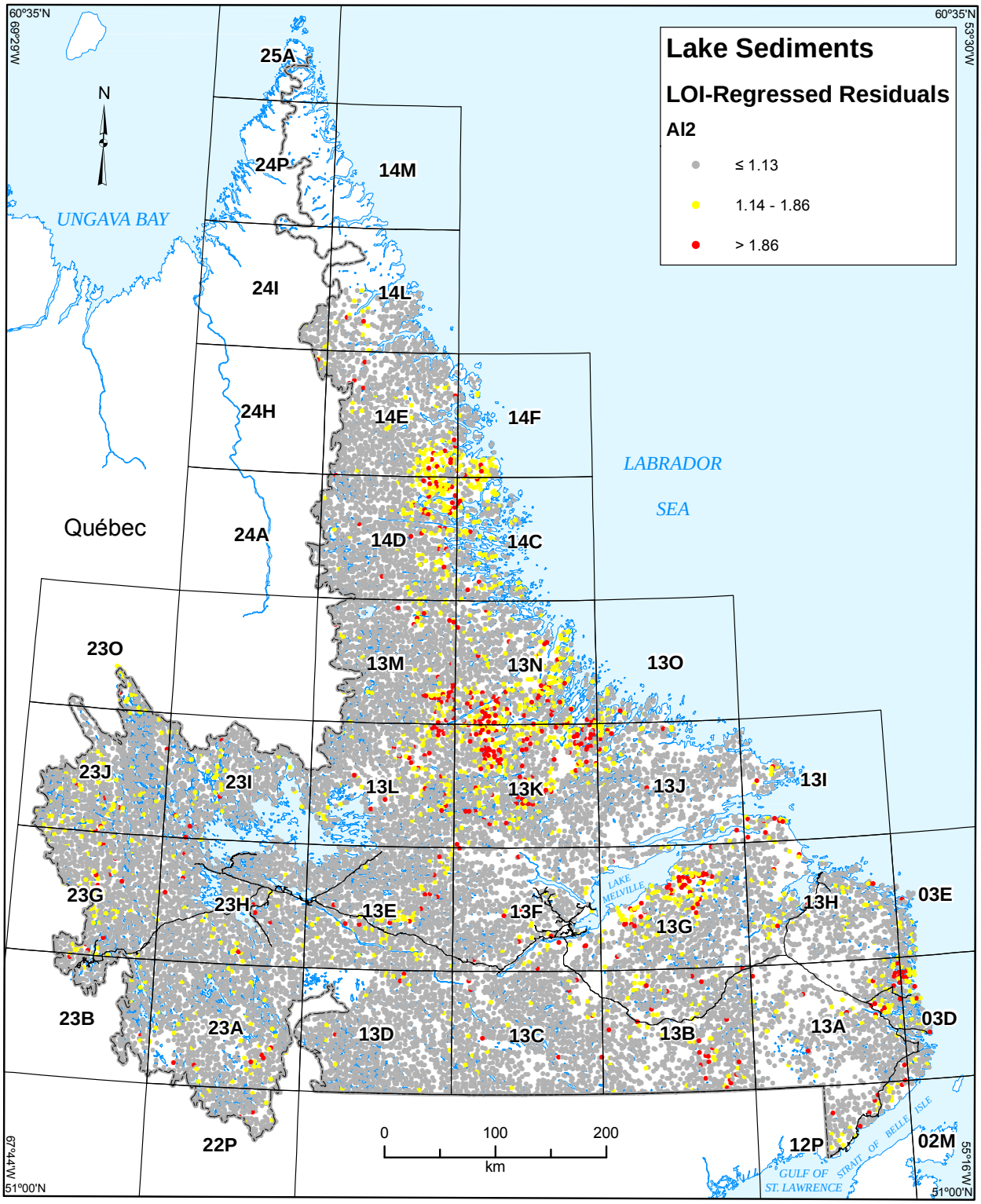


**Figure 13c.** *Standardized simple-regression residuals of Al2 in lake sediment, Labrador, with emphasis on highest values.*

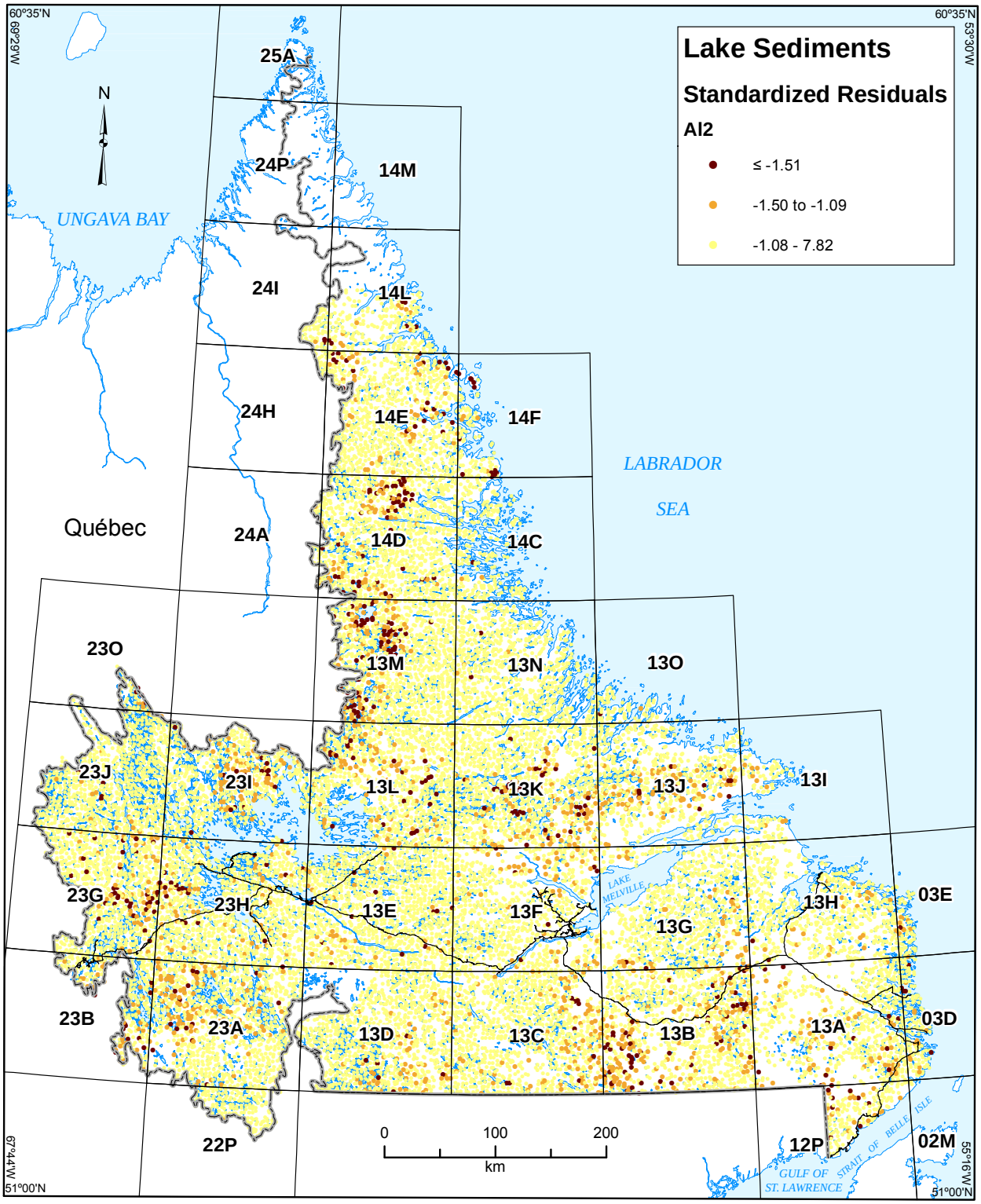


**Figure 13d.** *Standardized multiple-regression residuals of Al2 in lake sediment, Labrador, with emphasis on lowest values.*

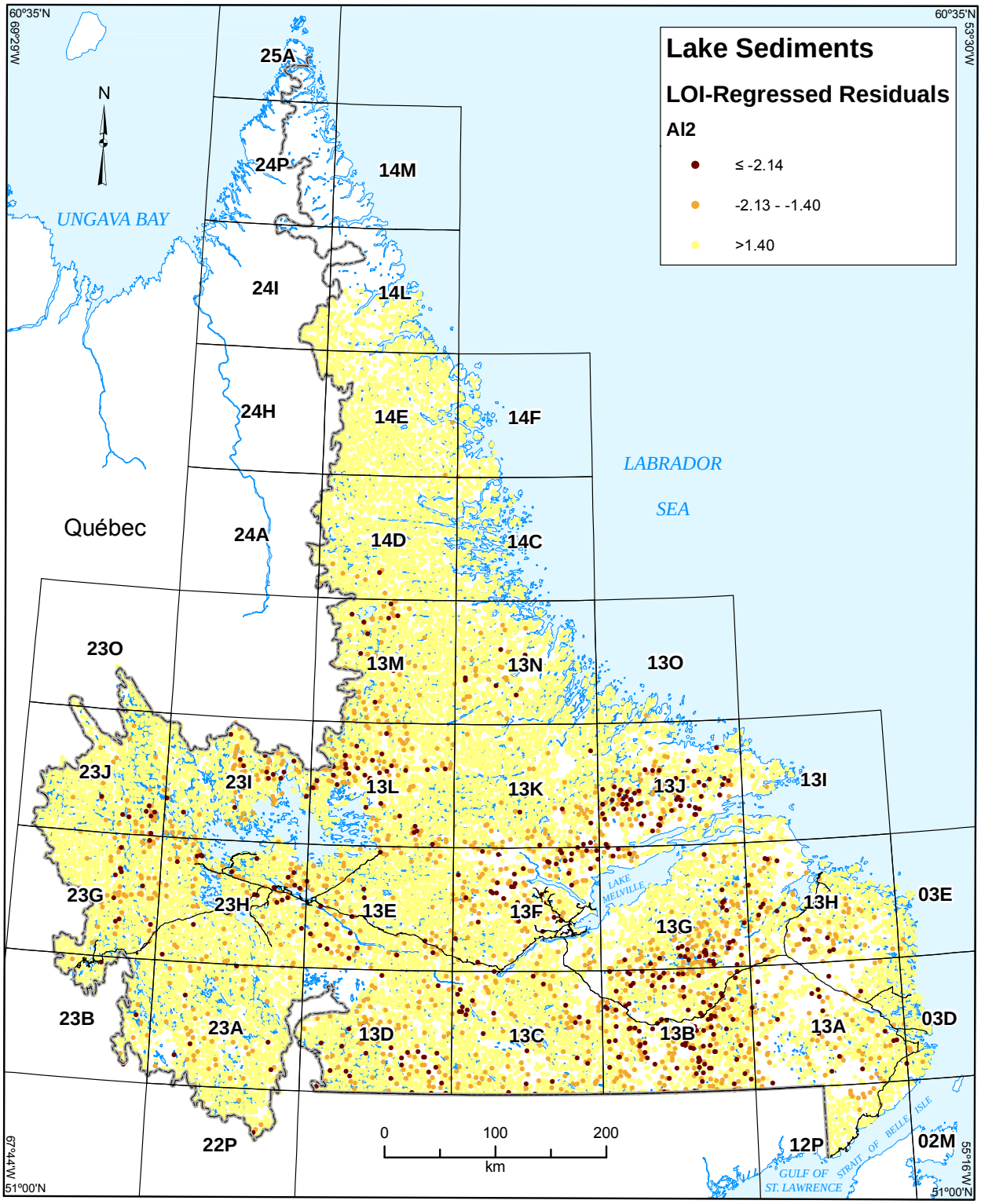


**Figure 13e.** *Standardized simple-regression residuals of Al2 in lake sediment, Labrador, with emphasis on lowest values.*

sion residuals is less focused. A similar feature is delineated by depleted and anomalously low multiple-regression residuals of Sc2, although it is absent in the LOI-regression residuals (Figure 22d).

Samples whose Al2 multiple-regression residuals are particularly low (Figure 13d) define foci west of Kingurutik Lake in northern Labrador (in the north of NTS map areas 14D/10, 11, 14 and 15), overlying the southern extension of the Umiakovik Lake batholith (Ryan 1990); in NTS map areas 13M/10, 11, 14 and 15, and in NTS 13M/03 and 04, overlying the Mistastin Batholith and lower Proterozoic and/or Archean gneissic and migmatitic country rock to the southeast (Wardle, 1993). These features are absent from the LOI-regression residuals (Figure 13e).

*Barium (Ba2)*

Anomalous and elevated raw values of Ba2, along with several other elements in the association, define an arcuate belt extending from south of Mistastin Lake (NTS map area 13M/06) eastward to the coast at Davis Inlet (NTS 13N/14; Figure 14a). Scattered anomalous and elevated values are present over a wide area of southeastern Labrador, and southwest of Hebron Fiord in the north. Most of the apparently anomalous samples indicated by the raw values disappear when residuals are examined, suggesting that the former are artefacts of the clastic content of the samples. An exception is south of Mistastin Lake, in NTS map areas 13M/06, 07 and 10, where an anomaly defined by residuals persists, over an area mainly underlain by Archean or Paleoproterozoic gneiss (Unit $P_1$-Agn) and two relatively small outliers of Mid-Mesoproterozoic arkose or quartzite of the Seal Lake Group (Unit $P_2$st; Wardle, 1993).

Although there are no obvious disparities between measured (Figure 9a) and predicted (Figure 9b) Ba2 values, examination of the positive Ba2 multiple-regression residuals (Figure 14b) indicates two areas of strong Ba2 enrichment in western Labrador (Figure 8c). These may have geological and possibly economic significance. The larger and more distinct one has no anomalous expression in the raw Ba2 values and is situated to the west of the Smallwood Reservoir in NTS map areas 23G/09 and 16; 23H/11, 12 and 13; and 23J/01. The larger of the two enrichment areas is termed the *Colville River anomaly*. The Ba is probably derived from the argillaceous Menihek Formation of the Knob Lake Group, although many of the component samples of the anomaly overlie the arenaceous Tamarack and Muriel formations of the Sims Lake Group (Ware and Wardle, 1979) and these were previously suggested (Brushett and Amor, 2013) as a possible source.

The second enrichment area (anomaly), defined both by anomalously high raw Ba2 values and (more strongly) by multiple-regression residuals, is situated in NTS map areas 23B/14 and 15, and 23G/02, north of Labrador City. This is termed the *Bondurant Lake anomaly*. In the southwest, the anomaly is closely spatially associated with the Menihek Formation, although to the northeast it overlies the older Sokoman, Wishart and Attikamagen formations; this may be due to eastward glacial displacement of Menihek Formation material.

Both of the above anomalies are less well defined by LOI-regression residuals (Figure 14c), particularly the former. In general, the impression is that the features defined by the latter are dilute and ‘noisy’.

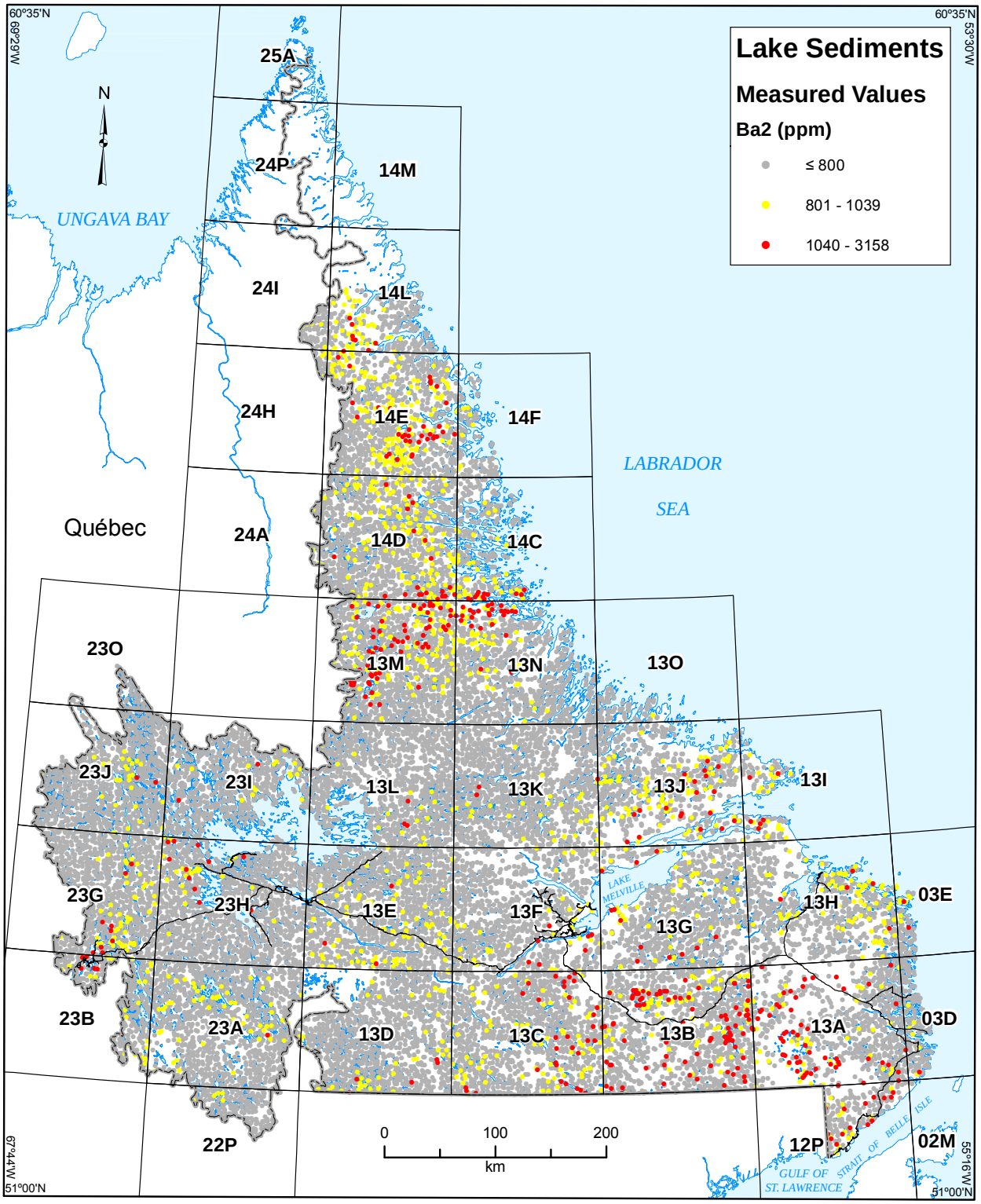


**Figure 14a.** *Measured values of Ba2 in lake sediment, Labrador, with emphasis on highest values.*

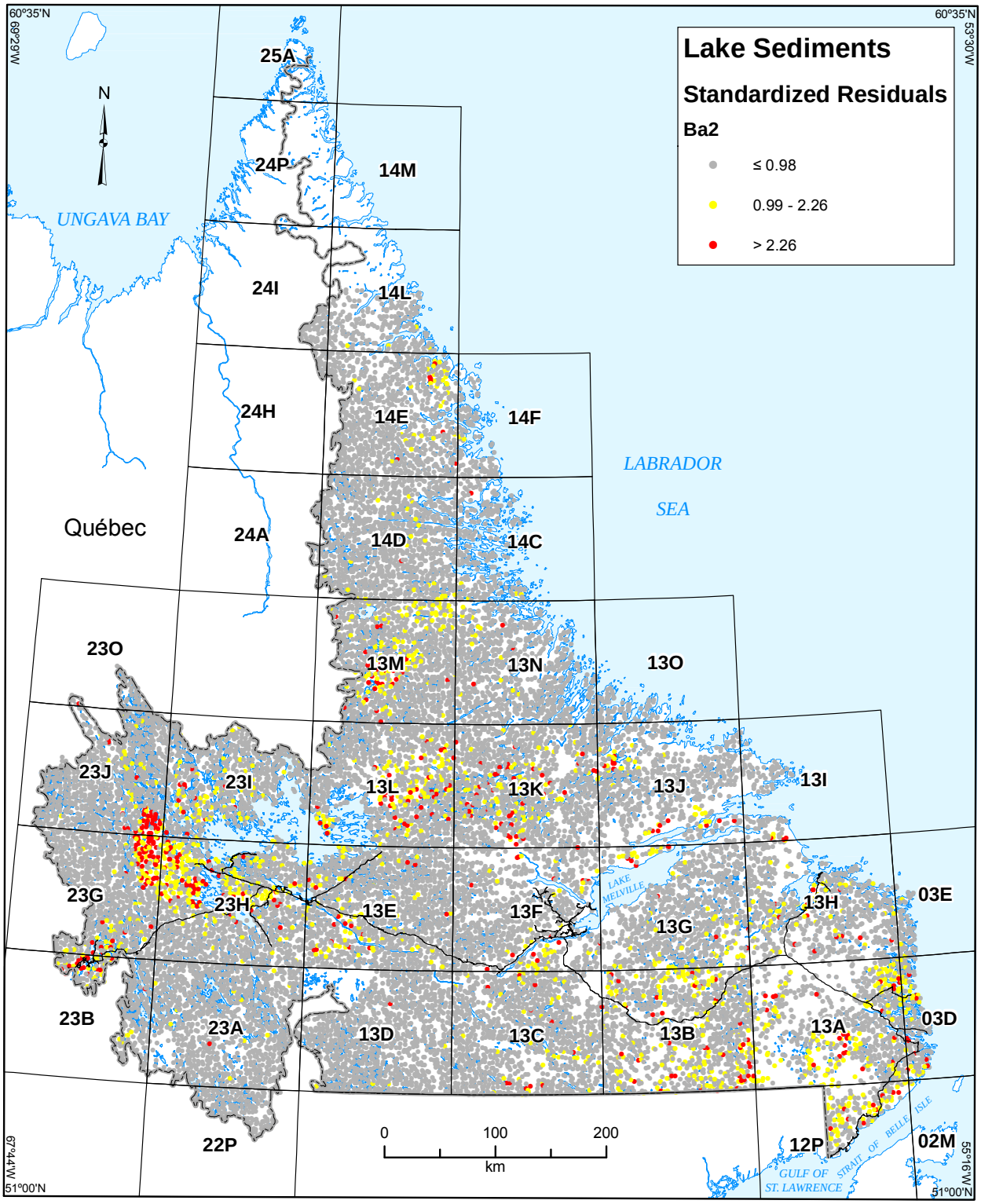


**Figure 14b.** *Standardized multiple-regression residuals of Ba2 in lake sediment, Labrador, with emphasis on highest values.*

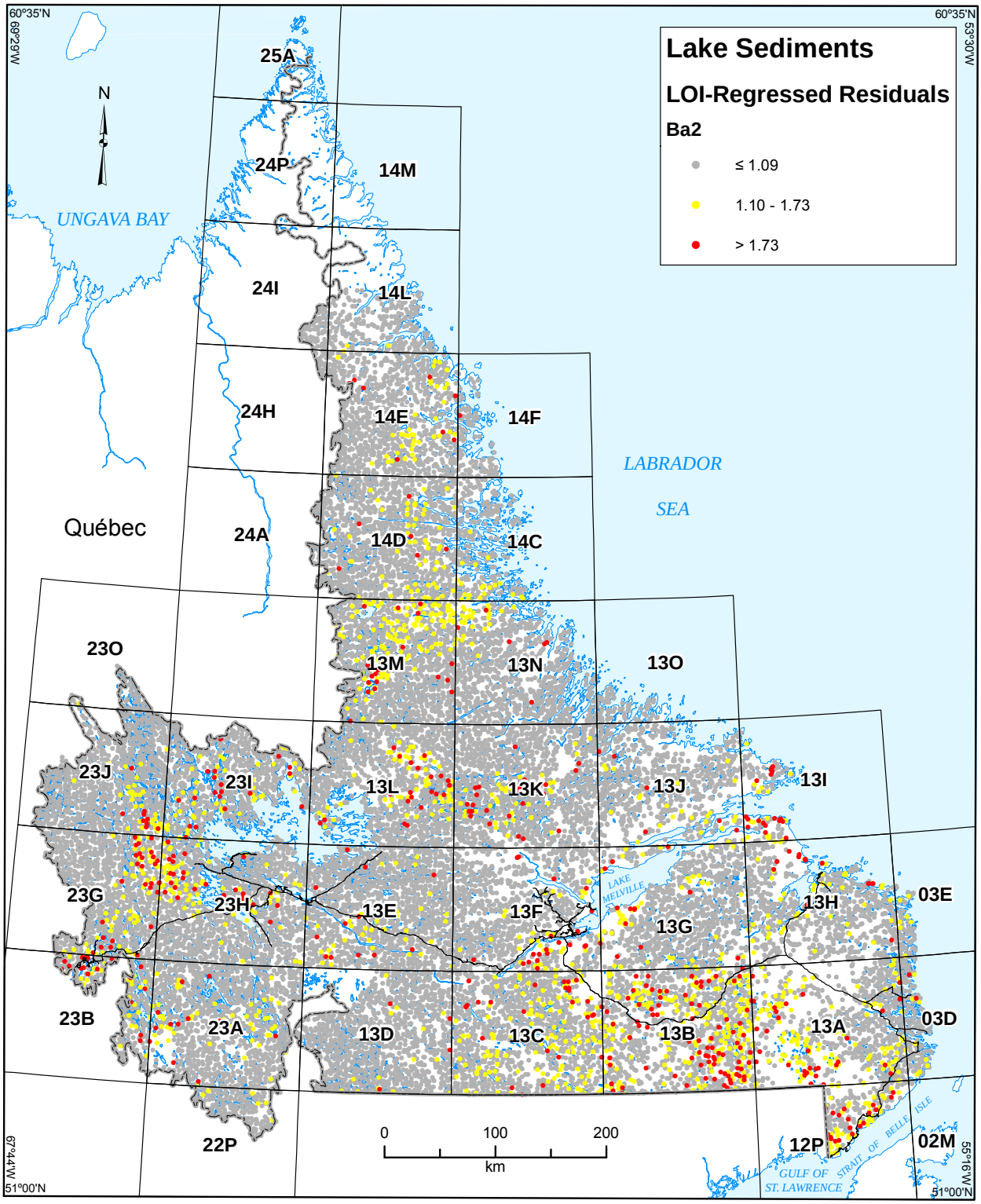


**Figure 14c.** *Standardized simple-regression residuals of Ba2 in lake sediment, Labrador, with emphasis on highest values.*

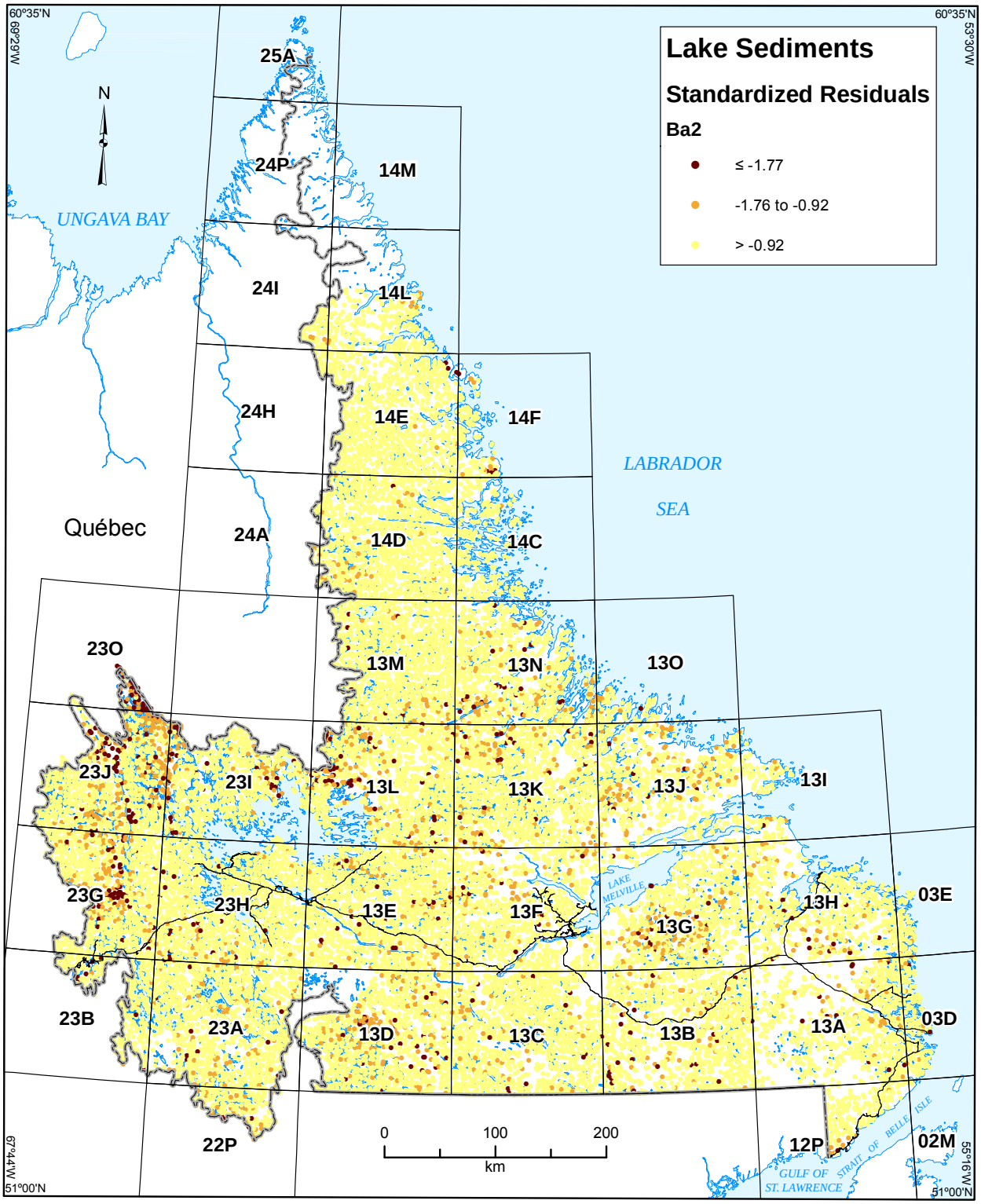


**Figure 14d.** *Standardized multiple-regression residuals of Ba2 in lake sediment, Labrador, with emphasis on lowest values.*

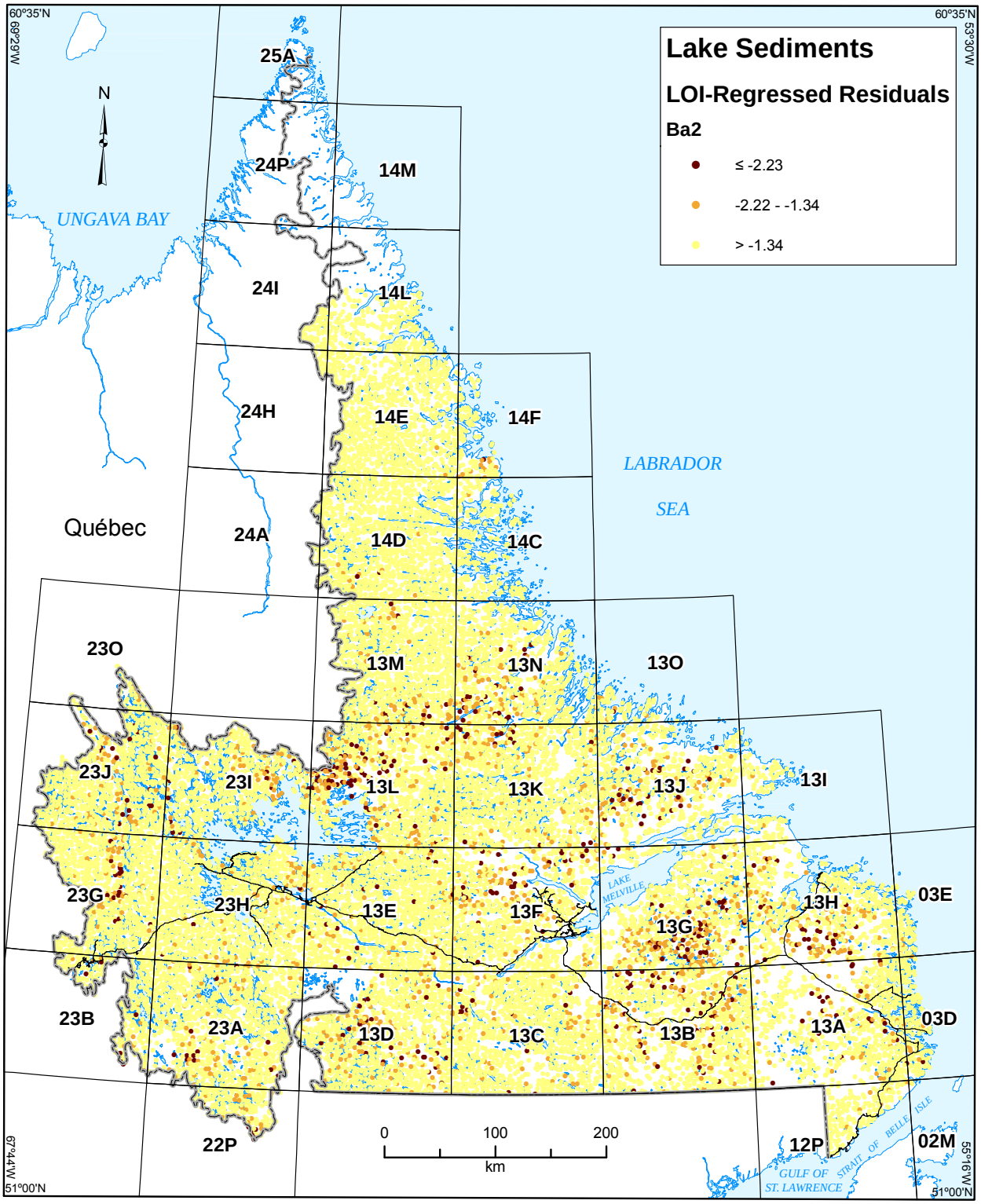


**Figure 14e.** *Standardized simple-regression residuals of Ba2 in lake sediment, Labrador, with emphasis on lowest values.*

Multiple-regression residuals of Ba are anomalously low in samples collected over rocks of the Labrador Trough in NTS map areas 23G and 23J (Figure 14d). In NTS map areas 23J/10, 11, 14 and 15, the depletion is associated with iron formation of the Sokoman Formation, although rocks assigned to the Menihek Formation have also been mapped in the area; Ba2 depletion is also noted over Menihek Formation rocks in NTS 23J/01, 02, 07 and 10, and in NTS 23G/07 and 10. In NTS map areas 23J/16 and 23O/01, 02 and 07, the depleted and anomalously low residuals are associated with argillaceous rocks of the Le Fer Formation, and the intruding Wakuach Gabbro (Wardle, 1982a). Anomalously low LOI-regression residuals (Figure 14e) do not define these features, although they do define two others: in NTS map area 13L/12, over the Michikamau Intrusion; and in NTS 13G/02 and 13G/07, over late Paleoproterozoic 'granite, monzonite, charnockite' (Unit $P_3$g, Wardle *et al*., 1997) or monzonite, quartz monzonite, monzonorite and porphyritic granite (Units $P_3$Cmz, $P_3$Cmq, $P_3$Cgp, $P_3$Cmn; Gower, 2010d). The latter feature is also defined, to a greater or lesser extent, by anomalously low LOI-regression residuals of all of the other elements.

*Hafnium (Hf1)*

Anomalously high raw values of Hf1 (Figure 15a) are mainly concentrated in northern Labrador; to the southeast and east of Mistastin Lake (*cf*. Ba2) in NTS map areas 13M/06, 09, 10, 11 and 16; 13N/11–15, over diverse rock units; in NTS 14C/04, 14D/01 and 02, underlain by the Cabot Lake gabbro and gneissic rocks to the west (Ryan, 1990); and in the dispersion train from the Strange Lake rare-earth element (REE) and rare-metal (RM) deposit in NTS map areas 24A/08, 14D/05–10. In NTS map areas 14E/02, 03, 06 and 07, anomalous raw Hf1 values coincide with a REE anomaly over the Umiakovik Lake batholith (Amor, 2011) and this anomaly is the only one that persists in the multiple-regression residuals (Figure 15b). Since the dispersion from Strange Lake is clearly not an artefact of the clastic component of the sediment, this suggests that, in some cases, the regression process can overcompensate for the latter's effects. LOI-regressed residuals (Figure 15c) tend to echo the raw Hf1 residuals, rather than their multiple-regression counterparts, in a more dilute form, including the dispersion from Strange Lake.

A positive multiple-regression residual anomaly of Hf1 is also present in the extreme southeastern corner of Labrador, in NTS map areas 12P/06, 07, 12P/10, 11, 14 and 15, over Neoproterozoic or Cambrian sediments (Units CFo, CBr) and older granitic rocks (Units PMgr and $M_3$Cmq; Gower, 2010b). The feature is smaller and less distinct as defined by Hf1 residuals and would probably not have been remarked upon in isolation. The K2 residuals of both types are also anomalously high in the same area, although their response is conspicuously stronger over the younger rocks (Figure 16b, 16c).

*Potassium (K2)*

Anomalously high raw values of K2 (Figure 16a) define the same arcuate belt defined by Al2 (Figure 13a), Hf1 (Figure 15a), and to a lesser extent by Ba2 (Figure 14a), in NTS map areas 13M, 13N, 14C and 14D. They are also focused over the granites of the Benedict Mountains (NTS map area13J), over Kaniapiskau Supergroup rocks on NTS map area 23J in the west, and coincident with the Hf-defined feature in the south of NTS map area 12P.

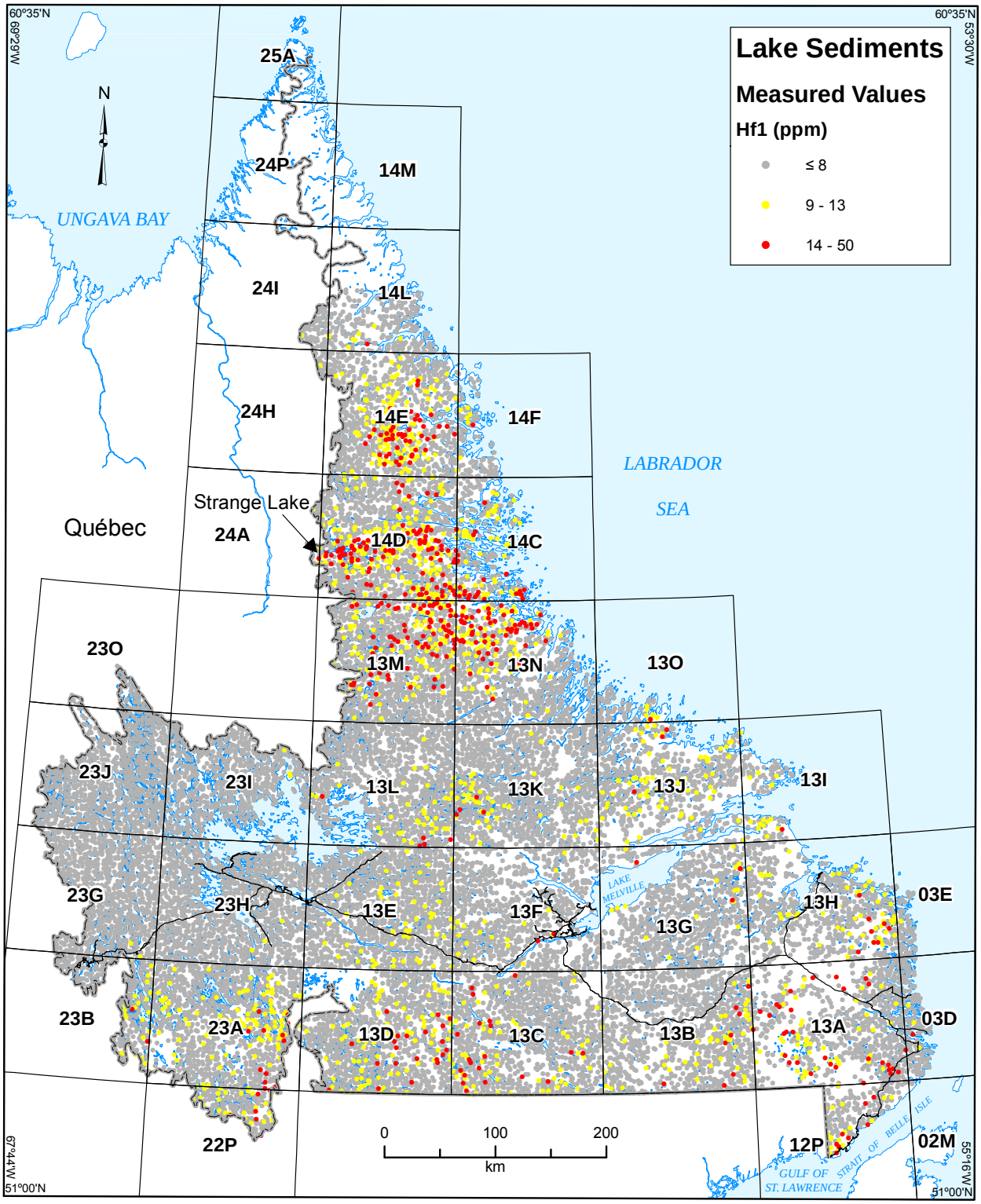


**Figure 15a.** *Measured values of Hf1 in lake sediment, Labrador, with emphasis on highest values.*

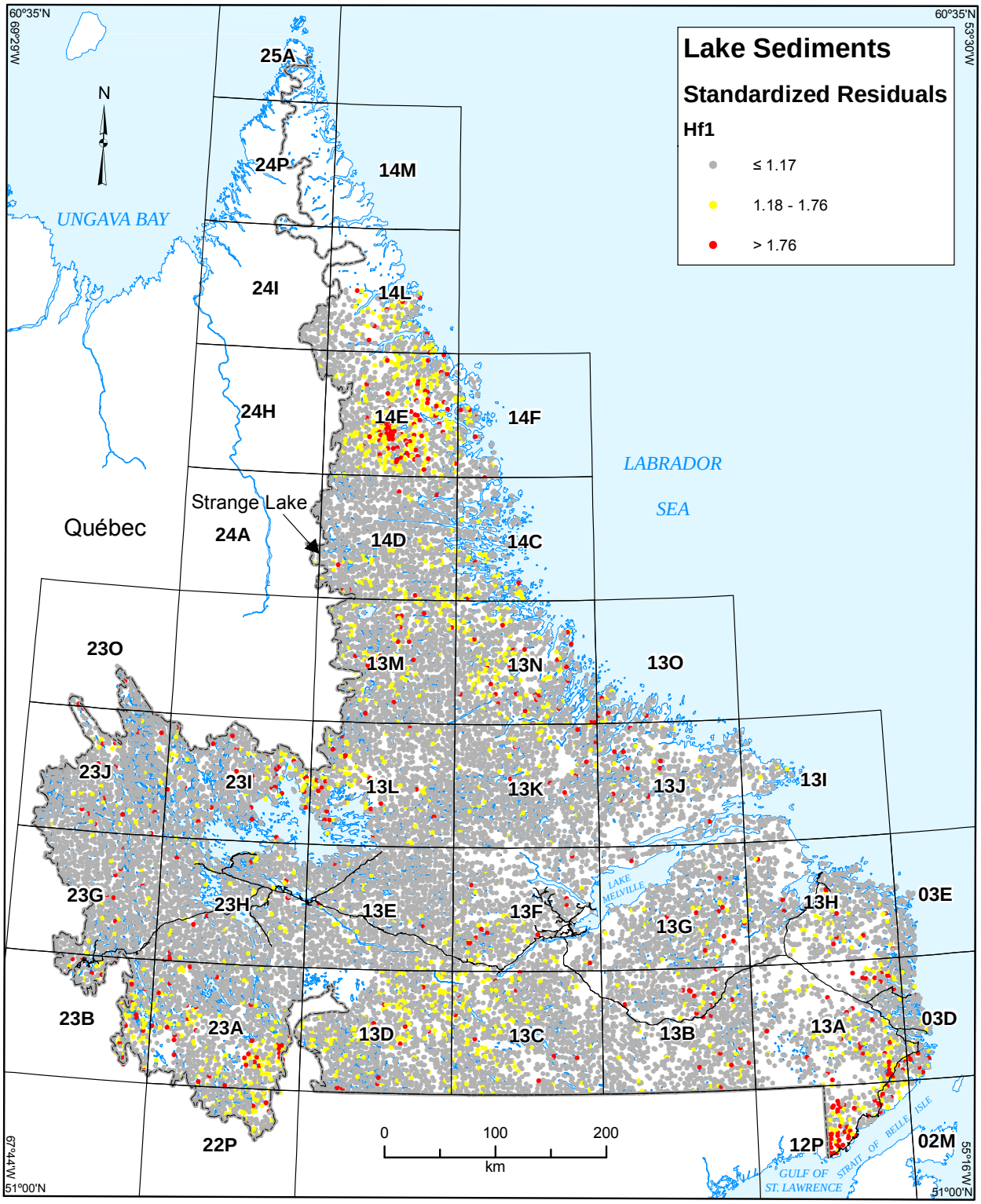


**Figure 15b.** *Standardized multiple-regression residuals of Hf1 in lake sediment, Labrador, with emphasis on highest values.*

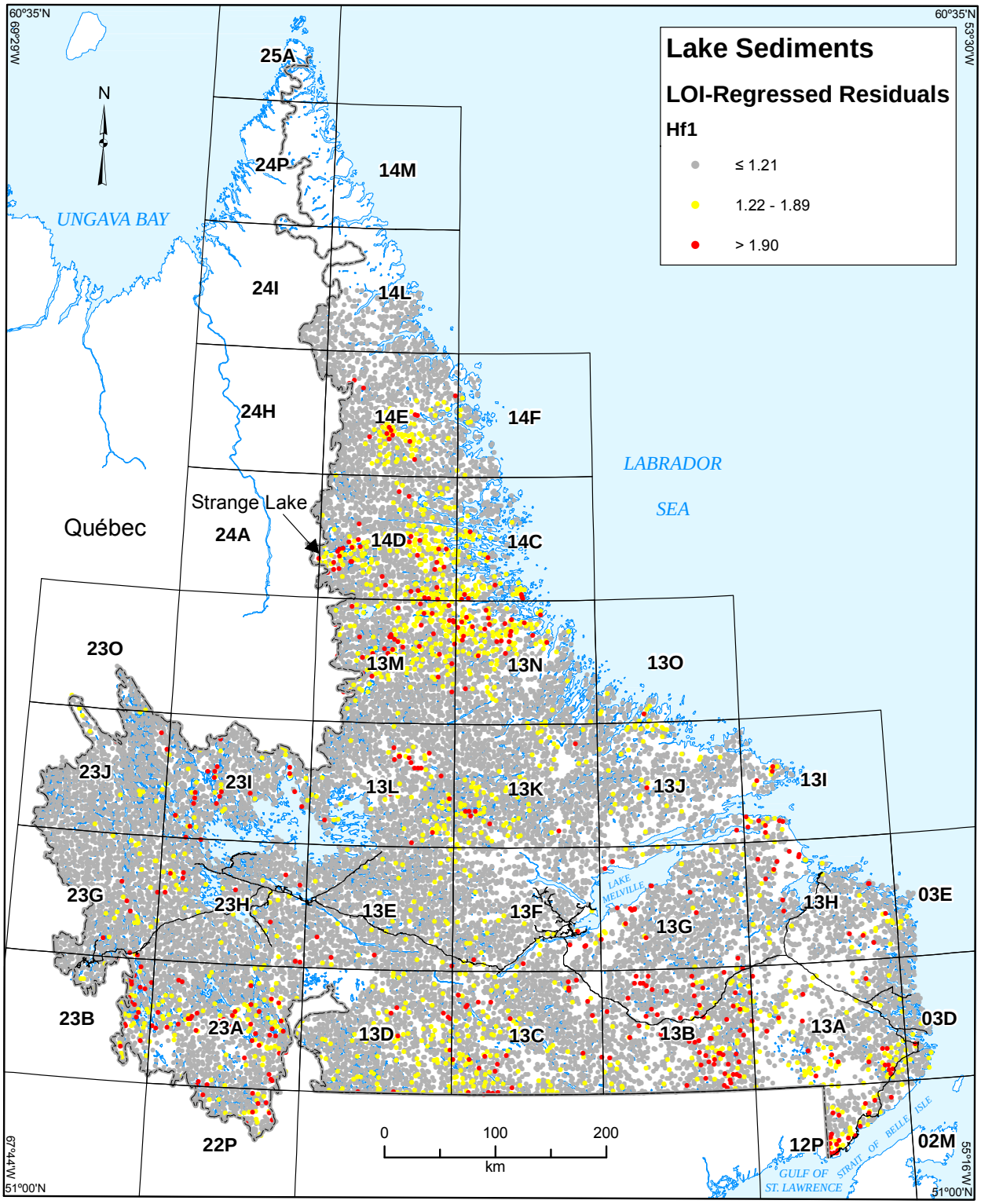


**Figure 15c.** *Standardized simple-regression residuals of Hf1 in lake sediment, Labrador, with emphasis on highest values.*

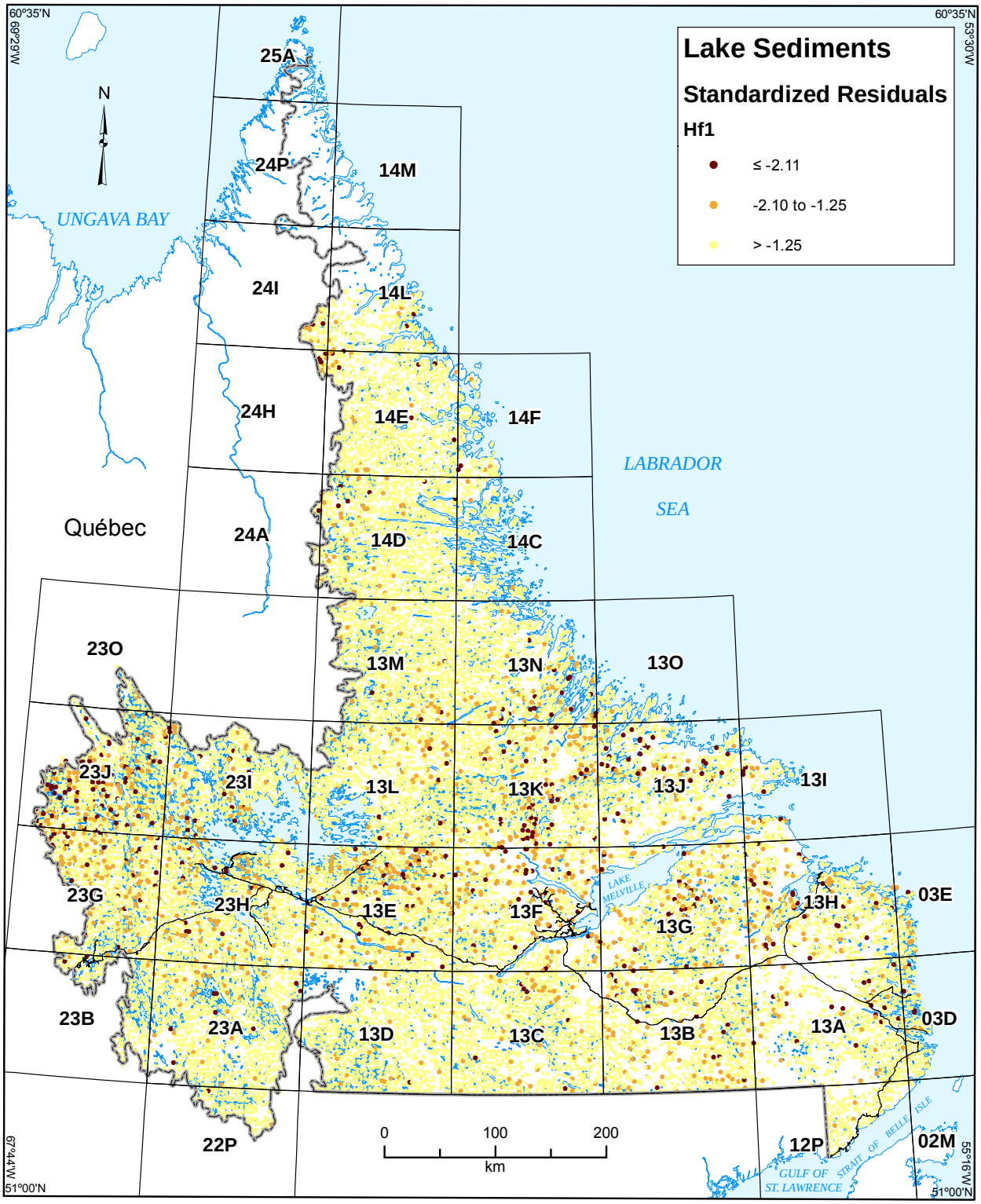


**Figure 15d.** *Standardized multiple-regression residuals of Hf1 in lake sediment, Labrador, with emphasis on lowest values.*

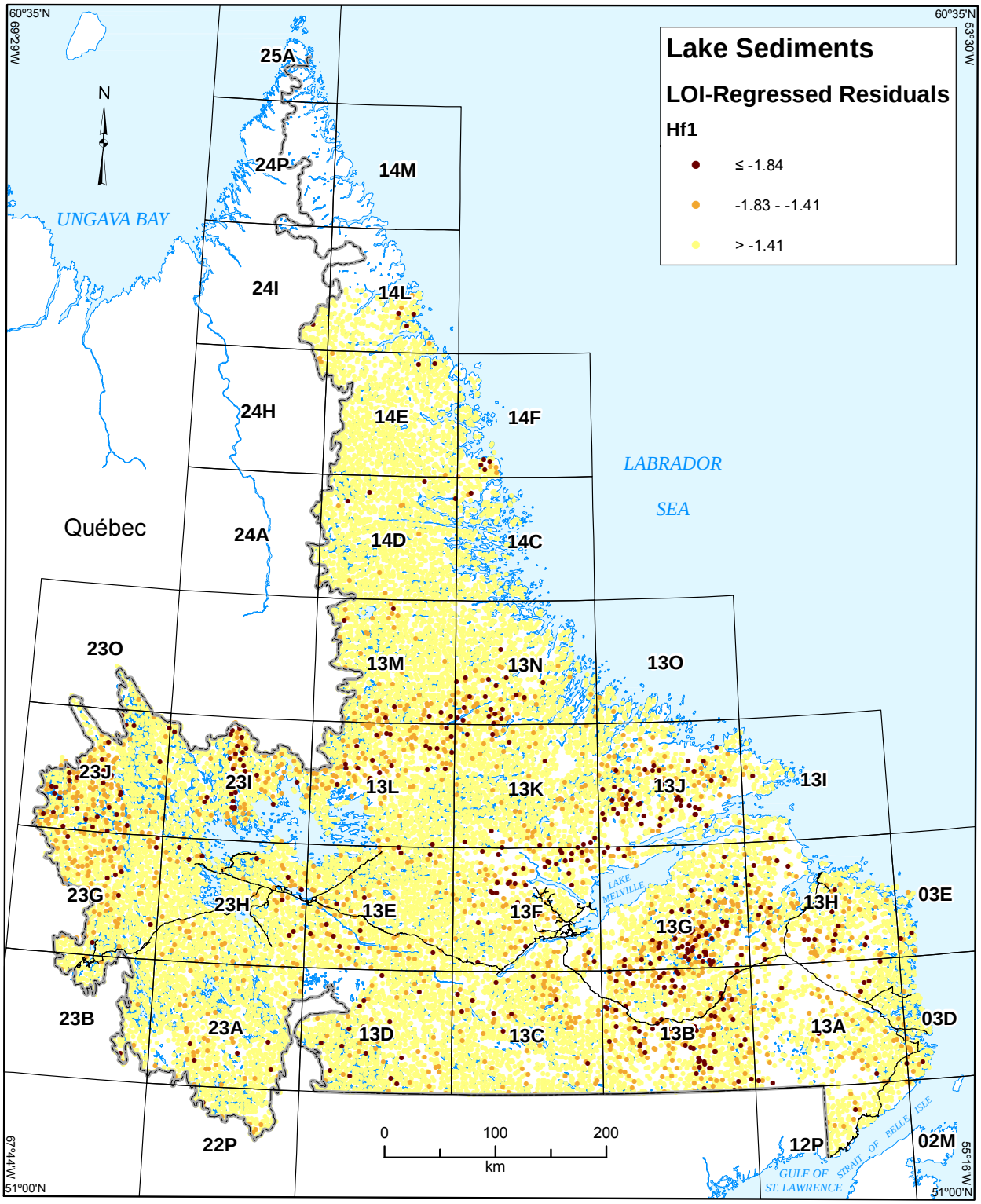


**Figure 15e.** *Standardized simple-regression residuals of Hf1 in lake sediment, Labrador, with emphasis on lowest values.*

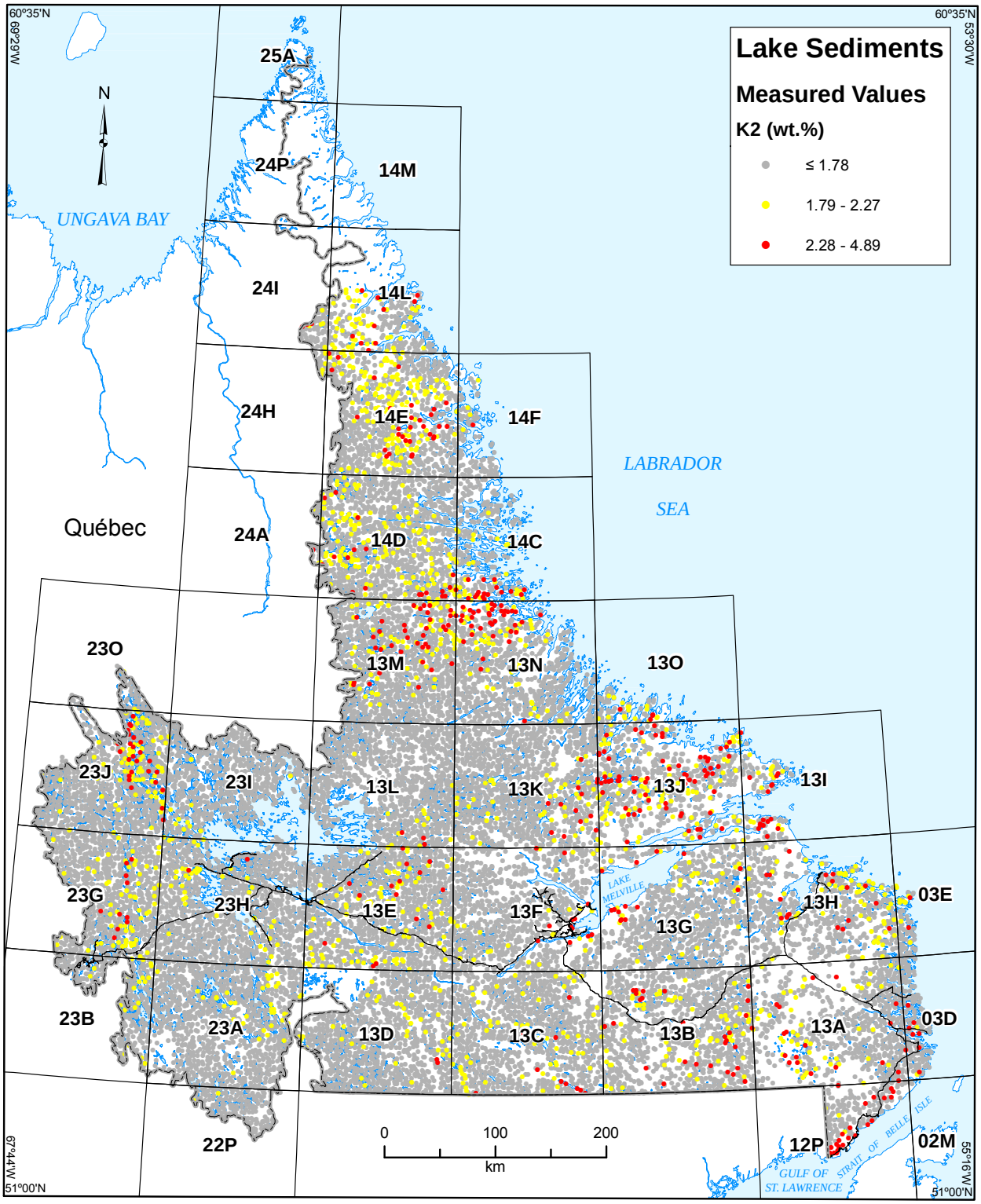


**Figure 16a.** *Measured values of K2 in lake sediment, Labrador, with emphasis on highest values.*

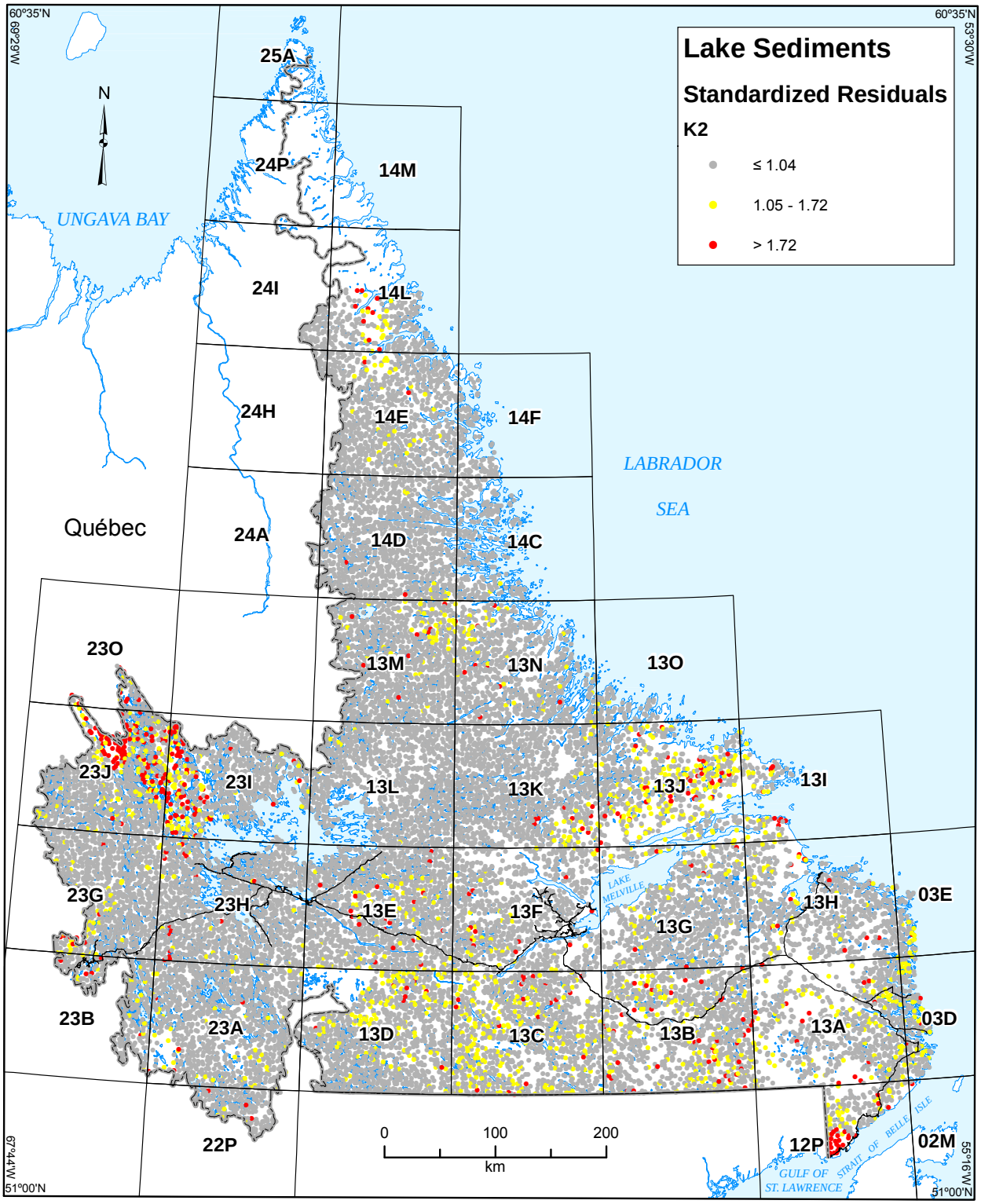


**Figure 16b.** *Standardized multiple-regression residuals of K2 in lake sediment, Labrador, with emphasis on highest values.*

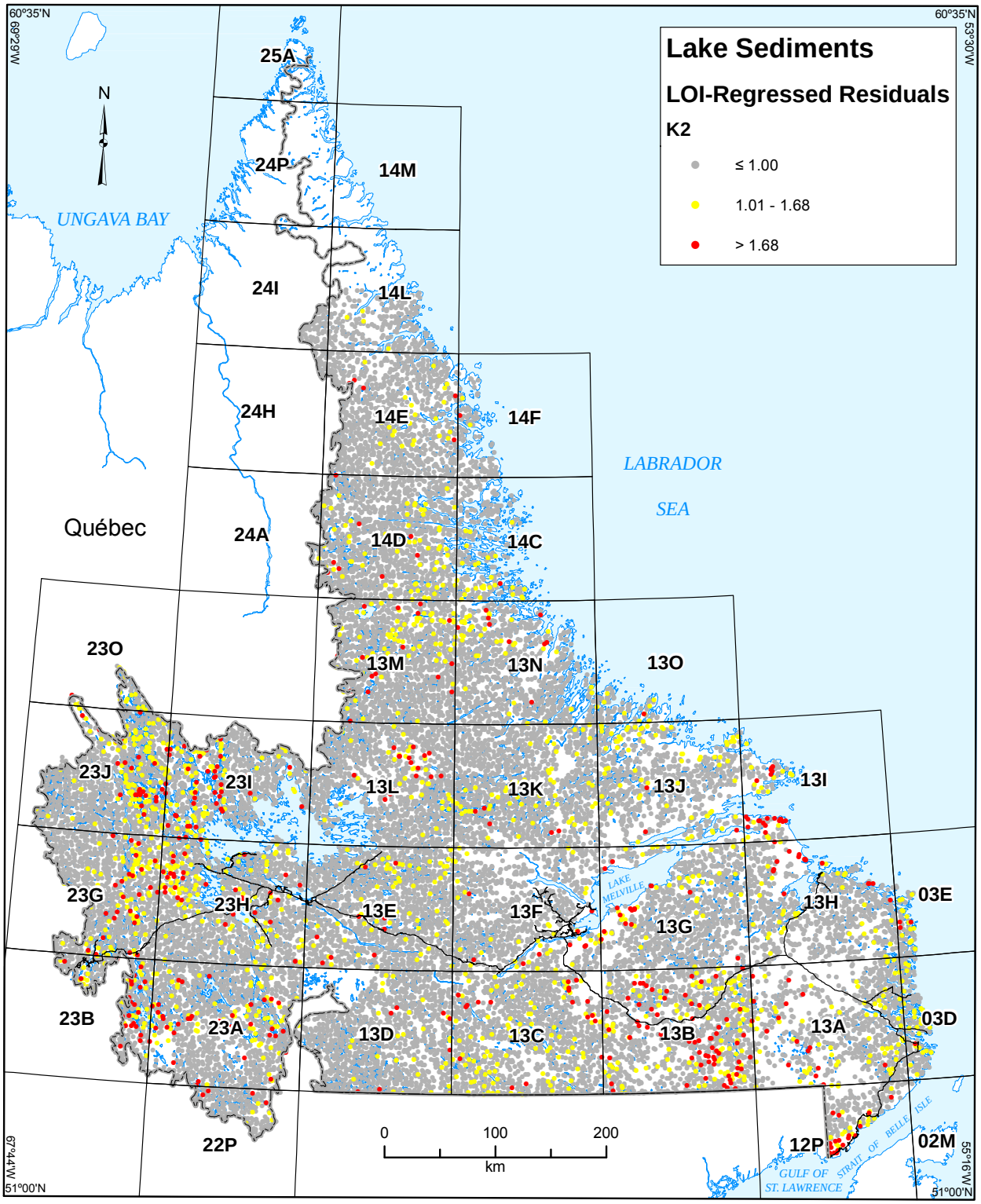


**Figure 16c.** *Standardized simple-regression residuals of K2 in lake sediment, Labrador, with emphasis on highest values.*

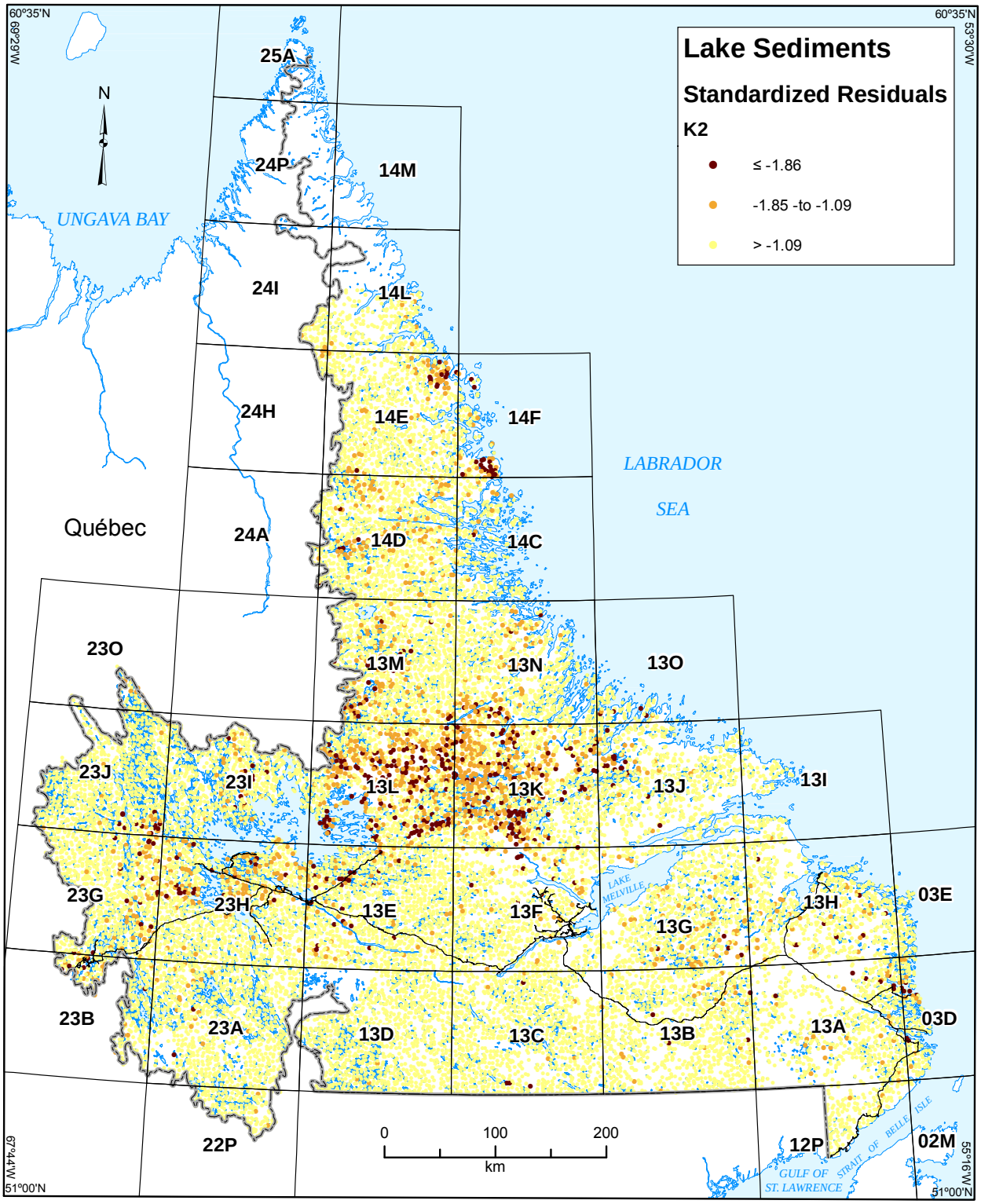


**Figure 16d.** *Standardized multiple-regression residuals of K2 in lake sediment, Labrador, with emphasis on lowest values.*

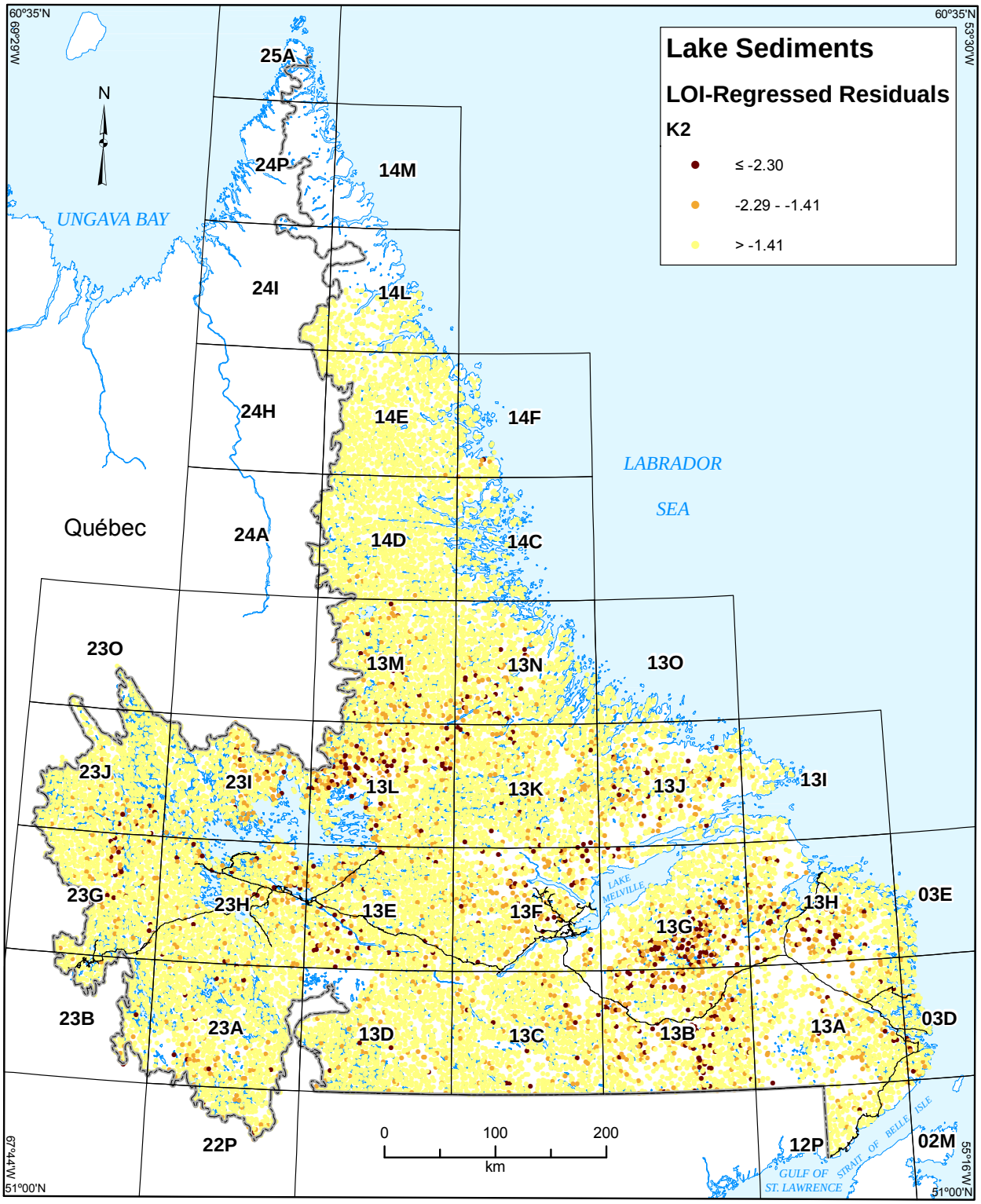


**Figure 16e.** *Standardized simple-regression residuals of K2 in lake sediment, Labrador, with emphasis on lowest values.*

In western Labrador, anomalously high multiple-regression residuals of K2 (Figure 16b) are present over a diverse package of Kaniapiskau Supergroup rocks (argillaceous rocks of the Le Fer and Dolly formations, dolomite of the Denault Formation, chert breccia of the Fleming Formation, arenaceous rocks of the Wishart Formation, basalt of the Nimish Formation, and iron formation of the Sokoman Formation; Wardle, 1982b) in NTS map areas 23I/04, 05, 12 and 13; and on 23J/08–14and 23J/16; multiple-regression residuals of Ba2 are anomalously low in the same area (Figure 14d). In common with the behaviour of many other elements in many other features, the overall response of LOI-regression K2 residuals (Figure 16c) is similar to that displayed by the multiple-regression residuals, but more 'noisy'.

An anomaly defined by high K2 multiple-regression residuals, and to a lesser extent by LOI-regression residuals, is also present in the extreme southeastern corner of Labrador, in NTS map areas 12P/06, 07, 10 and 11, over Neoproterozoic or Cambrian sediments (Units CFo, CBr) and older granitic rocks (Unit PMgr). A more areally extensive anomaly is defined by multiple-regression residuals of Hf1 (Figure 15b).

Anomalously low multiple-regression residuals of K2 (Figure 16d) are present in samples covering most of NTS map areas 13L and 13M; the underlying geology is extremely diverse (Wardle *et al.*, 1997). More areally restricted K2 residual lows are present over the Kiglapait troctolite intrusion in NTS map areas 14F/03 and 04 (this zone corresponds to an Na2 multiple-regression residual high (Figure 19b, as well as separate zones of high multiple-regression residuals of Mg2, Figure 18b; and Sc2, Figure 22b); over Archean granite gneiss, paragneiss and metamorphosed mafic intrusive rocks in NTS 14E/16 (Ryan, 1990), and over Archean and/or Paleoproterozoic gneiss southeast of the Mistastin batholith on NTS 13M/06 and 07. All of these zones are absent from the LOI-regression residuals, which only define a K2 low in NTS map areas 13G/02 and 13G/07, coincident with LOI-regression residual lows of all other elements under consideration (Figure 16e).

*Lithium (Li2)*

Raw lithium values (Figure 17a) are anomalously high over multiple units of the Kaniapiskau Supergroup in NTS map areas 23J/08, 09, 10, 15 and 16, and 23O/01, 02 and 07, and in the extreme north in NTS map areas 14E/16 (over Archean granite gneiss, paragneiss and metamorphosed mafic intrusive rocks), in NTS 14L/02, 06 and 07 over early Archean high-grade metamorphic rocks of the Nain Province, and in NTS 24H/16 and 24I/01 over granites and gneisses of the Southeast Churchill Province (Wardle *et al.*, 1997).

Multiple-regression residuals (Figure 17b) present a very different picture; the anomalies displayed by raw values are largely neutralized, but two concentrations of strongly anomalous samples are present in NTS map areas 13L/11–14, and 23I/08–10. In the former case, the underlying rock type consists primarily of Archean granite and gneiss, although a circular intrusion of syenogranite named the "13L Intrusion" by McConnell (1988) and the "Lac Ramusio pluton" by Nunn (1995), most of which is situated on the Québec side of the border, is situated at the northeastern extremity of the anomaly. The anomaly in NTS map area 23I is associated with two other intrusions: the Michikamats Intrusion to the southwest, and the Signal Hill intrusion, straddling the Labrador-Québec border, to the northeast. The significance of these two anomalous features,

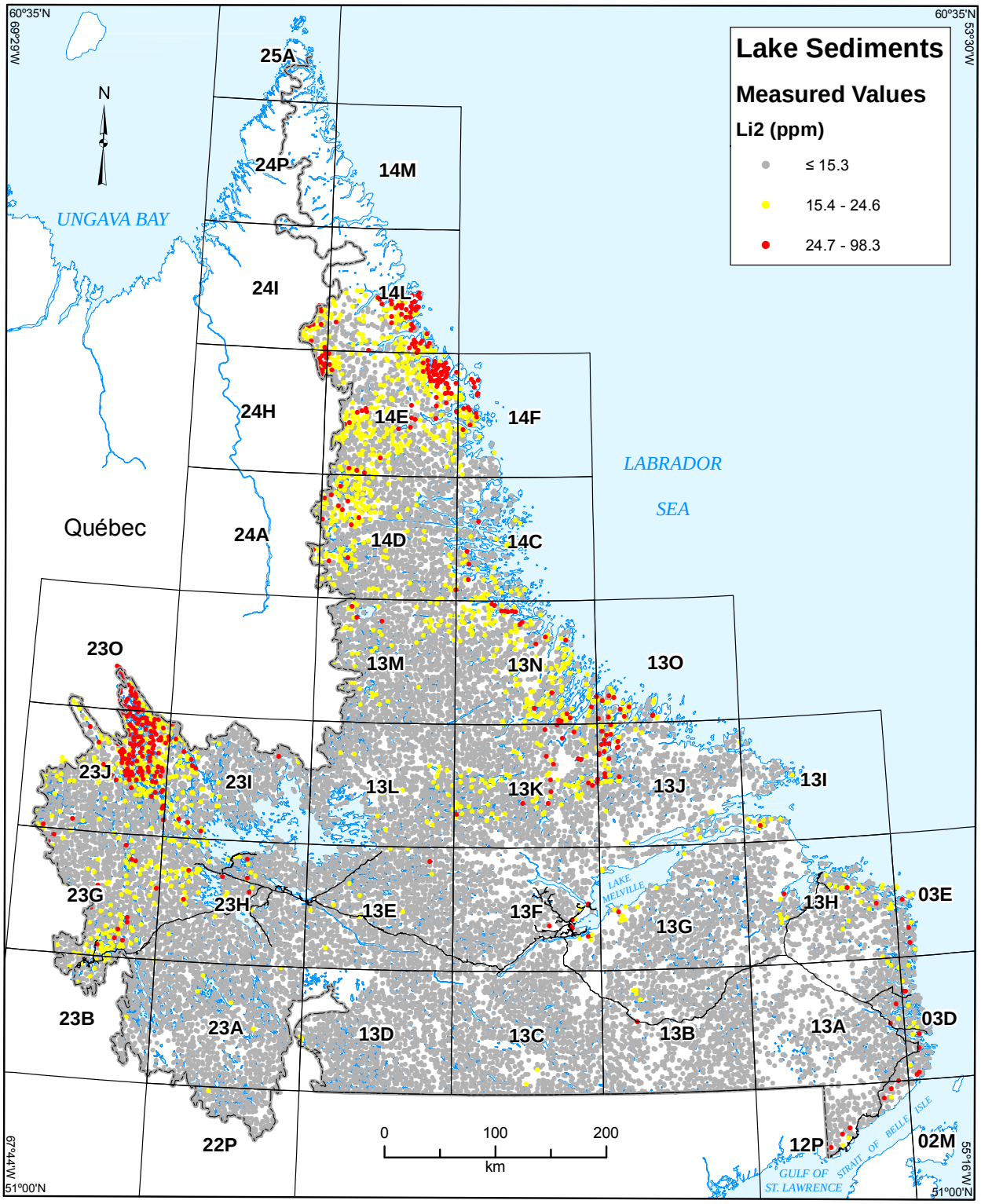


**Figure 17a.** *Measured values of Li2 in lake sediment, Labrador, with emphasis on highest values.*

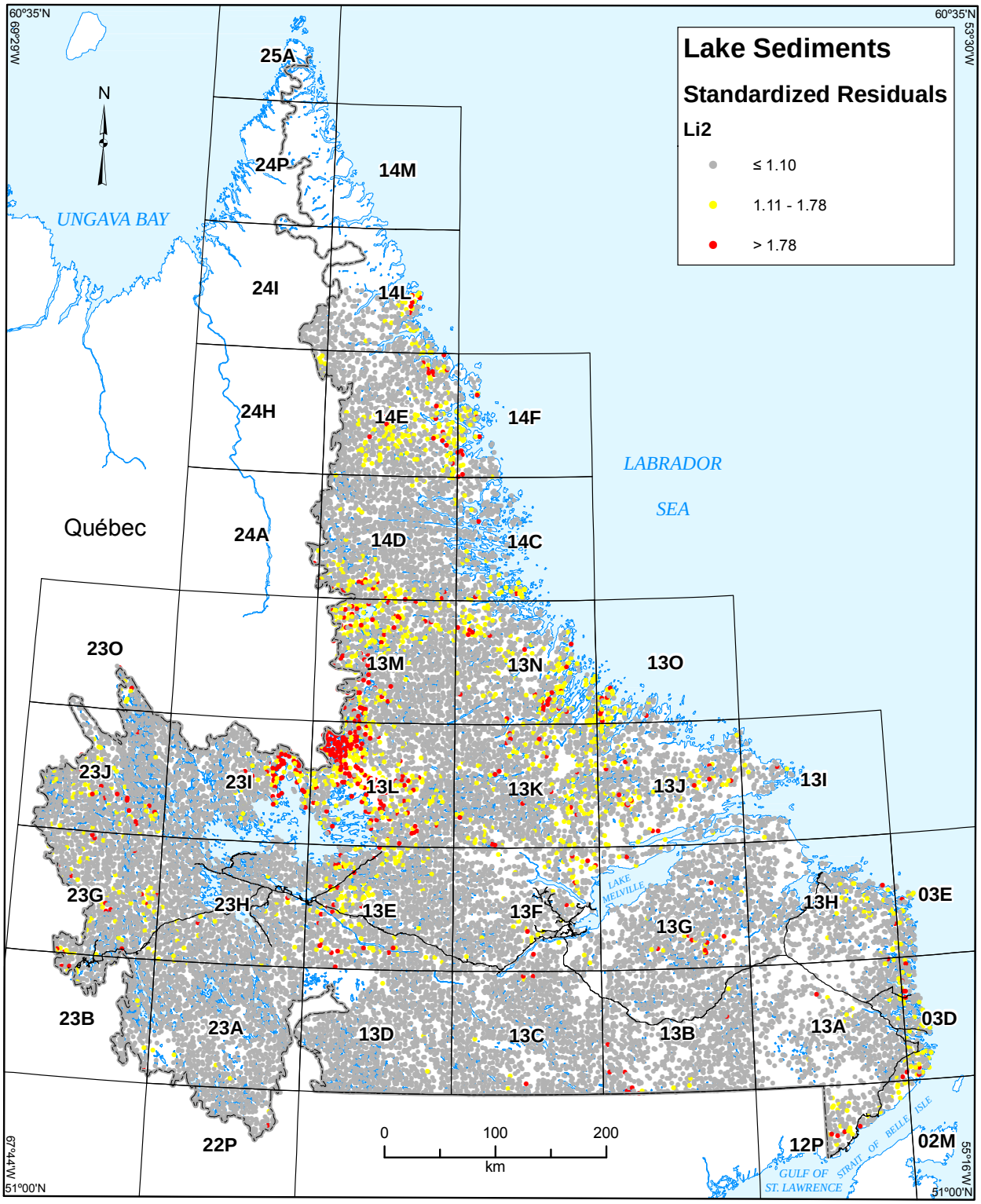


**Figure 17b.** *Standardized multiple-regression residuals of Li2 in lake sediment, Labrador, with emphasis on highest values.*

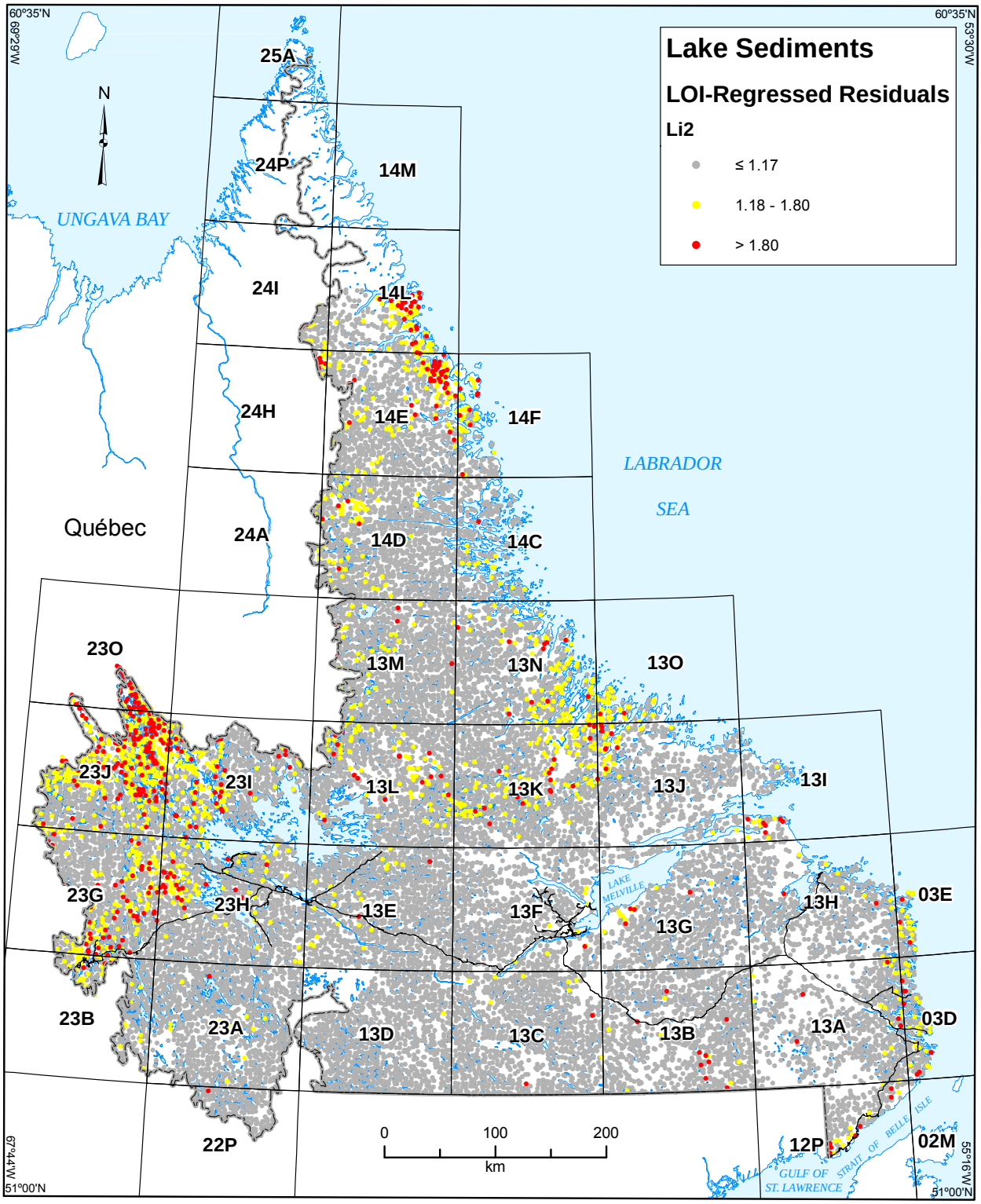


**Figure 17c.** *Standardized simple-regression residuals of Li2 in lake sediment, Labrador, with emphasis on highest values.*

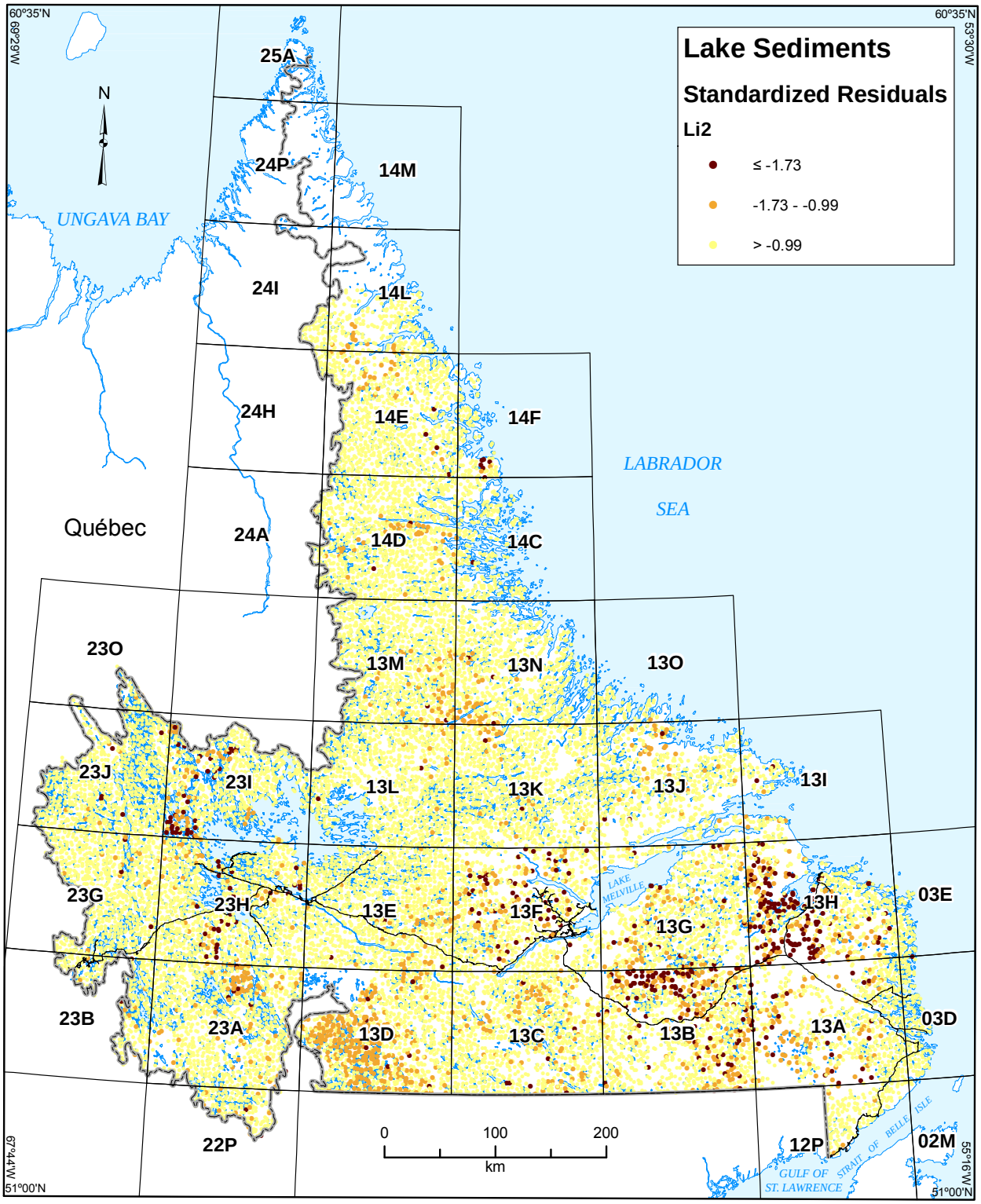


**Figure 17d.** *Standardized multiple-regression residuals of Li2 in lake sediment, Labrador, with emphasis on lowest values.*

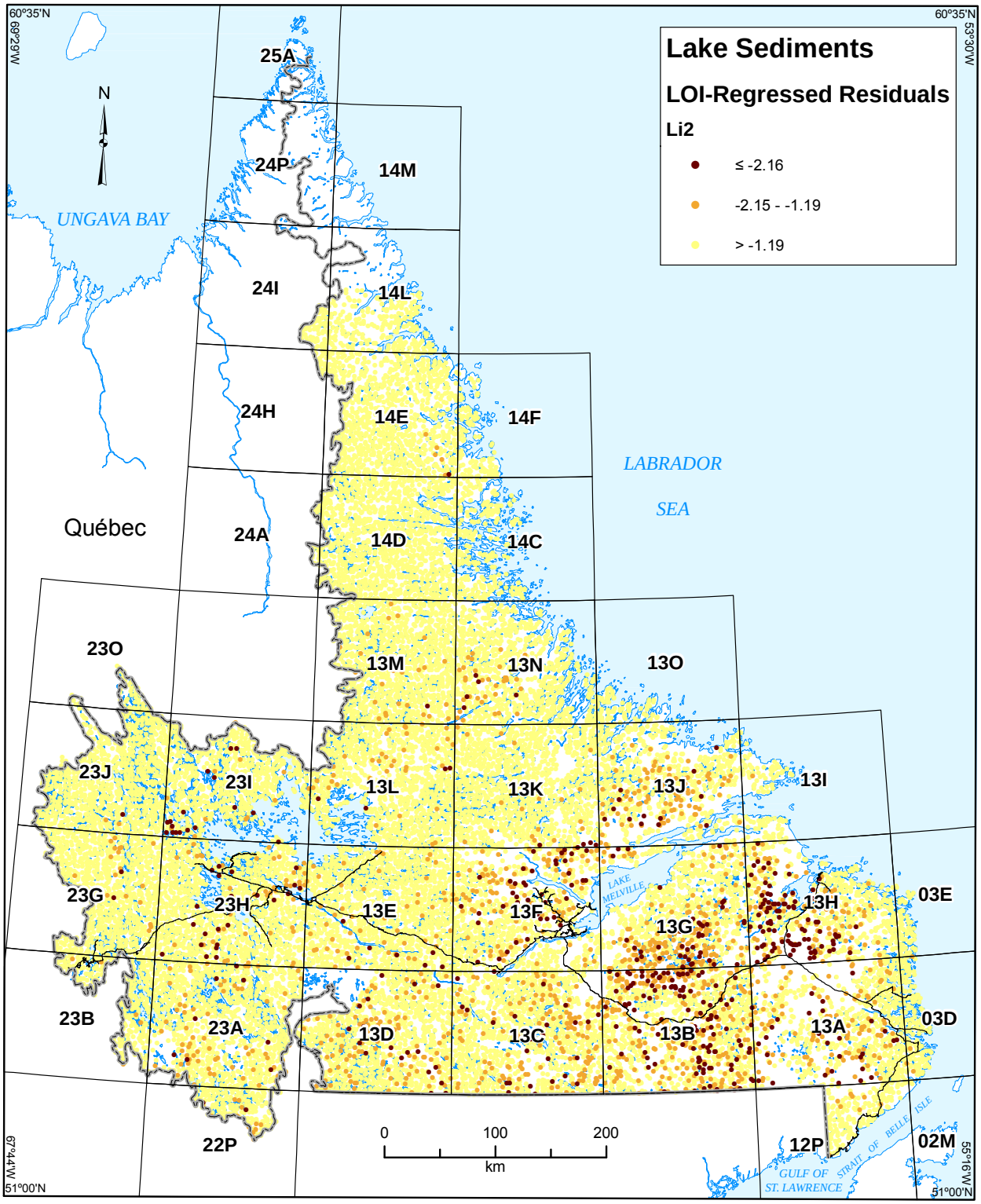


**Figure 17e.** *Standardized simple-regression residuals of Li2 in lake sediment, Labrador, with emphasis on lowest values.*

collectively named the *Thompson Lake/Michikamats anomaly*, will be discussed further, in the light of other indications of mineralization, in a later section.

A more diffuse Li2 multiple-regression residual anomaly, almost completely absent in raw values, is present over the Mistastin Batholith in NTS map areas 13M/11–14.

Both of the above features are absent from the LOI-regression residuals, which have more in common with the raw values, albeit in a dilute form (Figure 17c).

Conspicuous anomalously low multiple-regression residuals of Li2 are concentrated in NTS map area 23I/04, probably associated with the Menihek Formation; over Grenvillian granites and gneisses in NTS 13B/13–15; and over diverse Grenvillian intrusive and supracrustal units in NTS 13H/03–6, 11–13 (Figure 17d). The latter two features are also manifested in the LOI-regression residuals (Figure 17e).

*Magnesium (Mg2)*

Anomalous raw Mg2 values are concentrated in northern Labrador (NTS map areas 14E/09, 15 and 16; 14L/02, 06 and 07; 14E/13; 24H/16 and 24I/08; Figure 18a), over gneissic rocks (*cf.* Li2, Figure 17a) as well as over the Kiglapait Intrusion in NTS map areas 14F/03 and 14F/04.

High multiple-regression residuals of Mg2 (Figure 18b) persist over the Kiglapait Intrusion although they are restricted to the northwest, in NTS map area 14F/04; the zone they define lies within a larger area defined by anomalously high multiple-regression residuals of Na2 (Figure 19b), and anomalously low multiple-regression residuals of K2 (Figure 16d), but is both spatially distinct from an area defined by high multiple-regression Sc2 residuals (Figure 22b) and itself characterized by anomalously low Sc2 multiple-regression residuals (Figure 22d). According to Morse (1969), this high-Mg zone is underlain by the Lower Zone of troctolite, which also includes dunite and leucotroctolite. High multiple-regression residuals of Mg2 also delineate the previously documented (McConnell and Batterson, 1987) dispersion train from the REE-RM mineralization at Strange Lake in NTS map areas 14D/05, 6 and 10. Magnesium enrichment is a characteristic of the mineralization at Strange Lake that is not known to have been recognized previously. In common with features defined by anomalously high multiple-regression residuals of Al2 (Figure 13b), and anomalously low multiple-regression residuals of Sc2 (Figure 22d), the east-central portion of the Harp Lake Intrusive Suite (NTS map areas 13K/13 and 14, 13L/15 and 16, 13M/01–04), but not the northern, western or southern portions, have a distinct signature in Mg2 residuals. Anomalies over the Kaniapiskau Supergroup in the Labrador Trough of western Labrador (*e.g.,* those in NTS map areas 23I/04, and 23J/10 and 15) may be related to the presence of dolomite of the Denault Formation in the succession (Wardle, 1982a, b).

The anomaly defined by high Mg2 multiple-regression residuals in NTS map area 23I/11 may be derived from gabbro (Unit 29, James, 1994a; Unit $P_2$g, Wardle *et al.,* 1997). Other anomalies are present in NTS map areas 23B/14 and 15 and 23G/02 overlapping and extending beyond the Bondurant Lake anomaly, as defined by Ba2 residuals (see above); and in NTS 23A/15, possibly associated with slivers of Grenville amphibolitic and mafic-granulitic gneiss (Unit $P_3$mgn) within pelitic gneiss (Unit $P_3$sgn; Wardle *et al.*, 1997).

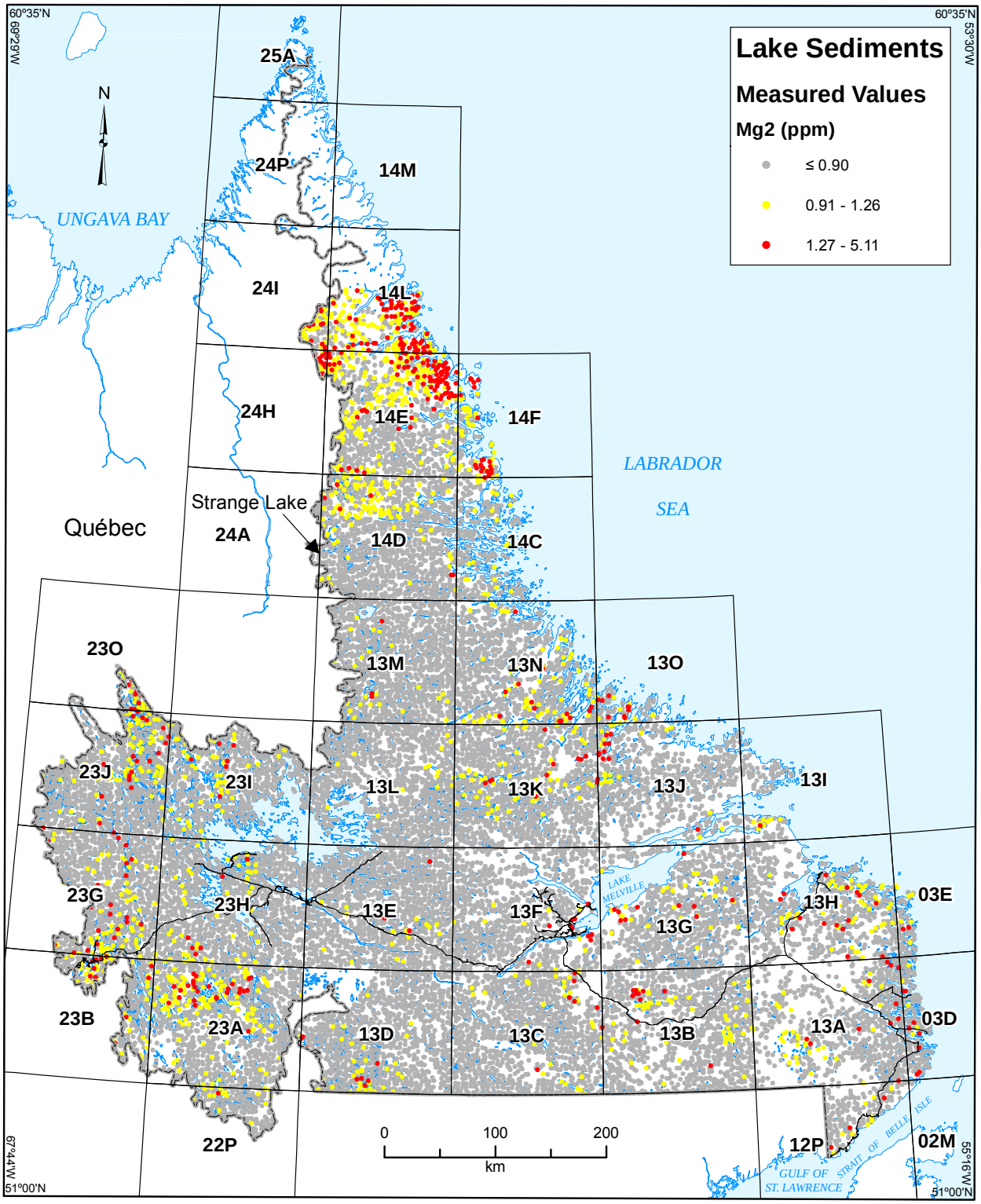


**Figure 18a.** *Measured values of Mg2 in lake sediment, Labrador, with emphasis on highest values.*

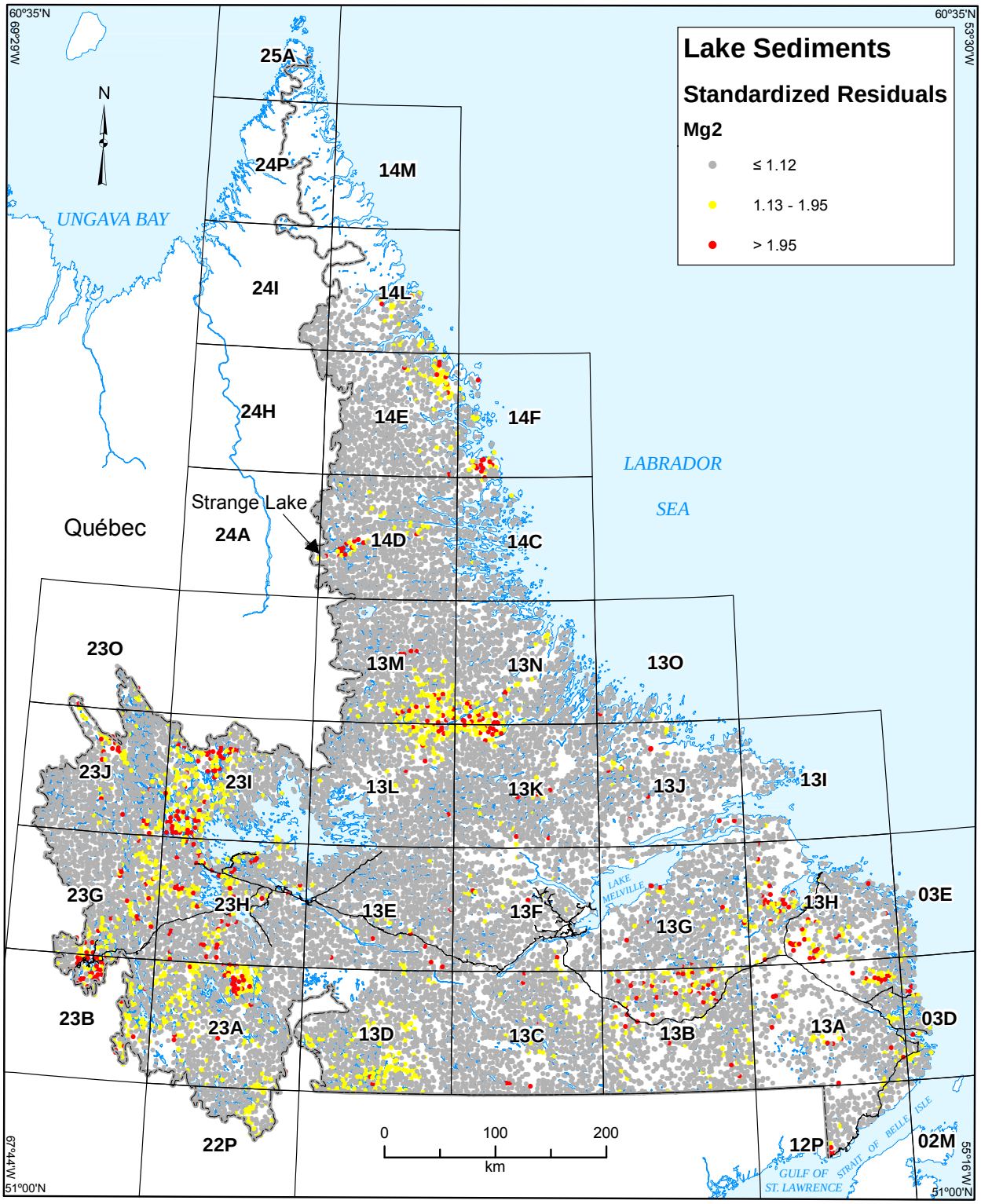


**Figure 18b.** *Standardized multiple-regression residuals of Mg2 in lake sediment, Labrador, with emphasis on highest values.*

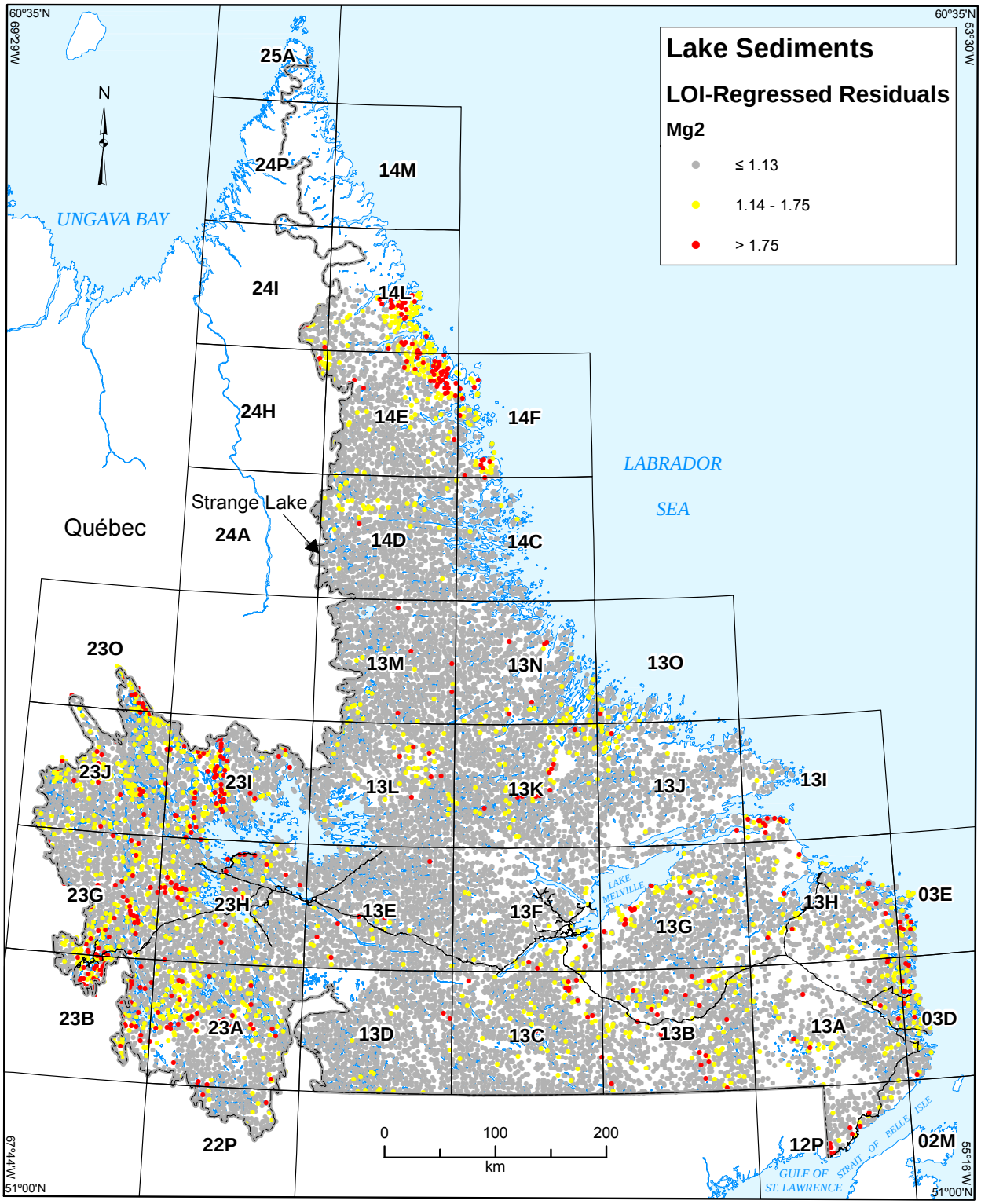


**Figure 18c.** *Standardized simple-regression residuals of Mg2 in lake sediment, Labrador, with emphasis on highest values.*

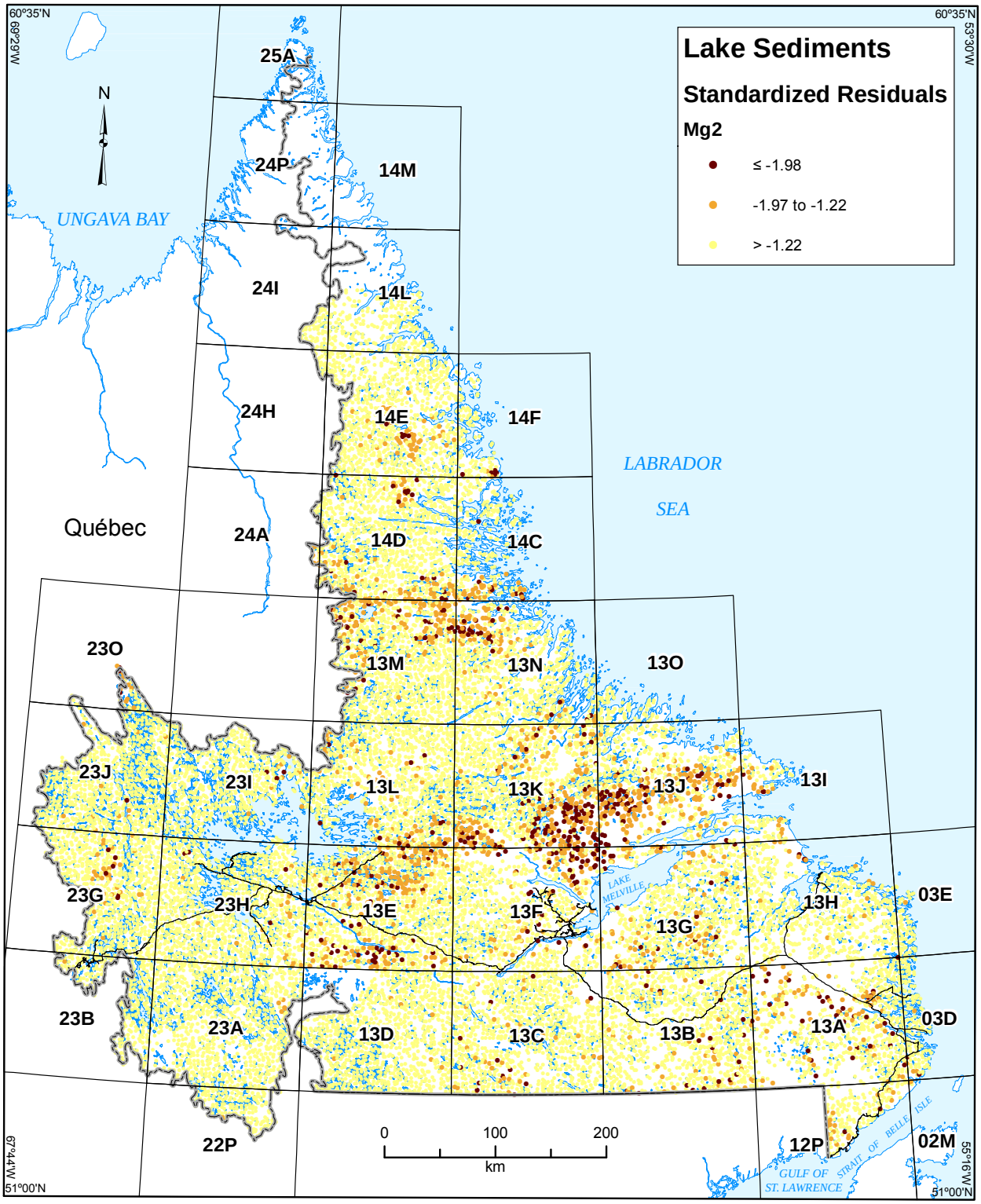


**Figure 18d.** *Standardized multiple-regression residuals of Mg2 in lake sediment, Labrador, with emphasis on lowest values.*

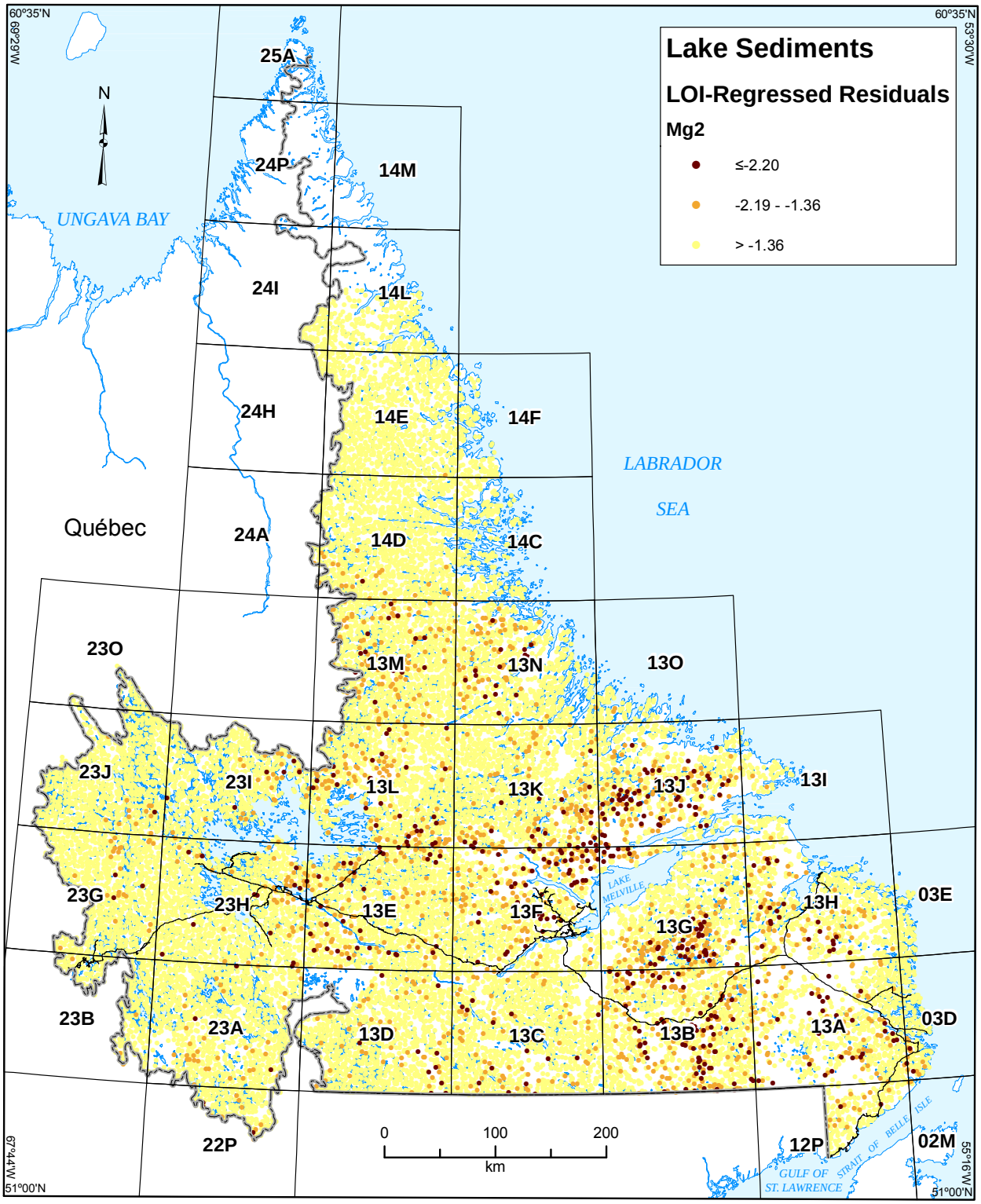


**Figure 18e.** *Standardized simple-regression residuals of Mg2 in lake sediment, Labrador, with emphasis on lowest values.*

In common with several other elements, the features defined by high LOI-regression Mg2 residuals (Figure 18c) have more in common with those defined by the raw values, than with their multiple-regression counterparts. In particular, they do not define the dispersion train from Strange Lake.

Anomalously low multiple-regression residuals of Mg2 (Figure 18d) are associated with granitic (Unit $P_3$gr) and gneissic (Unit $P_3$gdn) rocks in the eastern part of the Central Mineral Belt in NTS map areas 13F/15 and 16, 13J/04–11, and 13K/07 and 08 (a feature also defined by LOI-regression residuals; Figure 18e), and northwest of the Flowers River complex (Hill, 1982) on NTS 13M/09 and 16; and 13N/11–14; 14C/03 and 04; and 14D/01 and 02. This latter feature is not defined by LOI-regression residuals.

*Sodium (Na2)*

Anomalously high raw values of Na2 do not form well-defined features, with the exception of concentrations in the north over gneissic rocks in NTS map areas 14D/13–16 and 14E/01–08 (Figure 19a). The coincidence of these features with anomalous Mg2 and Li2 suggests that all are an artefact of the clastic component of the sediments. Anomalously high Na2 multiple-regression residuals (Figure 19b) are also rather widely dispersed, although there is a concentration of mostly elevated (as opposed to anomalous) values in NTS map areas 14E/03–06, over the northwestern part of the Umiakovik Lake batholith and the adjacent Archean gneiss (Ryan, 1990).

There is also, interestingly, a concentration of high Na2 multiple-regression residuals over the Kiglapait Intrusion in NTS map areas 14F/03 and 04; K2 multiple-regression residuals are depleted and anomalously low in the same samples (Figure 10e), which overlie the intrusion's Upper Gabbroic Zone, and the Lower Zone of troctolite, including dunite and leucotroctolite (Morse, 1969). The LOI-regression residuals (Figure 19c) do not define either of these features.

There are several concentrations of anomalously low Na2 multiple-regression residuals in western Labrador (Figure 19d). In NTS map areas 23B/14, 23G/02 and 23G/03, such samples were collected over Archean gneisses and migmatites of the Ashuanipi Complex (James, 1993), although low Na2 does not characterize the entire complex, as exposed in Labrador.

In NTS map areas 23J/10 and 23J/15, the zone of apparent Na2 depletion coincides closely with a multiple-regression residual high of K2 (Figure 16b), and over a diverse package of rocks of the Kaniapiskau Supergroup. In NTS map areas 13E/03–06, the Na2 low overlies granulite-facies Grenvillian metasediment (Wardle, 1994). Finally, the Neoproterozoic–Cambrian sediments in the extreme southeast of Labrador are characterized by anomalously low Na2 multiple-regression residuals; the low does not extend onto the granitic rocks to the north (*cf.* Hf1, K2).

There are no features by LOI-regression Na2 residuals, with the exception of a feature in NTS map areas 13G/02 and 13G/07, defined by residuals of all other elements and described previously (Figure 19e).

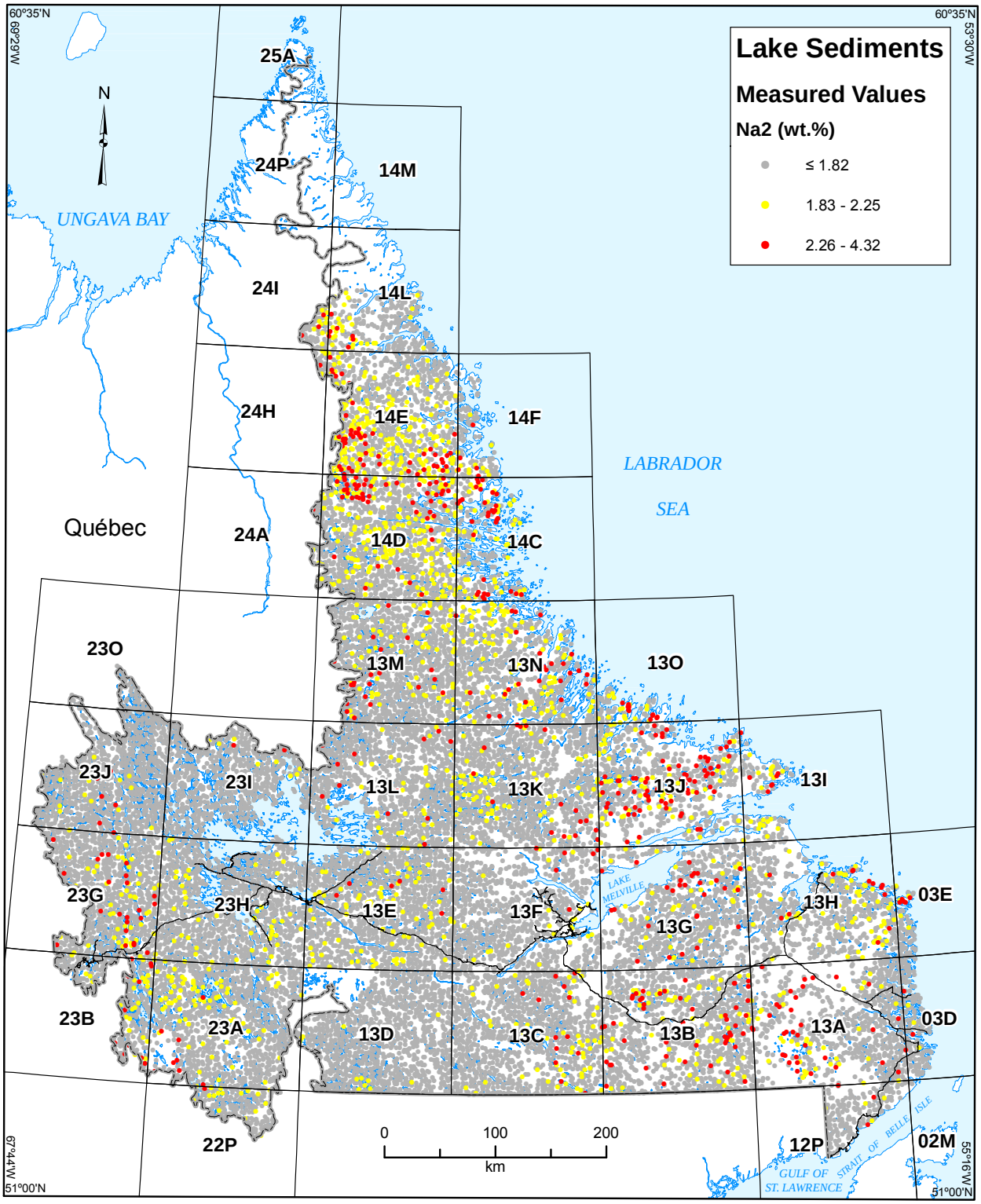


**Figure 19a.** *Measured values of Na2 in lake sediment, Labrador, with emphasis on highest values.*

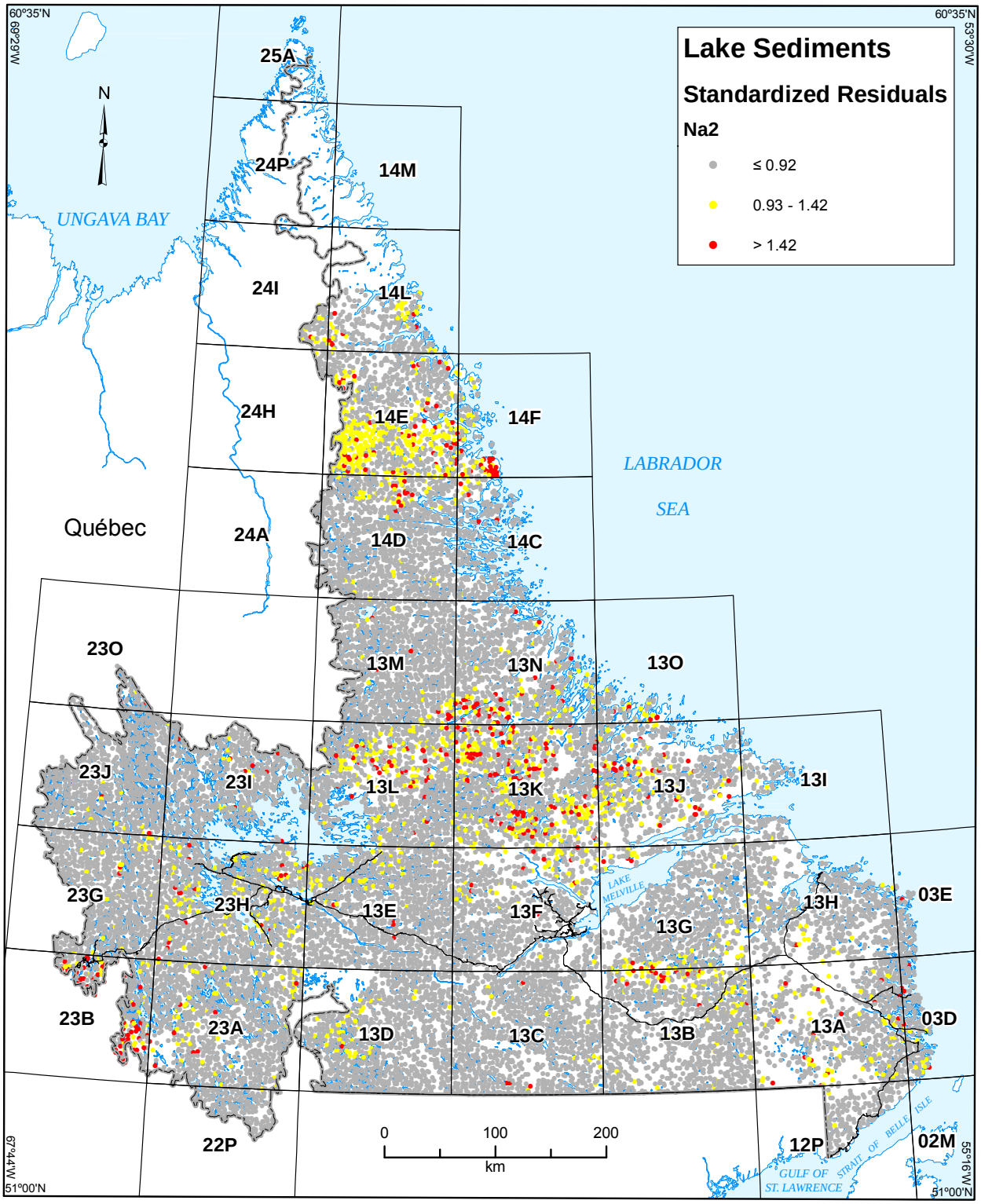


**Figure 19b.** *Standardized multiple-regression residuals of Na2 in lake sediment, Labrador, with emphasis on highest values.*

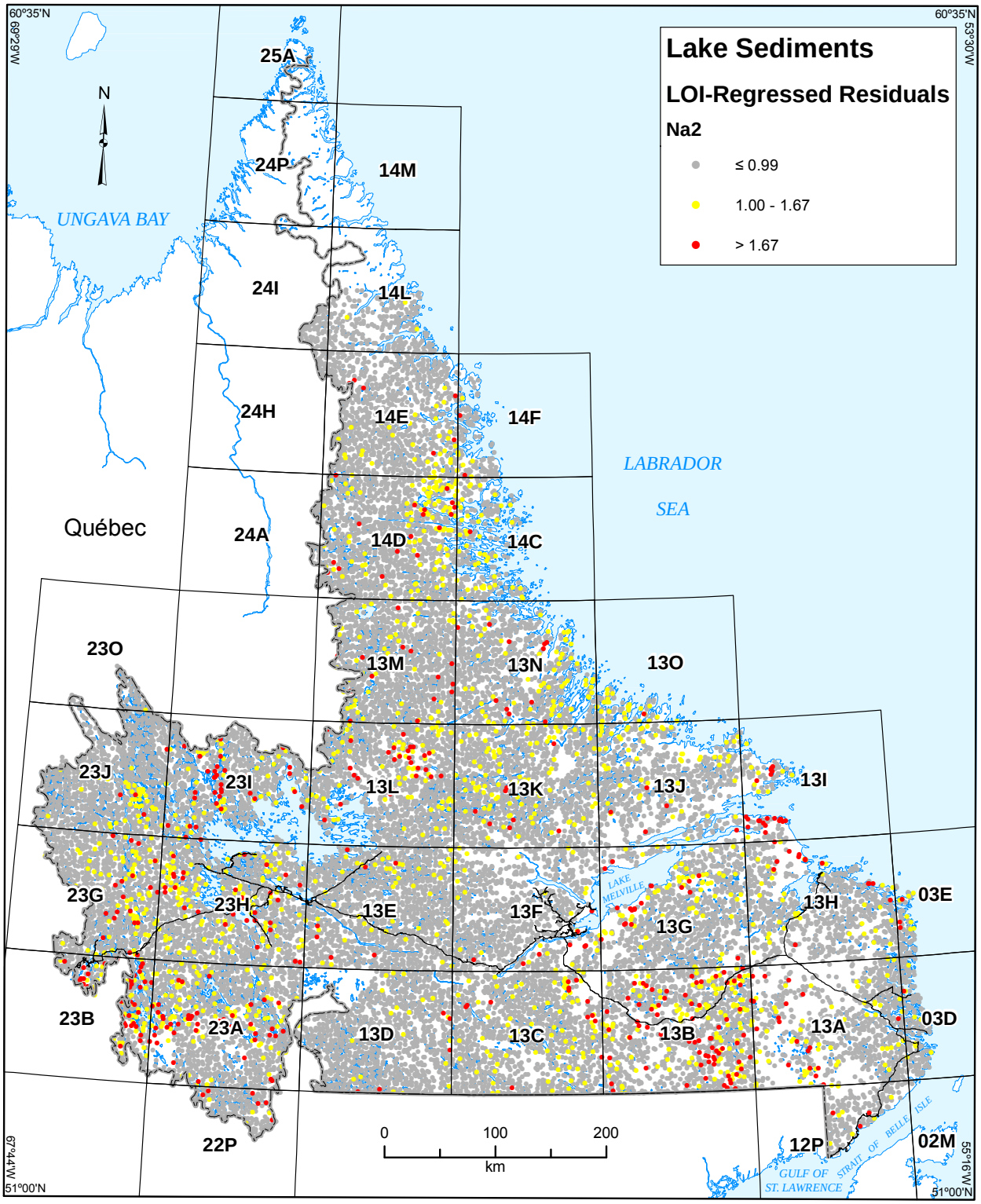


**Figure 19c.** *Standardized simple-regression residuals of Na2 in lake sediment, Labrador, with emphasis on highest values.*

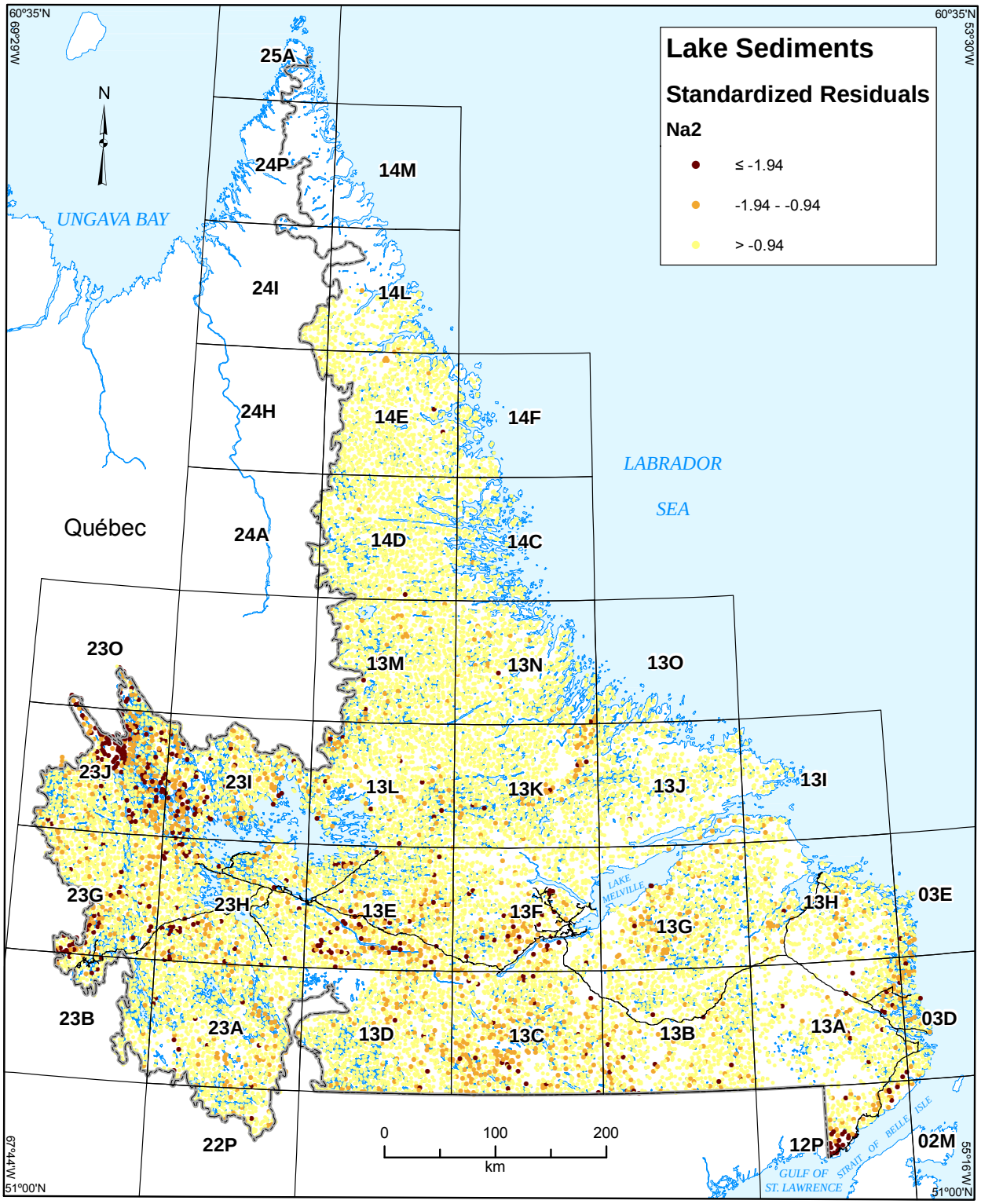


**Figure 19d.** *Standardized multiple-regression residuals of Na2 in lake sediment, Labrador, with emphasis on lowest values.*

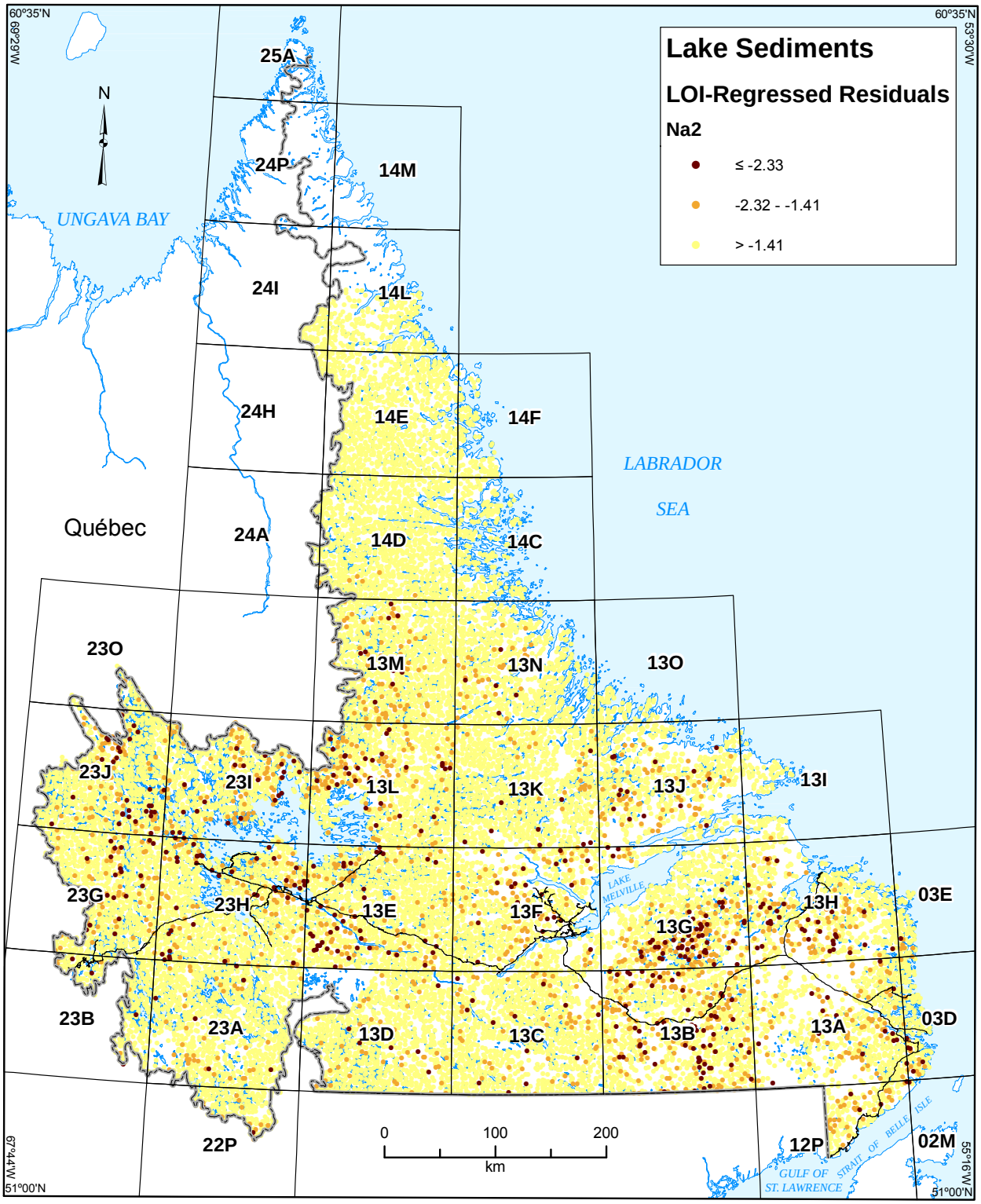


**Figure 19e.** *Standardized simple-regression residuals of Na2 in lake sediment, Labrador, with emphasis on lowest values.*

*Niobium (Nb2)*

The dispersion train from the Strange Lake deposit is equally apparent in both raw values (Figure 20a) and standardized multiple-regression residuals (Figure 20b) of Nb2. Anomalous raw Nb2 values also define a broad, arcuate zone in NTS map areas 13M/06, 9, 10, 11, 15 and 16; 13N/13–15; 14C/03 and 04; and 14D/01; a similar zone is defined by raw values of several other elements in the clastic (K–Na–Ti–Mg *etc*.) association.

Four features emerge in the multiple-regression residuals that are not apparent, or not as strong and extensive, in the raw values. In northern Labrador, accumulations of anomalous Nb2 residuals are present south of Mistastin Lake in NTS map areas 13M/03, 05, 06, 10, 11 and 13, over the Mistastin batholith and gneissic country rock; and in NTS 13N/10, 14 and 15, to the east and north of the Flowers River alkaline complex, apparently in response to the annulus of cumulate-zone gabbro surrounding the complex (Unit 14c; Hill, 1982);

In southeastern Labrador, anomalously high Nb2 multiple-regression residuals are present along the north shore of St. Lewis Sound, and over and to the northeast (possibly representing glacial dispersion) of the Chateau Pond granite (Unit PMgr, Gower, 2010c Gower *et al*., 1988) in southeastern Labrador (NTS map areas 13A/01, 08 and 03D/05). There is no Nb2 response to other nearby plutons of the same age.

Essentially, the features defined by positive residuals of both types (simple and multiple regression) are the same (Figure 20c).

Anomalously low or depleted Nb2 multiple-regression residuals define a vague northeastward-trending zone, extending from NTS map area 13L/08 to NTS 13K/14 and traversing a variety of geological domains (Figure 20d). They also define the Etagaulet Bay and Kennemich massifs, but not as well as the multiple-regression residuals of Al2 (high, Figure 13b) or of Sc2 (low, Figure 22d).

The corresponding LOI-regression residuals (Figure 20e) define the same low as all the other elements, in NTS map areas 13G/02 and 13G/07. An areally restricted but strong concentration of these residuals is present in NTS map areas 23I/10, 11, 14 and 15 and corresponds to the occurrence of the De Pas batholith (Unit $P_2$cg; Wardle *et al*., 1997). Multiple-regression residuals of Nb2 define neither this feature nor a similar, northward-trending feature at the eastern contact of the Ashuanipi Complex in NTS map area 23G/15.

*Rubidium (Rb1)*

Anomalous and/or elevated raw values of Rb1 (Figure 21a) form significant concentrations in western Labrador in NTS map areas 23J/07–10, 23J/15, 16 and 23H/12, both over clastic and chemical sediments of the Kaniapiskau Supergroup, of which the gneisses and schists of the Attikamagen Formation have the greatest exposure in the potential source area. The latter feature is also defined by anomalous Rb1 multiple-regression residuals (Figure 21b) in NTS map area 13J/12; anomalous values concentrate over Grenvillian granite (Unit $P_3$gr) and amphibolite (Unit $M_1$ga; Wardle *et al.*, 1997). There are also a few concentrations of anomalous raw values in NTS

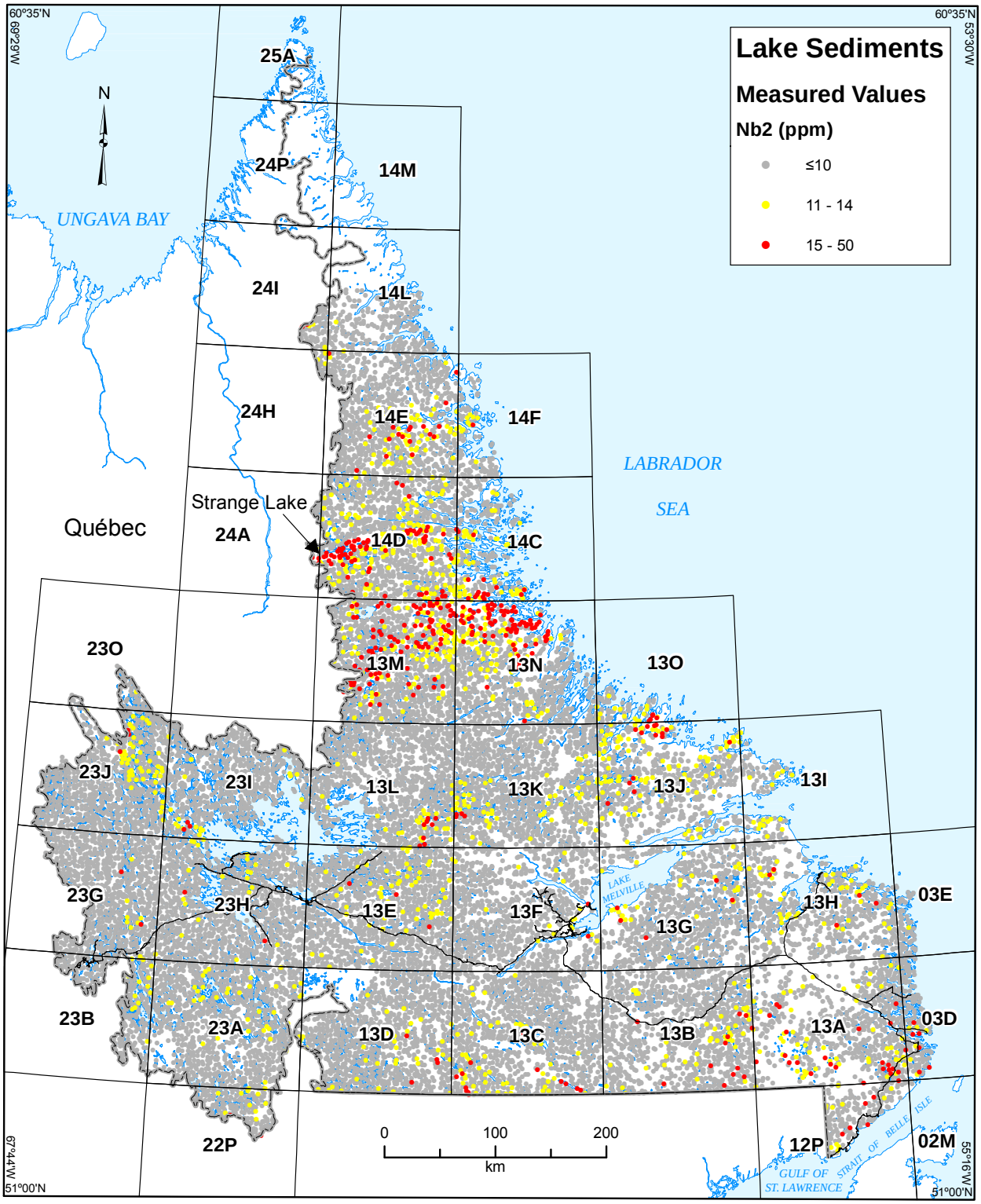


**Figure 20a.** *Measured values of Nb2 in lake sediment, Labrador, with emphasis on highest values.*

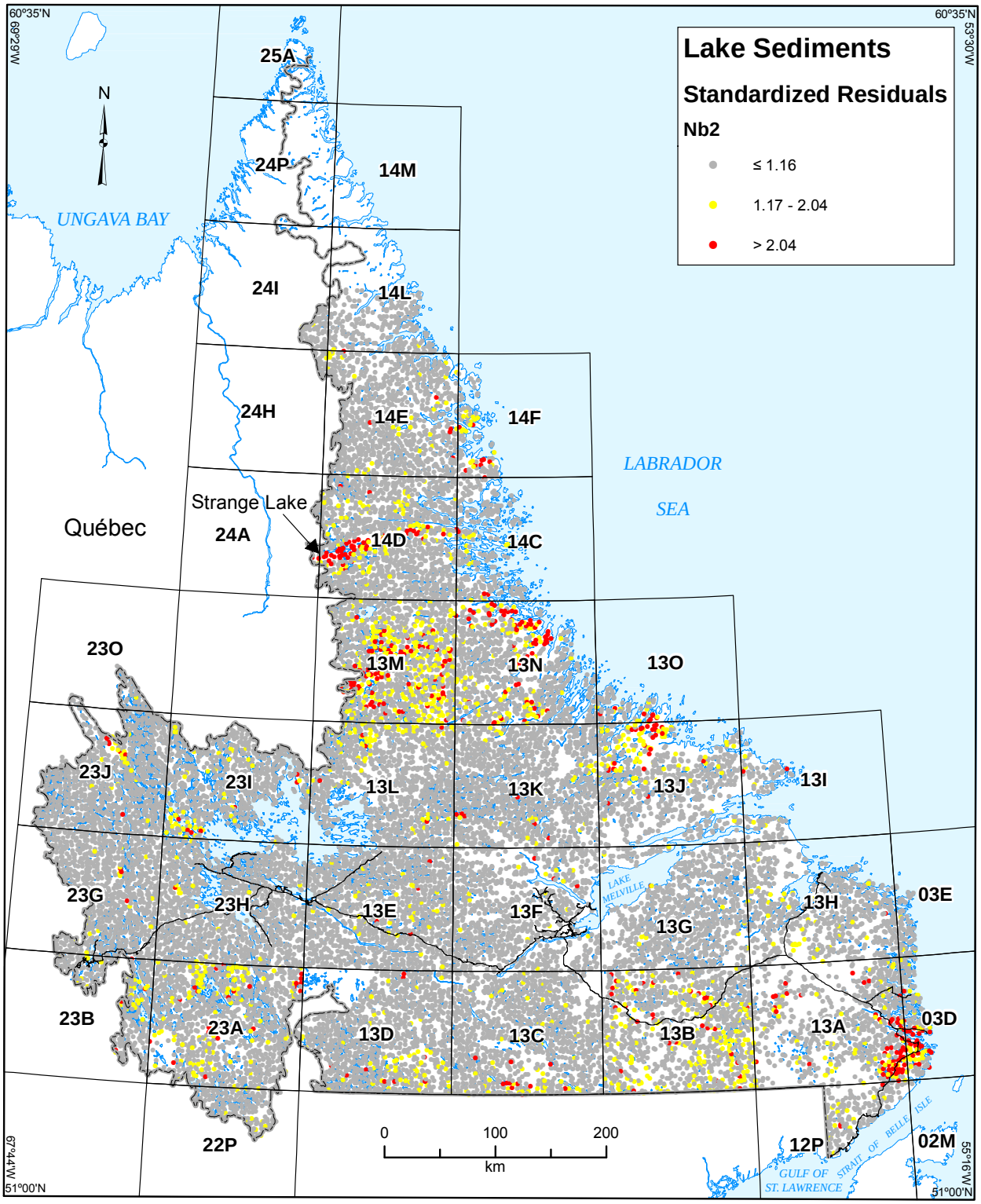


**Figure 20b.** *Standardized multiple-regression residuals of Nb2 in lake sediment, Labrador, with emphasis on highest values.*

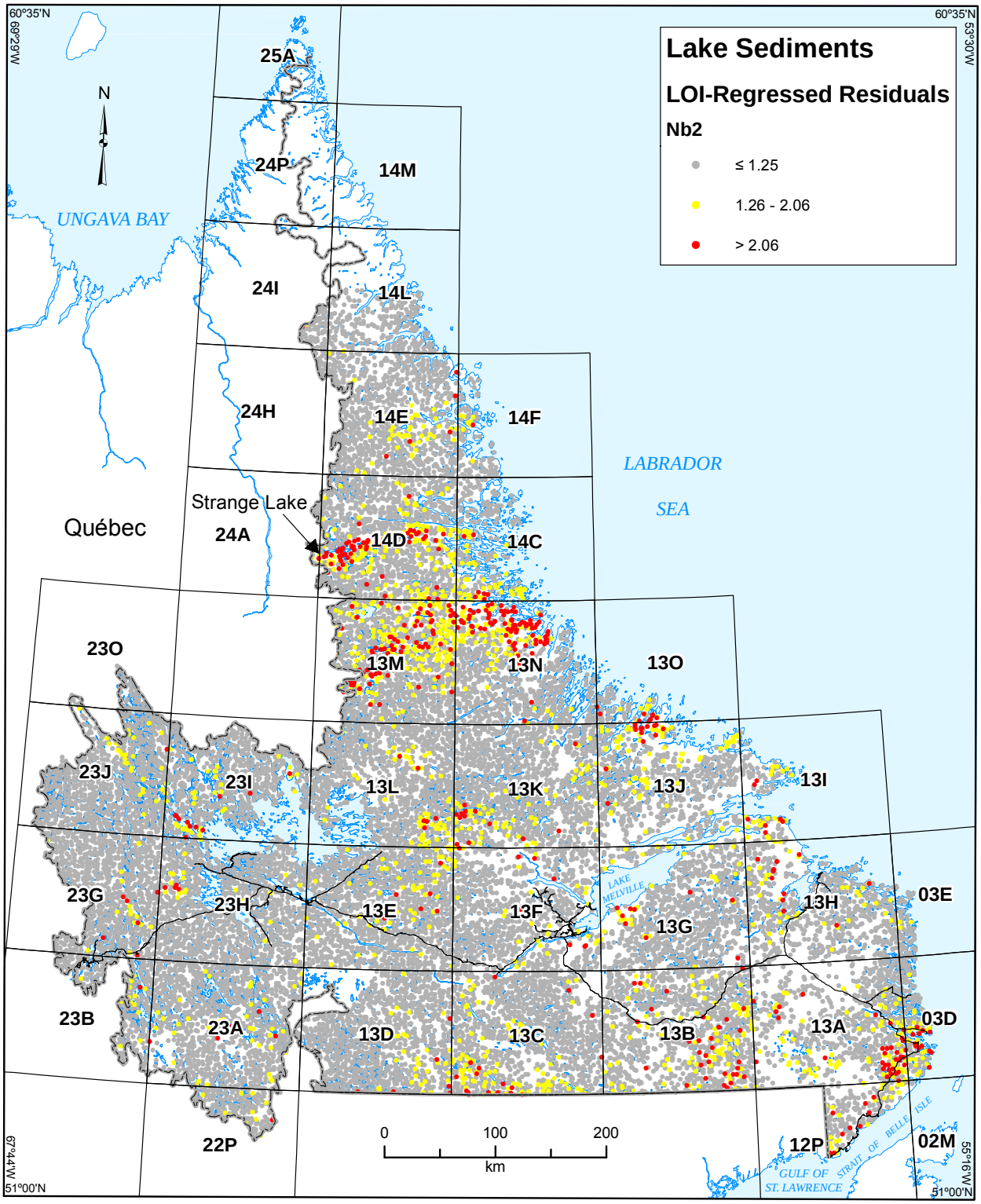


**Figure 20c.** *Standardized simple-regression residuals of Nb2 in lake sediment, Labrador, with emphasis on highest values.*

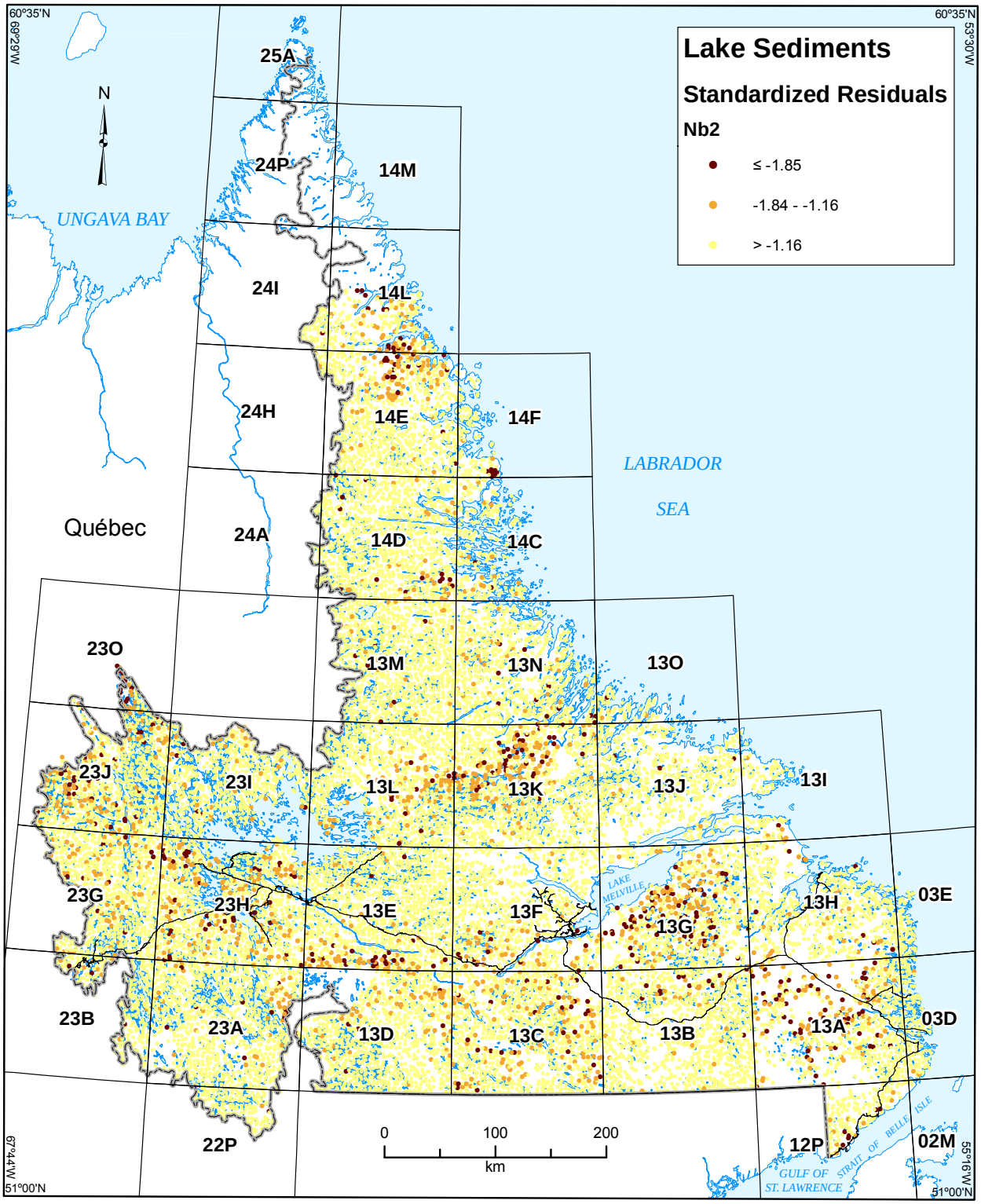


**Figure 20d.** *Standardized multiple-regression residuals of Nb2 in lake sediment, Labrador, with emphasis on lowest values.*

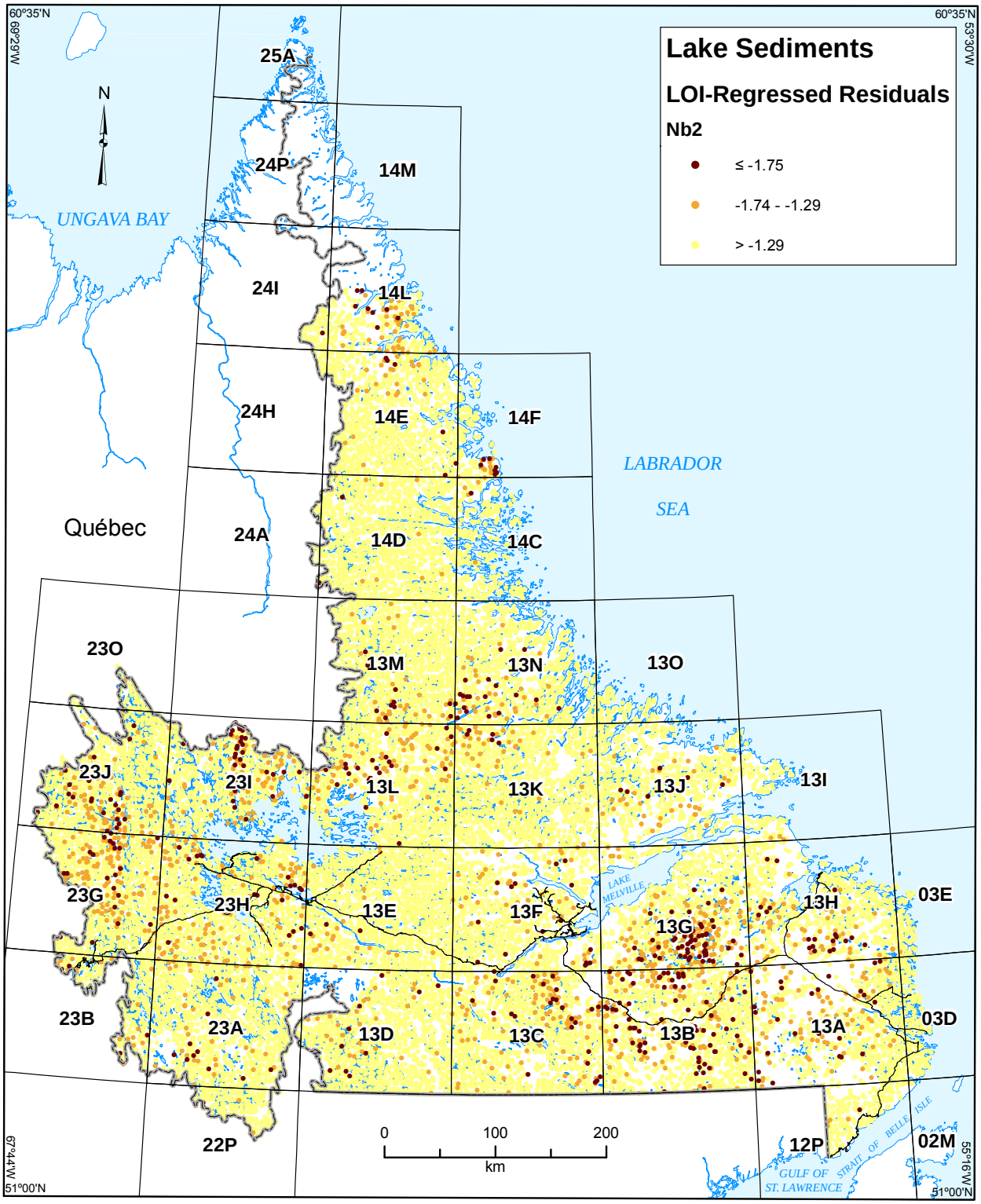


**Figure 20e.** *Standardized simple-regression residuals of Nb2 in lake sediment, Labrador, with emphasis on lowest values.*

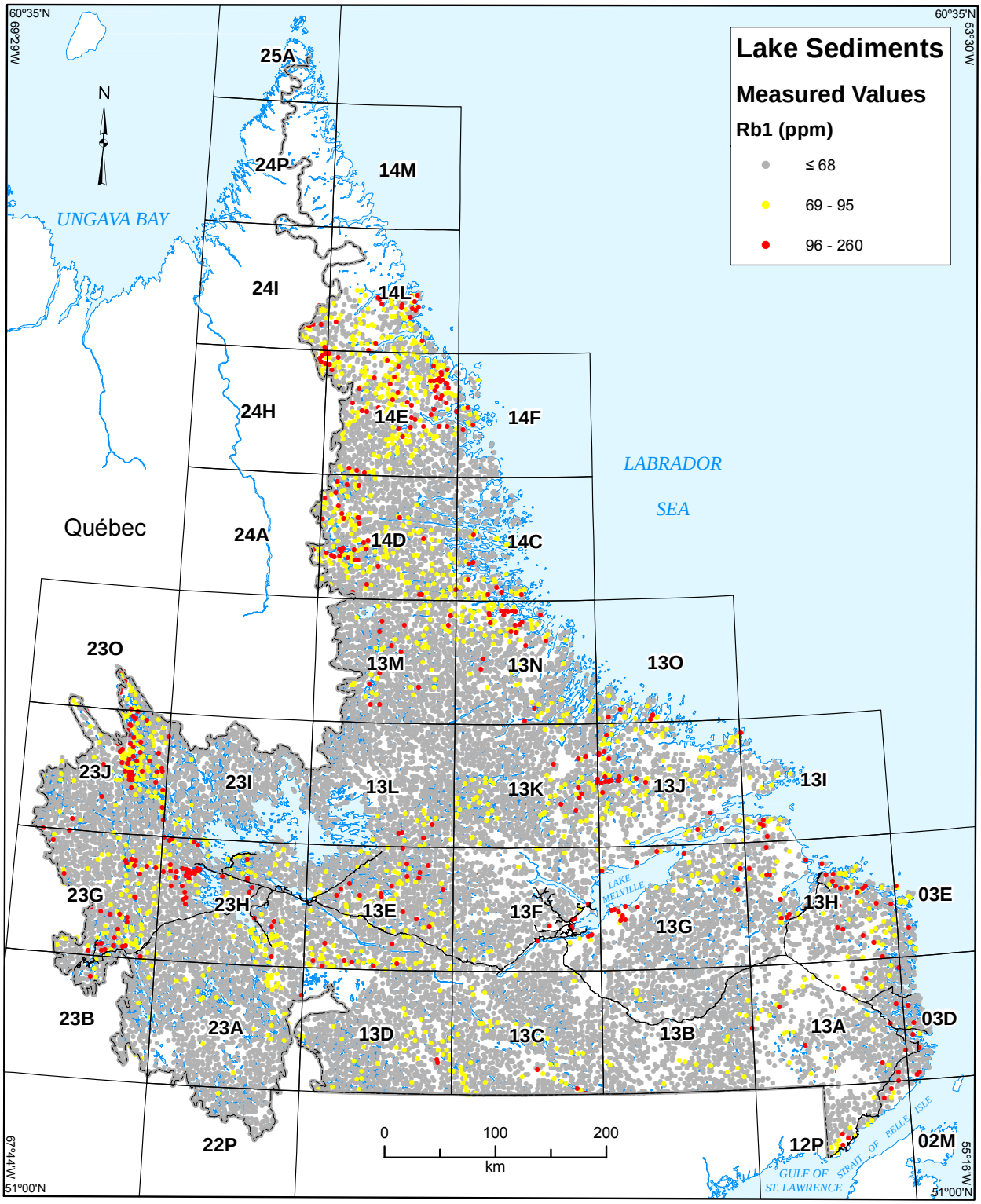


**Figure 21a.** *Measured values of Rb2 in lake sediment, Labrador, with emphasis on highest values.*

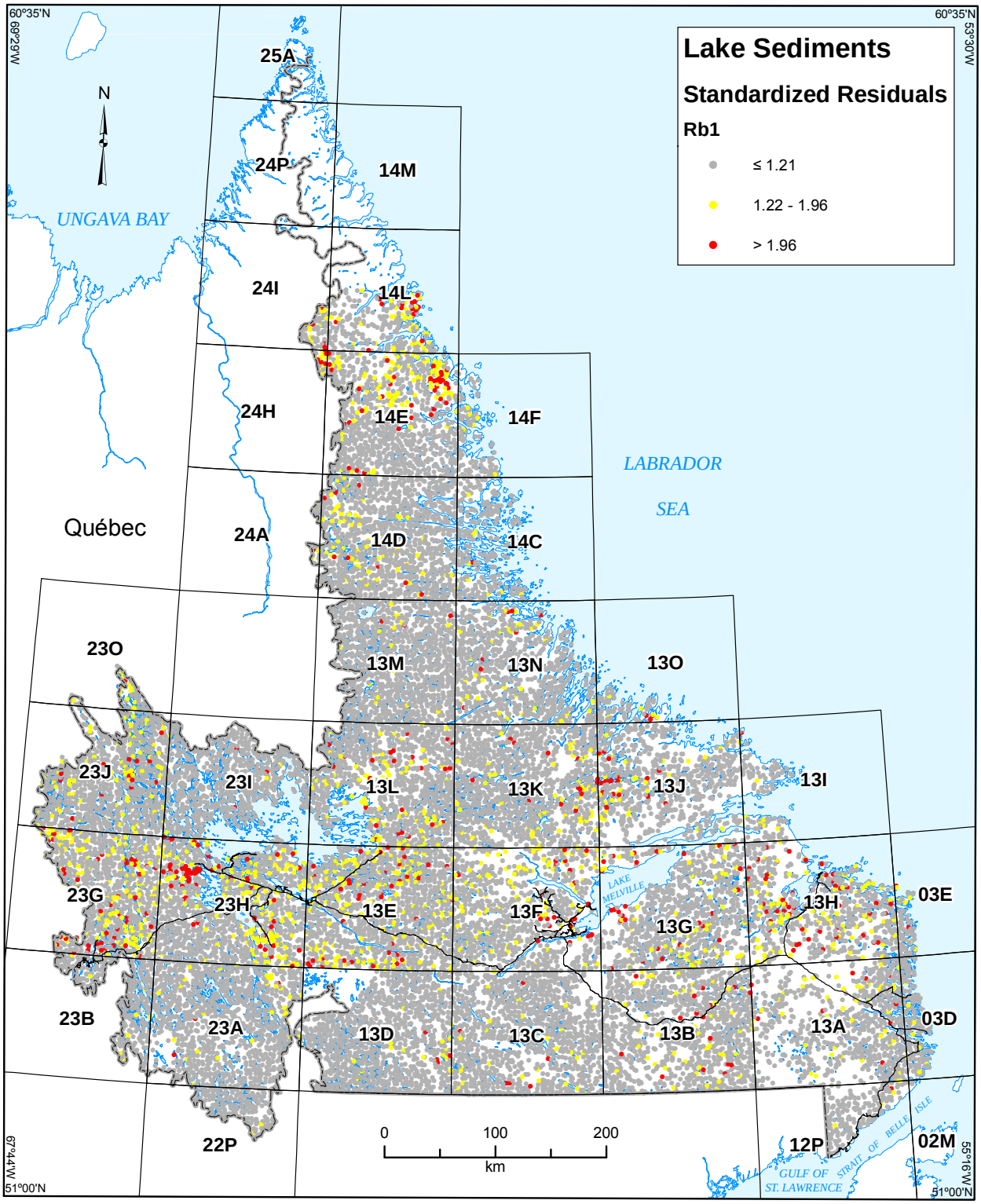


**Figure 21b.** *Standardized multiple-regression residuals of Rb2 in lake sediment, Labrador, with emphasis on highest values.*

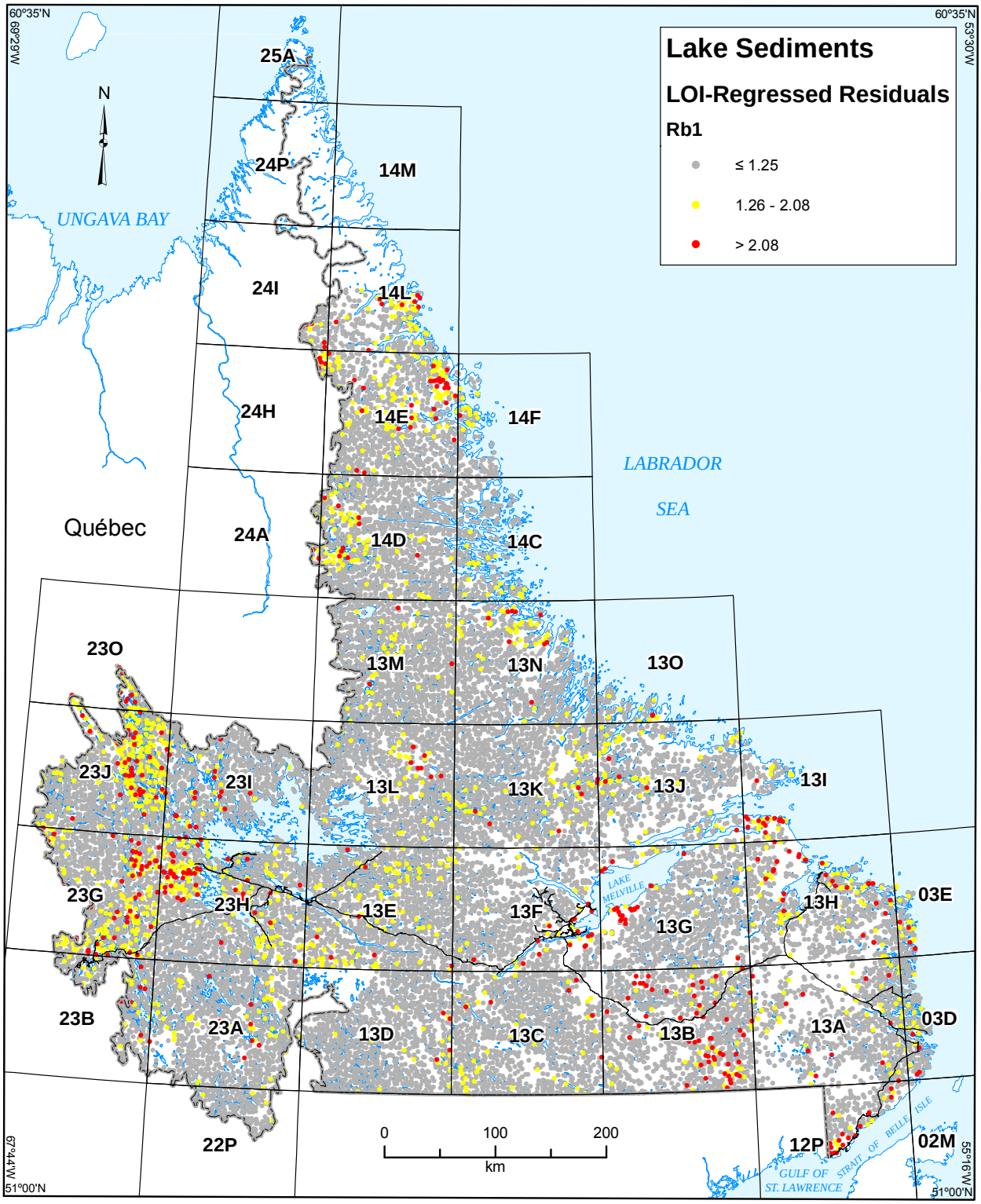


**Figure 21c.** *Standardized simple-regression residuals of Rb2 in lake sediment, Labrador, with emphasis on highest values.*

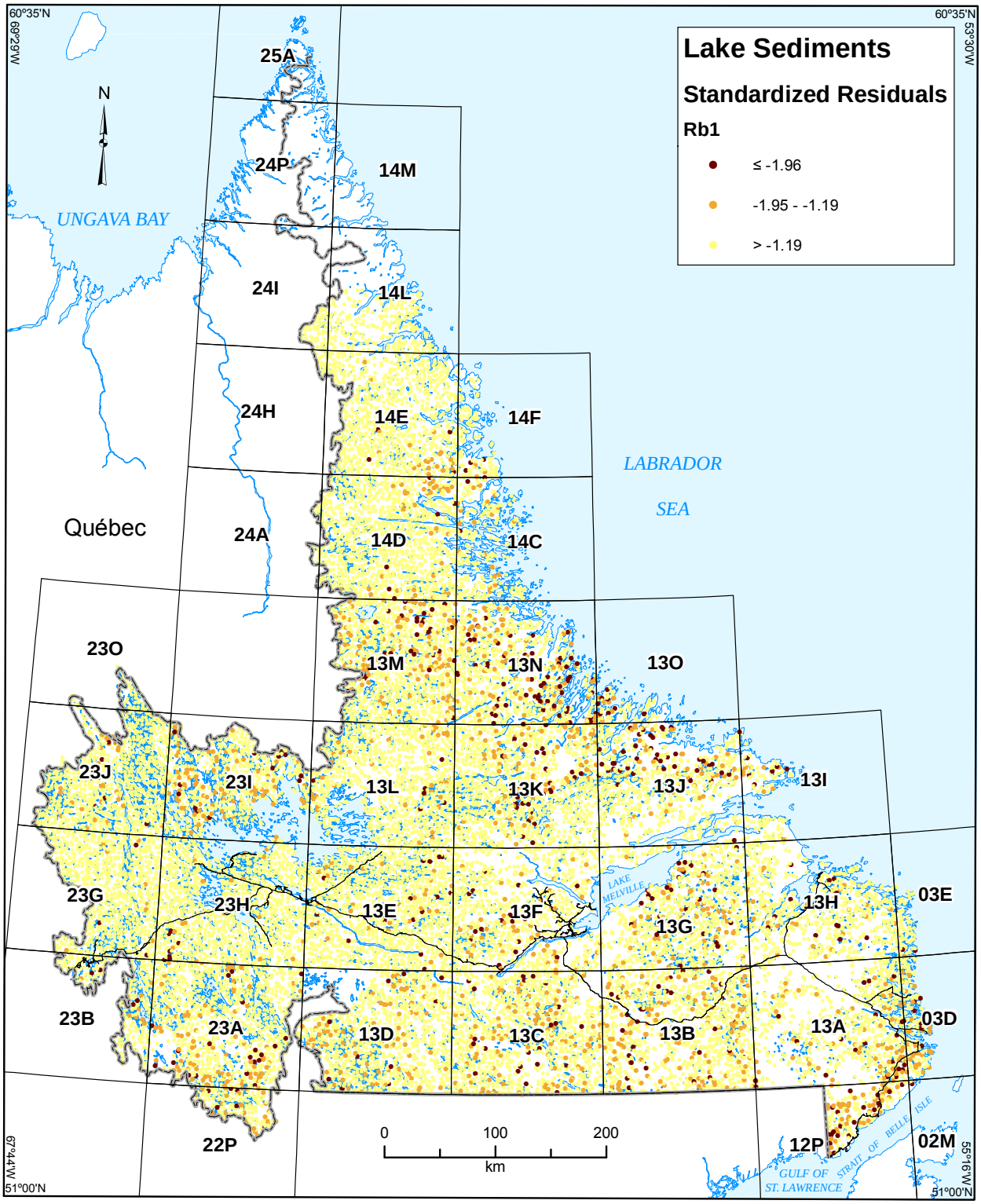


**Figure 21d.** *Standardized multiple-regression residuals of Rb2 in lake sediment, Labrador, with emphasis on lowest values.*

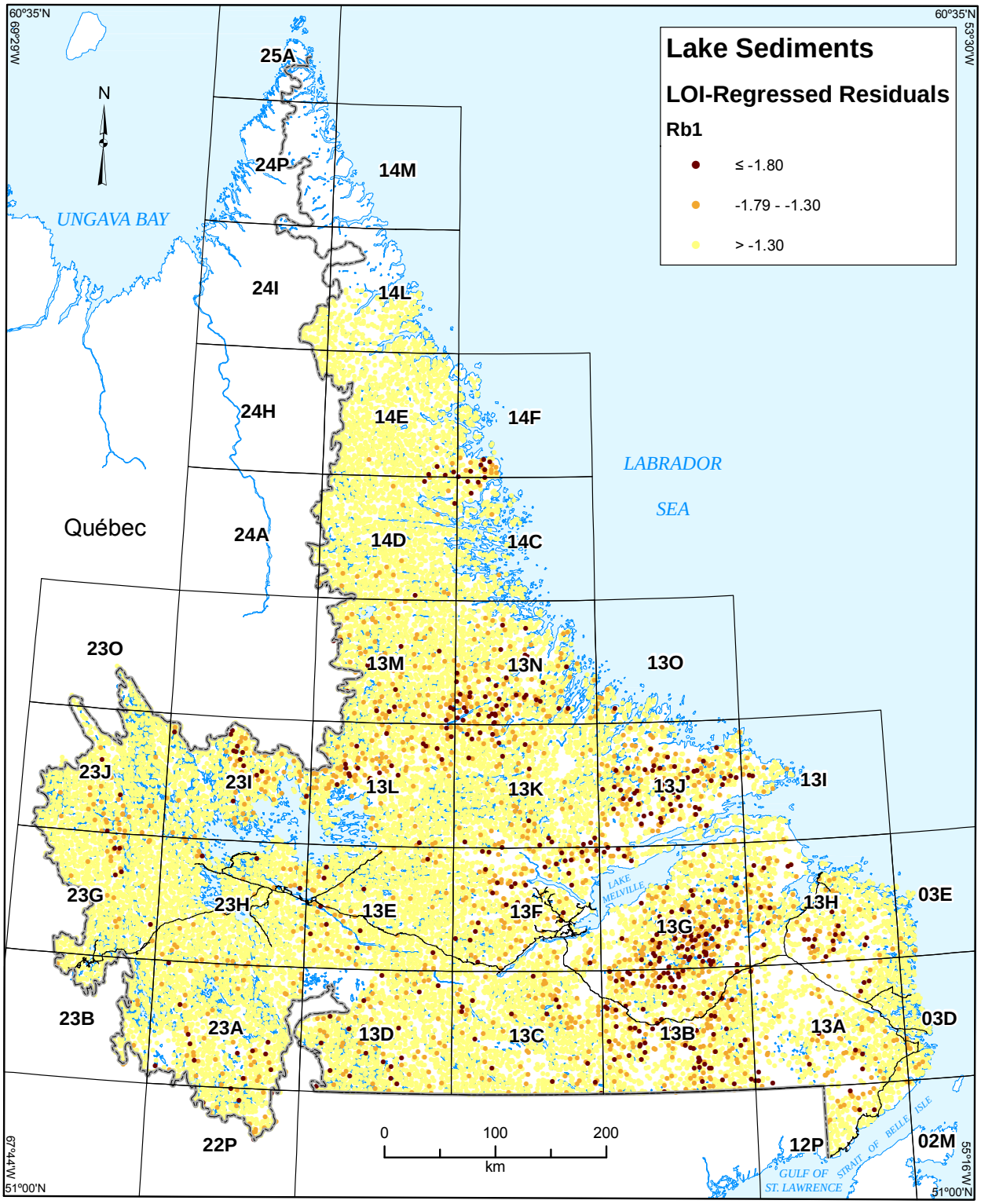


**Figure 21e.** *Standardized simple-regression residuals of Rb2 in lake sediment, Labrador, with emphasis on lowest values.*

map areas 14C and 14D in the north, as well as concentrations of anomalously high Rb1 multiple-regression residuals in NTS 14E/16 and 14L/07, over Archean (Nain Province) gneiss, and in NTS 24H/16 over Proterozoic (Southeast Churchill Province) gneiss.

There are no well-defined zones of anomalously low Rb1 multiple-regression residuals (Figure 21d, e). High LOI-regression residuals (Figure 21c) display similar patterns to their raw counterparts; there is a vague concentration of low LOI-regression residuals over the Harp Lake Intrusive Suite and the Central Mineral Belt.

*Scandium (Sc2)*

Anomalous and elevated raw values (and multiple-regression residuals) of Sc2 are concentrated over the Wakuach Gabbro (Ware and Wardle, 1979) in NTS map areas 23I/13, 23J/15 and 16, and 23O/01, 02 and 07 (Figures 22a, b). A similar area is delineated by depleted and anomalously low multiple-regression residuals of Ba2 (see Figure 14d). An extensive concentration of anomalous and elevated raw Sc2 values is present in northern Labrador, covering a diverse package of rocks in NTS map areas 14D/10, 14D/11, 14D/14, 14D/15, 14E/02, 14E/03, 14E/05, 14E/06, 14E//07, 14E/08, 14E//09, 14E/10, 14E/11, 14E/12, 14E/13, 14E/14, 14E/15, 14E/16, 14L/02, 14L/03, 14L/04, 14L/05, 14L/06, 14L/07 and 24I/01. A small area of the Kiglapait Intrusion (NTS map areas 14F/03 and 14F/04) is also characterized by anomalously high Sc2 raw values and multiple-regression residuals; this lies within a larger area defined by multiple-regression Na2 residuals (Figure 19b) that are anomalously high, and K2 residuals (Figure 16d) that are anomalously low, but is distinct from an area defined by high multiple-regression residuals of Mg2 (Figure 18b).

Although it is not discernible in the raw values, anomalous and elevated Sc2 multiple-regression residuals define a broad (30 km) zone over the Archean Ashuanipi Complex at its contact with the overlying Kaniapiskau Supergroup in NTS map areas 23G/09, 23G/10, 23G/15, 23G/16, 23J/01, 23J/02, 23J/07 and 23J/08; the same zone is marked by mostly depleted multiple-regression residuals of Ba2 (*see* Figure 14d). In the north, the large regional anomaly defined by raw Sc2 values is reduced to two principal foci: in NTS map areas 14D/10, 11, 14 over the southern extension of the Umiakovik batholith (Ryan, 1990), and on 14E/13 and 14L/04, over granitic and gneissic rocks of the Southeast Churchill Province.

Patterns displayed by high simple- (Figure 22c) and multiple-regression residuals are similar, although the former are generally more dilute.

There are a number of distinct Sc2 lows (Figure 22d), as defined by negative multiple-regression residuals, including the leuctotroctolitic, leucogabbroic and anorthositic Etagaulet Bay and Kennemich massifs in NTS map areas 13G/05, 06, 10, 11 and 15, which are also delineated by elevated and anomalous multiple-regression residuals of Al2 (see Figure 13b). Elsewhere, the central and eastern parts of the Harp Lake Intrusive Suite are similarly defined, but not the western or southern portions; anomalously high Al2 and Mg2 values define the same zones, which do not, however, appear to correspond to the petrologic phases of the intrusion as mapped by Emslie (1980). Within the anomaly defined by high Na2 (Figure 19b) and low K2 (Figure 16d) multiple-regression residuals within the Kiglapait Intrusion, most of the samples that are not characterized

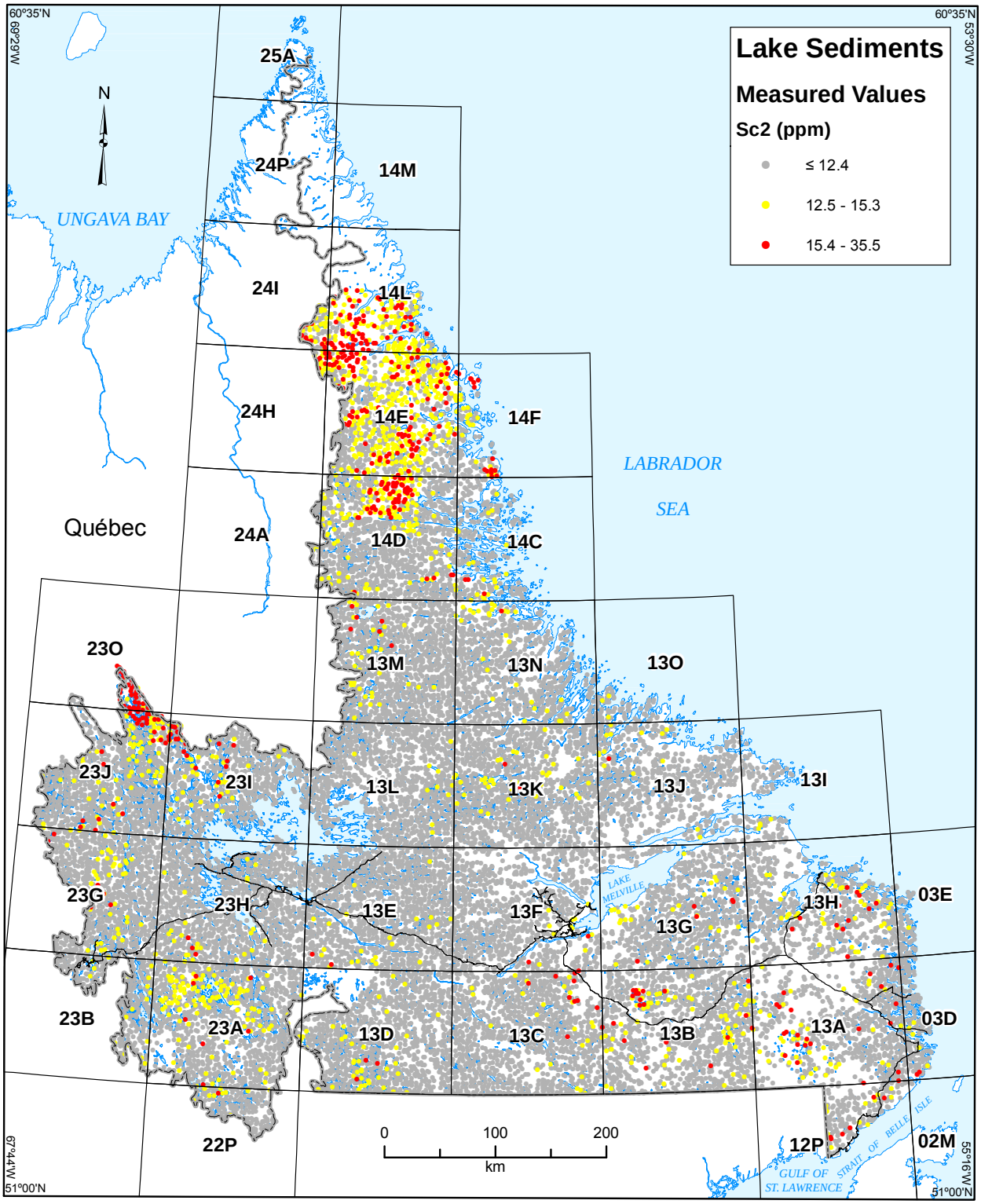


**Figure 22a.** *Measured values of Sc2 in lake sediment, Labrador, with emphasis on highest values.*

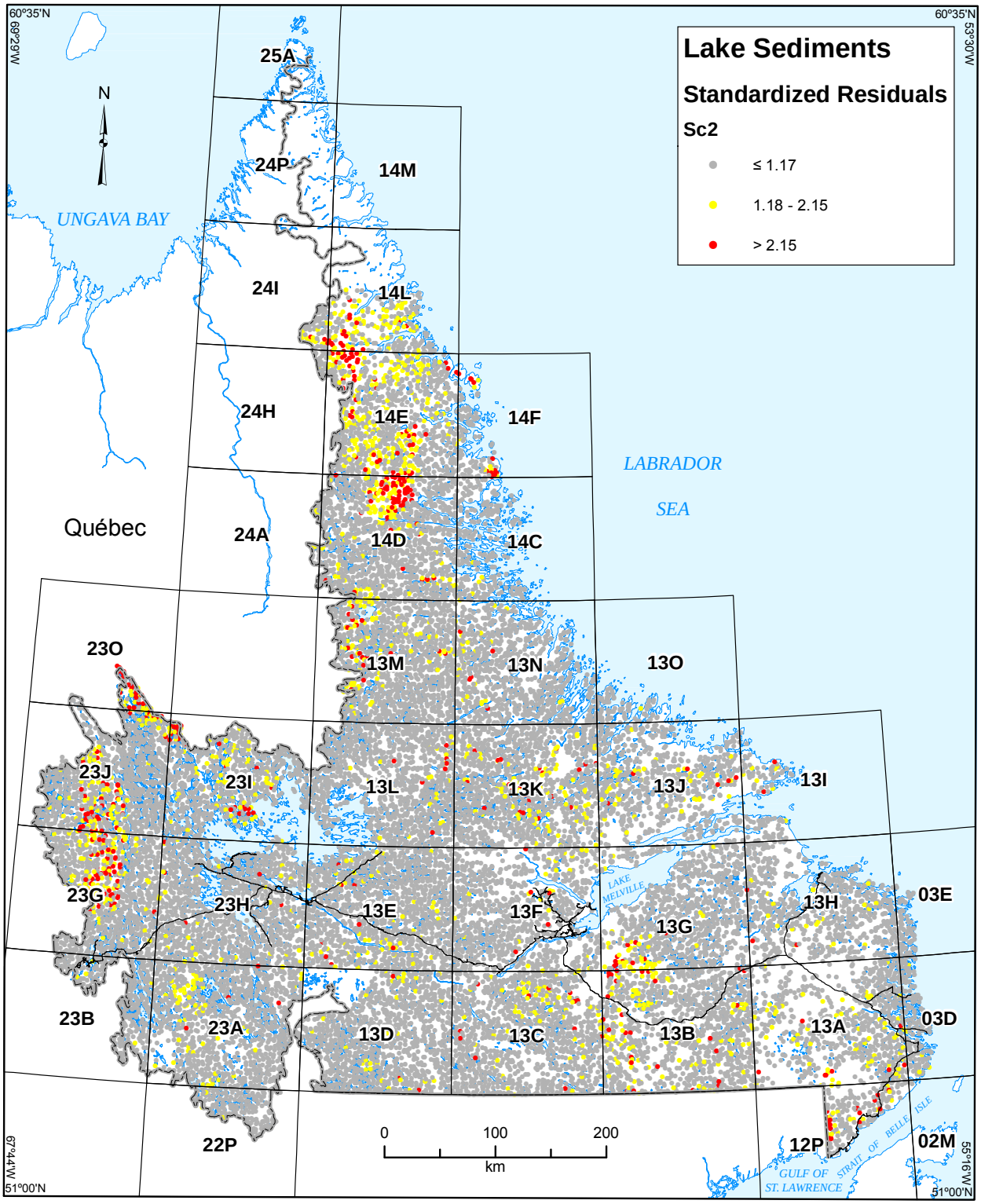


**Figure 22b.** *Standardized multiple-regression residuals of Sc2 in lake sediment, Labrador, with emphasis on highest values.*

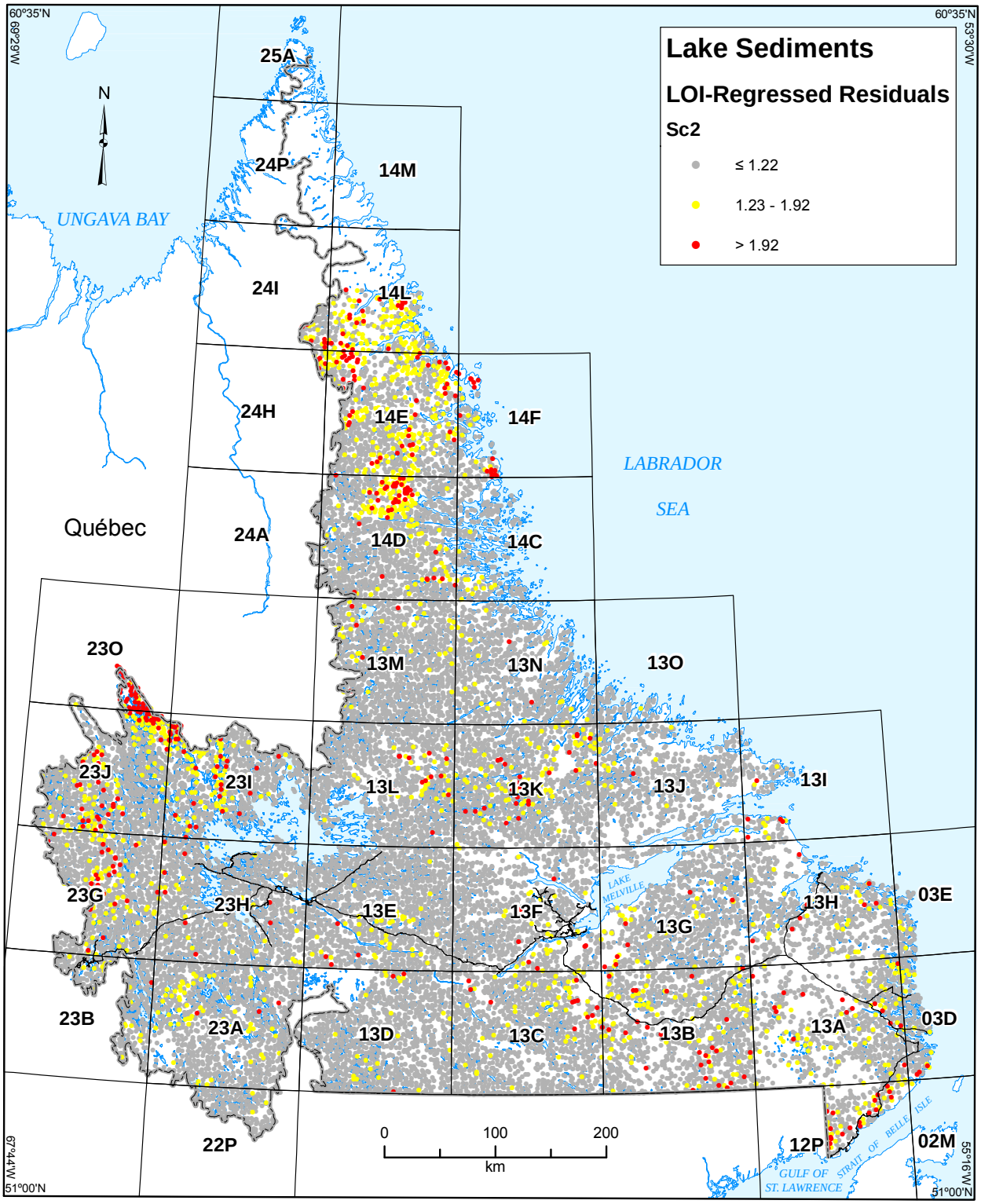


**Figure 22c.** *Standardized simple-regression residuals of Sc2 in lake sediment, Labrador, with emphasis on highest values.*

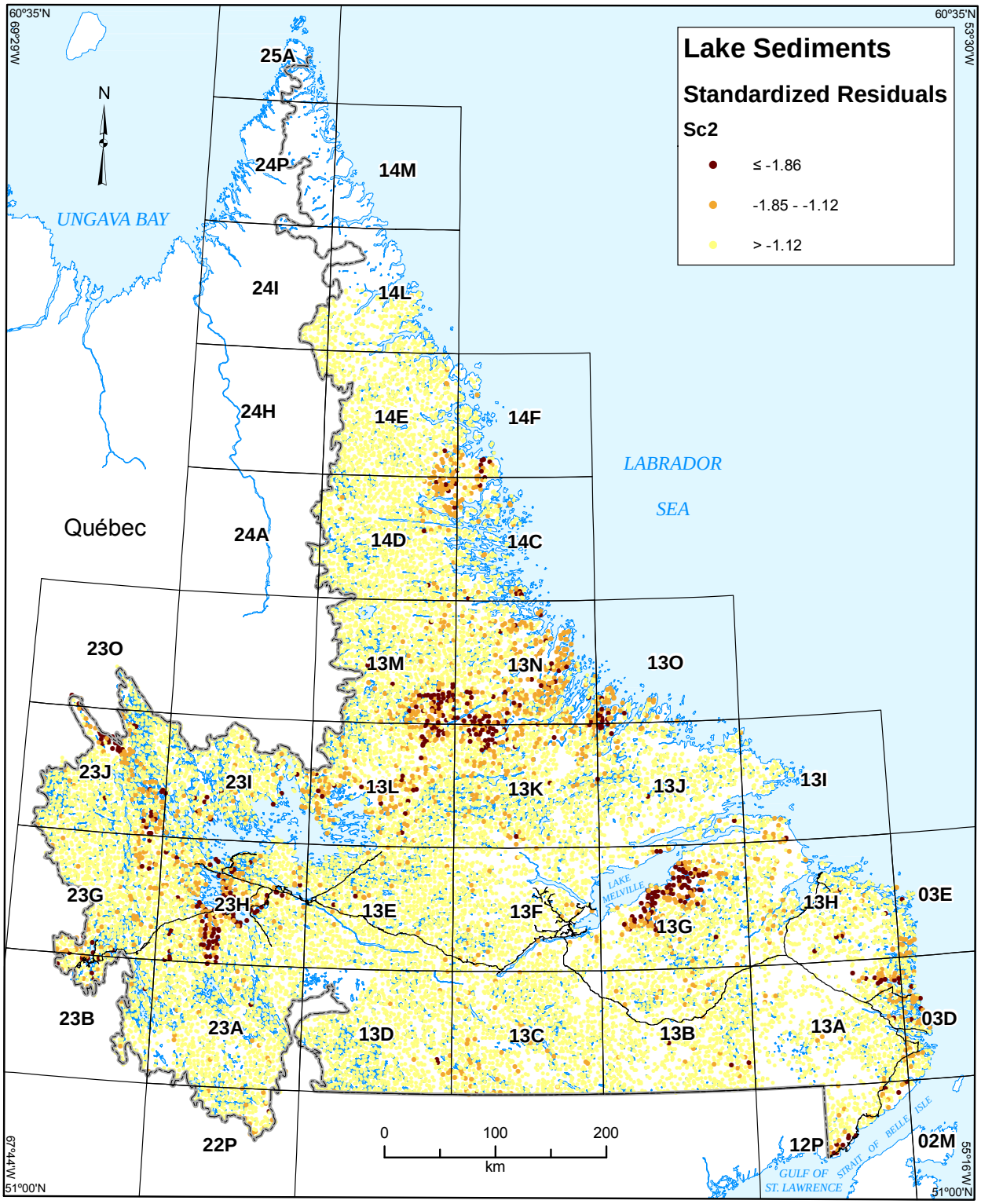


**Figure 22d.** *Standardized multiple-regression residuals of Sc2 in lake sediment, Labrador, with emphasis on lowest values.*

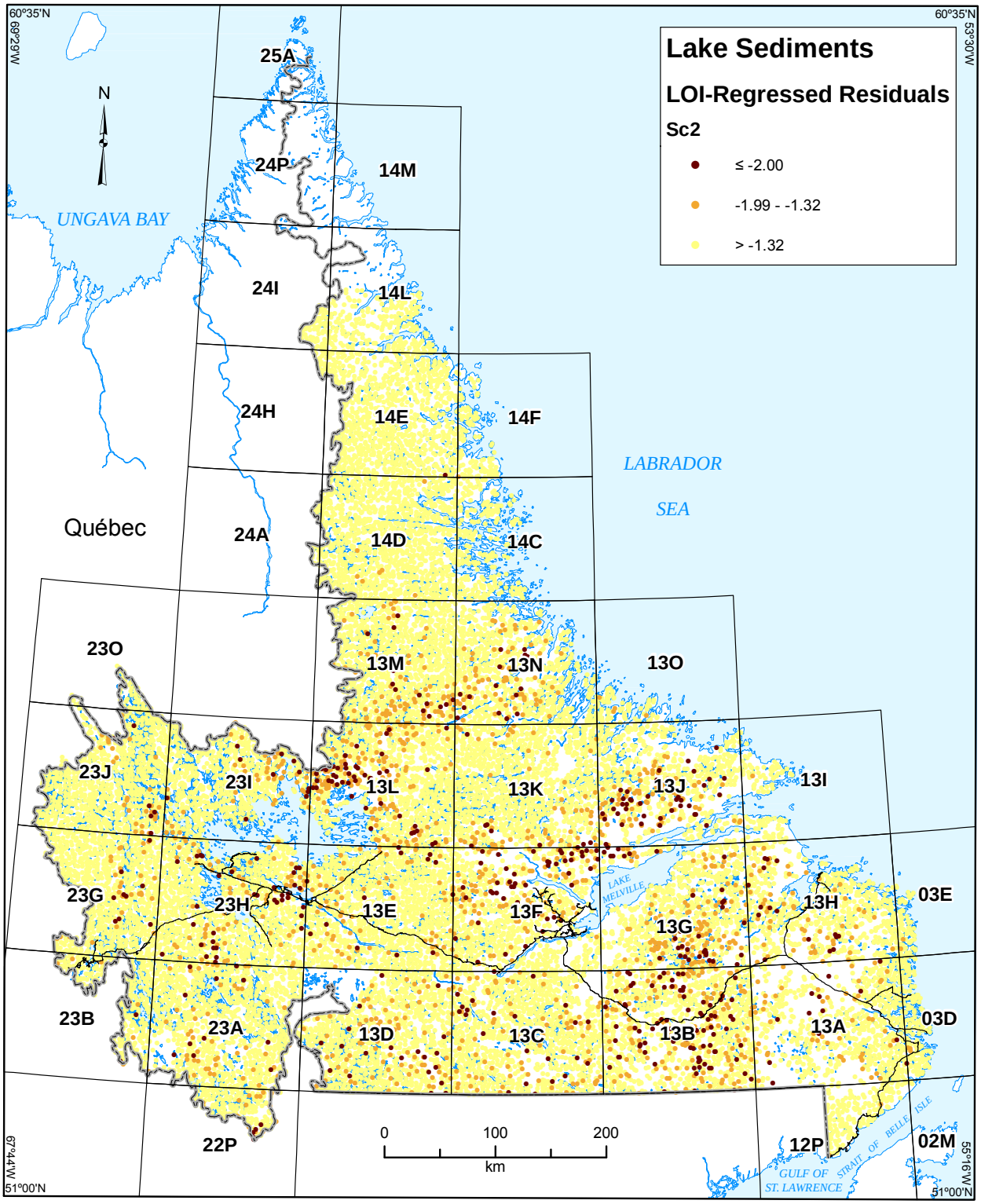


**Figure 22e.** *Standardized simple-regression residuals of Sc2 in lake sediment, Labrador, with emphasis on lowest values.*

by anomalously high Sc2 values (the latter being concentrated in the southeast, overlying the Upper Gabbroic Zone; Morse, 1969) are depleted and anomalously low in Sc2.

In southeastern Labrador in NTS map areas 03D/12 and 13A/16, multiple-regression residuals of Sc2 are anomalously low over gabbro of the White Bear Arm complex (Gower, 2010b), whereas in the west, an Sc2 low overlies Grenvillian paragneiss intruded by gabbronorite and amphibolite and mafic granulite (the Ossok Mountain intrusive suite; James, 1994b) in NTS map areas 23H/03 and 06; an areally restricted low comprising only four samples is present over similar rocks in NTS 23H/04. Finally, anomalously-low Sc2 multiple-regression residuals are concentrated over iron formation (Unit $P_2$i; Wardle *et al.*, 1997) in NTS map areas 23J/10 and 14.

LOI-regressed residual lows of Sc2 (Figure 22e) do not correspond to their multiple-regression counterparts and are generally poorly defined, although there are vague concentrations over the Central Mineral Belt, and in western Labrador over the northern part of the anorthositic Michikamau Intrusion, and the area to the east.

*Strontium (Sr2)*

Features defined by anomalous and elevated raw and simple- and multiple-regression residual Sr2 values (Figure 23a, b) are diffuse, and unlike most of the elements in the clastic association, concentrated mainly in southern Labrador. The strongest concentration of anomalous raw values is in NTS map areas 23A/11–14, west of an intrusion of Shabogamo Gabbro at Lac Joseph (James, 1994b), although the response is weaker in the multiple-regression residuals. A concentration of high LOI-regression Sr2 values (Figure 23c) is located to the south of this feature with very little overlap, located in NTS map areas 23A/05, 12, 13, 23B/08, 09 and 16. Its underlying geology also consists of some metamorphosed mafic intrusive rocks but is dominated by granite and metasediment.

In western Labrador, depleted and anomalously low multiple-regression residuals of Sr2 define most of the areas underlain by rocks of the Kaniapiskau Supergroup (with the possible exception of the Menihek Formation) in NTS map areas 23I, 23J and 23O (Wardle *et al.*, 1982a, b; Figure 23d). This is the only feature that is defined by LOI-regression residuals with comparable strength (Figure 23e).

On NTS map areas 23B/14, 15 and 23G/02, the Sr2 low coincides with a positive Ba2 simple- (Figure 14c) and multiple-regression (Figure 14b) residual anomaly of which the Menihek Formation is a possible source.

A concentration of depleted (but not many anomalously low) Sr2 multiple-regression residuals is also present over pyroxene granite and gneissic tonalite of the Grenvillian Atikonak River Intrusion (Units $P_2$Gr, $P_2$tgn; Wardle, 1994) in NTS map areas 13D/05, 06, 11 and 12 In NTS map areas 13A/01, 07 and 08, and 03D/04, strongly negative multiple-regression residuals of Sr2 overlie granitic rocks of the Grenvillian interior magmatic belt; they are also present on the north shore of St. Lewis Sound in NTS map areas 13A/08 and 3D/05 (where a positive Nb2 multiple-regression residual anomaly is also present; see Figure 20b) and over metagabbro and metanorite of the White Bear Arm complex in NTS 13A/16 and 13H/03.

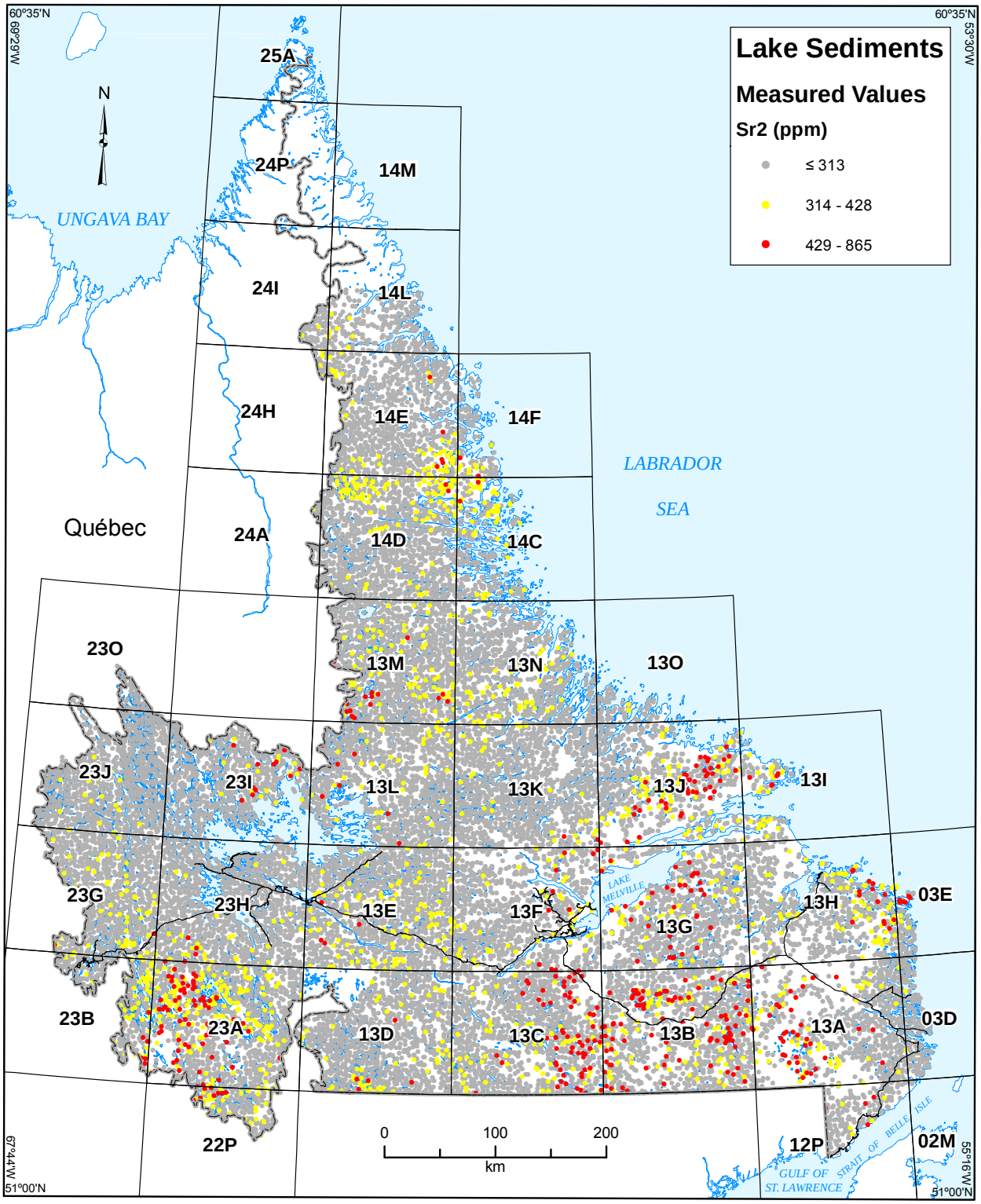


**Figure 23a.** *Measured values of Sr2 in lake sediment, Labrador, with emphasis on highest values.*

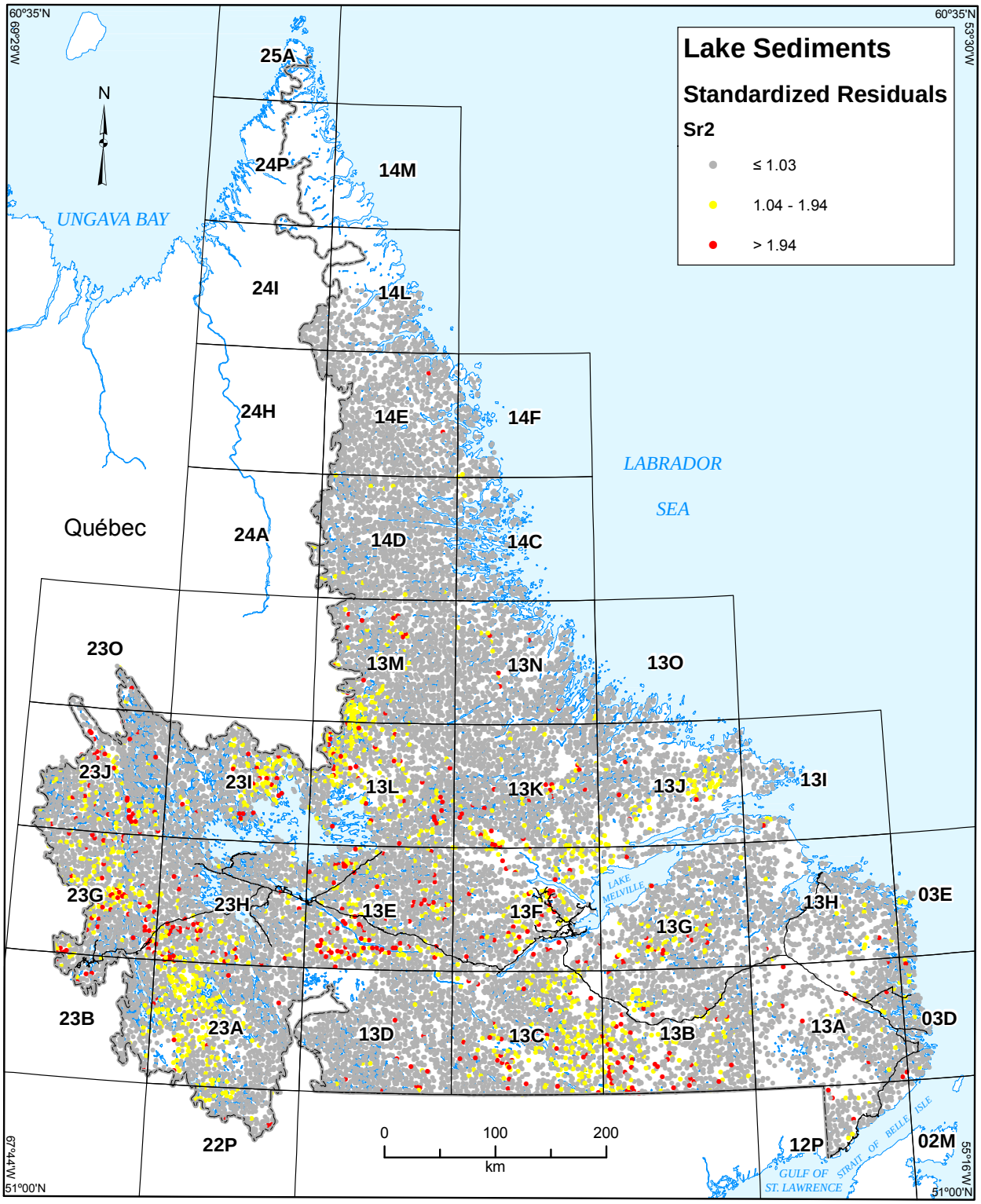


**Figure 23b.** *Standardized multiple-regression residuals of Sr2 in lake sediment, Labrador, with emphasis on highest values.*

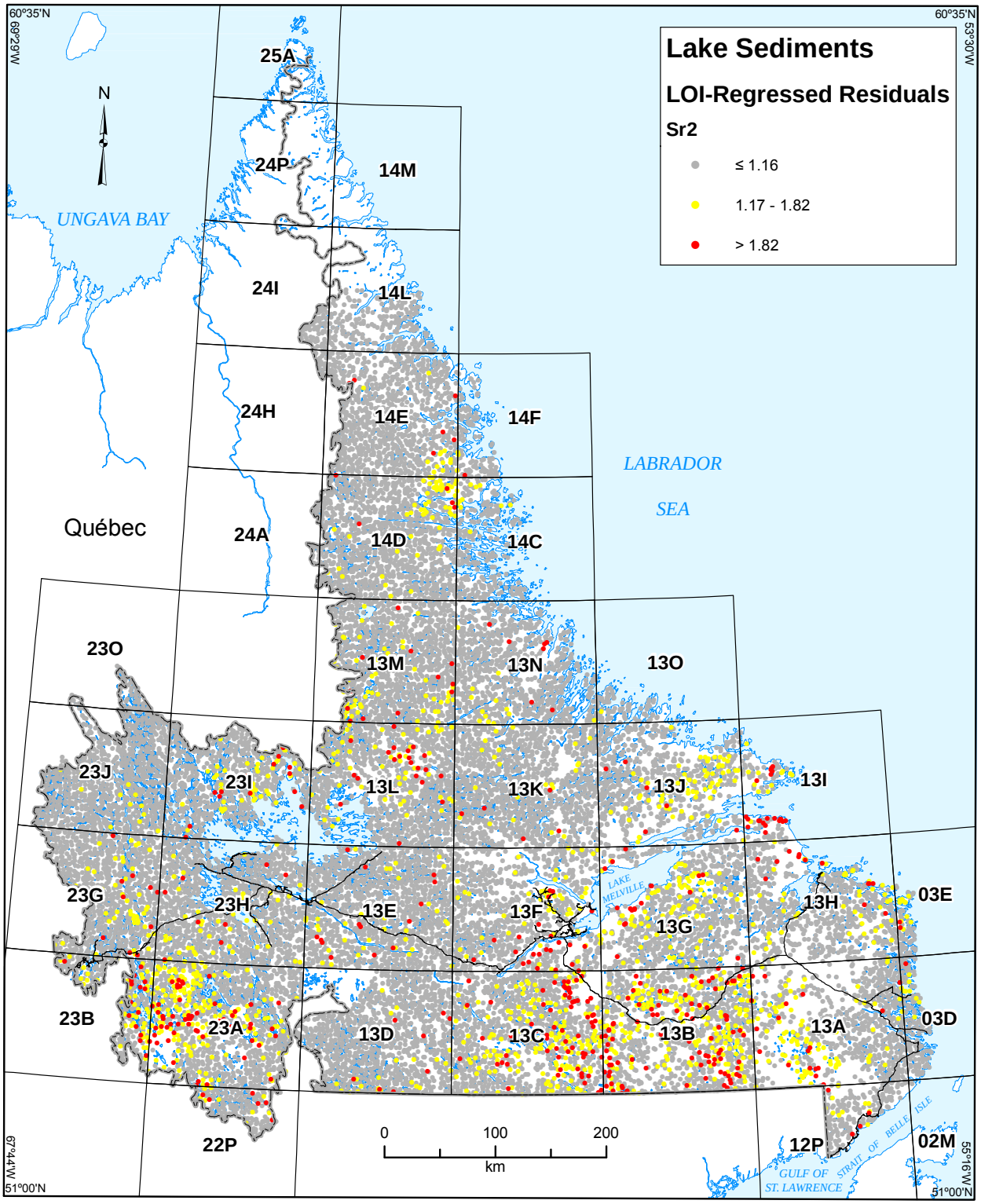


**Figure 23c.** *Standardized simple-regression residuals of Sr2 in lake sediment, Labrador, with emphasis on highest values.*

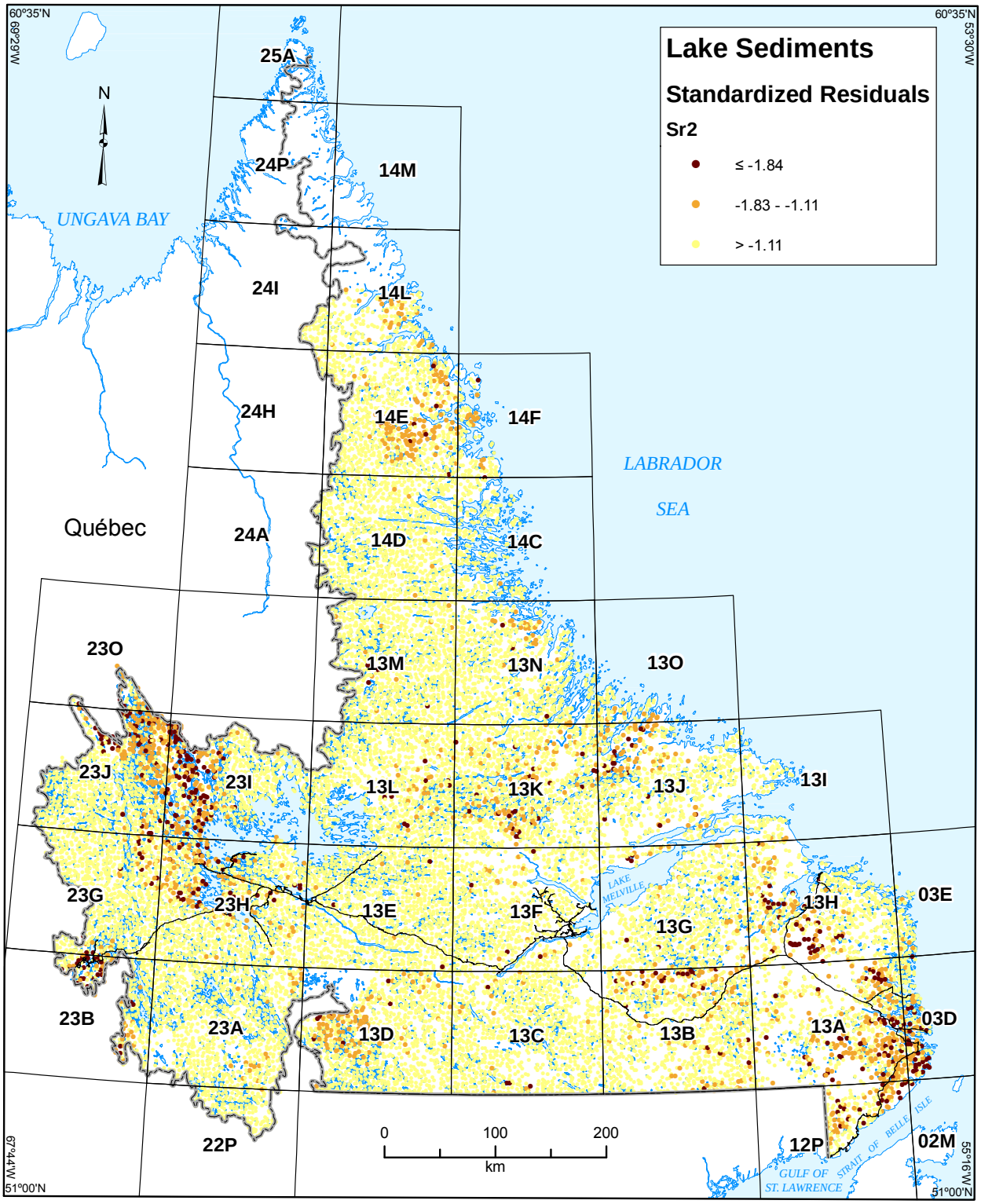


**Figure 23d.** *Standardized multiple-regression residuals of Sr2 in lake sediment, Labrador, with emphasis on lowest values.*

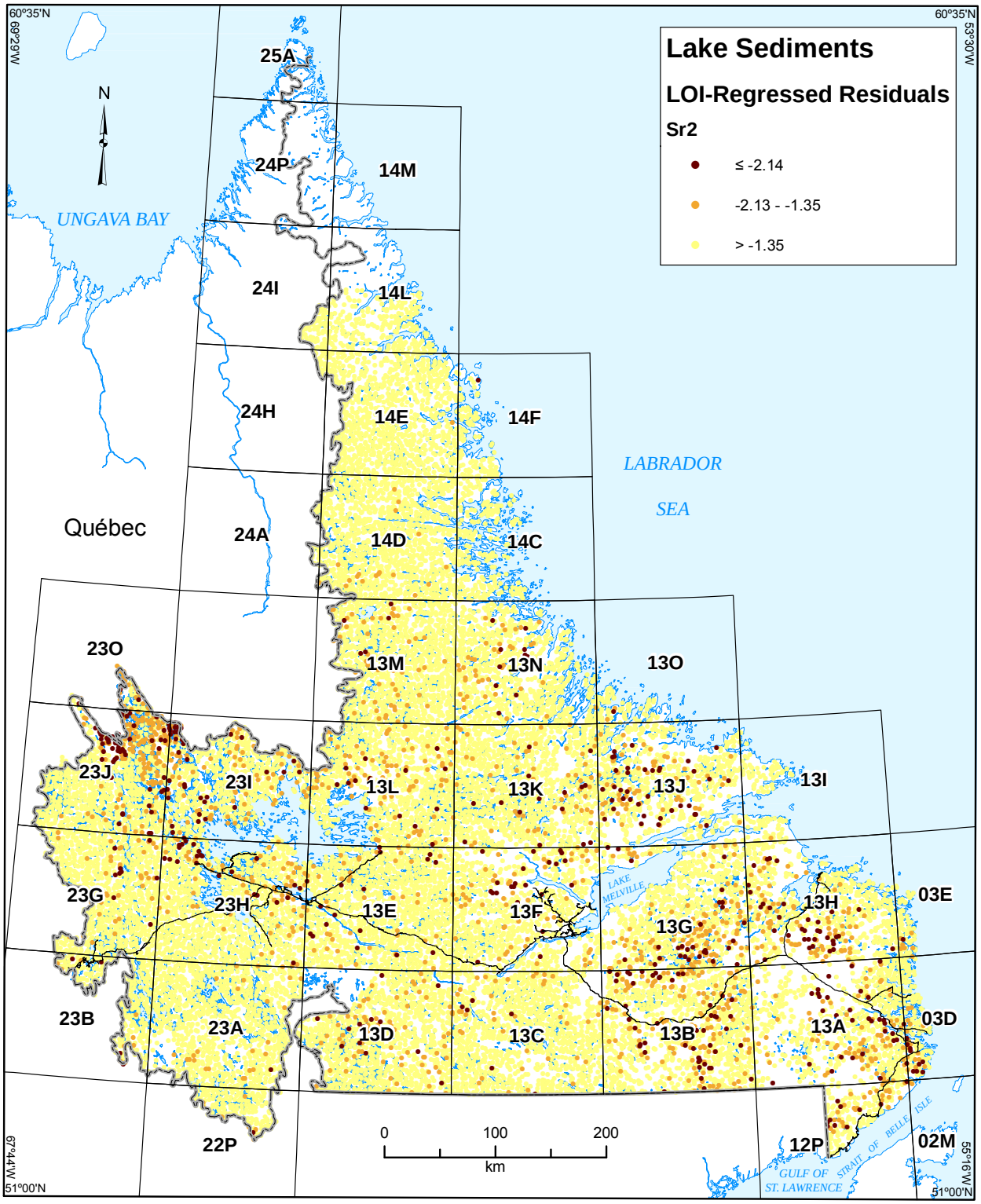


**Figure 23e.** *Standardized simple-regression residuals of Sr2 in lake sediment, Labrador, with emphasis on lowest values.*

*Titanium (Ti2)*

Anomalous and elevated raw Ti2 values define anomalies at a number of locations in Labrador (Figure 24a). These are better defined in the north: in NTS map areas 24H/16 and 24I/01; an extensive feature in NTS 14D/15, 16, 14E/01–03, 14E/07 and 08; in NTS 13M/15, 16, 13N/13, 14, 14C/03, 04 and 14D/01, mainly over the Voisey Bay–Notakwanon granitic batholith; in NTS 13K/05, 06 and 13K/12, overlying rocks of the Seal Lake Group (Wardle, 1993); and in NTS 23J/09, 23J/15, 16 and 23O/02 over rocks of the Kaniapiskau Supergroup in the Labrador Trough. There are also numerous samples with anomalous and elevated Ti2 values in southeastern Labrador, although they do not form well-defined clusters.

Positive multiple-regression residuals of Ti2 (Figure 24b) are more focussed: the anomalies in NTS map areas 24H/16 and 24I/01 persist, and overlie gneissic rocks of the Southeast Churchill Province. There is a concentration of anomalous samples over the upper gabbroic zone of the Kiglapait Intrusion (Morse, 1969) in NTS map areas 14F/03 and 04, that lies within a larger feature defined by high Na2 (Figure 19b) and low K2 (Figure 16c) multiple-regression residuals. This coincides with a zone defined by anomalous and elevated Sc2 multiple-regression residuals and encompasses a zone defined by low Mg2 multiple-regression residuals (*see* Figure 18d).

The feature in NTS map areas 13K/05, 06, and 12, also apparent in raw Ti2 values, persists in the multiple-regression residuals but is areally less extensive. A linear, northwestward-trending feature in NTS map areas 13K/02, 03 and 13F/15, not apparent in raw values, may be associated with arenaceous and basaltic rocks of the Bessie Lake Formation (Units 35a and 35b; Ryan, 1984). The response to the leucotroctolitic, leucogabbroic and anorthositic Etagaulet Bay and Kennemich massifs in NTS map areas 13G/05–11, and 15 is not absent in raw Ti2 values, or LOI-regression residuals, but that defined by the multiple-regression residuals is more homogeneous. Finally, the positive-residual anomaly (multiple-regression) in NTS map areas 13A/07–10, absent in raw Ti2 values, is underlain by a complex package of Pre-Labradorian (Late Paleoproterozoic; 1800–1710 Ma) quartzite and psammite, intruded by a variety of Early Labradorian (late Paleoproterozoic; 1710–1660 Ma) felsic and intermediate rocks. With the exception of the response to the Etagaulet Bay and Kennemich massifs, the response in high LOI-regression residuals of Ti2 is a weak echo of its multiple-regression counterpart (Figure 24c).

Although well-defined zones of depleted and anomalously low Ti2 multiple-regression residuals are not numerous, they have undoubted geological significance (Figure 24d). The dispersion train from the Strange Lake REE–RM deposit is well-defined, and reflects an aspect of the mineralization at Strange Lake that is not known to have been noted previously. The Ti2-defined feature extends to the northeast as far as NTS map areas 14D/07 and 10 (about 90 km), although this is not as long as the dispersion train defined by Nb2 (about 110 km).

Depleted and anomalously low Ti2 multiple-regression residuals are present over most of the northeastern two-thirds of the Harp Lake Intrusive Suite, and while the southeastern lobe of Unit *anln* (Emslie, 1980) is not distinctive in this respect (just as it is not anomalously high in Mg2; Figure 18b), or anomalously low in Sc2 (Figure 22d), the feature defined by the Ti2 residuals is not congruent, overall, with those defined by Mg2 and Sc2.

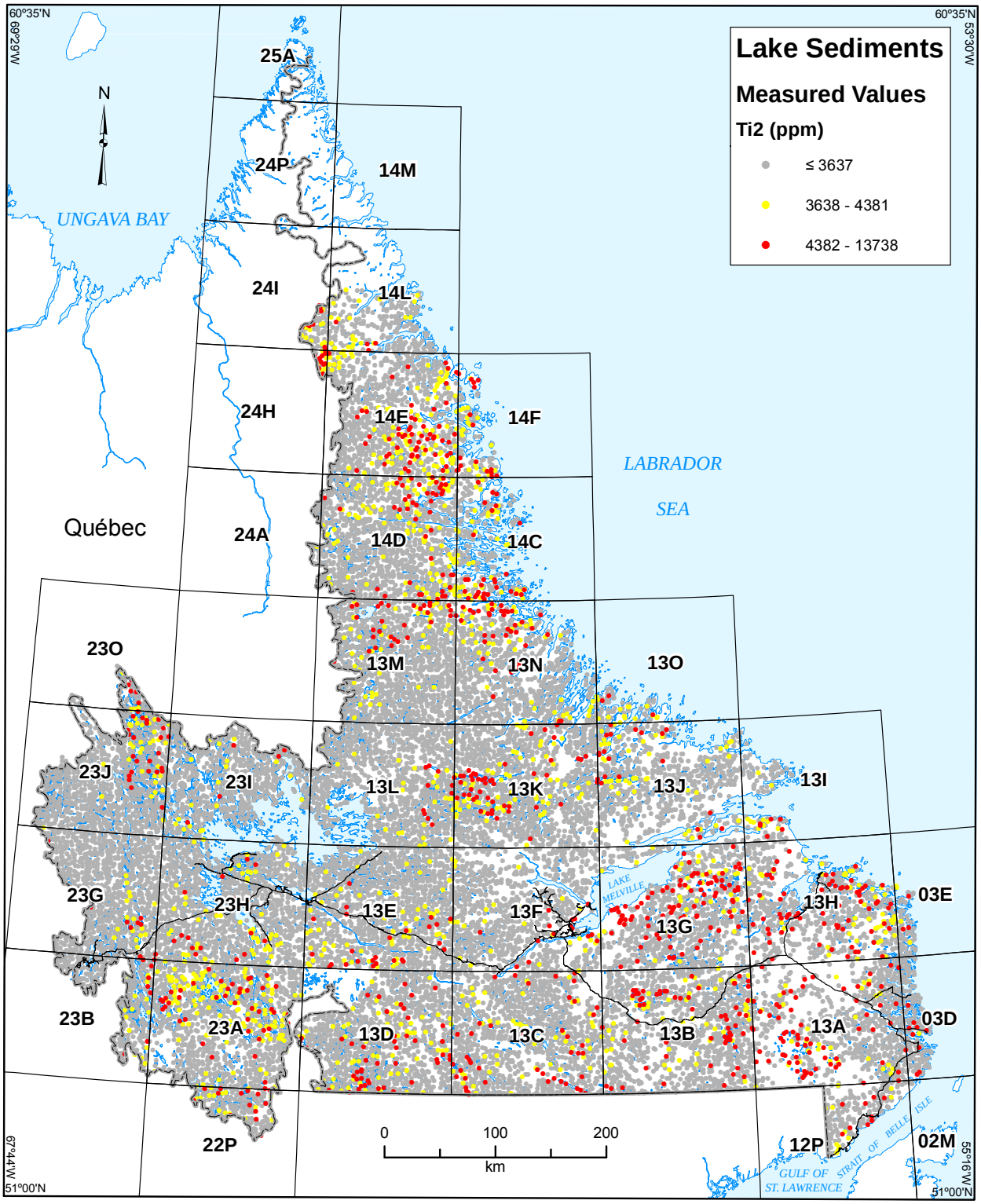


**Figure 24a.** *Measured values of Ti2 in lake sediment, Labrador, with emphasis on highest values.*

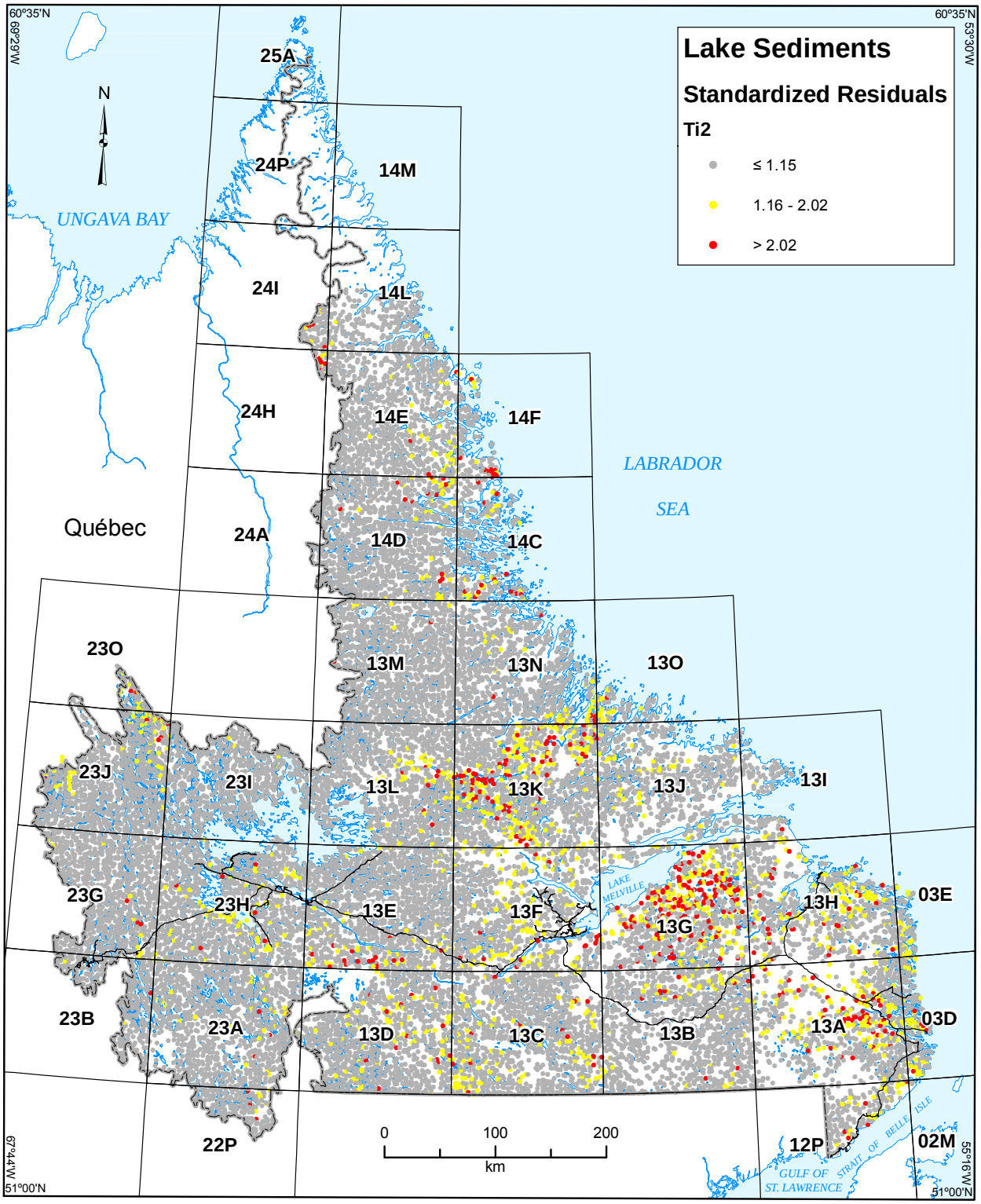


**Figure 24b.** *Standardized multiple-regression residuals of Ti2 in lake sediment, Labrador, with emphasis on highest values.*

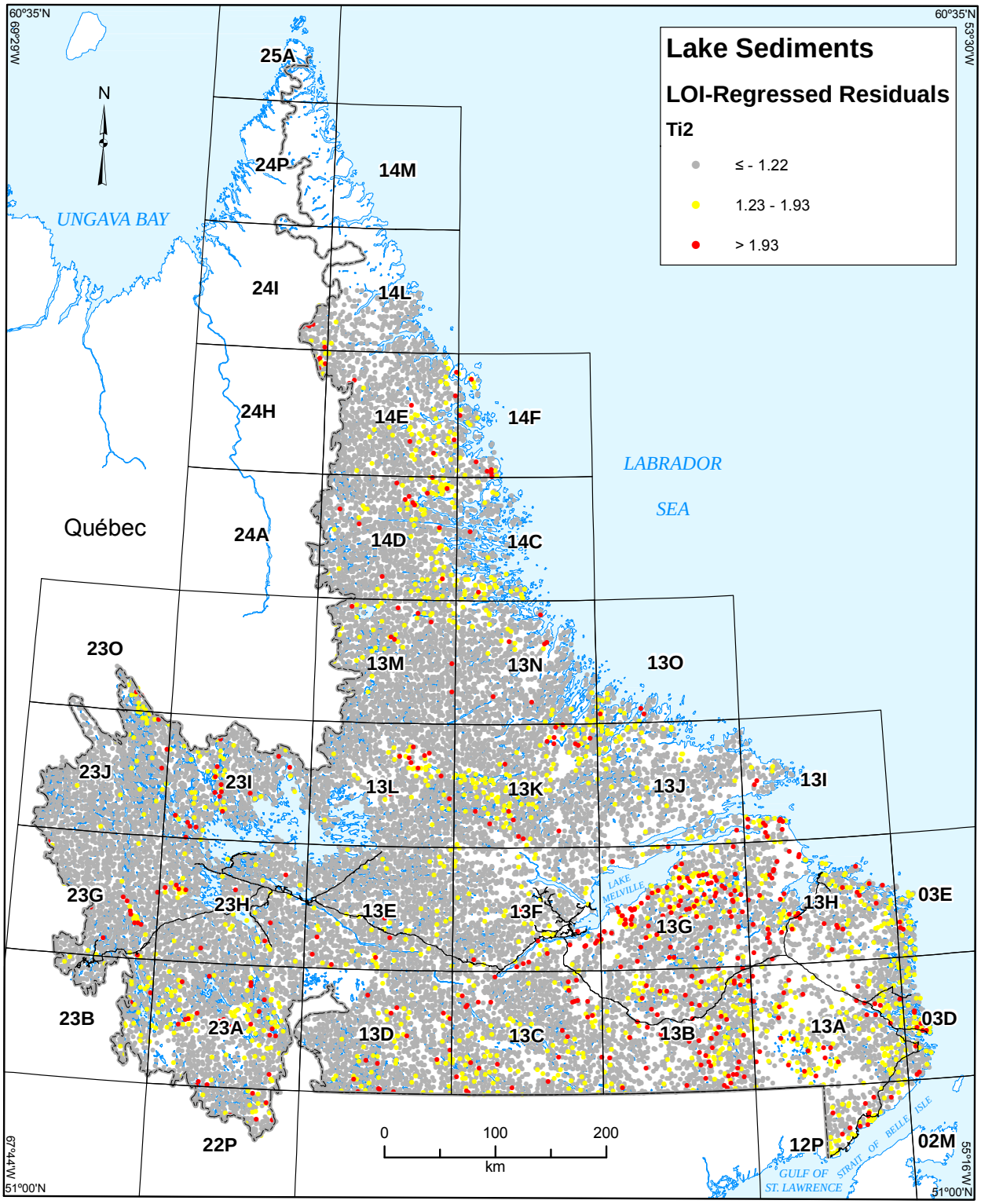


**Figure 24c.** *Standardized simple-regression residuals of Ti2 in lake sediment, Labrador, with emphasis on highest values.*

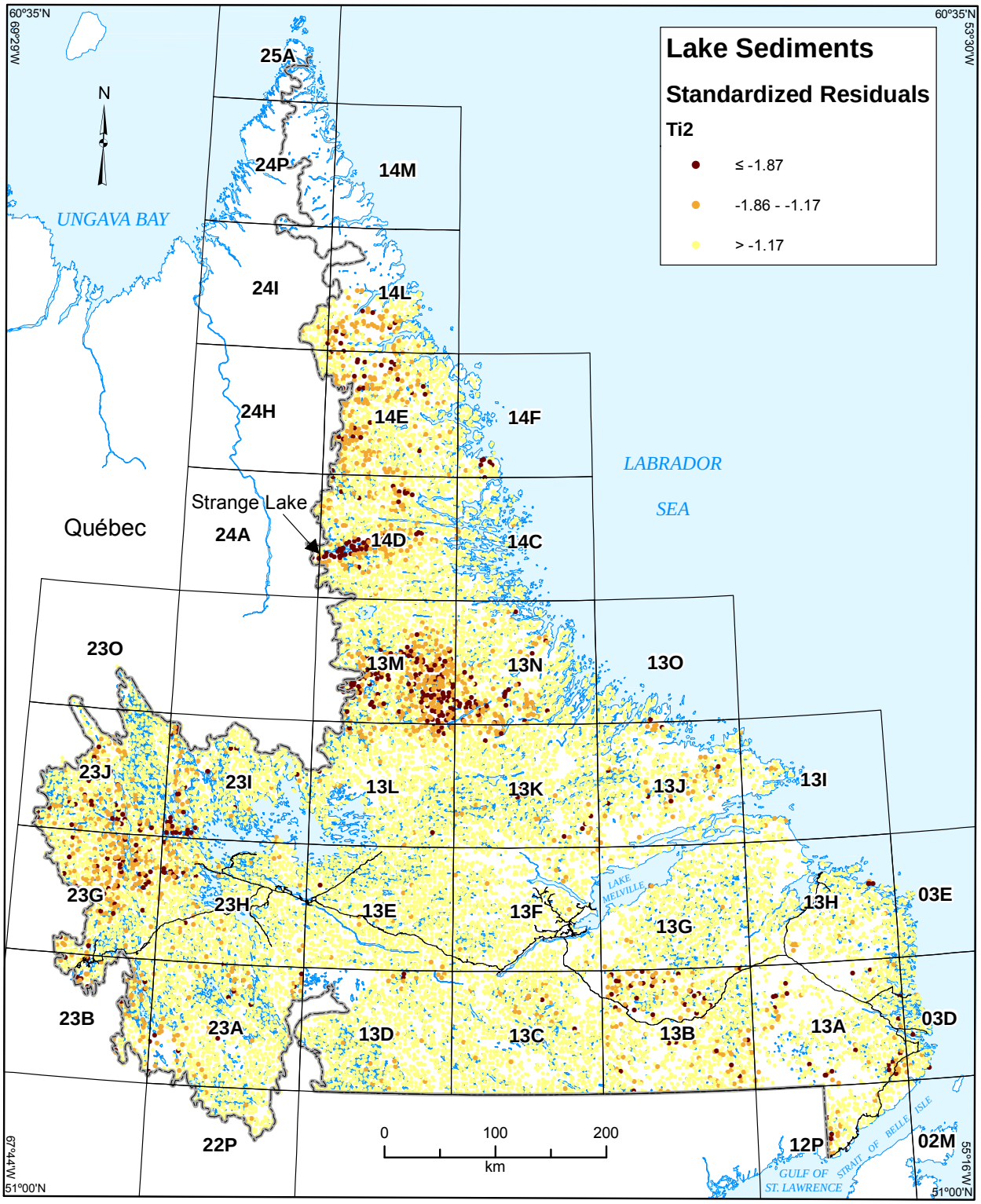


**Figure 24d.** *Standardized multiple-regression residuals of Ti2 in lake sediment, Labrador, with emphasis on lowest values.*

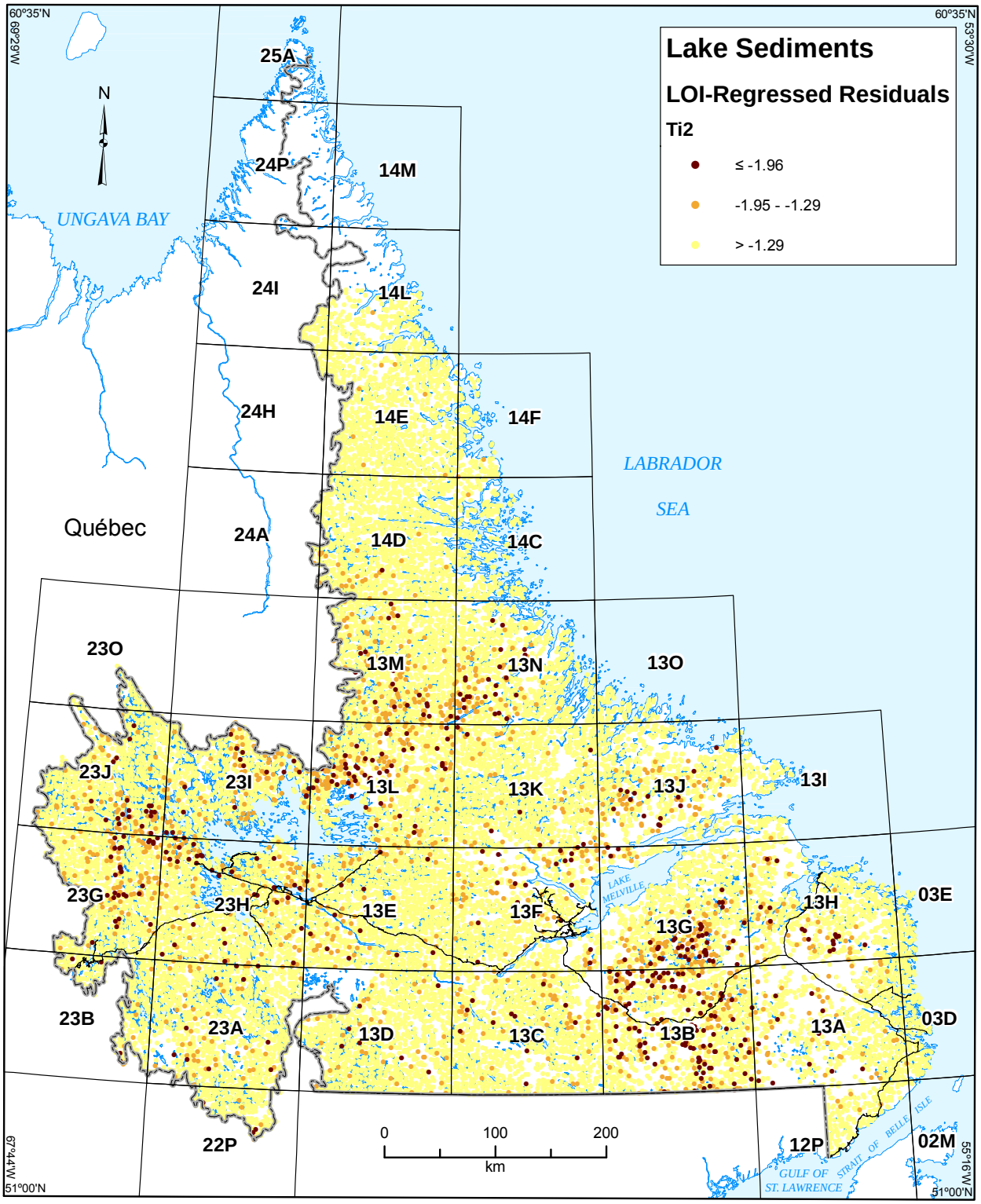


**Figure 24e.** *Standardized simple-regression residuals of Ti2 in lake sediment, Labrador, with emphasis on lowest values.*

The above two features are absent from the LOI-regression residuals (Figure 24e), which only define a concentration of low values in NTS map areas 13G/02 and 07, in common with all the other elements under consideration.

*Zirconium (Zr2)*

Grouping of samples defined by anomalous and elevated raw Zr2 values, as well as those defined by positive and negative multiple-regression residuals, are singular and distinct. The glacial dispersion train from Strange Lake, defined by raw values, extends as far as the coast, in NTS map area 14C/12 (Figure 25a); the anomaly defined by positive multiple-regression residuals (Figure 25b) is narrower and shorter, and it is clear that the regression process has in this case removed some of the anomalous response as well as the response to the clastic component in the sample (*cf.* Hf1, Figure 15b). A less homogeneous feature, as defined by anomalous raw values, extending in an east-northeastward direction from NTS map area 13M/06 to NTS 13N/15, is absent from the corresponding multiple-regression residuals and is probably an artefact of the clastic component; similar features are defined by Ba2, Hf1, K2, Nb2 and Ti2.

Unlike the dispersion from Strange Lake, the Zr2 multiple-regression residual response to the REE mineralization in the Red Wine Mountains and Letitia Lake in NTS map areas 13K/03–08, (Kerr, 2011) is homogeneous and more extensive than that defined by raw values. A separate, eastward-trending feature, possibly indicating a dispersion train, approximately 50 km long, from a source in the southeastern corner of NTS map area 13L/10, can also be discerned; this is absent from the raw values.

In western Labrador, the sample groupings defined by raw values and positive multiple-regression residuals of Zr2 are similar to one another in appearance and overlie most of the Kaniapiskau Supergroup rock types; there is also a concentration of anomalous and elevated residuals south of the Smallwood Reservoir in NTS map areas 23H/09–11 and 14–16, which may represent glacial dispersion from the former.

The LOI-regression residuals of Zr2 (Figure 25c) are superior to their multiple-regression counterparts in their stronger, homogeneous response to the dispersion train from Strange Lake and to the mineralization at Flowers River. Response to the Red Wine Mountains mineralization is less extensive. The responses of both parameters in western Labrador are similar.

Samples with depleted and anomalously low Zr2 multiple-regression residuals indicate two major zones (Figure 25d). In northern Labrador, they define the Umiakovik batholith, and the probable glacial dispersion from it; the lowest residual values of Zr2 in NTS map areas 14E/02 and 14E/07 are from the same samples that returned anomalously high Hf1 multiple-regression residuals in lake sediments (Figure 15b) as well as anomalous fluoride in lake water (Amor, 2011). The association of high Hf1 and low Zr2 values in the same samples is an interesting departure from very similar behaviour that these elements normally display.

On the coast of southeastern Labrador, a regional Zr2 low extending from NTS map area 12P/06 in the south to 03E/04 in the north has one of several foci over the Chateau Pond intrusion on map area 13A/01 and the area to the east and northeast, extending as far as the coast. Multiple-

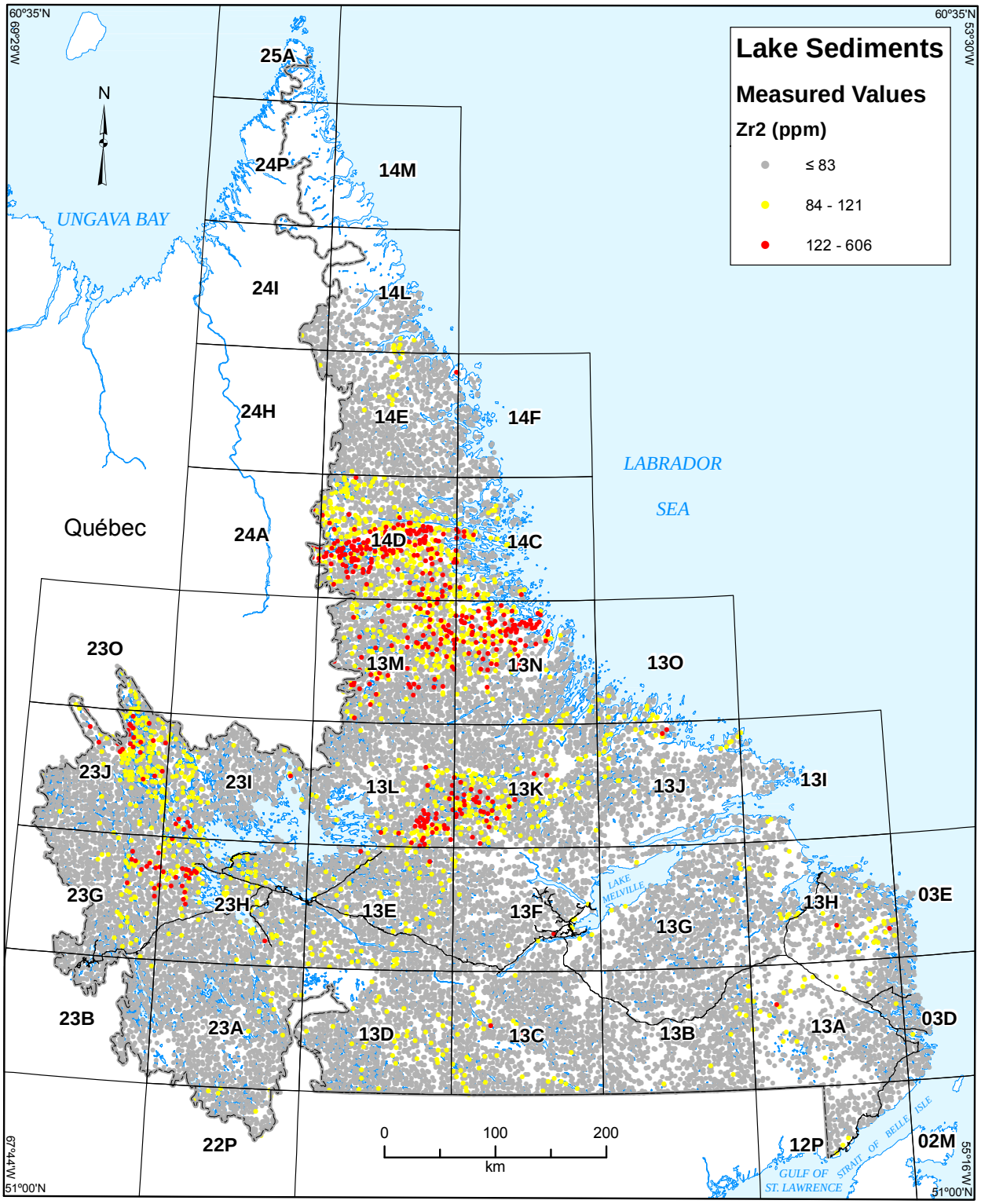


**Figure 25a.** *Measured values of Zr2 in lake sediment, Labrador, with emphasis on highest values.*

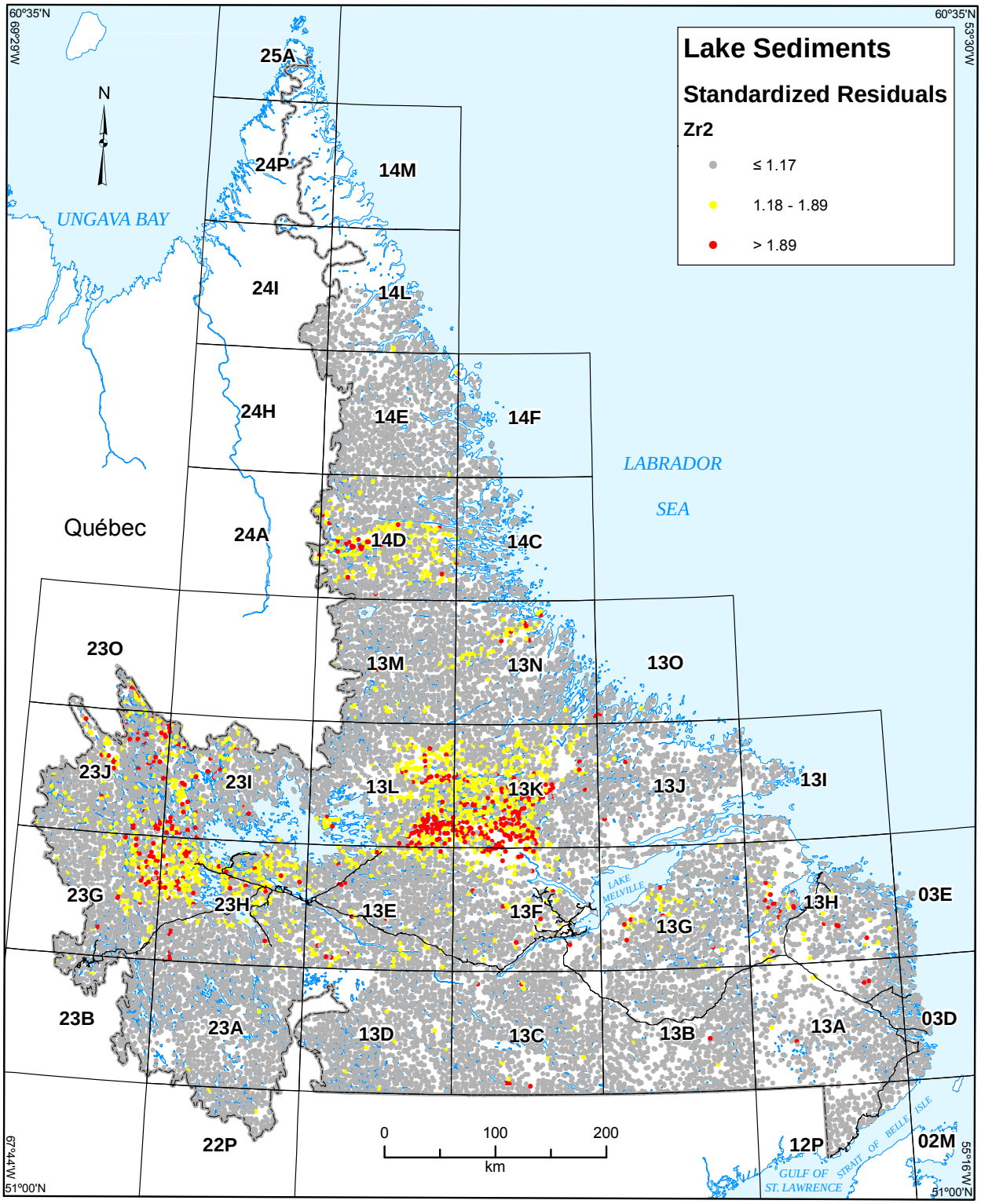


**Figure 25b.** *Standardized multiple-regression residuals of Zr2 in lake sediment, Labrador, with emphasis on highest values.*

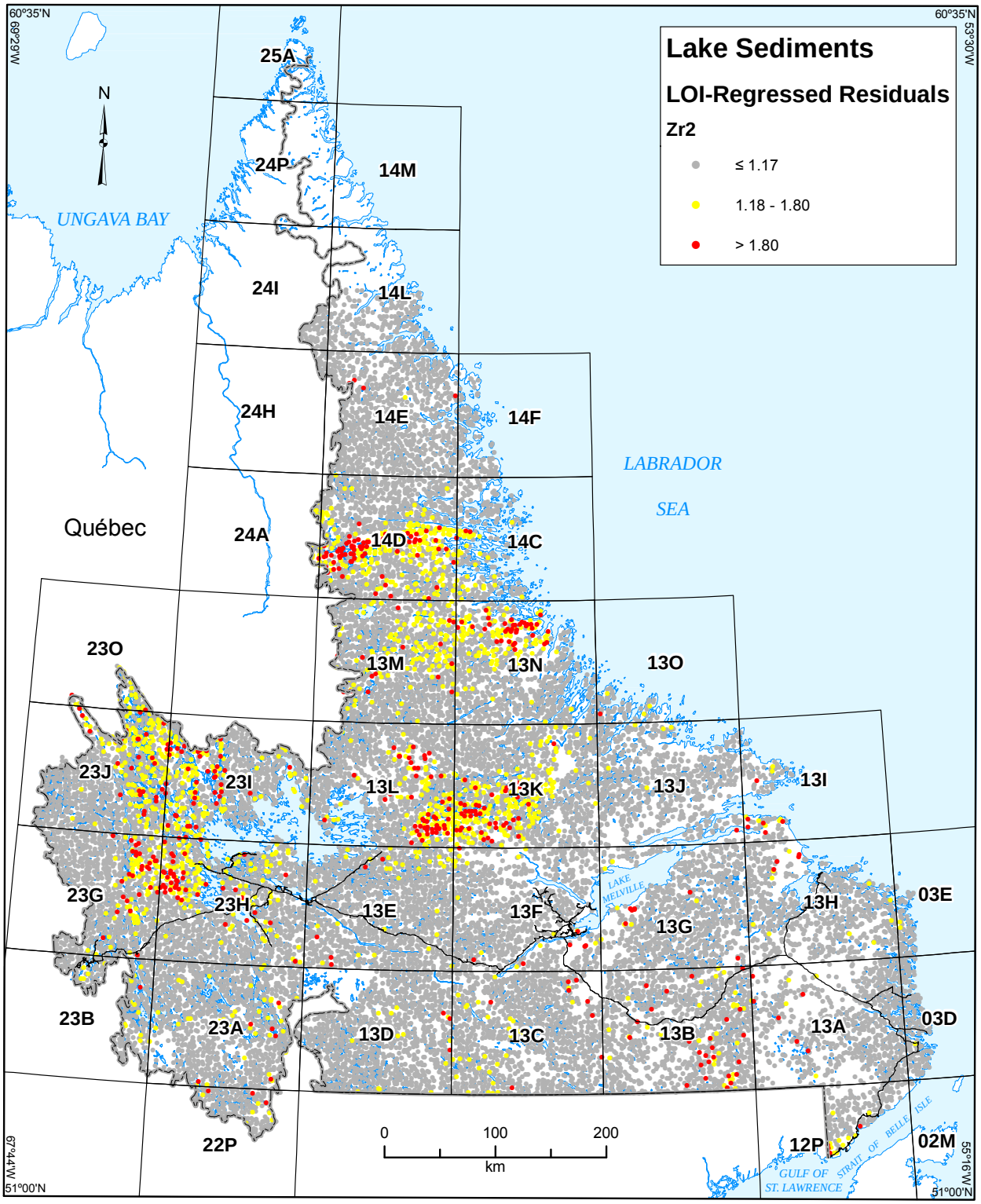


**Figure 25c.** *Standardized simple-regression residuals of Zr2 in lake sediment, Labrador, with emphasis on highest values.*

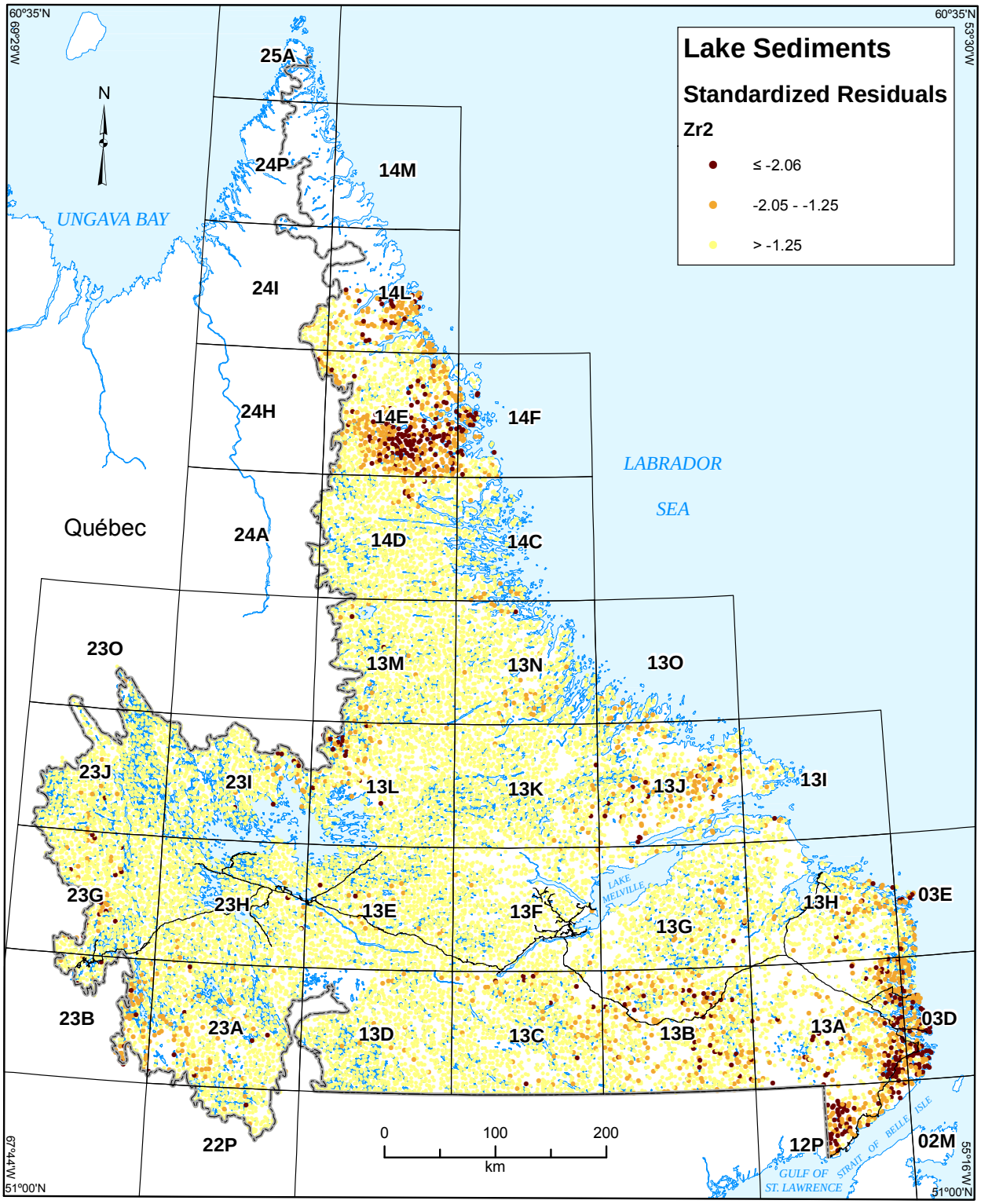


**Figure 25d.** *Standardized multiple-regression residuals of Zr2 in lake sediment, Labrador, with emphasis on lowest values.*

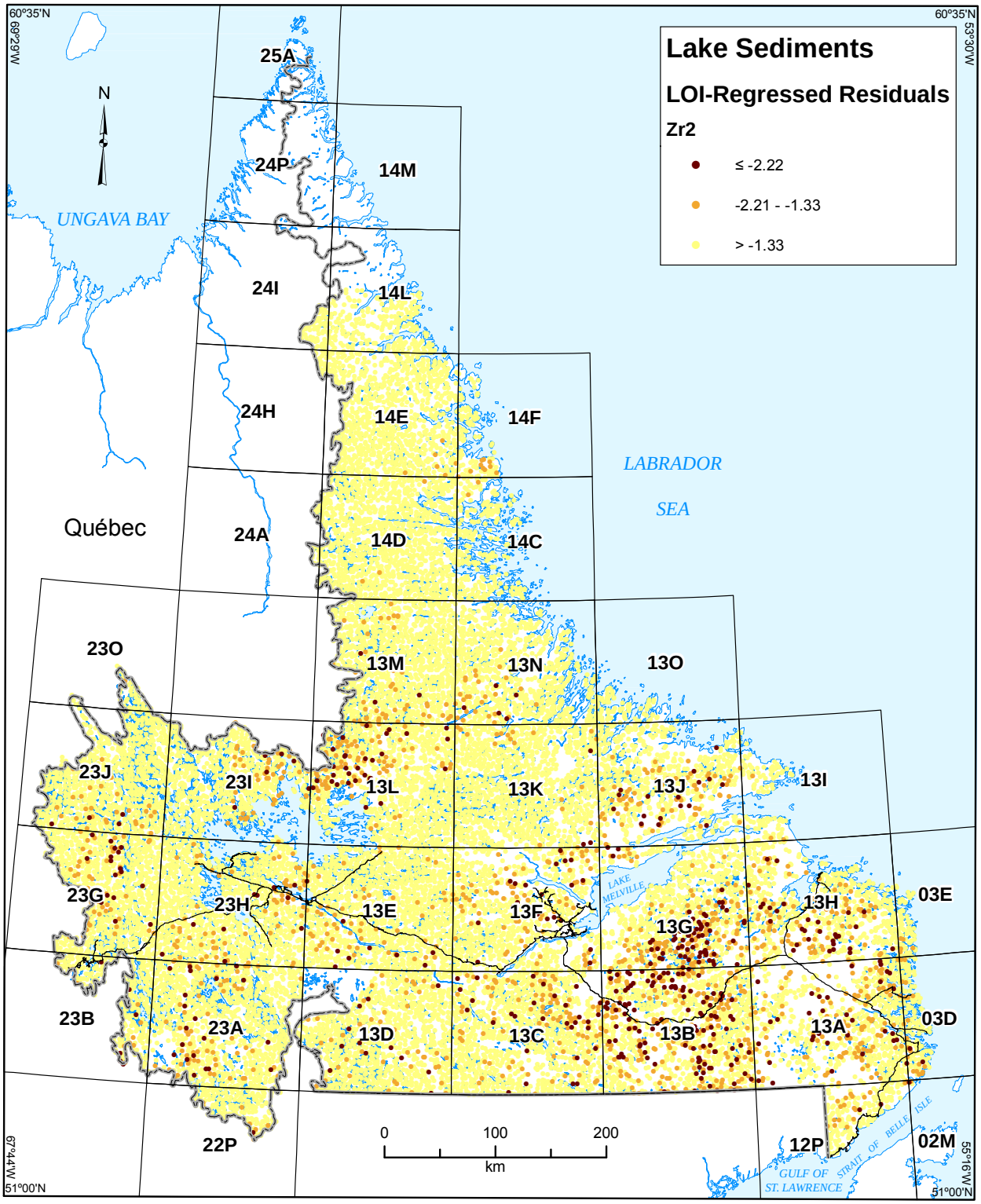


**Figure 25e.** *Standardized multiple-regression residuals of Zr2 in lake sediment, Labrador, with emphasis on lowest values.*

regression residuals of Zr2 are anomalously low on the north shore of St. Lewis Sound, although the anomaly is not as focused as the Nb2 high (Figure 20b) and Sr2 low (Figure 23d), noted previously. Finally, Zr2 multiple-regression residuals are depleted and anomalously low in the extreme south of Labrador in NTS map areas 12P/06, 07, 10, 11, 14 and 15 (Figure 25d), over late Neoproterozoic or Cambrian sediments (Units CFo and CBr) but more particularly (in this case) over older granite (Unit $M_3$Cgr) quartz monzonite (Unit $M_3$Cmg) and tonalite (Unit PMtn; Gower, 2010b). None of these features are defined by LOI-regression residuals (Figure 25e).

## DETAILED CONSIDERATION OF Ba AND Li ANOMALIES IN WESTERN LABRADOR

Attention is focused on features defined by residuals of Ba and Li in western Labrador because of the 13 elements in the clastic association, these are perceived to have the greatest economic potential, given the local geology.

### *Colville River Anomaly*

This anomaly is primarily defined by positive residuals of Ba2 (Figure 26); there is little or no anomalous response in the raw values. Most of the samples comprising the anomaly were collected over mid-Paleoproterozoic metasediments of the Sims Group: the mainly arenaceous Tamarack and Muriel formations (Ware and Wardle, 1979), assigned more generally to Unit $P_2$as by Wardle *et al*. (1997). However, despite the near-congruence of the Ba2 residual anomaly and the Sims Group outcrop, the association of Sedex-type barite mineralization with argillaceous host rocks (Lydon, 1996) suggests a more plausible source for the Ba2 in the Menihek Formation, the uppermost unit of the upper Knob Lake Group (Ware and Wardle, *op. cit.*), assigned to Unit $P_2$st (Wardle *et al*., *op. cit.*). Very few samples exhibiting anomalously high Ba2 residuals are situated to the west of the outcrop area of the Sims Group, although they do extend to the north, and south-southeast, where Menihek Formation rocks persist. To the north and west, the Ba2 regression residuals are anomalously low; this is consistent with eastward ice-movement directions described by Klassen and Thompson (1990).

There are supporting data for the lake-sediment Ba2 anomaly (Brushett and Amor, 2013). Esker-gravel samples containing barite grains were collected at six sites where rocks of the Sims Group or Menihek Formation constitute plausible (*i.e.*, up-postglacial drainage) sources; a seventh site is located over Archean rocks of the Ashuanipi Complex (Superior Province), and the sample is probably derived from the latter. Additionally, a single grain of gahnite (zinc spinel, considered to be diagnostic of metamorphosed exhalative massive-sulphide deposits) was also reported for a sample collected directly over Menihek Formation rocks in the southwest of NTS map area 23G/16.

Occurrences of Cu, Ni, Pb and pyrite mineralization are reported from Proterozoic rocks in the vicinity of the Colville River anomaly, whereas Au, Cu, Pb and pyrite occur over Archean rocks to the west. None of these occurrences constitute plausible sources for the barite (and barium). The Pb occurrences in the north (Galena Lake in NTS map area 23I/05: MODS # 023I/05/Pb 001, and Pogo Lake West in NTS 23J/08: 023J/08/Pb 001), although close to mapped outcrop of Menihek

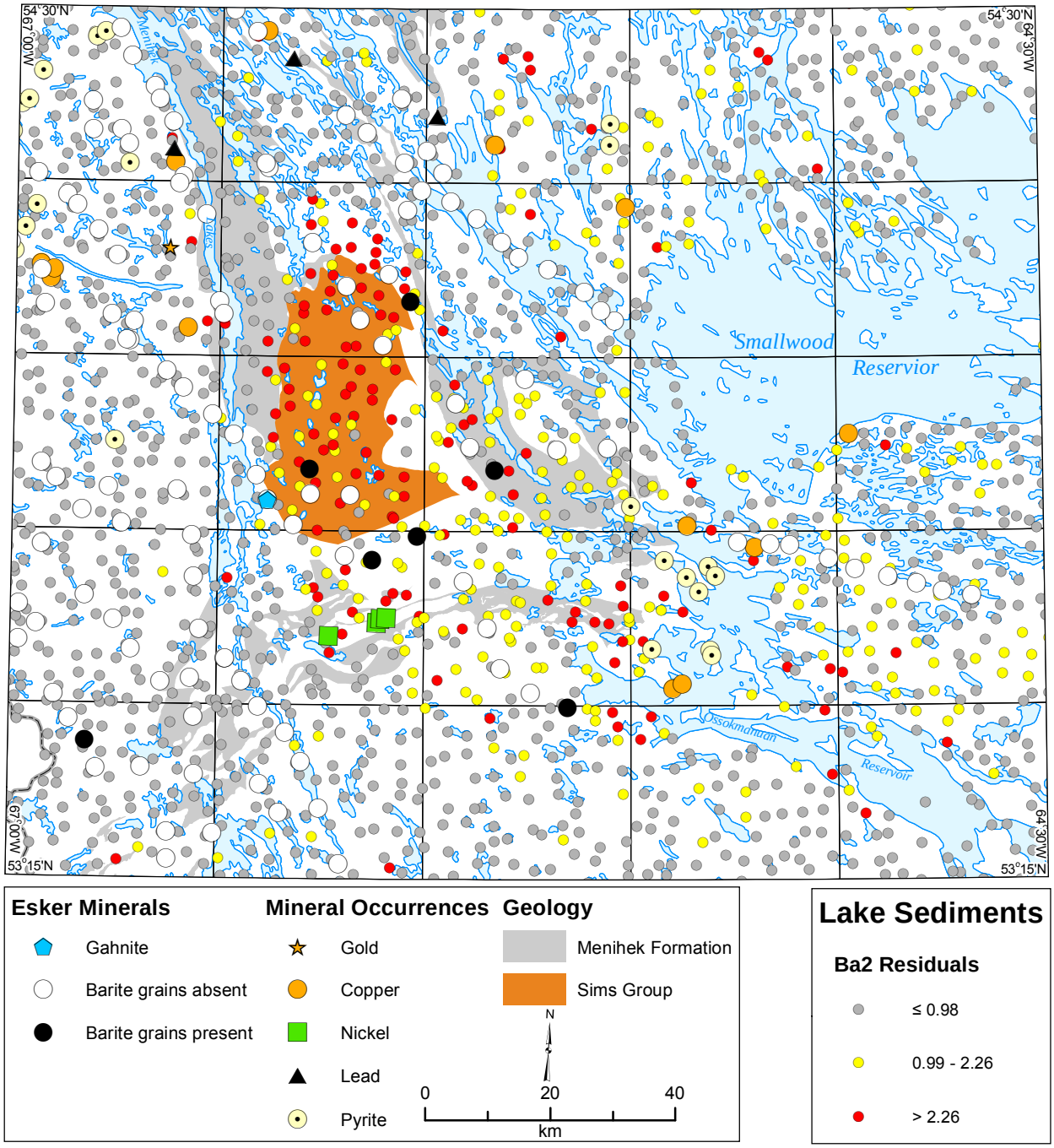


**Figure 26.** *Colville River Anomaly: Ba2 lake-sediment residuals, barite- and gahnite-bearing esker samples, and documented mineral occurrences, superimposed on mapped outcrop of the Menihek Formation and Sims Group rocks.*

Formation rocks, are reported to be volcanic-hosted. Where host geology is known, the pyrite occurrences in NTS map areas 23H/11 and 14 are hosted in argillaceous rocks, also close to Menihek Formation outcrop, although the pyrite occurrences have been assigned to the Grenville Province (MODS database; Stapleton *et al*., 2011), and such Pb and Zn analyses that were carried out were invariably undetectable.

Figure 26 shows the Ba2 lake-sediment residuals, the barite- and gahnite-bearing esker samples, and the documented mineral occurrences, superimposed on mapped outcrop of the Menihek Formation and Sims Group rocks.

Of the elements that are not in the K–Na–Ti–Mg association, anomalous and elevated values of As1 (Figure 27), Sb1 (Figure 28) and Pb2 (Figure 29) show a spatial relationship with mapped outcrop of the Menihek Formation, and although the anomalies are by no means congruent with that defined by the Ba2 residuals, they provide evidence of a chalcophile association in the argillaceous sediments. A very limited area, mostly over Menihek Formation rocks in NTS map area 23G/09 was covered by detailed sampling (McConnell, 1980). Many of the component samples were anomalous in Ag3, As1, Cd2, Pb2, Sb1, Se1 and Zn2.

*Bondurant Lake Anomaly*

Figure 30 shows Ba2 residuals from multiple-regression methods, aspects of local geology, and mineral occurrences in the area of the Bondurant Lake anomaly, within whose bounds lie the communities of Wabush and Labrador City. The anomaly is defined largely by positive residuals of Ba2, although unlike the Colville River anomaly, some raw Ba2 values are also anomalous or elevated. The most likely source for the anomaly is, once again, the Menihek Formation, consisting locally of "dark grey to black schist, phyllite and graphitic slate" (Rivers, 1985a, b, c), although many of the component samples overlie other formations: the metapelitic Attikamagen Formation, the dolomitic Denault Formation, iron formation of the Sokoman Formation and the arenitic Wishart Formation of the Knob Lake Group, as well as Shabogamo gabbro

Occurrences of Ag, Cu, Zn, graphite and kyanite occur within the bounds of the anomaly or are associated with its potential source rocks. The Duley Lake West pyritic Ag showing (MODS # 023B/15/Ag 001) occurs in narrow quartz stringers in quartzite of the Wishart Formation.

The Wetzel (MODS # 023G/02/Cu 002), North (Main) Weber (023G/02/Cu 003) and Weber Creek (023G/02/Cu 005) Cu showings are hosted in the Attikamagen, Sokoman and Menihek formations, while the South Weber showing (023G/02/Cu 004) is reported as being hosted in the Attikamagen Formation; the Macdermott Lake showing (023G/07/Cu 001) is hosted in the Menihek Formation. All consist of chalcopyrite-bearing quartz veins.

There is very little documented information on the Edluke Lake East (MODS # 023G/02/Zn 001) and Strawberry River South No. 1 (023G/02/Zn 002) Zn showings other than that the former is also enriched in Cu and U, and is hosted in graphitic slates and schist of the Menihek Formation, while the latter is enriched in V and U (Kerr *et al.*, 2013). Graphite mineralization at the Mart Lake developed prospect (MODS # 023B/14/Gf 001) consists of fine-grained quartz graphite schist, in the lower portion of the Menihek Formation near the contact with the underlying Sokoman

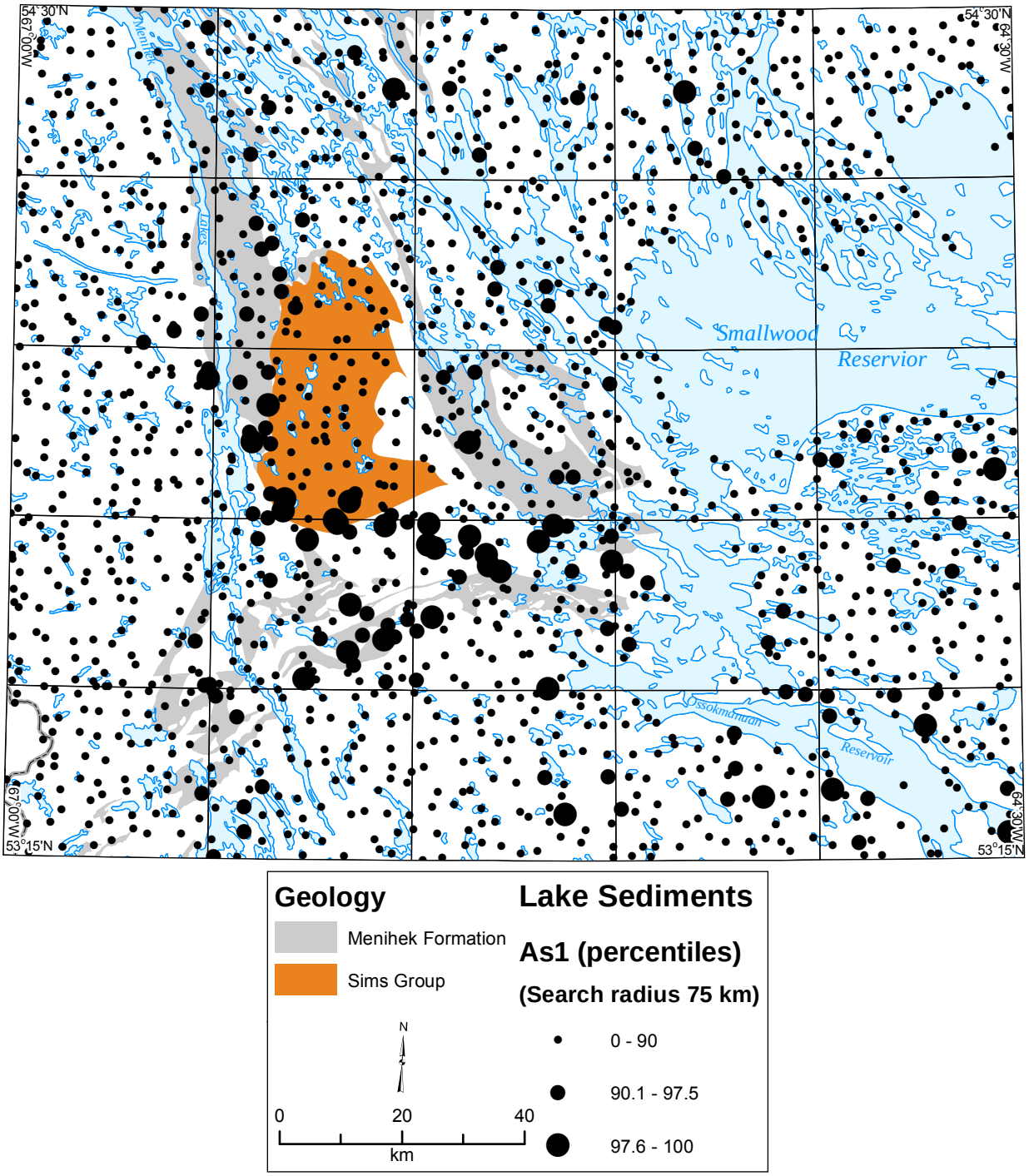


**Figure 27.** *Colville River Anomaly: Arsenic (As1) values in NGR lake-sediment samples superimposed on mapped outcrop of the Menihek Formation and Sims Group rocks.*

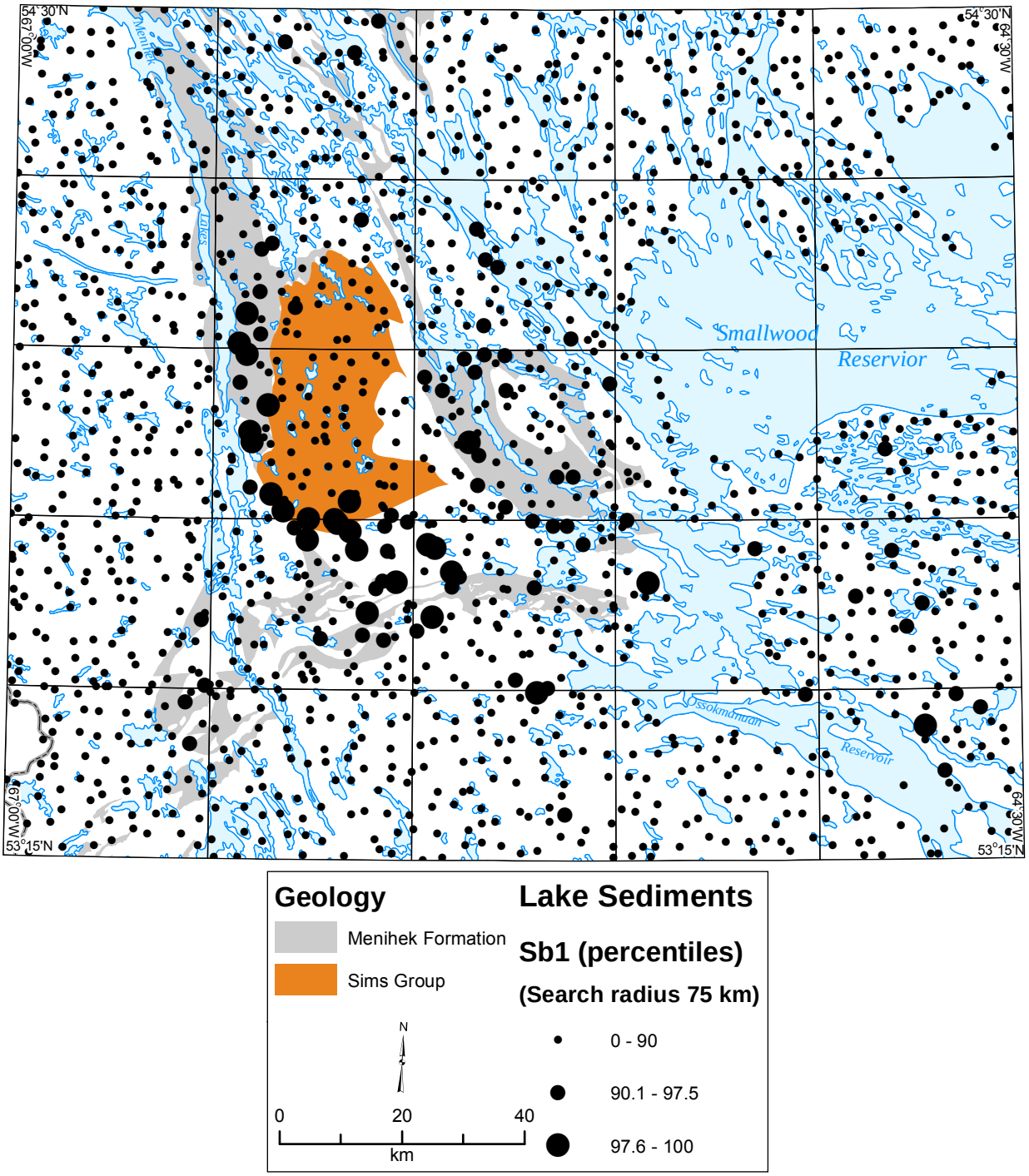


**Figure 28.** *Colville River Anomaly: Antimony (Sb1) values in NGR lake-sediment samples superimposed on mapped outcrop of the Menihek Formation and Sims Group rocks.*

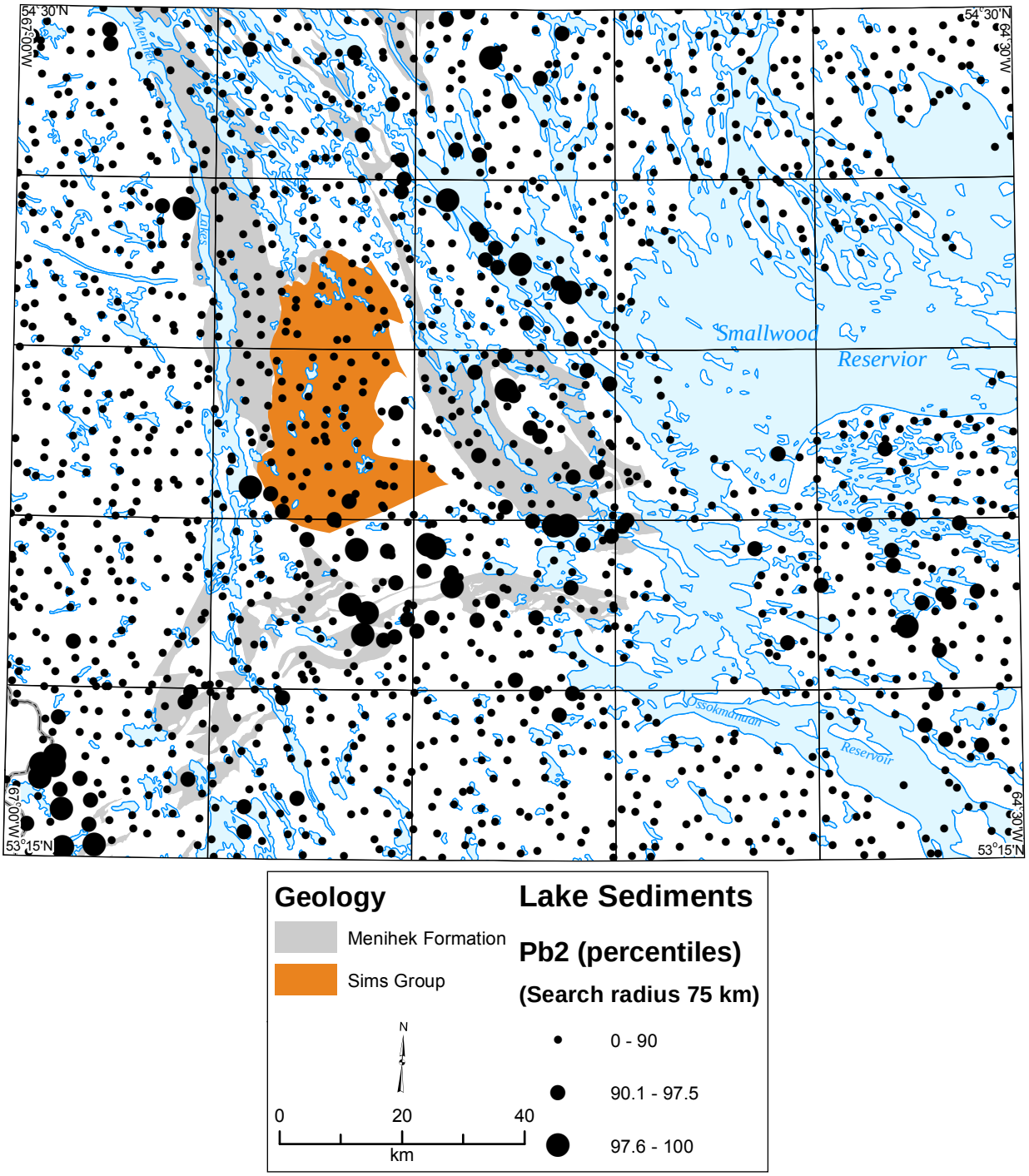


**Figure 29.** *Colville River Anomaly: Lead (Pb2) values in NGR lake-sediment samples superimposed on mapped outcrop of the Menihek Formation and Sims Group rocks.*

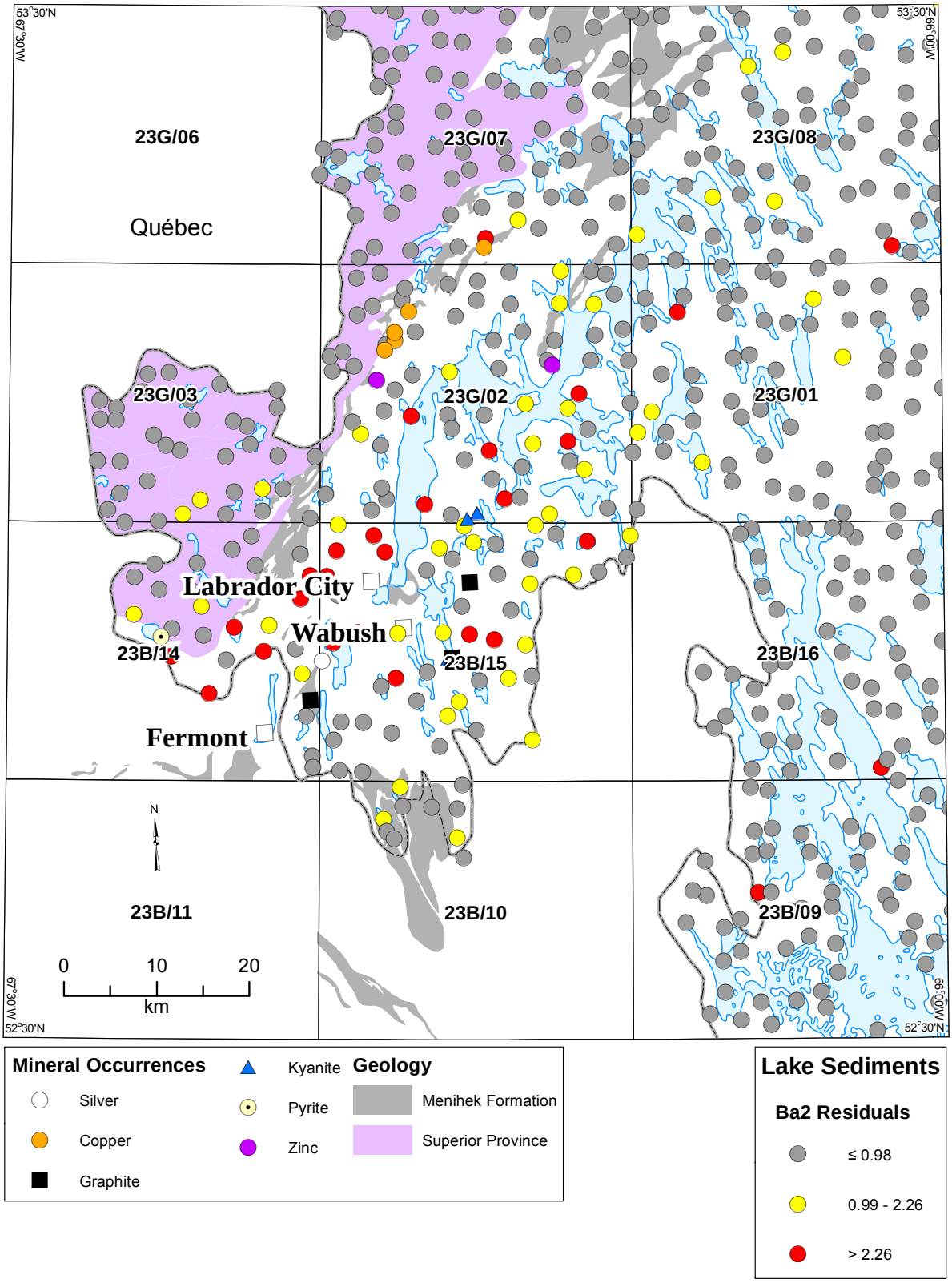


**Figure 30.** *Bondurant Lake Anomaly: Barium (Ba2) residuals in lake sediments, and documented mineral occurrences, superimposed on mapped outcrop of Menihek Lake Formation and Superior Province rocks.*

Formation. The mineralization also contains chalcopyrite and sphalerite. The Flora Lake South No. 3 (023B/15/Gf 003) and Moose Head Lake Southwest (023B/15/Gf 001) showings are both hosted in the metapelitic Attikamagen Formation, which also hosts three kyanite occurrences: the Moose Head Lake North Nos. 1 and 2 showings (023G/02/Kyn001 and 023G/02/Kyn002) and the Flora Lake South No. 2 prospect (023B/15/Kyn002).

The response defined by Mg2 residuals (Figure 31) covers a similar area to that defined by Ba2 residuals and it, too, is bounded to the west by the contact between the Menihek Formation and the Ashuanipi Complex.

Of the elements that are not in the K–Na–Ti–Mg association, there is supporting geochemical evidence in the form of Pb2 (Figure 32) and Zn2 (Figure 33) in the NGR sediments, and in the results of McConnell's (1980) detailed study, as well as Ag6 and Cd3 in the latter, which display local maxima in the area to the southeast of the outcrop of Menihek Formation. There is also some enrichment over rocks of the Ashuanipi Complex to the west, particularly in the case of Pb and Ag, which are unlikely to be derived from the Menihek Formation given that local striation directions indicate an ice-movement direction to the east or southeast.

*Thompson Lake/Michikamats Anomaly*

The contrast between raw values and positive regression residuals of any element is nowhere more striking than in the Thompson Lake/Michikamats Li2 anomaly in NTS map areas 13L/11–14. The Thompson Lake component, in the east, consists of a concentration of anomalous residuals to the southeast of the Lac Ramusio pluton, which straddles the Québec/Labrador border in NTS map area 13L/13. The Michikamats component, in the west, is centred over the Michikamats pluton in NTS 23I/09, but Li2 residuals are elevated over most of the sampled area between the two components (Figure 34).

The samples comprising the high-residual core of the Thompson Lake component were collected over lower Proterozoic and/or Archean mafic metavolcanic rocks (Unit $P_1$Amv), quartzofeldspathic gneiss and migmatite (Unit $P_1$Agn), and pelitic gneiss (Unit $P_1$Asgn); lower Proterozoic foliated granite (the Lac Ramusio pluton, Unit $P_1$gr); and mid-Proterozoic quartz monzonite (the Fazy Lake Pluton, Unit $P_2$qm), and anorthosite (the Michikamau Intrusion and Harp Lake Intrusive Suite, Unit $P_2$an; Wardle, 1993). Although it is not known how much of a role glacial processes have played in dispersing the Li2 from its source rocks, the Lac Ramusio pluton, in particular, appears to be significant in this respect.

The core of the Michikamats component is, as its name suggests, centred over the Michikamats Intrusion, an elliptical body of massive, megacrystic granite with a core of syenite in the west of NTS map area 23I/09 (James, 1994a). However, it extends in a northeastward direction over Archean granitoid gneiss and migmatite onto the Signal Hill intrusion, which straddles the Labrador/Québec border in NTS map area 23I/09 and is described as anorthosite by James (1994) and Thériault and Bilodeau (2002), and "monzonite, charnockite, granite" (like the Michikamats Intrusion) by Wardle *et al*. (1997).

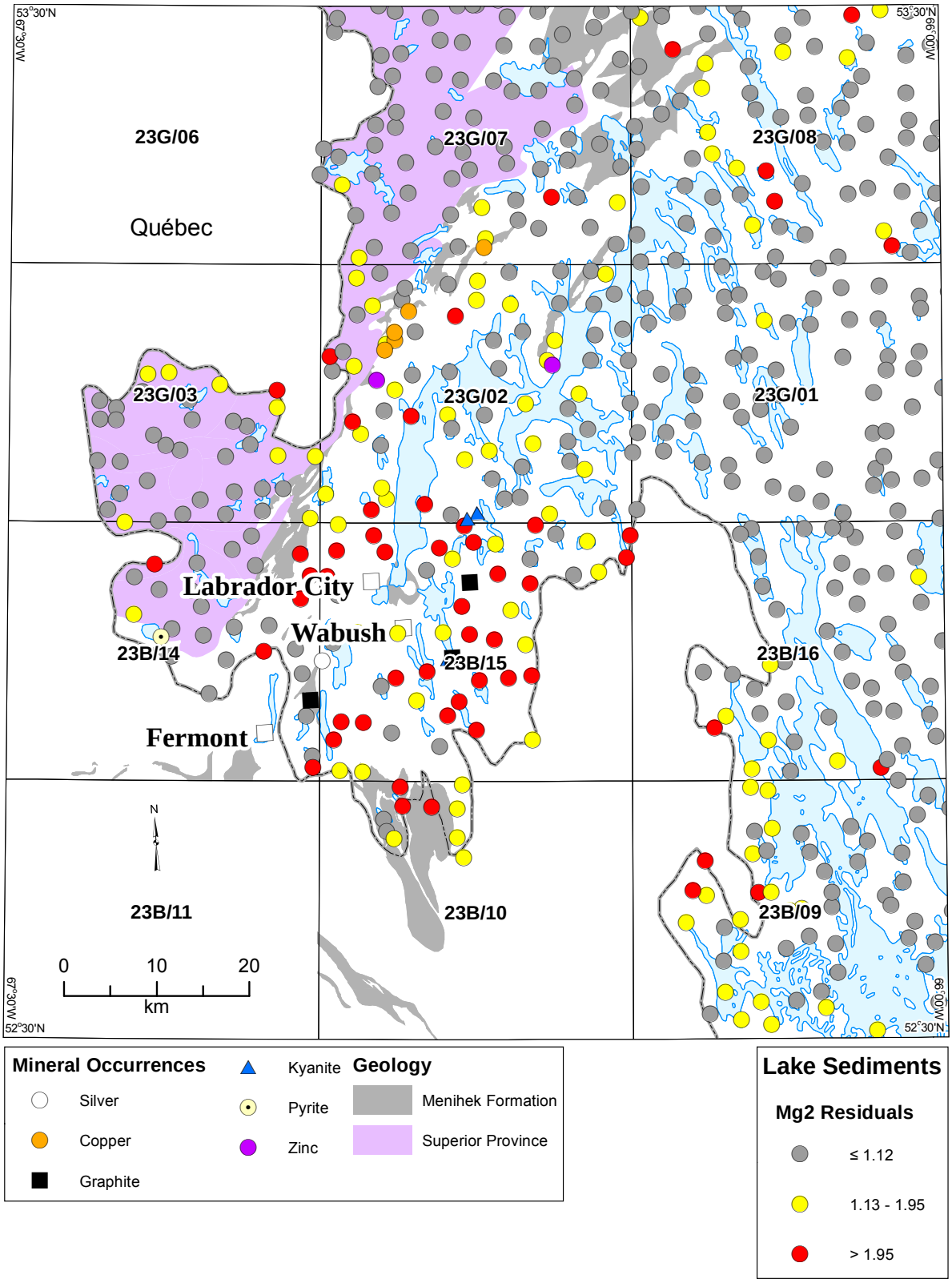


**Figure 31.** *Bondurant Lake Anomaly: Magnesium (Mg2) residuals in lake sediments, and documented mineral occurrences, superimposed on mapped outcrop of Menihek Lake Formation and Superior Province rocks.*

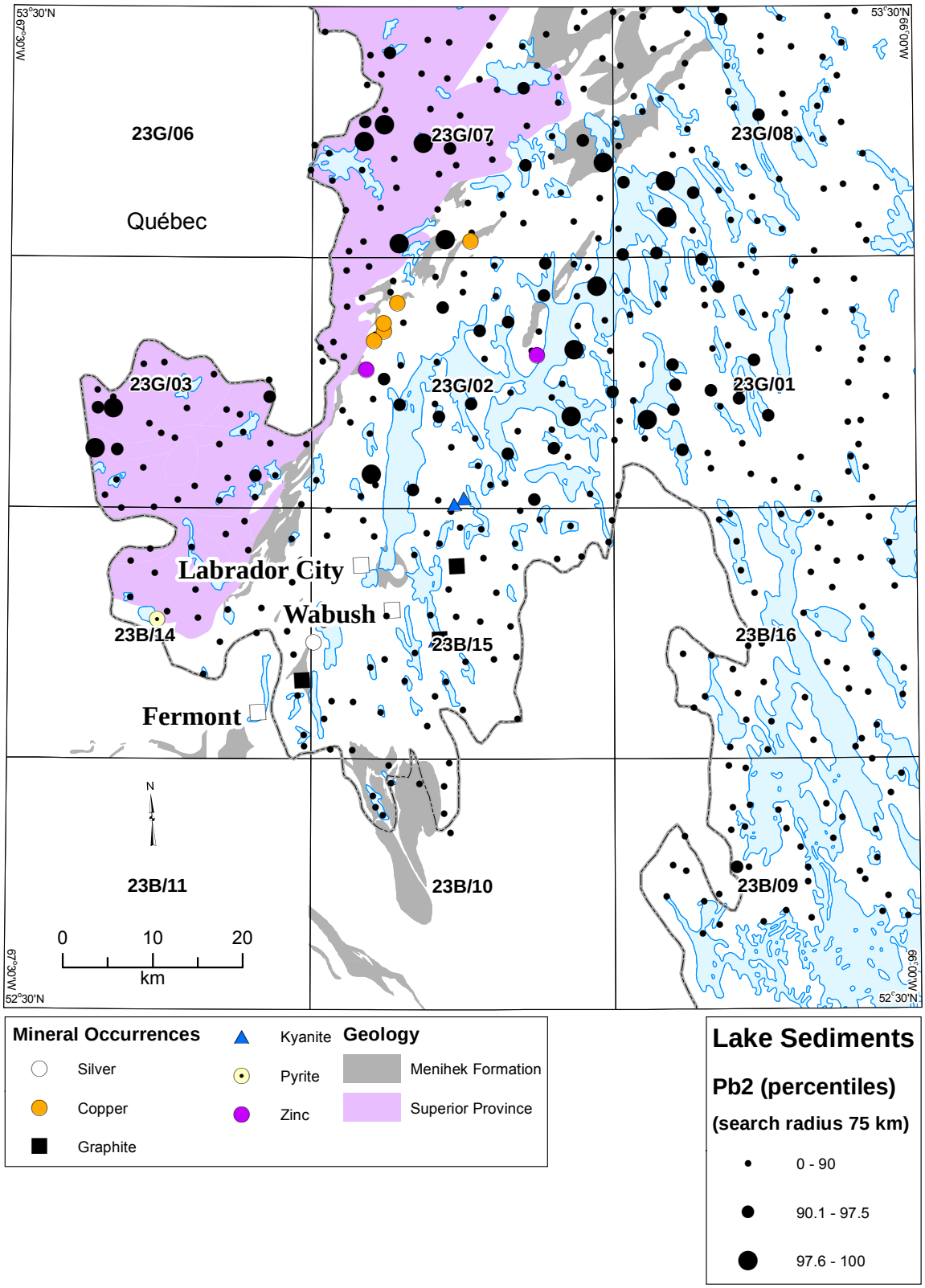


**Figure 32.** *Bondurant Lake Anomaly: Lead (Pb2) values in lake sediments, and documented mineral occurrences, superimposed on mapped outcrop of Menihek Lake Formation and Superior Province rocks.*

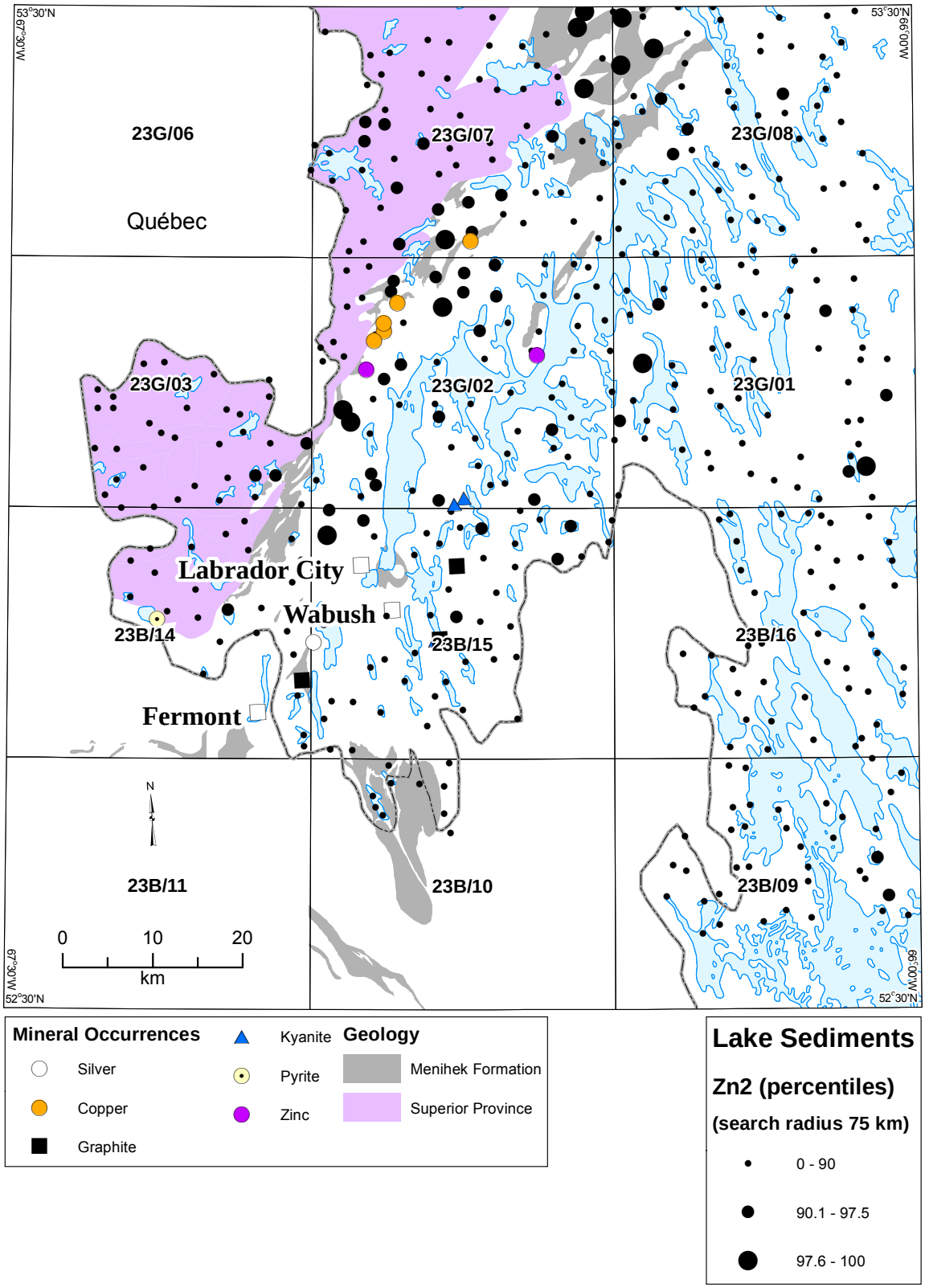


**Figure 33.** *Bondurant Lake Anomaly: Zinc (Zn2) values in lake sediments, and documented mineral occurrences, superimposed on mapped outcrop of Menihek Lake Formation and Superior Province rocks.*

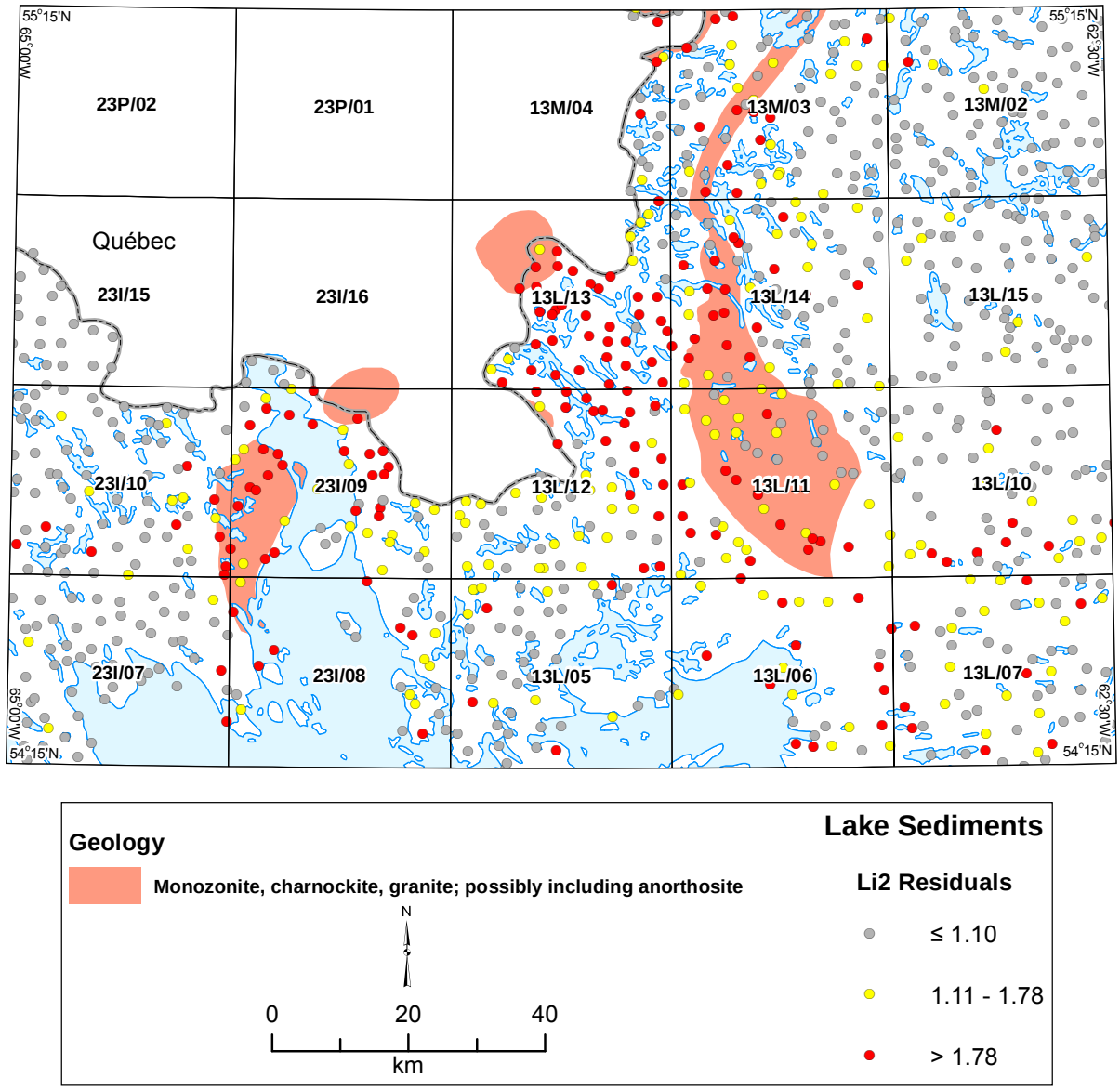


**Figure 34.** *Thompson River/Michikamats Anomaly: Lithium (Li2) residuals.*

The Ross Lake and Gossan 172 Ti showings (MODS #s 013L/14/Ti 001 and 013M/03/Ti 001) are the only documented mineral occurrences within the bounds of the Thompson Lake/Michikamats anomaly, and several Cu (± Ni) occurrences in the southeast of NTS map area 13M/03; all are hosted within the Harp Lake Intrusive Suite (Emslie, 1980) and are unlikely to be related to the Li enrichment.

Within the bounds of the Thompson Lake/Michikamats anomaly, anomalous Li contents in lake water were reported by Amor (2013a), particularly in the northern part of NTS map area 23I/09 against the Labrador/Québec border, along with anomalous responses of Mo2, Li2, Th1, La1 and La2 in sediment, and fluoride in water, with weaker responses in Ce1, Ce2, Mo1, Eu1, Tb1, Sm1, Dy2 and Cs1 in sediment and K, S and Y in water. Lake sediments and waters over the Michikamats Intrusion are anomalous in a number of REE, and REE pathfinders such as fluoride (Figure 35) and Mo (Amor, 2010; McConnell, 1988). Although Li analyses were not carried out in the McConnell(1988) study, lake-water samples collected over the eastern and western edges of the intrusion in later studies (Amor, 2013a, b) are highly anomalous in Li2.

## DISCUSSION

### *Significance of the Groupings of Samples Defined by Residuals*

That the value of one element in the clastic association can be predicted from the values of others, by simple or multiple regression, is an interesting statistical conclusion. It is also of interest that some of the regression residuals, when plotted, show good spatial correlations. Although some of the sample groupings thus defined have only been postulated as indicators of hitherto-unknown mineralization, there are a number of others whose relation to singular, already-known geological or geomorphological features is hard to dispute. These include several zones, defined by multiple-regression residuals: of Mg2 and Sc2, that delineate precisely the contact between the gabbroic and troctolitic zones of the Kiglapait Intrusion; within the Harp Lake Intrusive Suite, the dispersion train in Mg2 (enrichment) and Ti2 (depletion) associated with the Strange Lake REE-RM deposit; and the Nb2 residuals that characterize the Chateau Pond granite. Simple regression is generally not as effective, although anomalously low LOI–regression residuals of Nb2 define granite of the De Pas batholith in western Labrador.

Other zones have independent geochemical confirmation; for example, an anomaly of fluoride in lake water and REE in sediment over the Umiakovik pluton in northern Labrador, associated with a ring-shaped magnetic anomaly (Amor, 2011) is also characterized by a congruent anomaly of positive Hf1 and negative multiple-regression Zr residuals identified during the current study.

### *Universality of the Clastic Associations*

Examination of inter-element correlations in lake-sediment data, on the Island of Newfoundland and from elsewhere in the Canadian Shield (Amor, unpublished data, 2014) indicates that the element association described in the current study is widespread. However, the NGR samples from Labrador are the only ones that have been subjected to such a wide array of analyses, and of the 13 elements in the clastic association identified in the current investigation, only

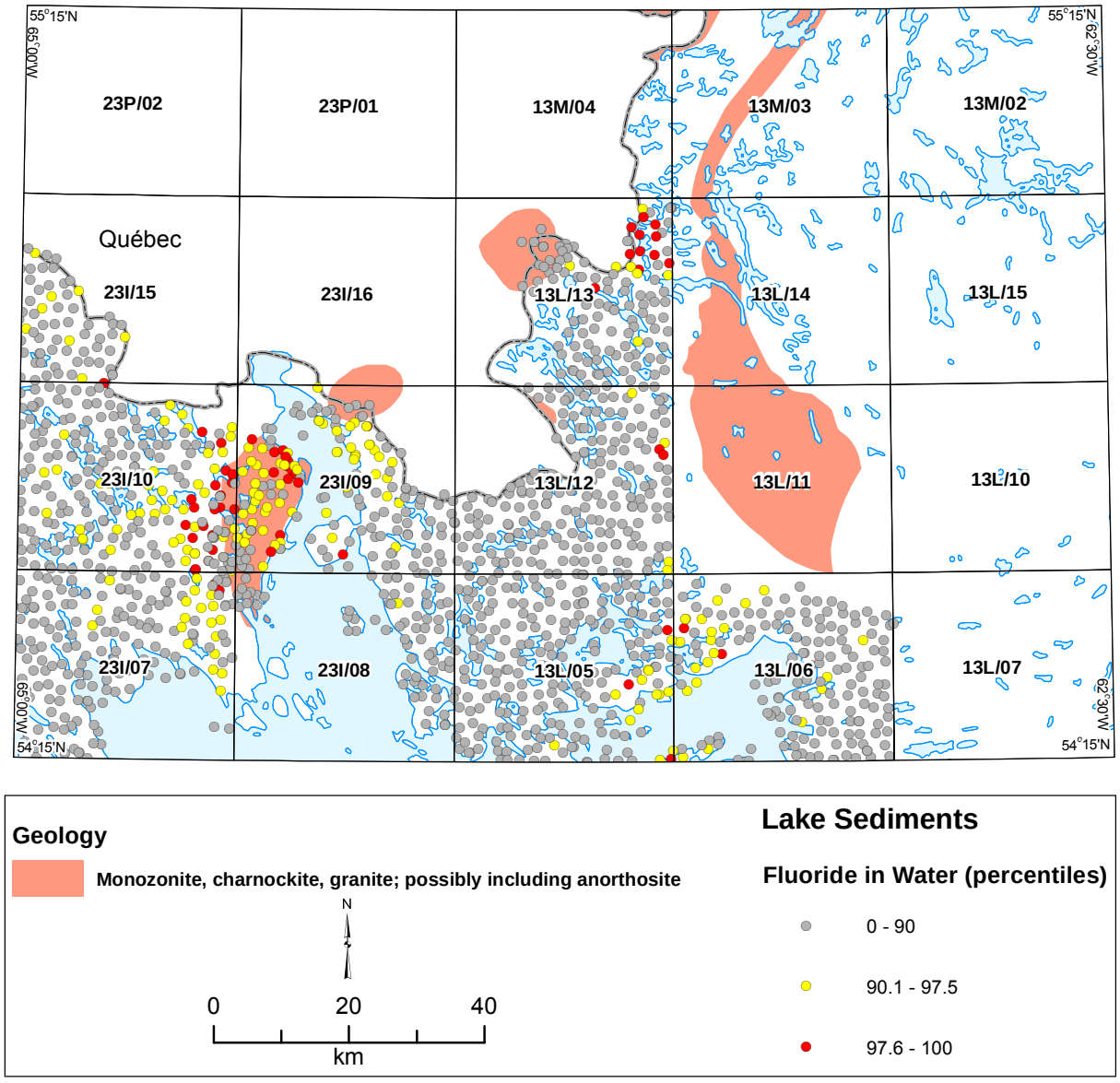


**Figure 35.** *Thompson River/Michikamats Anomaly: Fluoride in lake water.*

Hf1 and Rb1 are included in the more generally (although not universally) available INAA suite. Acceptable INAA analyses are also available for Ba, Na and Sc, although they were omitted in favour of ICP-ES analyses of the same elements in the current study because the latter have generally lower detection limits. Still, any study of element associations in lake sediments from elsewhere in Canada would be subject to the limitation that the association is represented by a smaller (and possibly rather different) suite of elements from that described here. Nevertheless, studies similar to the current one could probably be carried out and the results compared with those of the current study.

With the partial exception of F (absent from the clastic association only in the northern Labrador data subset), all of the elements in the clastic association were analyzed during the second or third phase of analyses, so that the association would likely not have been recognized during initial study of the lake-sediment data. However, a significant number of the elements associated with the more widely documented phenomenon of co-precipitation with Fe and Mn hydroxides were analyzed during the initial phase of the program, allowing for its earlier recognition.

*Role of Factor Analysis*

The application of factor analysis in the current investigation involves the characterization of an element association in terms of elements, the absolute value of whose loadings exceeds 0.5. This provides an objective and consistent means of identifying the important elements in an association: a task for which a graphical correlation matrix (e.g., Figure 1) is not as suitable, despite its intuitive visual appeal. Although methods exist to automate and accelerate the process, the routine application of factor analysis to evaluate the relationship between the variables in a multi-element dataset is inevitably a time-consuming business. In the current investigation, the Labrador dataset was split up into four subsets to identify the elements that feature consistently in the clastic association. A more thorough evaluation of the data would require splitting the data up into smaller subsets, and subjecting each to the process of cross-validation to identify appropriate factor models.

Other workers have employed a combination of factor and regression analysis in pursuit of similar goals to that of the current investigation. Closs and Nichol (1973) used stream-sediment factor scores as independent variables in regression against the raw geochemical variables from which the factor scores were derived, and concluded that the regression residuals thus derived provided a better indication of mineralization than the raw analytical values. This approach (Amor, unpublished data, 2014) has resulted in similar results, in terms of the anomalies thus delineated in the NGR data, to the use of uncombined elements as independent variables, as described in the current investigation. However, it suffers from at least three drawbacks: first, the estimation of the expected value of an element (and, consequently, of its residual) using the element itself, even in combination with other elements, is not unbiased; second, factor analysis is less widely used, and understood, than is regression analysis; and third, regression analysis is more readily incorporated into a GIS application: an extension of the current investigation that may prove rewarding.

The results of the factor analysis suggest that the relationship between the clastic elements and LOI are not entirely complementary: a conclusion supported by the different results of using the former and the latter as independent variables in regression analysis.

*Advantages of Residuals over Raw Values*

It would be an overgeneralization to state that regression residuals, as calculated in the current investigation, are the only parameters that show a response to variations in bedrock composition. Examples where a response to bedrock composition is, with the benefit of hindsight, visible in the raw lake-sediment values include Al2, Mg2 and Ti2 over the Harp Lake Intrusive Suite and the Kiglapait Intrusion; Hf1, Nb2, Sc2 and Zr2 over the dispersion train from Strange Lake; and Zr2 in the dispersion train from the REE-RM mineralization in the Red Wine Mountains. However, for most of these elements there are other features that are not bedrock-derived. Therefore, because the responses to these bedrock features compete with the 'noise' created by artefacts of the clastic contribution, they would be unlikely, in isolation, to draw attention to the geological features they represent. Furthermore, other features of undoubted geological significance, such as the Mg and Ti multiple-regression residual signatures of the glacial dispersion train from Strange Lake, the Nb2 multiple-regression residual anomaly over and to the northeast of the Chateau Pond granite in southeastern Labrador, and the the grouping of samples defined by low LOI–regression residuals of the same element over the De Pas granite in western Labrador (Figure 20e), are not apparent at all in the raw values of the respective elements.

*Economic Significance and Exploration Potential*

The clastic association in Labrador lake sediments includes some elements that are unlikely to be present in economic quantities in any Labrador rocks (Al, K, Mg, Na, Sr), elements of limited industrial application (Hf, Rb, Sc), and potentially economic elements (Ba, Li, Nb, Ti, Zr). Of the last group, the Ba and Li anomalies in western Labrador appear to be of the most interest, particularly the former, because they are indicated by both simple- and multiple-regression residuals. The Colville River (Ba) anomaly has the greatest residual exploration potential since there is no evidence that its potential source has been prospected at all east of Menihek Lake in NTS map areas 23G/16, 23J/01, 07 and 08. Prospecting in NTS map area 23G/09 has been mainly directed toward sandstone-hosted uranium, and magmatic Ni–Cu mineralization in the Shabogamo Gabbro.

The Colville River anomaly is also greatly strengthened by the supporting information from the 2012 esker-sampling program, which revealed barite at six locations and gahnite (Zn spinel), albeit one grain only, at one (Brushett and Amor, 2013). The latter is considered an important pathfinder for metamorphosed volcanic- and sedimentary-exhalative massive sulphide (Sedex) deposits (Averill, 2001). The argillaceous Menihek Formation constitutes a potential source for the latter deposit type, which typically hosts barite also, at least in deposits younger than 1.67 Ga in age (Lydon, 1996). Because the anomaly is largely congruent with the outcrop of the slightly younger, arenaceous Tamarack River and Muriel formations of the Sims Group, it was previously ascribed to these rocks (Brushett and Amor, *op. cit.*), but the Menihek Formation constitutes a more plausible source and has been proposed previously as a potential Sedex host (Wardle *et al.*, 1995, page 32).

The Bondurant Lake (Ba) anomaly has less residual exploration potential than the Colville River anomaly because it lies in an area with extensive exploration history, albeit mostly for iron, magmatic Ni–Cu, uranium and various industrial minerals. Nevertheless, some of the company

airborne geophysical data acquired during these programs, now in the public domain, may draw attention to untested features within the Menihek Formation.

Other than the results of other lake-sediment and lake-water surveys in the area, there is little supporting information for the economic potential of the Thompson Lake/Michikamats (Li) anomaly and it may represent exceptionally high Li background in the alkaline intrusions and their country rocks, rather than mineralization. Any follow-up prospecting should be focused on pegmatite or aplite veins.

*Relative Merits of Simple and Multiple Regression*

It is not possible to state definitively that one of the two regression methods is effective at isolating the bedrock- or till-related component of the lake sediments' composition in the elements of the clastic association, while the other is not. Although more of such features are delineated by multiple-regression residuals than their LOI–regression counterparts, certain features are manifest only in the latter. The reason for this is not known.

Residual features delineated by both methods are clearly the ones most likely to be representative of real variations in the composition of the source material of the sediment, whether the latter consists of bedrock, or glacially transported material. One such feature is the Colville River anomaly, defined primarily by Ba2 in the form of a strong, homogeneous multiple-regression anomaly, and a more dilute but essentially congruent LOI–regression anomaly. The Thompson Lake/Michikamats (Li) anomaly only has an expression in multiple-regression residuals; although the anomaly is homogeneous and laterally extensive, the absence of a feature defined by LOI–regression Li2 residuals makes it less striking.

The different results achieved when the 'clastic' elements are regressed against each other, or against LOI, indicate that whatever process the clastic-element association represents, it is not directly complementary to the amount of organic material (of which the LOI content is a reasonable first approximation); this confirms the impression gained from results of the factor analysis of lake-sediment data from four regions of Labrador.

## CONCLUSIONS

Certain elements in lake sediments from Labrador show a high level of intercorrelation suggesting that they are largely controlled by a single process. These elements comprise Al, Ba, Hf, K, Li, Mg, Na, Nb, Rb, Sc, Sr, Ti and Zr, which correlate strongly with one another in subsets of the Labrador data from southeastern, south-central, southwestern and northern Labrador, and are referred to as 'clastic elements'. The correlation of Be, Br, Ca, Cr, F, Fe, Hg, LOI, Mn, Pb, Th and V with the former elements, and with each other, is weaker, but still significant. The natural property giving rise to the co-association of these elements is believed to be the amount of inorganic clastic material in the sample, because samples rich in such material show demonstrably higher concentration levels in these elements, in comparison to their organic-rich counterparts. The element association, and the process it is believed to represent, are largely independent of the bedrock source of the sediments, and in most cases strong enough to mask any bedrock response.

The correlations between the elements in the first (Al to Zr) association are so strong that it is possible to predict the value of any one element in a sample, from the values of the other twelve, with a fair degree of accuracy. At the scale of Labrador, geochemical symbol plots of predicted and real values are on initial examination indistinguishable. Such differences as do exist constitute attributes of the lake sediments' composition that cannot be explained in terms of this process alone, and it is postulated that many of these represent local variations in composition of local bedrock, possibly including mineralization, or the glacial sediments derived from it.

It is also possible to predict the value of each of these elements using LOI alone. This is to be expected, because this parameter is considered an approximate measure of the organic (*i.e.* non-clastic) content of the sediment. However, the predictive power of LOI is not as great as that of the elements themselves; this suggests that the inorganic content of the sediment, as modelled by the content of the clastic elements, and the organic content, as represented by LOI, are not entirely complementary.

The discrepancies (positive or negative) between real and regression-predicted values of these elements can be quantified in the form of residuals. When plotted as geochemical symbol maps, the residuals show responses to a number of known geological features, including the Kiglapait Intrusion (K, Mg, Na, Sc, Ti), the Harp Lake Intrusive Suite (Al, Mg, Sc), the dispersion train from the Strange Lake REE-RM deposit (Mg, Ti), and the Chateau Pond and De Pas granites (Nb). They also form unexplained features of which the Ba anomalies at Colville River and Bondurant Lake, and the Li anomaly at Thompson Lake/Michikamats are of the greatest significance.

In conclusion, with the recent ICP-OES analyses of the entire Labrador NGR sample archive, much remains to be discovered in these data, particularly if the effects of non-geological agencies are quantified and compensated. Regression analysis offers a practical method of achieving this. A modification of the technique is applicable to lake-sediment data from Newfoundland, and elsewhere in Canada.

## ACKNOWLEDGEMENTS

Early versions of this report were critically reviewed by Andrew Kerr, John McConnell and Martin Batterson.

## REFERENCES

The reference list has been subdivided into three sections: General References, References to Geological Maps and Reports and References to NGR lake geochemical data releases.

*General References*

Amor, S.D

2010: Lake-sediment and water-sampling survey in the Knox Lake region, western Labrador. *In* Current Research, Government of Newfoundland and Labrador, Department of Natural Resources, Geological Survey, Report 10-1, 2010, pages 111-117

2011: An untested rare-earth element target in northern Labrador. Government of Newfoundland and Labrador, Department of Natural Resources, Geological Survey, Open File 14E/0229, 2011, 45 pages.

2012: A filtering technique for identifying local maxima in regional geochemical data sets. Government of Newfoundland and Labrador, Department of Natural Resources, Geological Survey, Open File NFLD/3167

2013a: A high-density lake-sediment and water survey in the Fraser Lake region, western Labrador (NTS map areas 13L/05, 06, 12, 13, 23I/08 and 09). Government of Newfoundland and Labrador, Department of Natural Resources, Geological Survey, Open File LAB/1616, 2013, 215 pages.

2013b: A high-density lake-sediment and water survey in the Knox Lake region, western Labrador (NTS map areas 023I/06, 07, 10, 11, 12, 13, 14 and 15). Government of Newfoundland and Labrador, Department of Natural Resources, Geological Survey, Open File 23I/0101, 2013, 239 pages.

Brushett, D. and Amor, S.
2013: Kimberlite-indicator mineral analysis of esker samples, western Labrador. Government of Newfoundland and Labrador, Department of Natural Resources, Geological Survey, Open File LAB/1620, 58 pages.

Chao, T.T. and Theobald, P.K. Jr.
1976: The Significance of Secondary Iron and Manganese Oxides in Geochemical Exploration. Econ. Geol, Volume 71, pages 1560-1569.

Closs, L.G. and Nichol, I.
1975: The Role of Factor and Regression Analysis in the Interpretation of Geochemical Reconnaissance Data. Canadian Journal of Earth Sciences, Volume 12, pages 1316-1330.

Davis, J.C.
1973: Statistics and Data Analysis in Geology. John Wiley and Sons, 550 pages.

Kerr, A.
2011: Rare-earth-element [REE] mineralization in Labrador: a review of known environments and the geological context of current exploration activity. *In* Current research, Government of Newfoundland and Labrador, Department of Natural Resources, Geological Survey, Report 11-1, 2011, pages 109-143.

Kerr, A., Walsh, J.A., Sparkes G.W. and Hinchey, J.G.
2013: Vanadium potential in Newfoundland and Labrador: A review and assessment Current Research (2013) Newfoundland and Labrador Department of Natural Resources, Geological Survey, Report 13-1, pages 137-165

Klovan, J.E.,
1968: Selection of Target Areas by Factor Analysis: Paper Presented at the Symposium on Decision-Making in Exploration, January 26th 1968; reprinted in The Western Miner, February 1968, pages 44-54.

Koch, G.S. Jr. and Link, R.F.
1970: Statistical Analysis of Geological Data, Volume II. Dover, 438 pages.

Lydon, J.W.
1996: Sedimentary Exhalative Sulphides (Sedex). *In* Geology of Canadian Mineral Deposit Types, Eckstrand, O.R., Sinclair, W.D and Thorpe, R.I., Editors. Geological Survey of Canada, Geology of Canada, No. 8, pages 130-152.

McConnell, J.W.
1976: Geochemical dispersion in wallrocks of Archean massive sulphide deposits. Unpublished M.Sc thesis, Queen's University, 230 pages.

1980: Detailed lake sediment, water and radiometric surveys of 14 base metal and uranium anomalies in Labrador. Government of Newfoundland and Labrador, Department of Mines and Energy, Mineral Development Division, Open File LAB/0224, 1980, 37 pages.

1988: Lake sediment and water geochemical surveys for rare metal mineralization in granitoid terranes in Churchill Province, Labrador. Government of Newfoundland and Labrador, Department of Mines, Mineral Development Division, Open File LAB/0772, 107 pages.

2009: Complete geochemical data for detailed-scale Labrador lake surveys, 1978-2005. Government of Newfoundland and Labrador, Department of Natural Resources, Geological Survey, Open File LAB/1465, 25 pages.

McConnell, J.W. and Batterson, M.J.
1987: The Strange Lake Zr-Y-Nb-Be-REE deposit, Labrador: A geochemical profile in till, lake and stream sediment, and water. *In* Geochemical Exploration 1985, R.G. Garrett, *Editor.* Journal of Geochemical Exploration, Volume 29, pages 105-127.

McConnell, J.W. and Finch, C.
2012: New ICP-ES geochemical data for regional Labrador lake-sediment and lake-water surveys. Government of Newfoundland and Labrador, Department of Natural Resources, Geological Survey, Open File LAB/1602, 50 pages.

Morse, S.A.
1969: The Kiglapait Layered Intrusion, Labrador. Geological Society of America, Memoir 112, 204 pages and map.

Rose, A.W., Dahlberg, E.C. and Keith, M.L.
1970: A Multiple Regression Technique for Adjusting Background Values in Stream sediment Geochemistry: Economic Geology, Volume 65, pages 156-165

Stapleton, G.J., Smith, J.L. and Rafuse, H.M.
2011: Mineral Occurrence Data System. Current Research, Newfoundland and Labrador Department of Natural Resources, Geological Survey, Report 11-1, pages 341-345.

Wardle, R. J., Swinden, S. and James, D. T.
1995: The southeastern Churchill Province. *In* The geology and mineral deposits of Labrador: a guide for the exploration geologist, Compiled by R. J. Wardle, Government of Newfoundland and Labrador, Department of Natural Resources, Geological Survey, Open File LAB/1130, 1995, pages 26-42.

*References to Geological Maps and Reports*

Emslie, R.F.
1980: Geology and Petrology of the Harp Lake Complex, Central Labrador: An Example of Elsonian Magmatism. Geological Survey of Canada, Bulletin 293, 136 pages.

Gower, C.F.
2010a: Geology of the English River area (NTS sheets 13G/09, 10, 15 & 16), Southeastern Labrador. Geological Survey, Mines Branch, Department of Natural Resources, Government of Newfoundland and Labrador. Map 2010-10, Scale 1:100 000, Open File 013G/0055.

2010b: Geology of the Pinware River area (NTS sheets 12P/10, 15 & 16; and parts of 12P/06, 07, 09, 11, 14 & 2M/13), Southeastern Labrador. Geological Survey, Mines Branch, Department of Natural Resources, Government of Newfoundland and Labrador. Map 2010-25, Scale 1:100 000, Open File LAB/1567.

2010c: Geology of the St. Lewis River area (NTS sheets 03D/04 & 05; 13A/01, 02, 07 & 08), Southeastern Labrador. Geological Survey, Mines Branch, Department of Natural Resources, Government of Newfoundland and Labrador. Map 2010-24, Scale 1:100 000, Open File LAB/1566.

2010d: Geology of the southeast Mealy Mountains area (NTS sheets 13G/01, 02, 07 & 08), Southeastern Labrador. Geological Survey, Mines Branch, Department of Natural Resources, Government of Newfoundland and Labrador. Map 2010-14, Scale 1:100 000, Open File 013G/0057.

Gower, C.F, van Nostrand, T. and Smyth, J.
1988: Geology of the St. Lewis River map region, Grenville Province, eastern Labrador. *In* Current Research, Newfoundland and Labrador Department of Mines, Mineral Development Division, Report 88-1, pages 59-73.

Hill, J.D
1982: Flowers River area, Labrador. Map 81-136. Scale: 1:100 000. In Geology of the Flowers River - Notakwanon River area, Labrador. Government of Newfoundland and Labrador, Department of Mines and Energy, Mineral Development Division, Report 82-6, 140 pages.

James, D.T.

1993: Geology of the Archean Ashuanipi Complex in western Labrador: Map 2. Map 93-018. Scale 1:100 000. Government of Newfoundland and Labrador, Department of Mines and Energy, Geological Survey Branch.

James, D.T.

1994a: Geology of the Woods Lake area (NTS 23I), western Labrador. Map 94-239. Scale: 1:200 000. *in* Geology of the eastern Churchill Province in the Woods Lake area (NTS 23I), western Labrador. Government of Newfoundland and Labrador, Department of Mines and Energy, Geological Survey Branch, Open File 23I/0076, 102 pages.

1994b: Geology of the Grenville Province in the Lac Joseph area (NTS 23A/NW), western Labrador. Map 93-53. Scale: 1:100 000. In Geology of the Grenville Province in the Lac Joseph and Ossokmanuan Lake areas (23A/NW and 23H/SW), western Labrador. Government of Newfoundland and Labrador, Department of Mines and Energy, Geological Survey Branch, Report 94-2, 58 pages.

Nunn, G.A.G

1995: Bedrock geology of the Kanairiktok River headwaters, NTS area 13L/NW, Labrador. Scale: 1:100 000. Government of Newfoundland and Labrador, Department of Mines and Energy, Geological Survey Branch, Map 94-122.

Rivers, T.

1985a: Geology of the Opocopa Lake area, Labrador - Quebec. Map 85-24. Scale: 1:100 000. Government of Newfoundland and Labrador, Department of Mines and Energy, Mineral Development Division. Colour map. GS# 023B/0133

1985b: Geology of the Evening Lake area, Labrador (23G/NE). Map 85-27. Scale: 1:100 000. Government of Newfoundland and Labrador, Department of Mines and Energy, Mineral Development Division. Colour map GS# 023G/0229.

1985c: Geology of the Lac Virot area, Labrador/Quebec. Map 85-025. Scale 1:100,000. Government of Newfoundland and Labrador, Department of Mines and Energy, Mineral Development Division, GS#LAB/0696.

Rivers, T. and Massey, N.

1985: Geology of the Wightman Lake area, Labrador - Quebec. Map 85-28. Scale: 1:100 000. Government of Newfoundland and Labrador, Department of Mines and Energy, Mineral Development Division. Colour map 023G/0228 .

Ryan, B.

1984b: Geology of the Central Mineral Belt (central part - sheet 2). Map 82-4. Scale: 1:100 000. In Regional geology of the central part of the Central Mineral Belt, Labrador. Government of Newfoundland and Labrador, Department of Mines and Energy, Mineral Development Division, Memoir 3, 195 pages.

1990: Preliminary geological map of the Nain Plutonic Suite and surrounding rocks (Nain-Nutak, NTS 14 S.W.). Map 90-44. Scale: 1:500 000. Government of Newfoundland and Labrador, Department of Mines and Energy, Geological Survey Branch. Colour map GS# LAB/0964

Thériault, R. and Bilodeau, C. (compilers)
2002: Geological map of Québec. Edition 2002. Ministère des Ressources Naturelles; DV 2002-07, scale 1 : 2 000 000.

Wardle, R.J.
1982a: Map 1. Geology of the south-central Labrador Trough. Map 82-5. Scale: 1:100 000. Government of Newfoundland and Labrador, Department of Mines and Energy, Mineral Development Division, accompanied by Figure 1 (legend to accompany Maps 1 and 2) and Figure 2 (cross-sections). Colour map GS# LAB/0603a

1982b: Map 2. Geology of the south-central Labrador Trough. Map 82-6. Scale: 1:100 000. Government of Newfoundland and Labrador, Department of Mines and Energy, Mineral Development Division, accompanied by Figure 1 (legend to accompany Maps 1 and 2) and Figure 2 (cross-sections). Colour map GS# LAB/0603b

1993: Geology of the Naskaupi River region, central Labrador (13NW). Map 93-16. Scale: 1:500 000. Government of Newfoundland and Labrador, Department of Mines and Energy, Geological Survey Branch. Colour map GS# LAB/0981

1994: Geology of the North West River area, central Labrador, NTS 13 SW. Map 94-117. Scale: 1:500 000. Government of Newfoundland and Labrador, Department of Mines and Energy, Geological Survey Branch.

Wardle, R.J., Ware, M.J., Noel, N., Rivers, T. and Britton, J.M.
1985: Geology of the Gabbro Lake area, Labrador. Map 85-26. Scale: 1:100 000. Government of Newfoundland and Labrador, Department of Mines and Energy, Mineral Development Division. Colour map GS# 023H/0091.

Ware, M.J. and Wardle, R.J.
1979: Geology of the Sims-Evening Lake area, western Labrador, with emphasis on the Helikian Sims Group. Government of Newfoundland and Labrador, Department of Mines and Energy, Mineral Development Division, Report 79-05, 26 pages.

*References to NGR Lake Geochemical Data Releases*

Boyle, D.R., Coker W.B. and Ellwood D.J.
1981a: National Geochemical Reconnaissance, northern Labrador (23G, 23H, 23I, 23J, 14D, 13N, 13L). Geological Survey of Canada, Open File 748, 1981, 24 pages.

1981b: National geochemical reconnaissance, eastern Labrador [13B,F,G,H,I,J and O; 3E]. Geological Survey of Canada, Open File 749, 1981; 25 pages,

Friske, P.W.B., McCurdy, M.W., Lynch, J.J., Gross, H., Day, S.J., Adcock, S.W., Durham, C.C. and Karam, H.

1992a: Regional lake sediment and water geochemical reconnaissance data, central Labrador. Geological Survey of Canada, Open File 2471, 119 pages.

Friske, P. W. B. McCurdy, M. W., Lynch, J. J., Gross, H,. Adcock, S.W., Durham, C. C., Day, S. J. and Karam, H.

1992b: Regional lake sediment and water geochemical reconnaissance data, eastern Labrador. Geological Survey of Canada, Open File 2472, 122 pages.

Friske, P.W.B., McCurdy, M.W., Gross, H., Day, S.J., Lynch, J.J. and Durham, C. C.

1993a: National geochemical reconnaissance lake sediment and water data, central Labrador [NTS 13E]. Geological Survey of Canada, Open File 2474, 140 pages.

1993b: National geochemical reconnaissance lake sediment and water data, central Labrador [NTS 13K]. Geological Survey of Canada, Open File 2645, 136 pages.

1993c: National geochemical reconnaissance lake sediment and water data, eastern Labrador [NTS 13I, 13J, 13O]. Geological Survey of Canada, Open File 2646, 126 pages.

1993d: National geochemical reconnaissance lake sediment and water data, central Labrador [NTS 13L]. Geological Survey of Canada, Open File 2647, 131 pages.

1993e: National geochemical reconnaissance lake sediment and water data, eastern Labrador [NTS 13N]. Geological Survey of Canada, Open File 2648, 121 pages.

1993f: National geochemical reconnaissance lake sediment and water data, west-central Labrador [NTS 13M]. Geological Survey of Canada, Open File 2649, 131 pages.

Friske, P.W.B., McCurdy, M.W., Day, S.J., Gross, H., Lynch, J.J and Durham, C.C.

1993g: Regional lake sediment and water geochemical reconnaissance data, western Labrador. Geological Survey of Canada, Open File 2475, 195 pages.

1993h: Regional lake sediment and water geochemical reconnaissance data, southwestern Labrador. Geological Survey of Canada, Open File 2689, 170 pages.

1993i: Regional lake sediment and water geochemical reconnaissance data, northern Labrador. Geological Survey of Canada, Open File 2690, 150 pages.

1993j: Regional lake sediment and water geochemical reconnaissance data, northern Labrador. Geological Survey of Canada, Open File 2691,; 154 pages.

Friske, P.W.B., McCurdy, M.W., Gross, H., Day, S.J., Balma, R.G., Lynch, J.J. and Durham, C.C.
1994a: National Geochemical Reconnaissance lake sediment and water data, southeastern Labrador (NTS 3E and 13H). Geological Survey of Canada, Open File 2473, 110 pages.

1994b: National Geochemical Reconnaissance, regional lake sediment and water geochemical reconnaissance data, southern Labrador (NTS 13B). Geological Survey of Canada, Open File 2791, 1994; 135 pages (1 sheet).

1994c: National Geochemical Reconnaissance, regional lake sediment and water geochemical reconnaissance data, southeastern Labrador (NTS 3D, 13A, and parts of 2M and 12P). Geological Survey of Canada, Open File 2790, 1994; 135 pages (1 sheet).

1994d: National Geochemical Reconnaissance, regional lake sediment and water geochemical reconnaissance data, southern Labrador (NTS 13C). Geological Survey of Canada, Open File 2792, 1994; 140 pages (1 sheet)

1994e: National Geochemical Reconnaissance, regional lake sediment and water geochemical reconnaissance data, southern Labrador (NTS 13D). Geological Survey of Canada, Open File 2793, 1994; 135 pages (1 sheet)

1994f: National Geochemical Reconnaissance, regional stream sediment and water geochemical reconnaissance data, northern Labrador (NTS 14M and parts of 14L, 24I, 24P, and 25A). Geological Survey of Canada, Open File 2794, 1994; 165 pages (1 sheet)

Hornbrook, E. H. W., Lund, N. G. and Lynch, J. J.
1983a: Geochemical lake sediment and water, Labrador [13E], maps and data. Open File 901, 1983; 75 pages

1983b: Geochemical lake sediment and water, Labrador [22P,23A,23B], maps and data. Geological Survey of Canada, Open File 902, 1983; 84 pages

1983c: Geochemical lake sediment and water, Labrador [23G,23H], maps and data. Geological Survey of Canada, Open File 903, 1983; 94 pages

1983d: Geochemical lake sediment and water, Labrador [23I,23J,23O], maps and data. Geological Survey of Canada, Open File 904, 1983; 89 pages

1984a: Geochemical lake sediment and water, Labrador [13D], maps and data. Geological Survey of Canada, Open File 996, 1984; 65 pages

1984b: Geochemical lake sediment and water surveys, Labrador [13K], maps and data. Geological Survey of Canada, Open File 997, 1984; 66 pages

1984c: Geochemical lake sediment and water, Labrador [13L], maps and data. Geological Survey of Canada, Open File 998, 1984; 66 pages

Hornbrook, E. H. W. and Friske, P. W. B.
1988: Regional Lake Sediment and Water Geochemical Reconnaissance Data, east - central Labrador. Geological Survey of Canada, Open File 1636, 150 pages

1989: Regional lake sediment and water geochemical data, western Labrador. Geological Survey of Canada, Open File 2037, 185 pages.

Hornbrook, E. H. W., Maurice, Y. T. and Lynch, J. J.
1977a: National geochemical reconnaissance release NGR 23-1977, regional lake sediment and water geochemical reconnaissance data eastern Labrador: Geological Survey of Canada, Open File 512.

1977b: National geochemical reconnaissance release NGR 24-1977, regional lake sediment and water geochemical reconnaissance data, eastern Labrador. Geological Survey of Canada, Open File 513

1978a: National geochemical reconnaissance release NGR 20-1977, regional lake sediment and water geochemical reconnaissance data, eastern Labrador. Geological Survey of Canada, Open File 509.

1978b: National geochemical reconnaissance release NGR 21-1977, regional lake sediment and water geochemical reconnaissance data, eastern Labrador. Geological Survey of Canada, Open File 510.

1978c: National geochemical reconnaissance release NGR 22-1977, regional lake sediment and water geochemical reconnaissance data, eastern Labrador. Geological Survey of Canada, Open File 511.

1978d: National geochemical reconnaissance release NGR 23-1977, regional lake sediment and water geochemical reconnaissance data, eastern Labrador. Geological Survey of Canada, Open File 511.

1979a: National geochemical reconnaissance release NGR 37- 1978, regional lake sediment and water geochemical reconnaissance data, central Labrador. Geological Survey of Canada, Open File 557

1979b: National geochemical reconnaissance release NGR 38- 1978, regional lake sediment and water geochemical reconnaissance data, central Labrador. Geological Survey of Canada, Open File 558

1979c: National geochemical reconnaissance release NGR 39- 1978, regional lake sediment and water geochemical reconnaissance data, central Labrador. Geological Survey of Canada, Open File 559.

1979d: National geochemical reconnaissance release NGR 40- 1978, regional lake sediment and water geochemical reconnaissance data, central Labrador. Geological Survey of Canada, Open File 560.

# APPENDIX A

## Box Plots of Field Observations *vs.* Geochemical Data

## EXPLANATION OF BOX-PLOT CLASSES

**Depth Class**

Compositional and accompanying lake-sediment analytical data from Geoscience Atlas and McConnell and Finch (2012)

1. < 1 metre
2. 1 metre
3. 2 metres
4. 3-4 metres
5. 5-8 metres
6. 9-16 metres
7. > 16 metres

**Area Class**

1. <0.25 $km^2$
2. 0.25 to 1 $km^2$
3. 1 to 5 $km^2$
4. > 5 $km^2$

**Relief**

1. Low
2. Moderate
3. High

**Sample Colour**

1. Black
2. Brown
3. Yellow
4. Green
5. Grey

**Observed Sample Composition**

*Compositional and accompanying lake-sediment analytical data from McConnell (2010)

1. Clastic, fine-grained
2. Clastic, coarse-grained
3. Organic Ooze
4. Organic Granular
5. Organic, Peaty

| | Depth | Area | Relief | Colour | Composition* |
|---|---|---|---|---|---|
| Al2 | 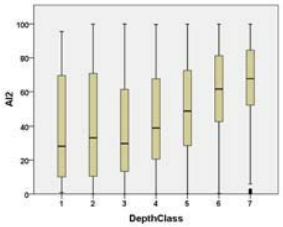 | 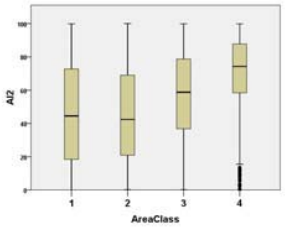 | 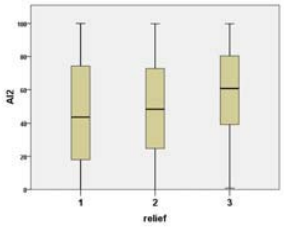 | 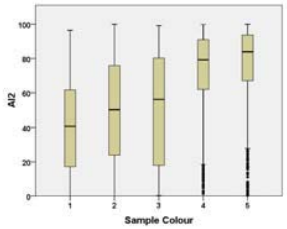 | 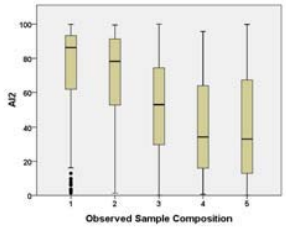 |
| Ba2 | 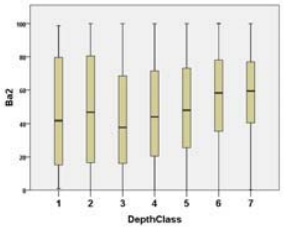 | 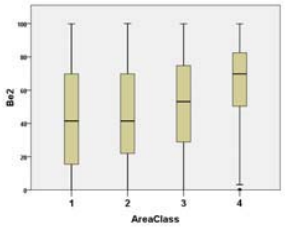 | 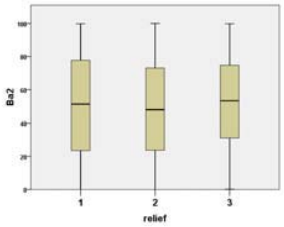 | 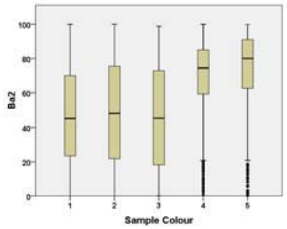 | 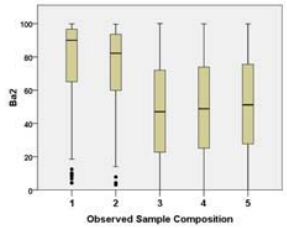 |
| Be2 | 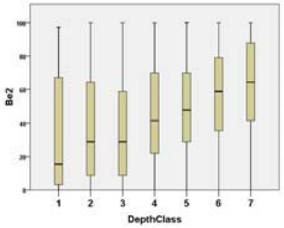 | 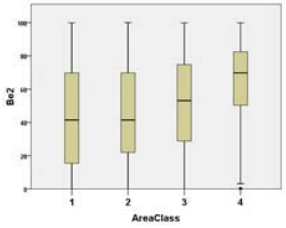 | 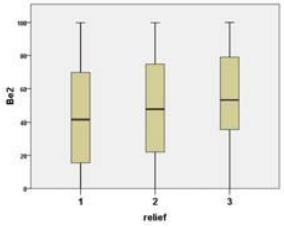 | 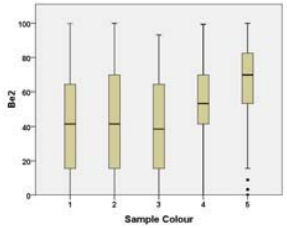 | 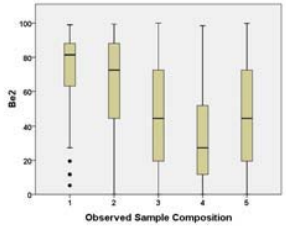 |
| Br1 | 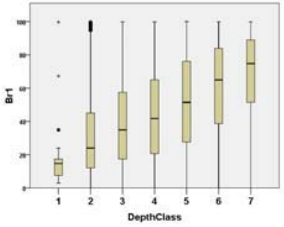 | 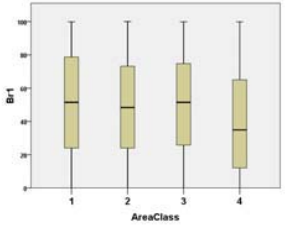 | 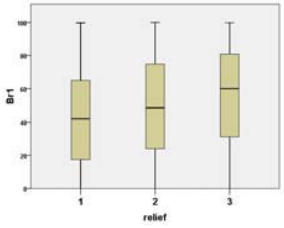 | 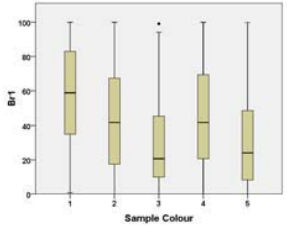 | 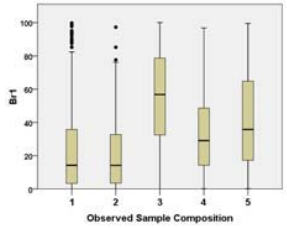 |

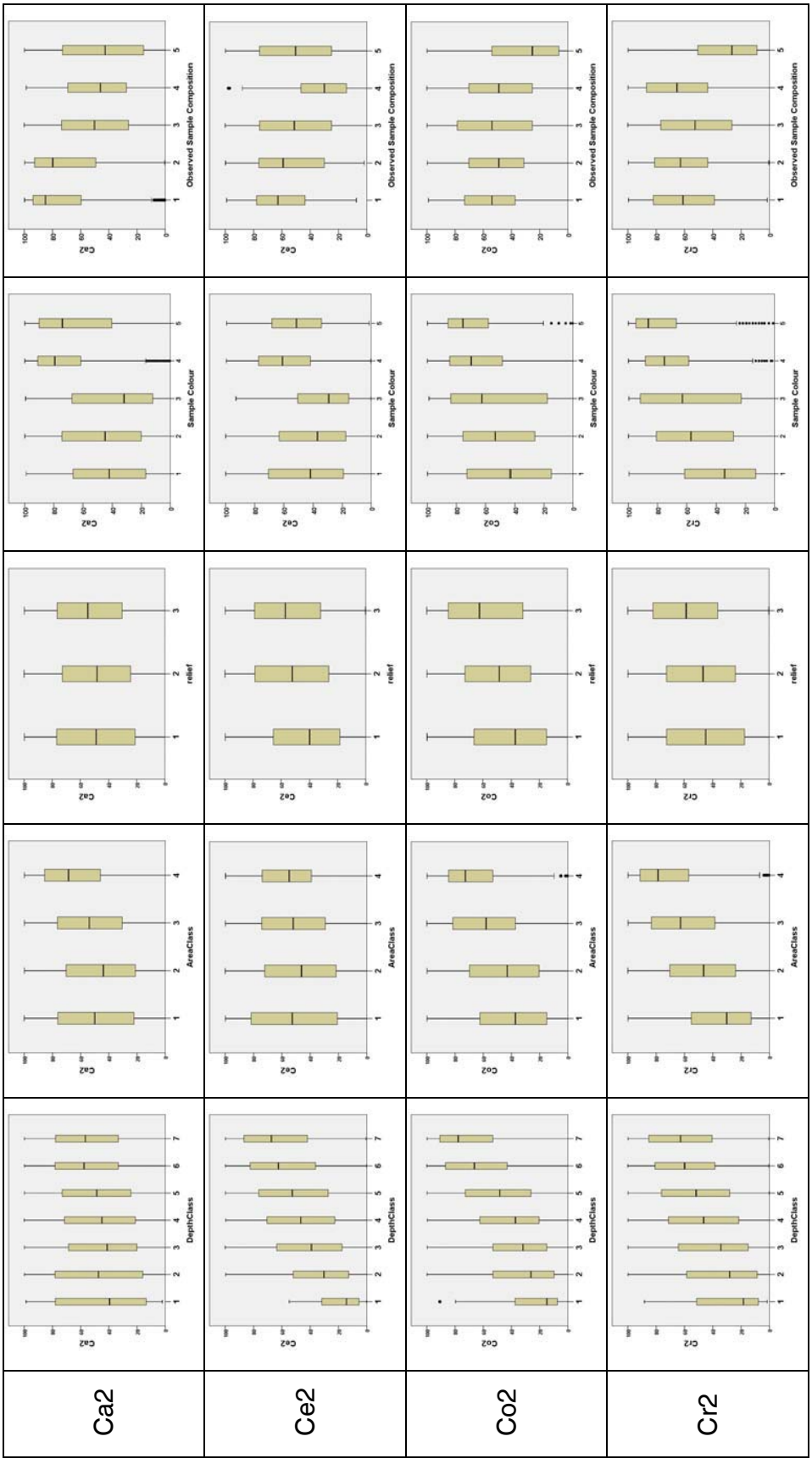
Ca2
Ce2
Co2
Cr2
DepthClass
AreaClass
relief
Sample Colour
Observed Sample Composition

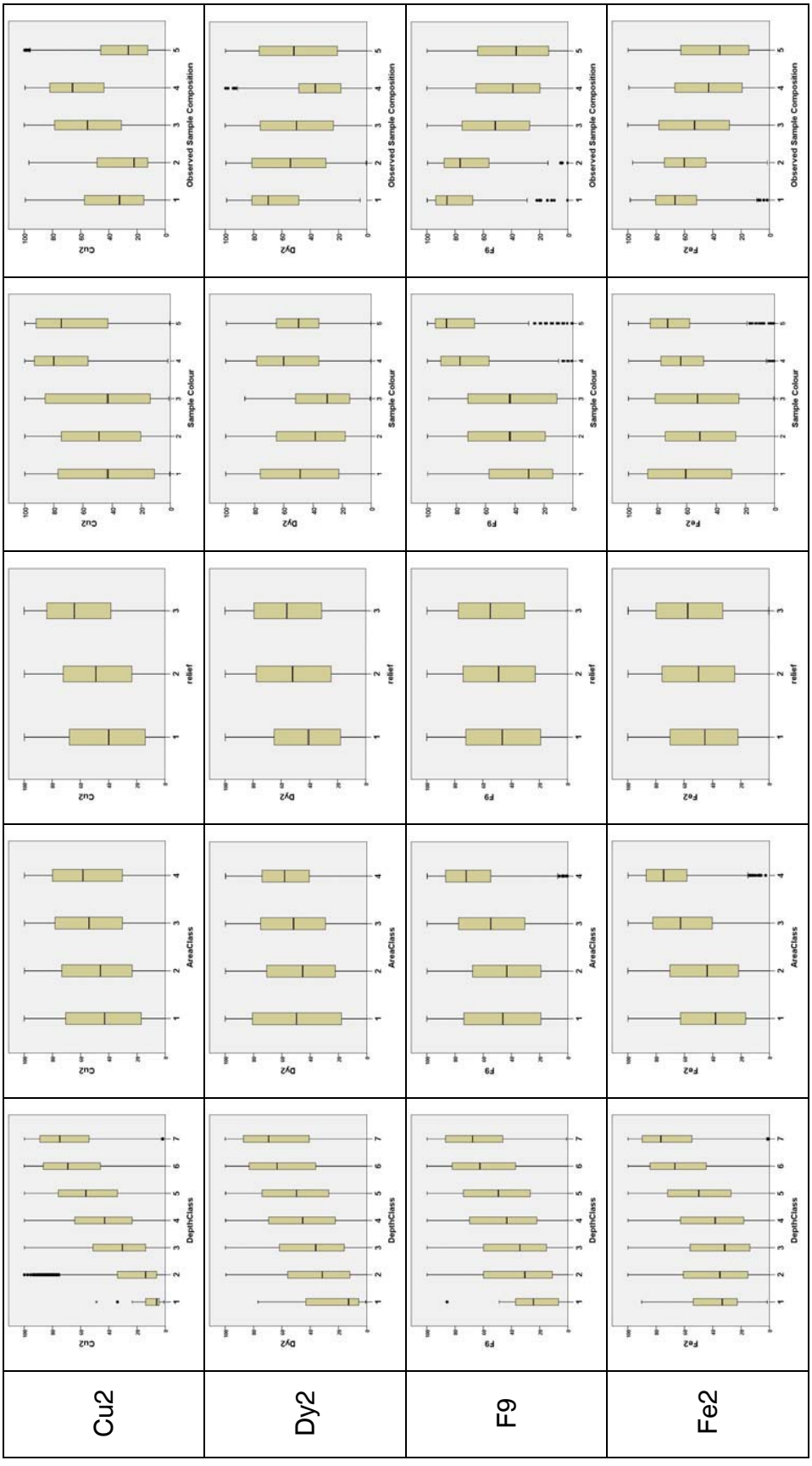
Cu2
Dy2
F9
Fe2
DepthClass
AreaClass
relief
Sample Colour
Observed Sample Composition

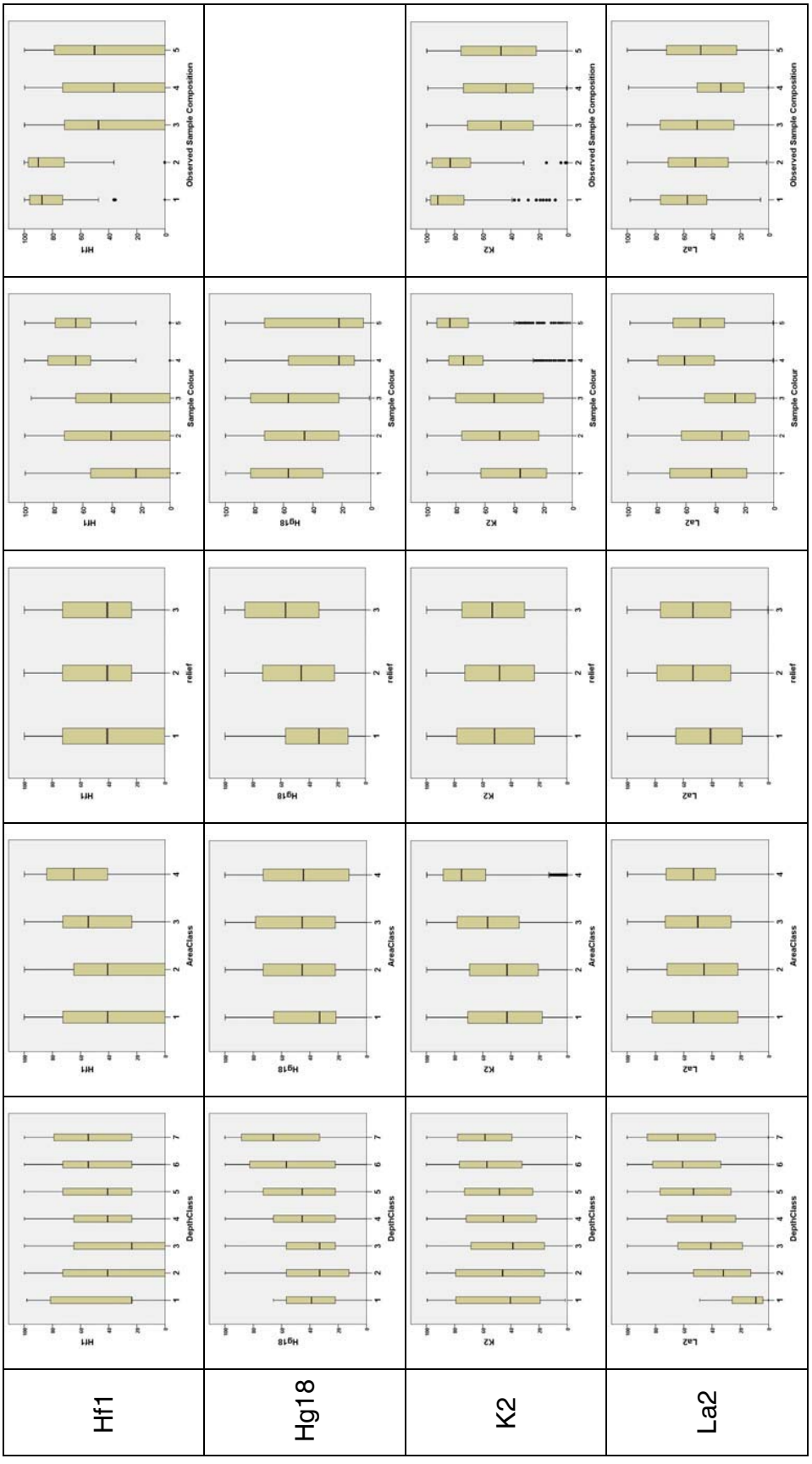
Hf1
Hg18
K2
La2
Observed Sample Composition
Sample Colour
relief
AreaClass
DepthClass

| | | | | | |
|---|---|---|---|---|---|
| Li2 | 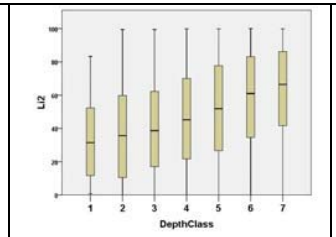 | 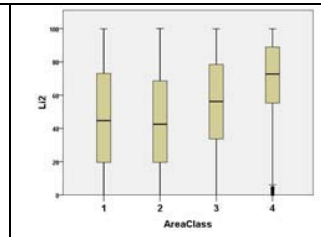 | 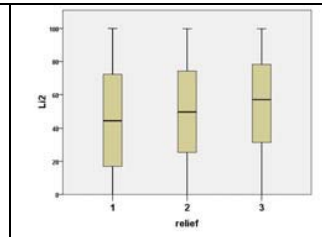 | 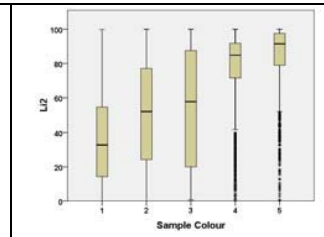 | 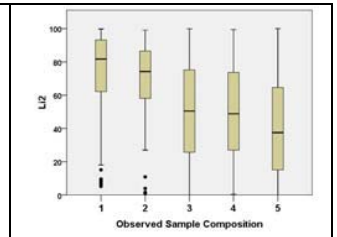 |
| LOI | 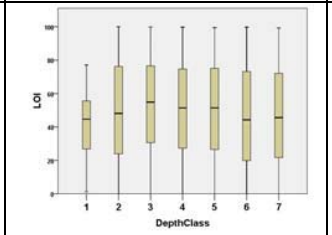 | 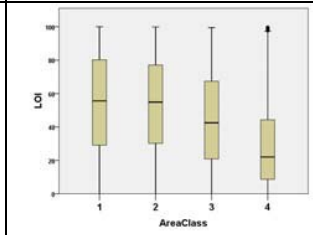 | 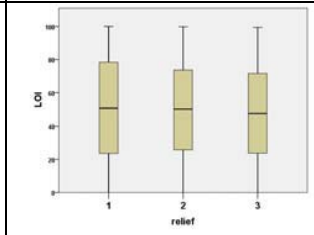 | 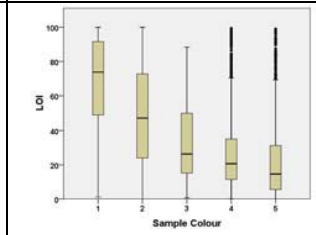 | 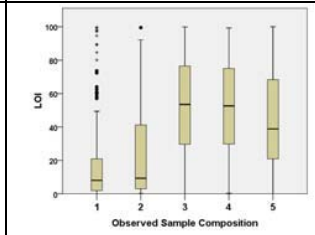 |
| Mg2 | 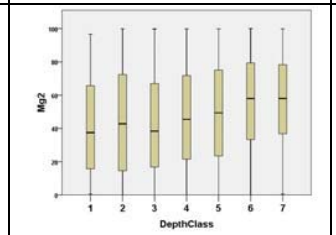 | 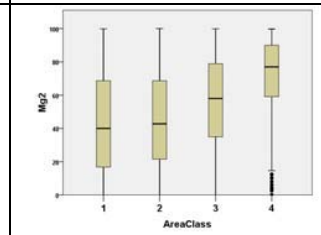 | 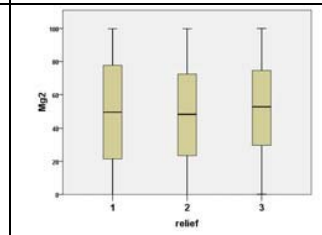 | 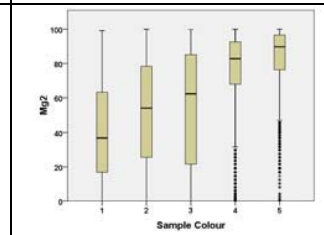 | 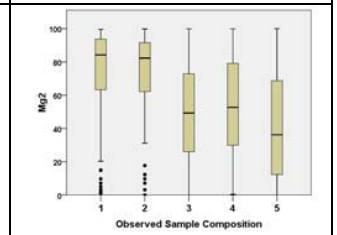 |
| Mn2 | 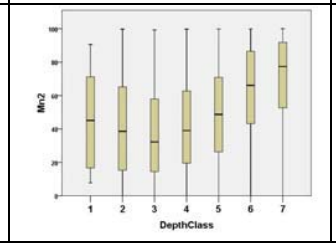 | 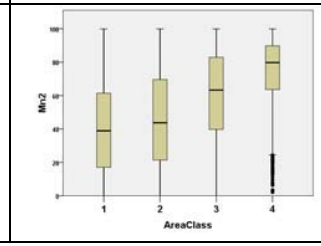 | 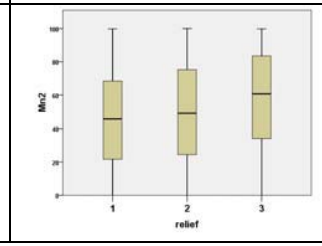 | 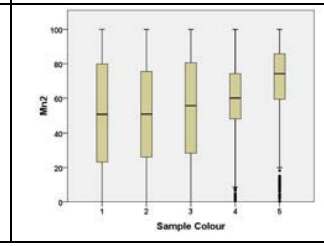 | 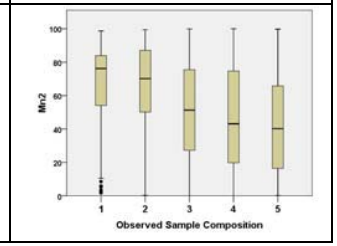 |

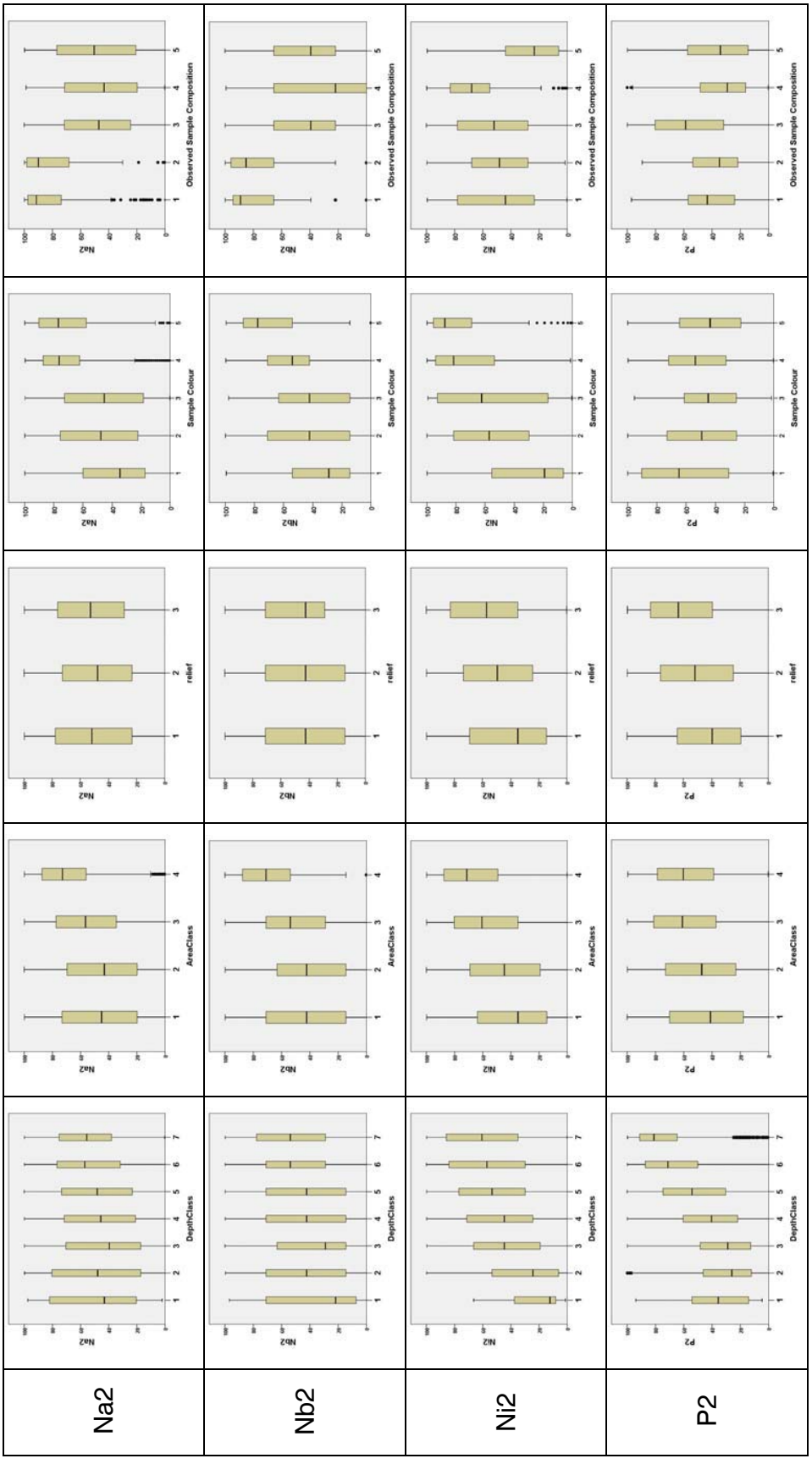
Na2
Nb2
Ni2
P2
Observed Sample Composition
Sample Colour
relief
AreaClass
DepthClass

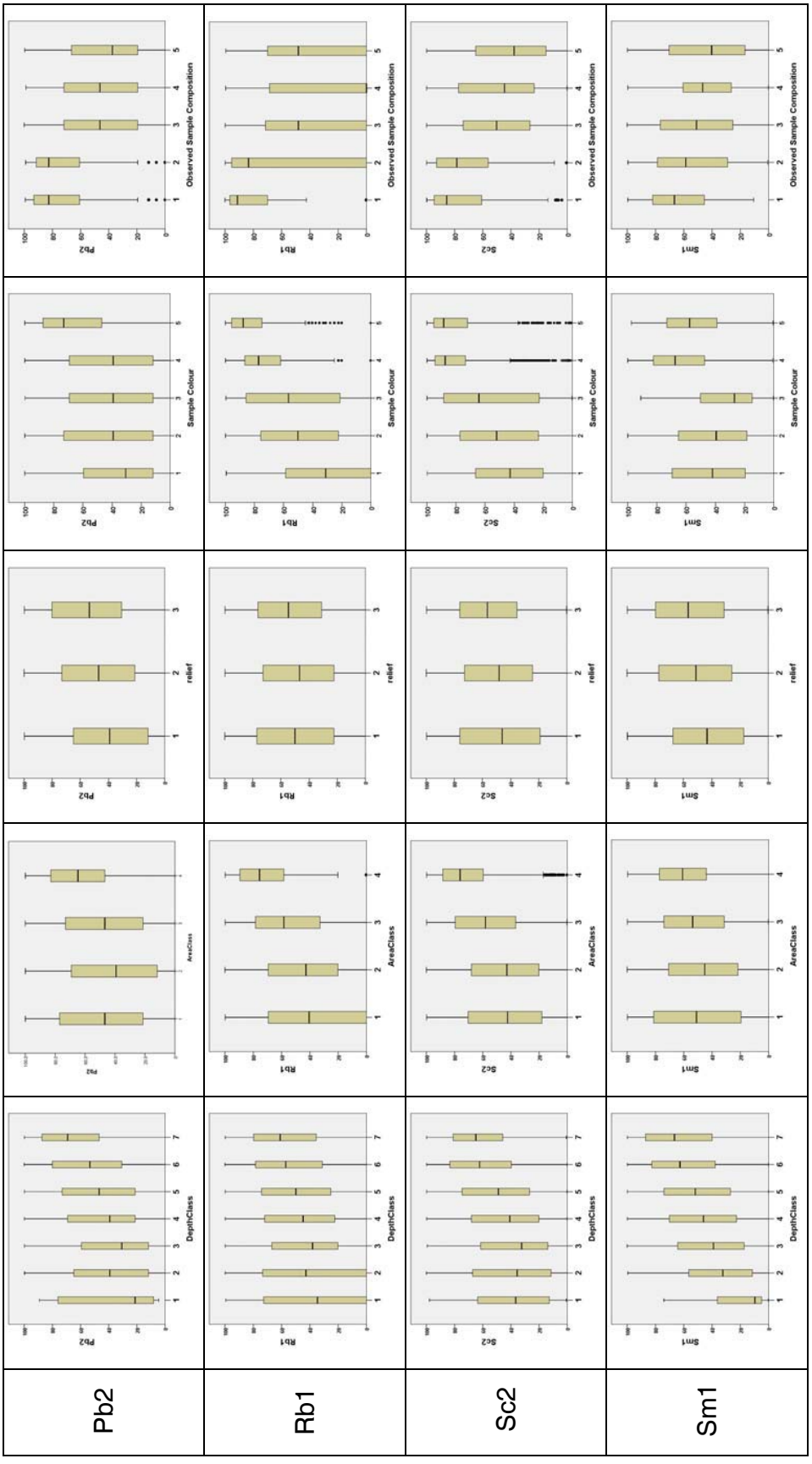
Pb2
Rb1
Sc2
Sm1
Observed Sample Composition
Sample Colour
relief
AreaClass
DepthClass

| | | | | | |
|---|---|---|---|---|---|
| Sr2 | 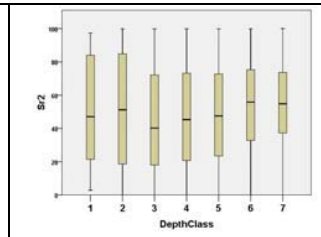 | 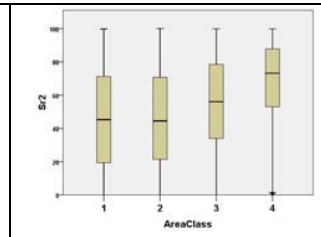 | 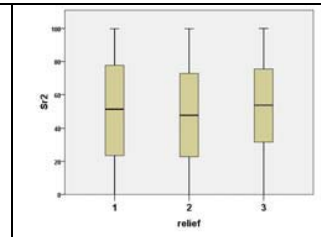 | 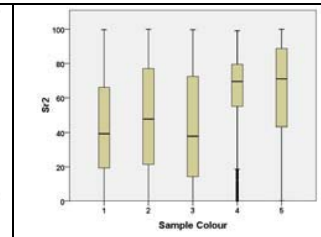 | 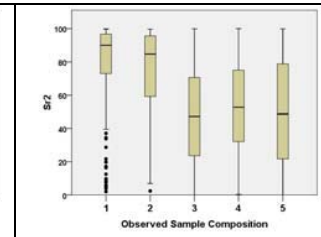 |
| Th1 | 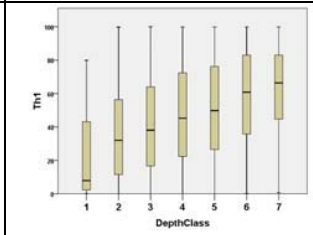 | 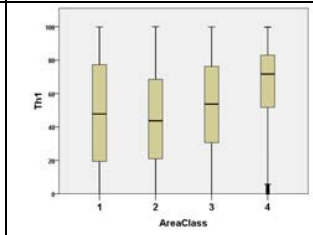 | 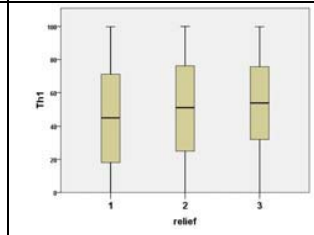 | 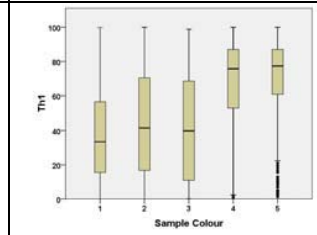 | 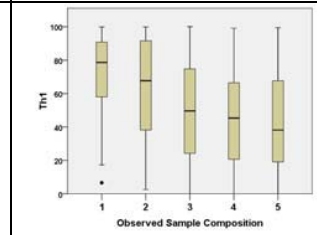 |
| Ti2 | 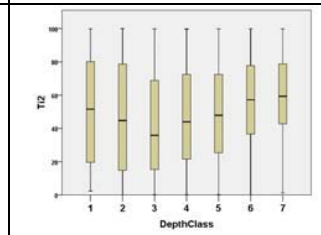 | 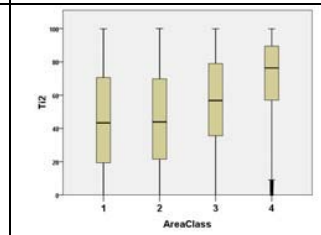 | 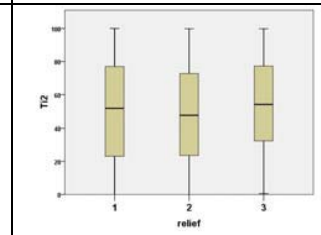 | 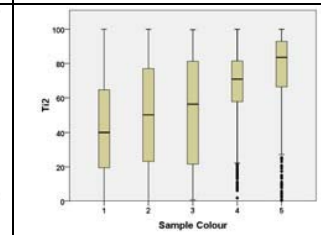 | 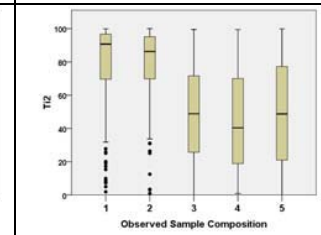 |
| U1 | 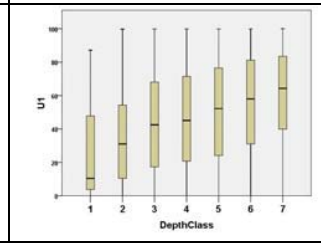 | 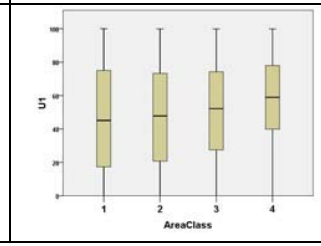 | 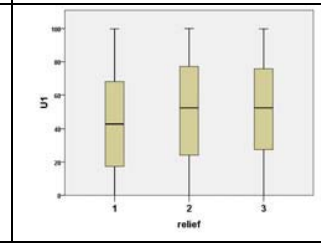 | 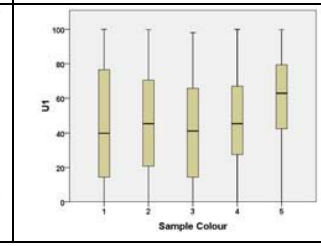 | 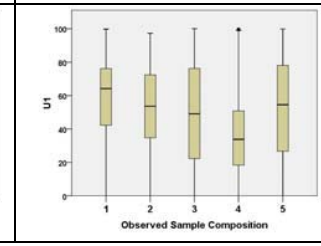 |

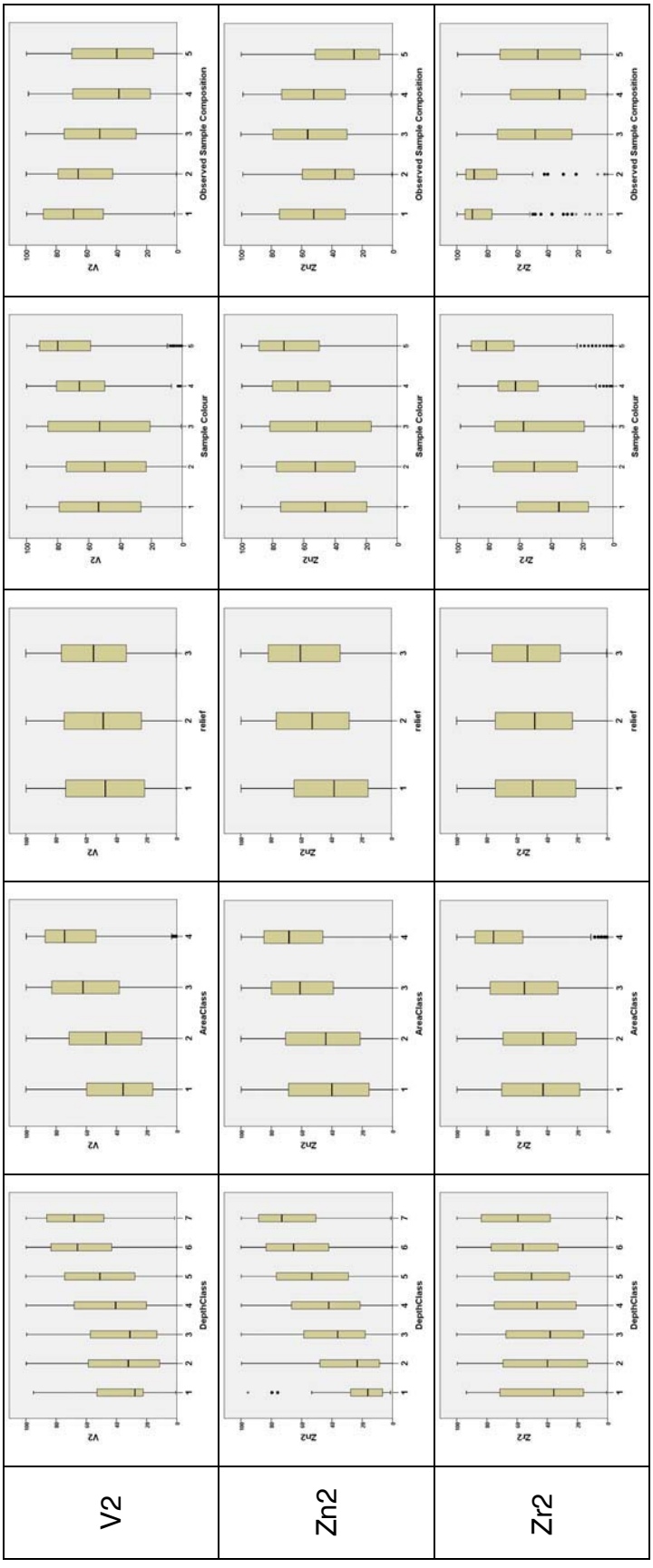
V2
Zn2
Zr2
Observed Sample Composition
Sample Colour
relief
AreaClass
DepthClass

# APPENDIX B

## Application of Factor Analysis to the NGR Lake-sediment Data

*Process and Response*

The analytical data in a typical multielement geochemical dataset may consist of analyses for more than 30 different chemical variables, but it is reasonable to assume that these elements are not emplaced in the sample medium by as many different natural processes, each one unique to a single element response.

Furthermore, the amount of a particular element in a sample is unlikely to be the result of only one process acting on the sample material. The strength of the correlations between certain elements in most naturally occurring media, including those in the current study, bears witness to this. Typically, for example, one might expect the content of a lake-sediment sample to be influenced by the composition of the rocks in the lake's catchment, subsequent glacial action, fluvial processes in the streams feeding the lake, iron and manganese scavenging, and the presence of organic matter.

"R-mode" factor analysis (because it is based on r, the correlation coefficient and deals with relationships between variables; "Q-mode" factor analysis, which is little used in geochemistry, deals with relationships between samples) is a general term given to a variety of related techniques that seek to identify a limited number of controls on a much greater number of observational variables. These controls are modelled in the form of linear combinations of those variables which are known as "factors". In geochemistry, it is reasonable to suppose that such factors will be more closely related to the processes that have acted on the naturally occurring medium in question, than are the individual variables themselves, although this does not necessarily follow.

A useful bi-product of R-mode factor analysis is that it often provides a means of concisely describing and summarizing the behaviour of a large number of elements in a geochemical dataset – for example, in a suitably ordered correlation matrix (Figure B1).

A particularly lucid description of the principles and application of factor analysis in geology is given by Klovan (1968).

*Graphical Demonstration*

In mathematical terms, factor analysis involves the extraction of the eigen-vectors of the correlation matrix, although for non-mathematicians the process is more readily demonstrable graphically. In the simplest, two-dimensional case, a "straight-line" graphical relationship between two elements in a naturally occurring medium implies that the compositions of both elements are essentially controlled by the same process (and not that the content of one of the two elements controls that of the other). The use of the term "straight-line" normally means not literally that, but at best that the data points concentrate in the form of a rather elongate, cigar-shaped ellipse whose long axis represents the straight line, and whose short axis represents some minor component of random variation. Figure B2 demonstrates this principle in two and three dimensions.

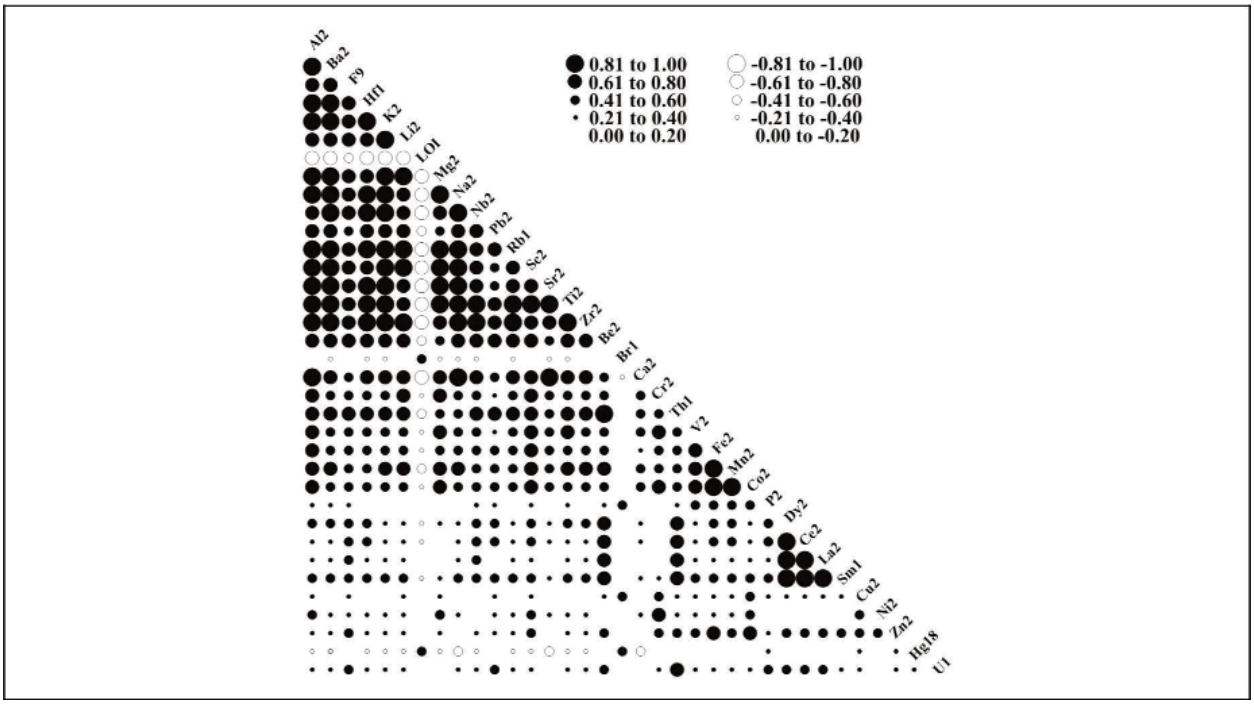


**Figure B1:** *Graphical correlation matrix of input data, current investigation.*

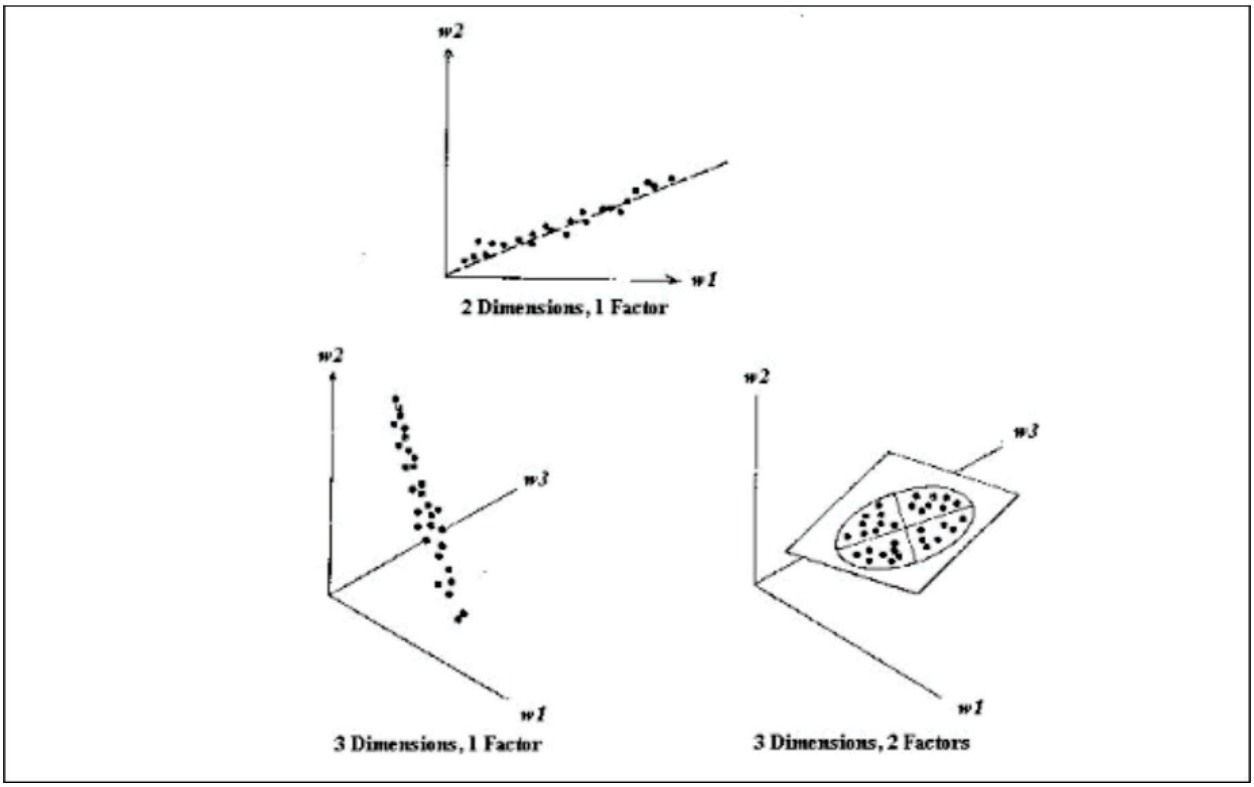


**Figure B2:** *Graphical demonstration of factor analysis. In the first plot, points plotted in two dimensions fall on a single line; in the second, points plotted in three dimensions fall on a single line; in the third, points plotted in three dimensions fall on a single plane. From Koch and Link (1970).*

*Expansion into more than 3 Dimensions*

The multielement analyses of a group of samples can be conceptualized as a cluster of points in multidimensional space. Factor analysis and the closely related technique of principal-components analysis (PCA) can be seen as involving the treatment of this cluster of points as a multidimensional ellipsoid, or hyperellipsoid, and extraction of its principal axes (Davis, 1973, page 473; Koch and Link, 1970, page 119). These are expressed as linear combinations of the input variables; they are mutually at right angles to one another and are, therefore, uncorrelated and mutually independent.

The dimensionality of the modelled hyperellipsoid is limited by the number of dimensions in which the data are "plotted", and in principal-components analysis, the number of eigen-vectors (or principal axes) extracted is always the same as the number of input variables. If a certain amount of variability is ascribed to random agencies, most of the variance and covariance can often be expressed by a much smaller number of such axes and this is the role of factor and analysis. These axes of the hyperellipsoid (compared to the dimensionality of the data) are known as factors.

The strength of an individual input variable in a factor is referred to as its *loading*. Loadings vary between -1 and +1. It is convenient to describe, characterize, and compare factors in terms of the input variables whose loading exceeds |0.5|, after rotation (*see* below).

*Factor Rotation*

Some form of factor rotation is generally applied in factor analysis. This has the effect of increasing the loadings on the more important input variables in a factor, and reducing the loadings on the less important variables. The interpretation of the factors, in terms of familiar natural geochemical procedures, is thus facilitated. The most commonly applied method of factor rotation is known as Kaiser's Varimax, and has as its objective the moving of each factor axis to positions so that projections from each input variable onto the factor axes are either ±1 or near zero; in other words, that the angle between each factor and each axis is as close as possible either to zero, or 90º (Davis, 1973, page 510).

*Number of Factors to Extract*

The number of factors to extract must be determined first, before the analysis takes place. The "correct" number of factors is not determined automatically (although some software packages may have default settings that may make it appear that this is what is taking place) and there are no universally agreed criteria for determining it. Amongst the methods that can be applied are the following:

1. Continuing to extract factors until the eigen-value of a new factor (essentially, the relative length of the axis it represents) drops below 1.0, meaning that the new factor explains less of the total variance than a single input variable.

2. Observing the plot of factor number *vs.* eigen-value and looking for a flattening out of the line. This indicates a sudden reduction in the capacity of the factor-extraction process to account for the variance of the data.

3. Observing the loadings on the factors and only extracting those factors that can be recognized as representing familiar geological and environmental processes, or which have been recognized in datasets from similar geological and physical environments.

4. Ceasing the factor-extraction when factors begin to appear in which only one input variable is heavily loaded.

5. Randomly splitting the dataset into two equal parts, applying factor analysis to both, and discontinuing the extraction of factors when factor characteristics differ significantly between the two splits. This method is known as "Cross-Validation" and it has an intuitive, logical appeal. It may appear tedious but methods exist for expediting the process.

*The Importance of Data Integrity*

It was stated above that factor analysis is based upon the Pearson correlation matrix. The successful and reliable calculation of the correlation coefficient is dependent on the input data being normally distributed and free of outliers. In factor analysis, the presence of outliers in the data will result not only in the creation of an erroneous factor, strongly weighted in the element or elements whose analyses created the outlier, and probably no other, but also, since they are by definition constrained to be mutually perpendicular, in all the other factors in the model being erroneous as well. The outliers are normally readily identifiable in histograms or cumulative-frequency diagrams and should be removed from the input data.

*Application to the Current Study*

Four subsets of the entire Labrador lake-sediment dataset (southeastern, south-central, southwestern, northern) were subjected to factor analysis. In general, when a choice was possible between two analyses of the same variable (ICP or INAA) the variable with the most detectable values was chosen. For some elements, too many values (more than 25% of the total) were undetectable for their inclusion in the calculations. This resulted in the exclusion from the factor analysis of Ba1, Ce1, Co1, Co3, Cr1, Cu3, Fe1, Fe3, La1, Mn3, Ni3, Sc1, U8, Zn3 and Zr1 for the first reason and Ag3, As19, As1, Au1, Cd3, Cs1, Eu1, Lu1, Mo1, Mo2, Mo5, Ni1, Pb3, Sb1, Ta1, Tb1, W1, Y2 and Yb1 for the second.

To comply with the requirement that the frequency distributions of the input variables be normally distributed, the input elements were subjected to linear transformation *(i.e.*, none), square-root transformation, log-transformation or log-log transformation, as listed in Table 1.

**Table 1:** Transformations applied to input data

| Region | No Transformation | Square-Root Transformation | Log-Transformation | Log-Log-Transformation |
|---|---|---|---|---|
| Southeastern Labrador | LOI | Cr1, Hg18, V2 | Al2, Be2, Br1, Ce2, Co2, Cr2, Cu2, Dy2, Fe2, Hf1, K2, La2, Li2, Mn2, Na2, Nb2, Ni2, P2, Pb2, Rb1, Sc2, Sm1, Th1, Ti2, Zn2, Zr2 | Ba2, Ca2, F9, Mg2, Sr2, U1 |
| South-central Labrador | LOI | F9, Sc2, V2 | Al2, Ba2, Be2, Br1, Ce2, Cr2, Dy2, Fe2, Hf1, Hg18, K2, La2, Li2, Mg2, Mn2, Na2, Nb2, Ni2, Pb2, Rb1, Sm1, Th1, Ti2, Zn2, Zr2, | Ca2, Co2, Cu2, P2, Sr2, U1 |
| Southwestern Labrador | LOI | Al2, Be2, Br1, Ce2, Cr2, Dy2, F9, Pb2, Rb1, Sc2, Sm1, Ti2, V2 | Ba2, Cu2, Fe2, Hf1, Hg18, K2, La2, Li2, Mg2, Mn2, Na2, Nb2, Th1, U1, Zr2 | Ca2, Co2, Ni2, P2, Sr2, Zn2 |
| Northern Labrador | Al2, Ba2, K2, Na2, Sc2, Ti2 | Ca2, F9, Hf1, Li2, LOI, Mg2, Nb2, Pb2, Rb1, Sr2, Th1, V2 | Be2, Br1, Ce2, Fe2, Hg18, La2, Sm1, Zn2, Zr2 | Co2, Cr2, Cu2, Dy2, Mn2, Ni2, P2, U1 |

The cross-validation method (Method 5, above) was applied, to decide on appropriate factor models for each of the four regions. When an appropriate model had been decided upon, the two splits were combined for the final factor analysis, whose results are presented in Table 2. Communalities of the input variables (*i.e.*, the percentage of each variable's variance explained by the chosen factor model) are listed in Table 3.

**Table 2:** Factor Models. Variables are listed in decreasing order of strength; negative loadings are listed in red.

| Factor # | Southeastern Labrador | | South-central Labrador | | Southwestern Labrador | | Northern Labrador | |
|---|---|---|---|---|---|---|---|---|
| 1 | K2, Na2, Sr2, Zr2, Mg2, Hf1, Rb1, Ti2, Ba2, Ca2, Nb2, Al2, Li2, Sc2, F9, Pb2, Cr2, Be2 | 37% | Na2, Sr2, K2, Ti2, Ba2, Mg2, Hf1, Zr2, Ca2, Rb1, Nb2, Al2, Sc2, Li2, Pb2, F9, Cr2, Th1, LOI | 38% | K2, Ti2, Rb1, Al2, Mg2, Nb2, Zr2, Na2, Hf1, Ba2, Sc2, F9, Be2, V2, Li2, Cr2, Th1, Sr2, Pb2, Fe2, Mn2, LOI | 43% | Na2, Sr2, K2, Ba2, Ti2, Al2, Ca2, Hf1, Rb1, Nb2, Zr2, Mg2, Sc2, Li2, Br1, Hg18, LOI | 33% |
| 2 | La2, Ce2, Sm1, Dy2, Th1, U1, Be2, | 20% | La2, Ce2, Sm1, Dy2, Th1, Be2, U1 | 19% | La2, Sm1, Ce2, Dy2 | 13% | Sm1, La2, Ce2, Dy2, Th1, Be2, Zn2, U1, F9 | 21% |
| 3 | Fe2, Co2, Mn2, Zn2, P2, V2 | 12% | V2, Fe2, P2, Mn2, Cr2 | 9% | Ni2, Cu2, Zn2 | 10% | Ni2, Cr2, Cu2, Mg2, V2, Li2, Sc2 | 15% |
| 4 | Ni2, Cu2, Cr2 | 8% | Br1, Cu2, Hg18, P2, LOI | 7% | P2, Br1 | 5% | P2, Fe2, Mn2, Br1 | 8% |
| 5 | Br1, LOI, | 4% | Co2 | 6% | Co2, Fe2, Zn2 | 5% | Pb2 | 4% |
| 6 | Hg18, P2 | 3% | Ni2 | 5% | U1 | 4% | Co2 | 3% |
| 7 | Pb2 | 2% | U1 | 2% | Ca2 | 4% | U1 | 2% |
| 8 | | | Hg18 | 2% | Hg18 | 4% | | |
| **Total Variance Explained** | **87%** | | **88%** | | **88%** | | **86%** | |

**Table 3:** Communalities of the input variables

| | Southeastern Labrador | South-central Labrador | Southwestern Labrador | Northern Labrador |
|---|---|---|---|---|
| Al2 | 92% | 91% | 94% | 87% |
| Ba2 | 82% | 87% | 83% | 84% |
| Be2 | 90% | 86% | 83% | 81% |
| Br1 | 83% | 86% | 84% | 79% |
| Ca2 | 78% | 82% | 88% | 85% |
| Ce2 | 95% | 93% | 90% | 93% |
| Co2 | 90% | 87% | 86% | 91% |
| Cr2 | 91% | 90% | 89% | 87% |
| Cu2 | 74% | 75% | 85% | 86% |
| Dy2 | 92% | 90% | 78% | 89% |
| F9 | 77% | 79% | 81% | 73% |
| Fe2 | 90% | 90% | 87% | 84% |
| Hf1 | 87% | 87% | 87% | 86% |
| Hg18 | 84% | 87% | 87% | 73% |
| K2 | 97% | 96% | 95% | 91% |
| La2 | 95% | 93% | 91% | 93% |
| Li2 | 81% | 82% | 85% | 84% |
| LOI | 86% | 80% | 71% | 81% |
| Mg2 | 93% | 95% | 94% | 94% |
| Mn2 | 85% | 86% | 80% | 78% |
| Na2 | 95% | 96% | 89% | 94% |
| Nb2 | 87% | 87% | 86% | 85% |
| Ni2 | 87% | 93% | 90% | 88% |
| P2 | 76% | 85% | 84% | 79% |
| Pb2 | 82% | 81% | 79% | 87% |
| Rb1 | 81% | 81% | 90% | 89% |
| Sc2 | 90% | 88% | 90% | 87% |
| Sm1 | 93% | 94% | 94% | 92% |
| Sr2 | 89% | 91% | 89% | 88% |
| Th1 | 92% | 91% | 89% | 85% |
| Ti2 | 93% | 95% | 94% | 82% |
| U1 | 80% | 91% | 78% | 84% |
| V2 | 81% | 86% | 85% | 82% |
| Zn2 | 89% | 81% | 85% | 82% |
| Zr2 | 93% | 90% | 89% | 86% |

# APPENDIX C

## Maps of Raw and Predicted Values of Hf1, K2, Mg2, Na2, Nb2, Rb1, Sc2 and Sr2 in Labrador Lake Sediments

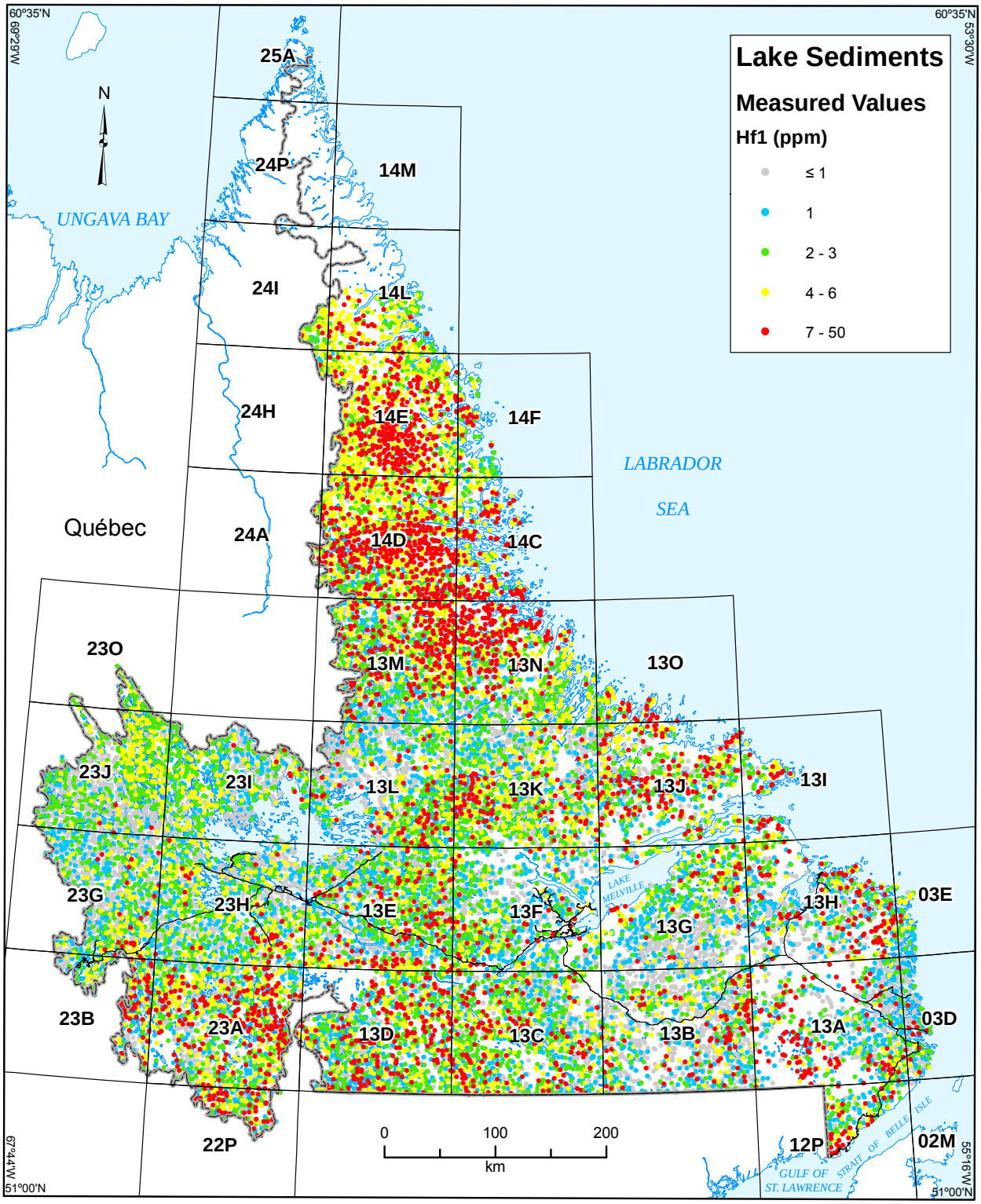


**Figure C1a.** *Measured values of Hf1 in lake sediment, Labrador.*

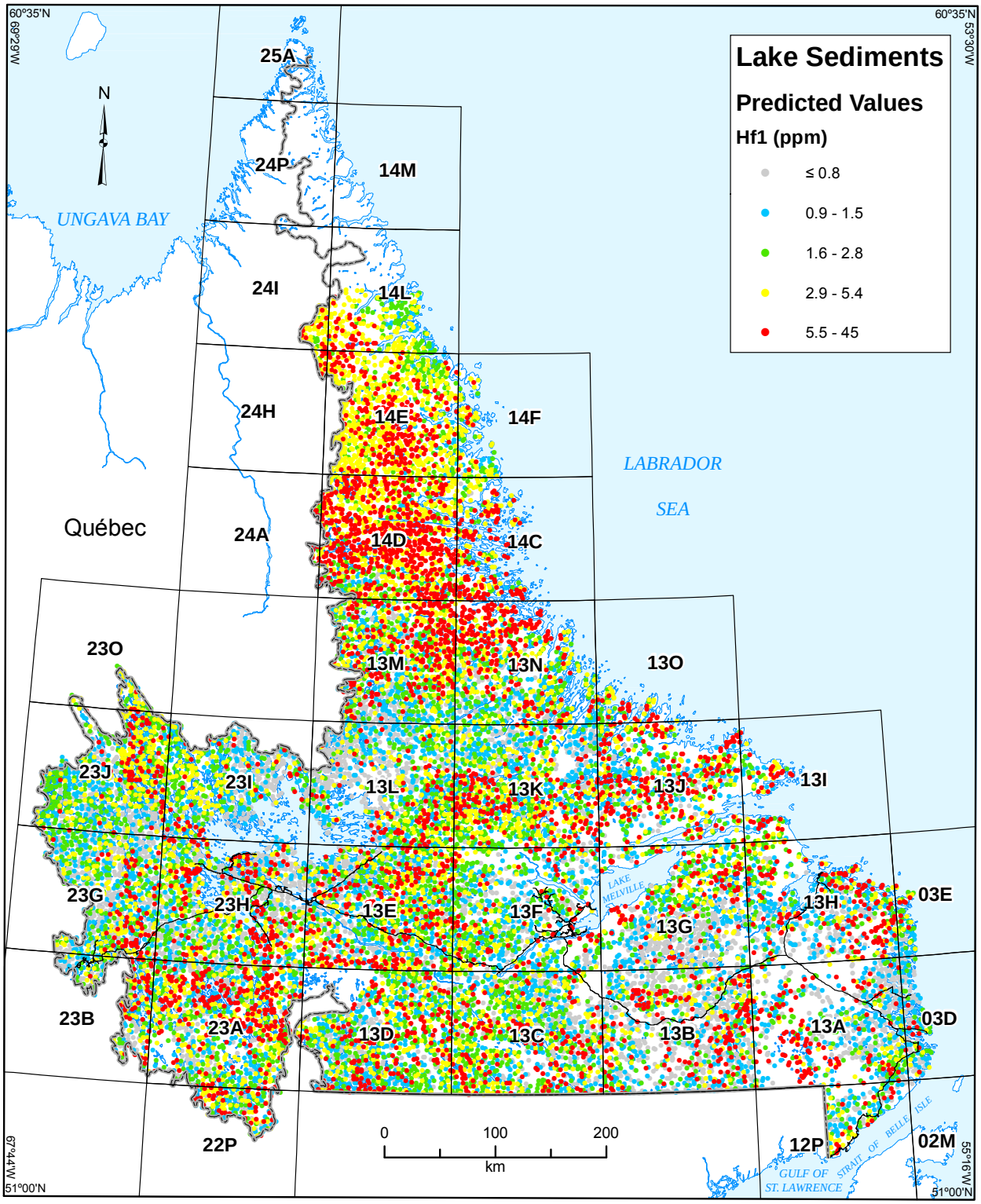


**Figure C1b.** *Multiple regression-predicted values of Hf1 in lake sediment, Labrador.*

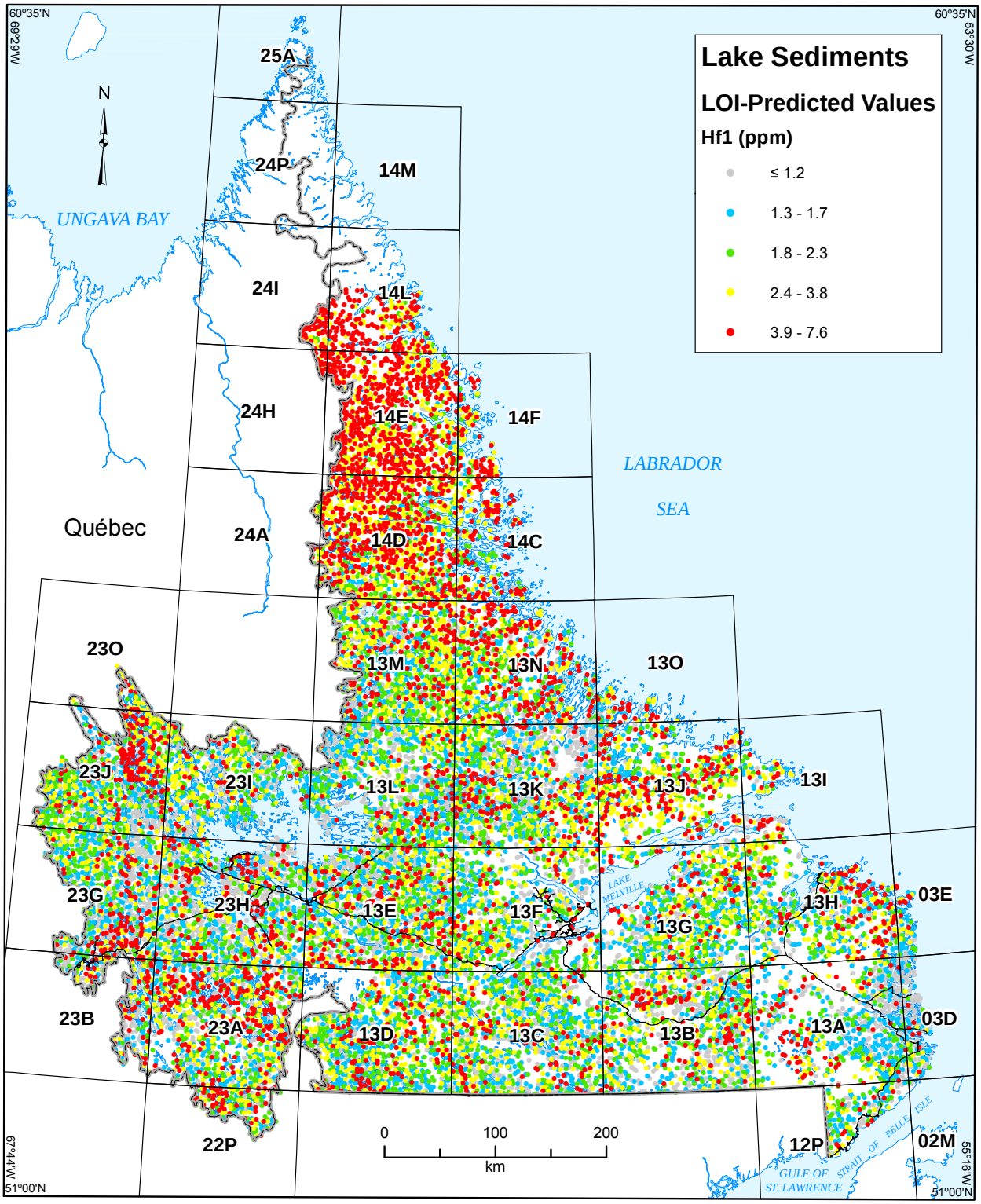


**Figure C1c.** *Simple regression-predicted values of Hf1 in lake sediment, Labrador.*

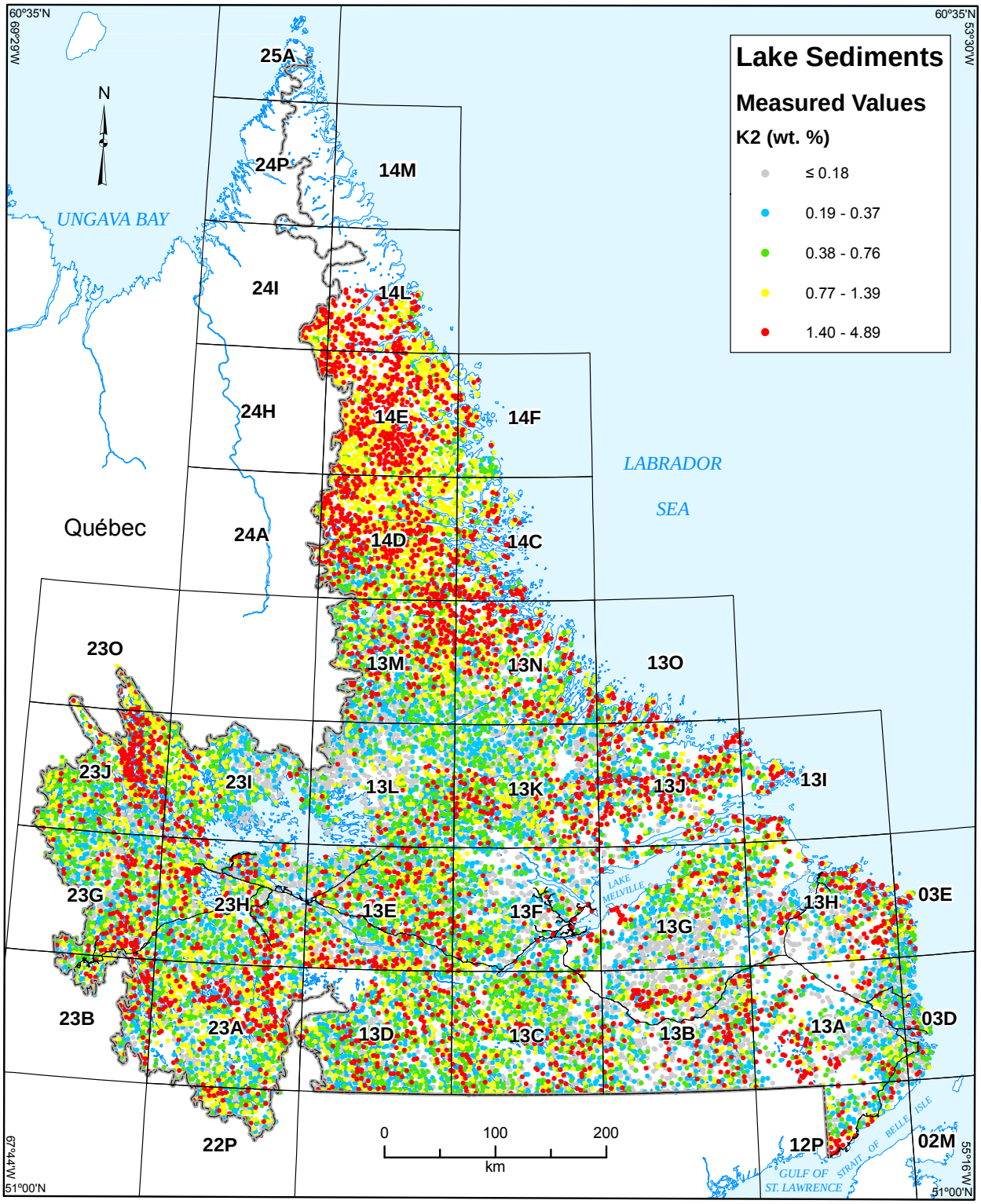


**Figure C2a.** *Measured values of K2 in lake sediment, Labrador.*

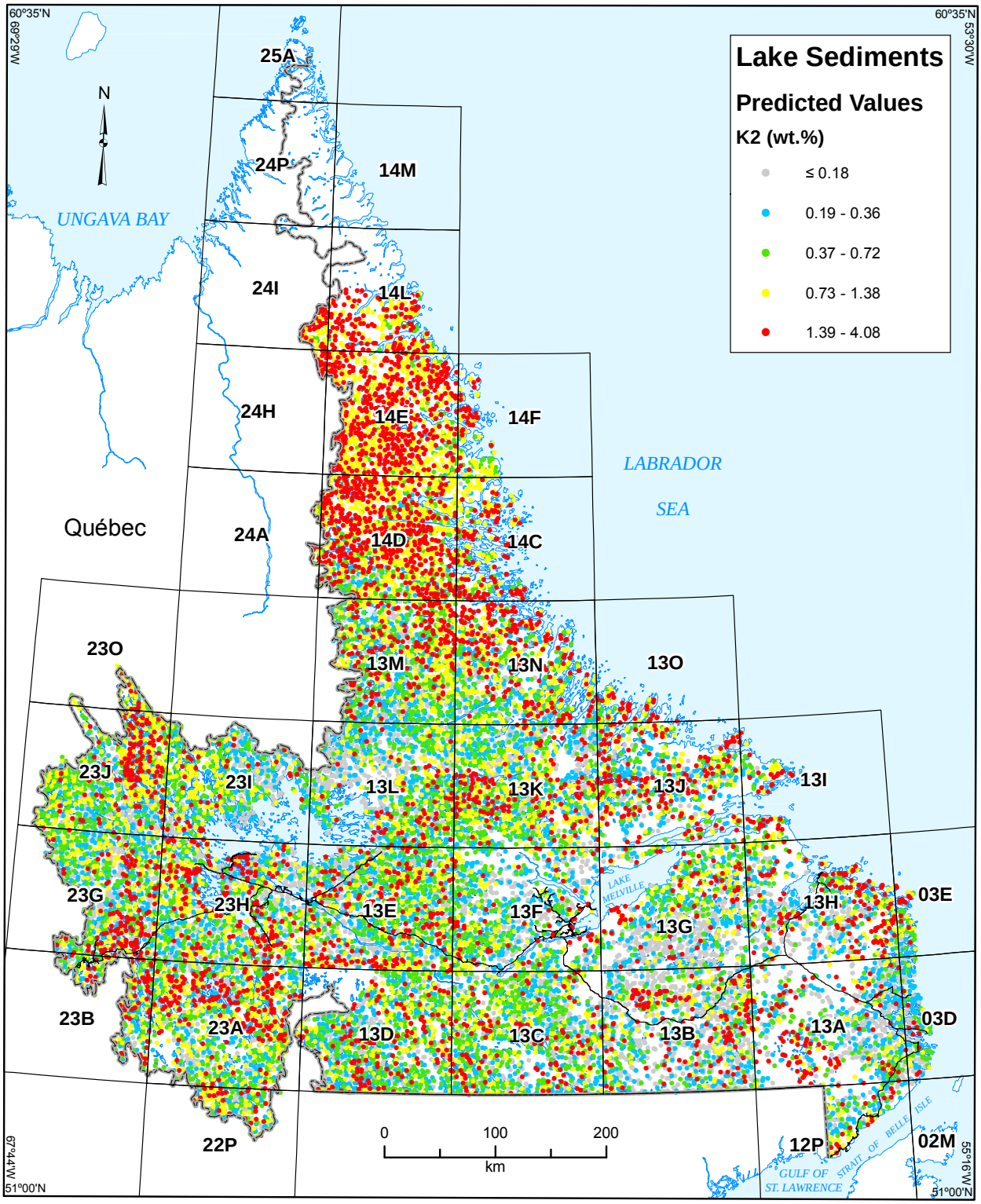


**Figure C2b.** *Multiple regression-predicted values of K2 in lake sediment, Labrador.*

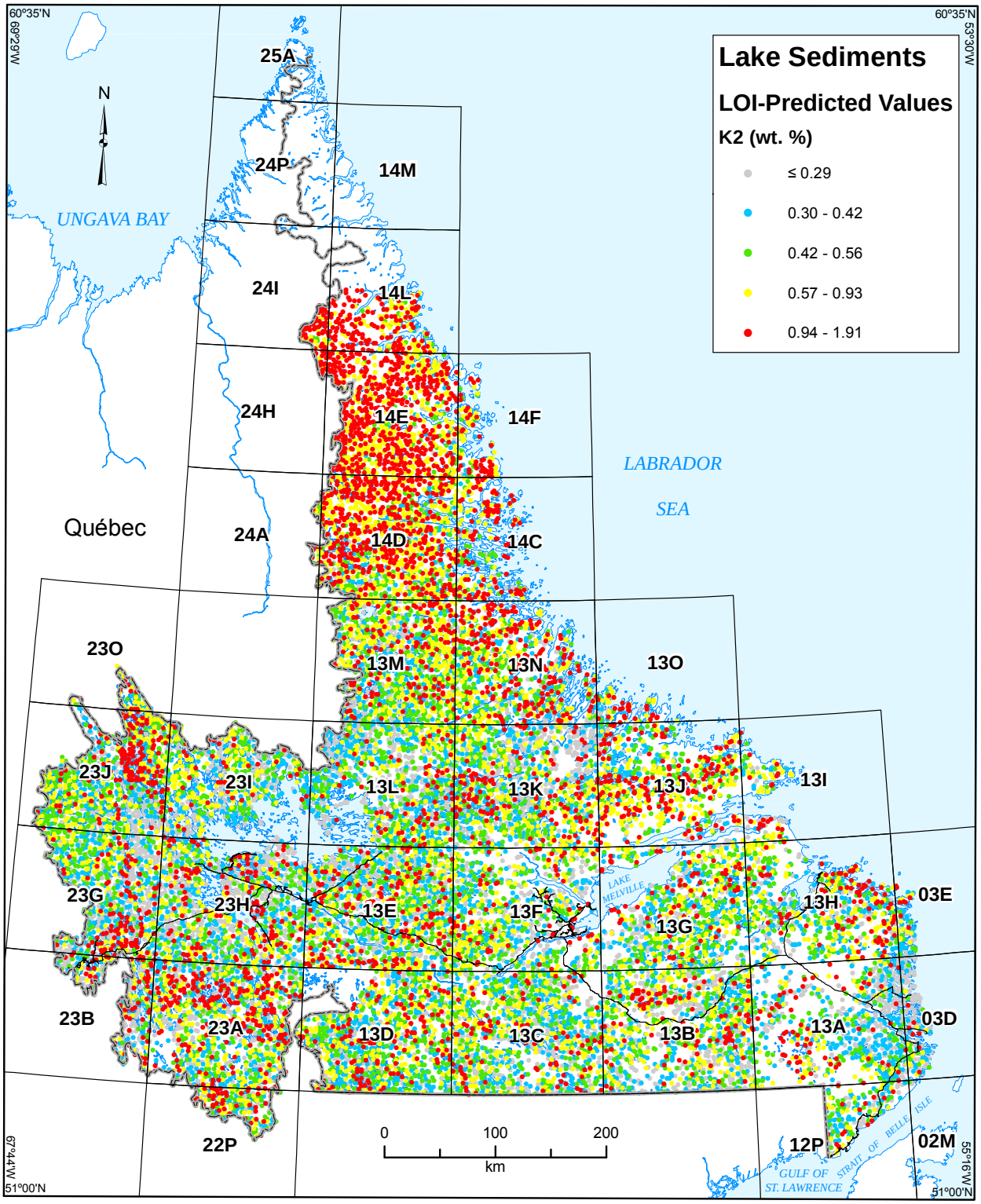


**Figure C2c.** *Simple regression-predicted values of K2 in lake sediment, Labrador.*

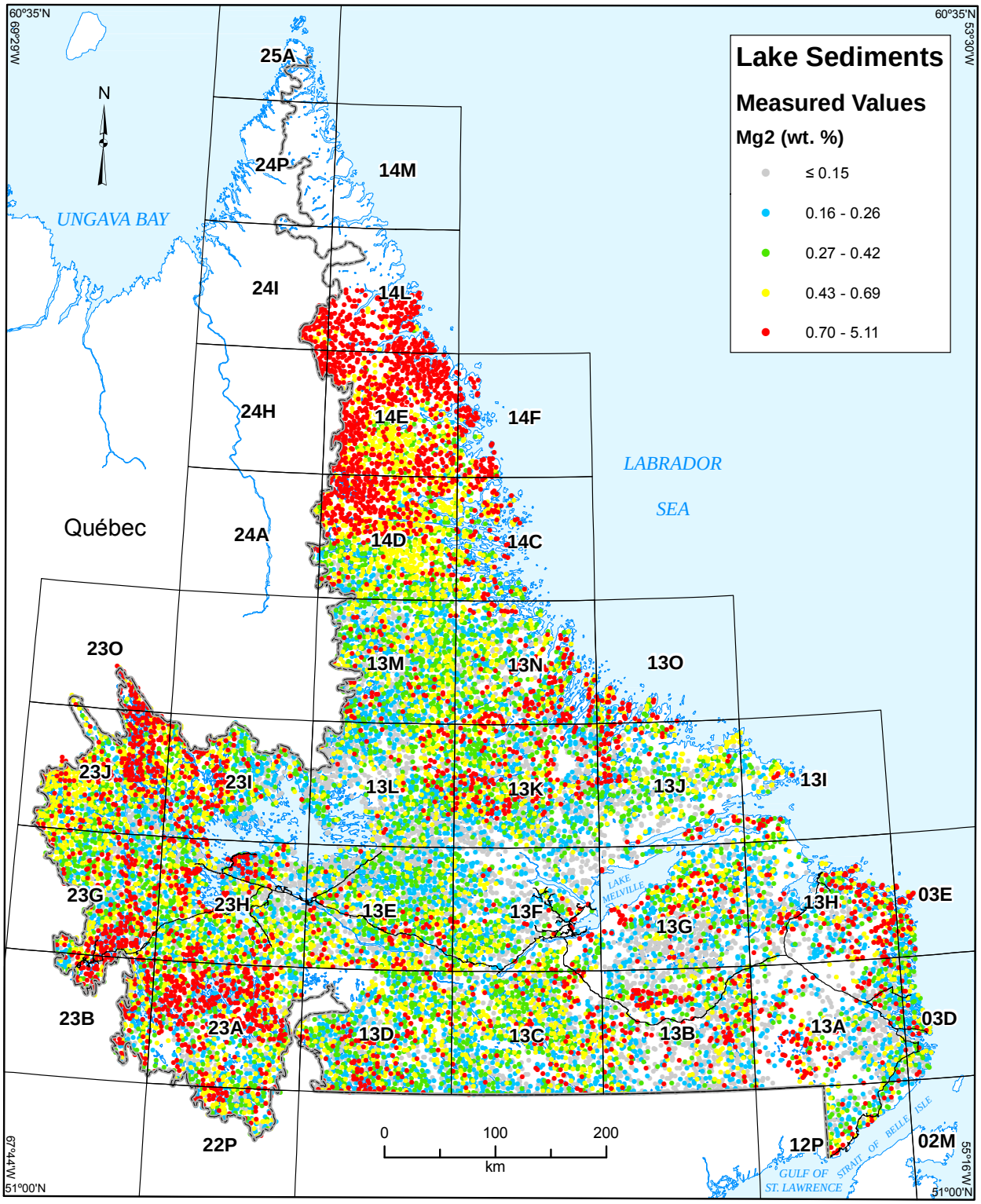


**Figure C3a.** *Measured values of Mg2 in lake sediment, Labrador.*

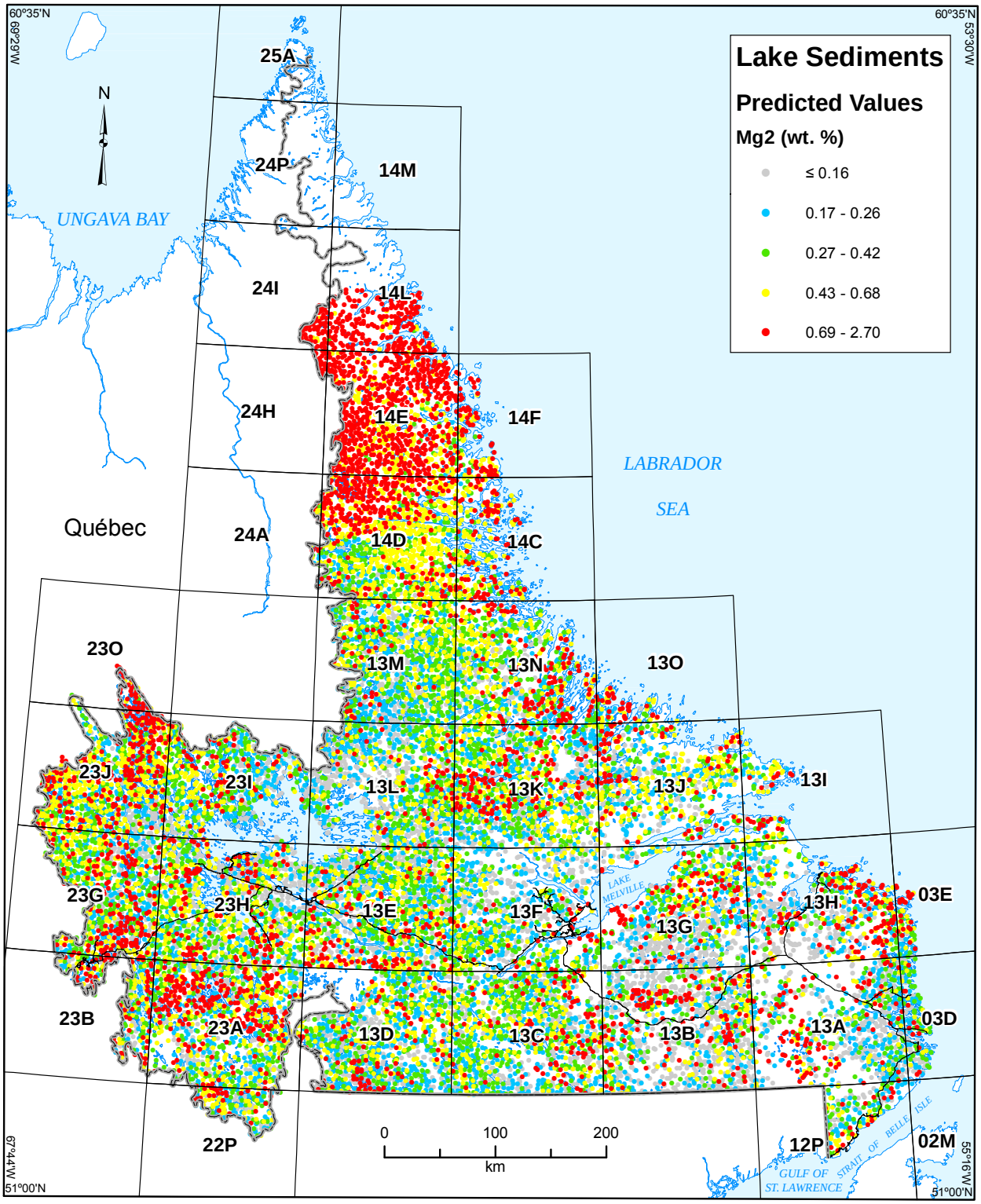


**Figure C3b.** *Multiple regression-predicted values of Mg2 in lake sediment, Labrador.*

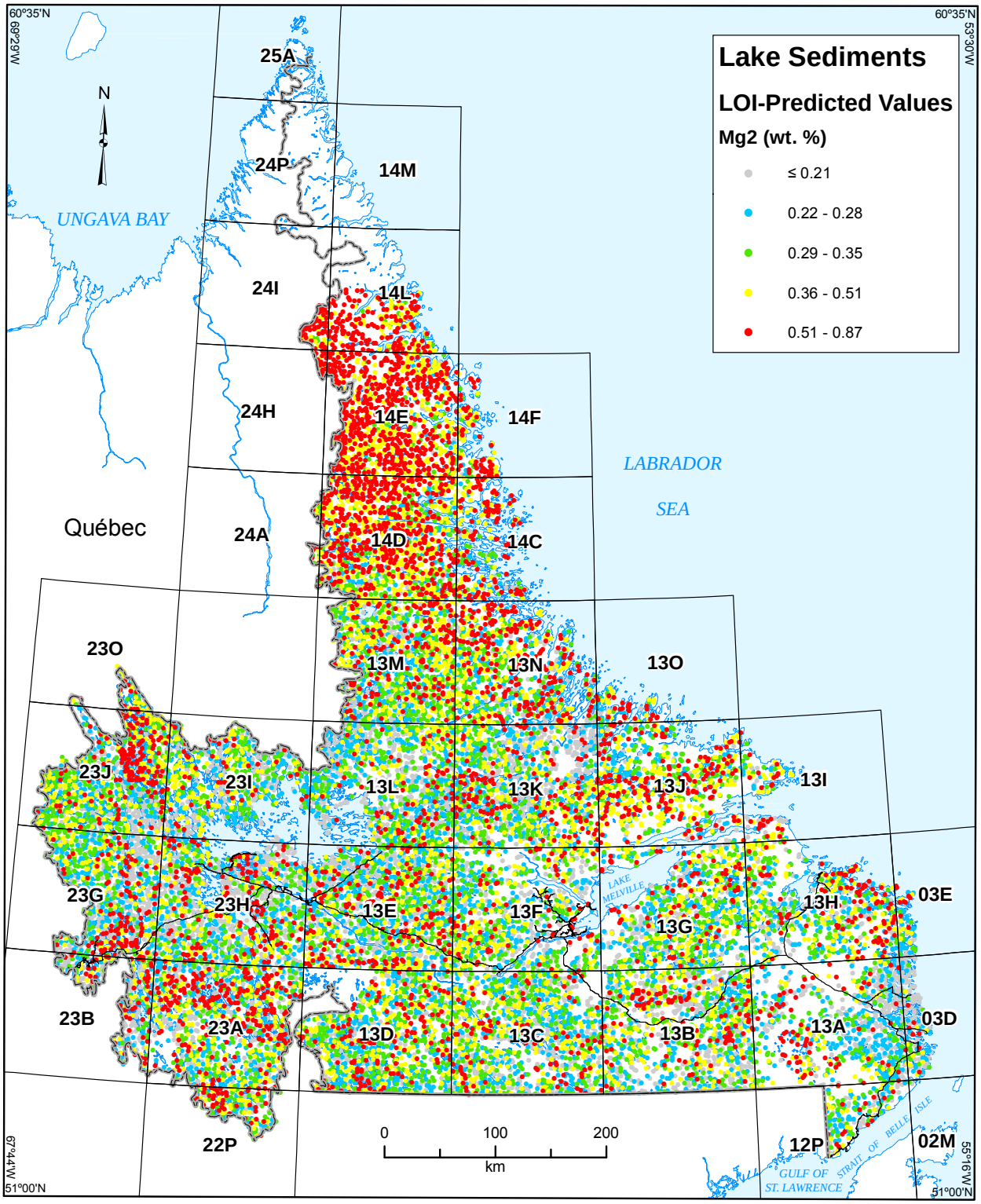


**Figure C3c.** *Simple regression-predicted values of Mg2 in lake sediment, Labrador.*

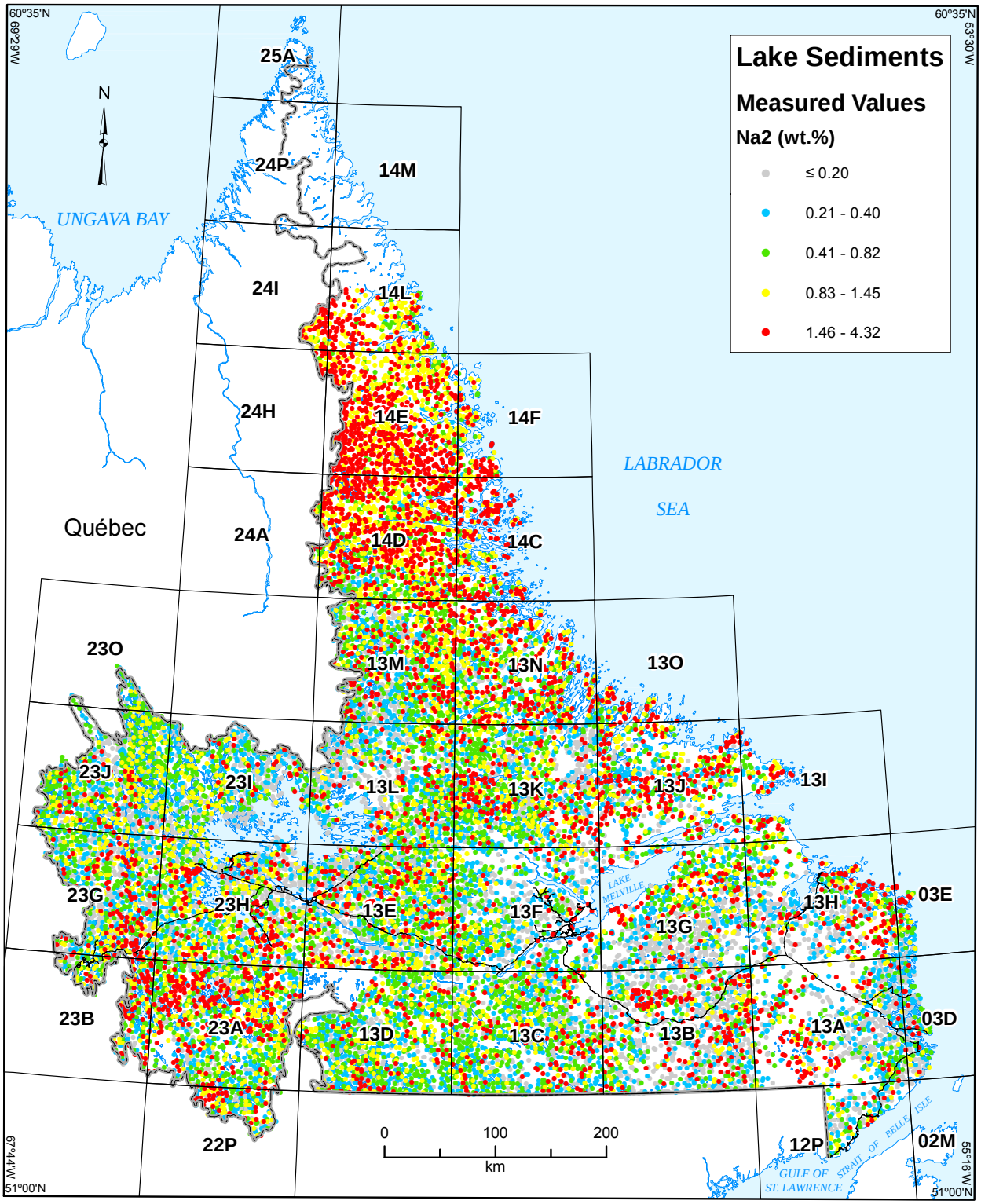


**Figure C4a.** *Measured values of Na2 in lake sediment, Labrador.*

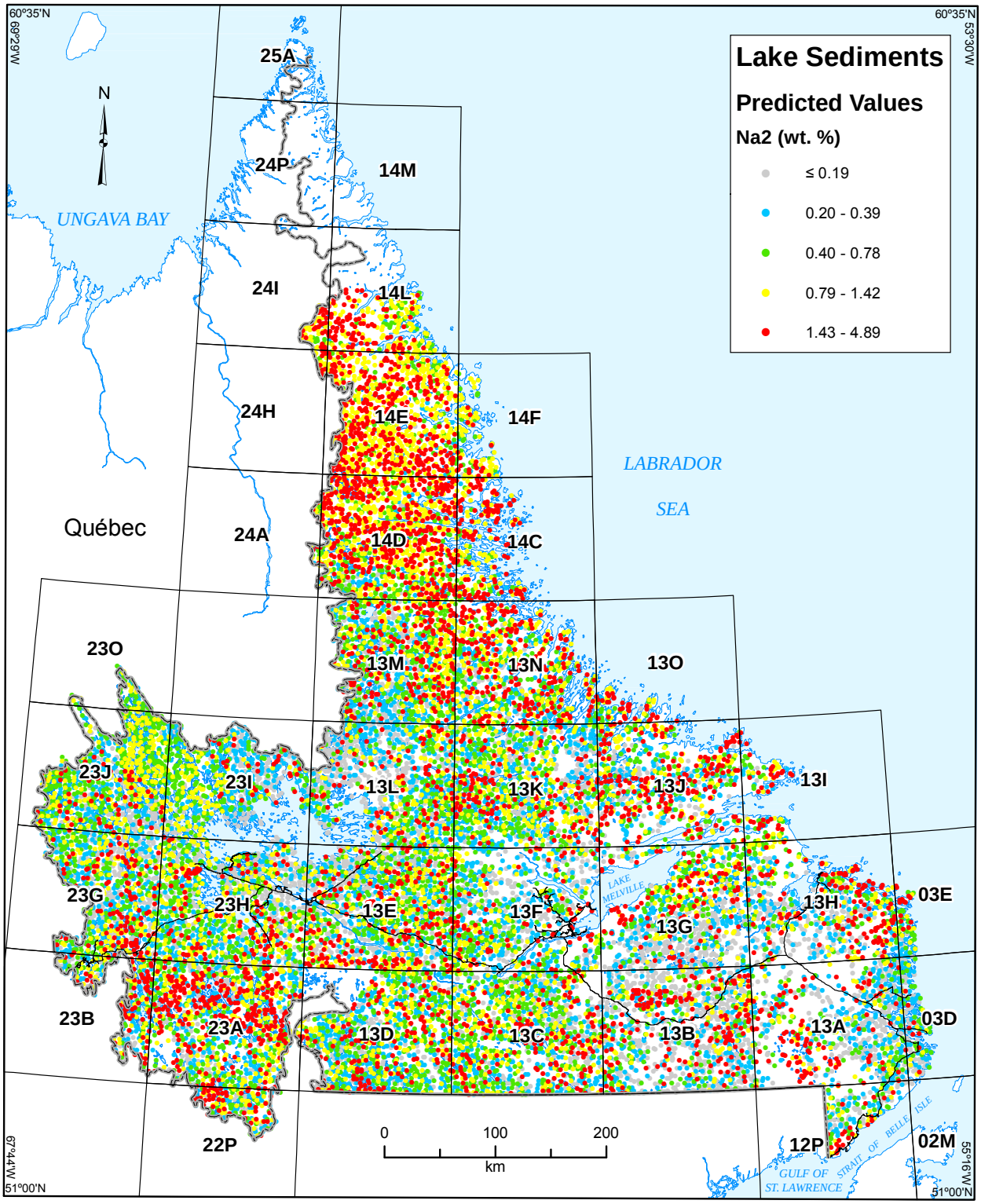


**Figure C4b.** *Multiple regression-predicted values of Na2 in lake sediment, Labrador.*

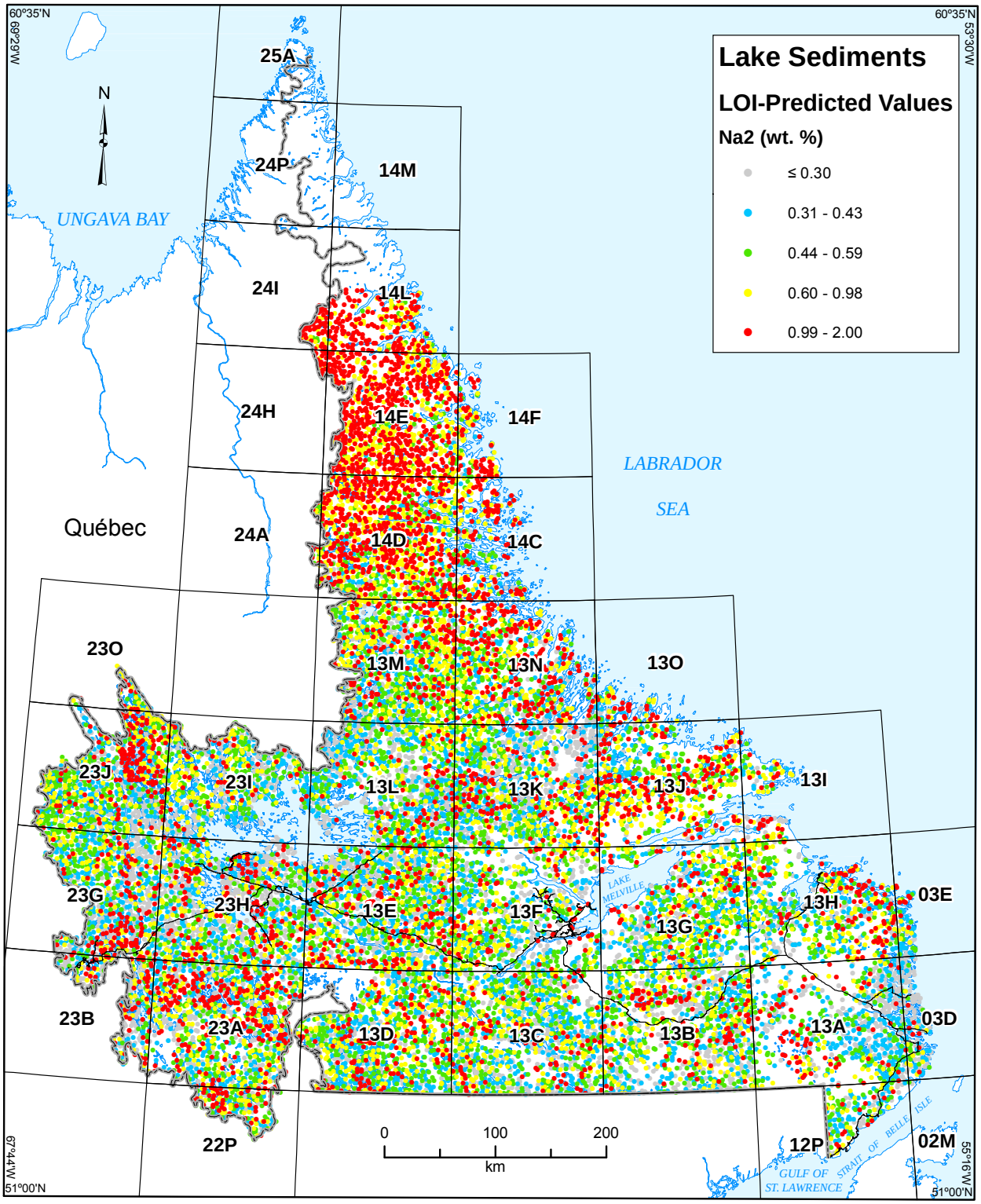


**Figure C4c.** *Simple regression-predicted values of Na2 in lake sediment, Labrador.*

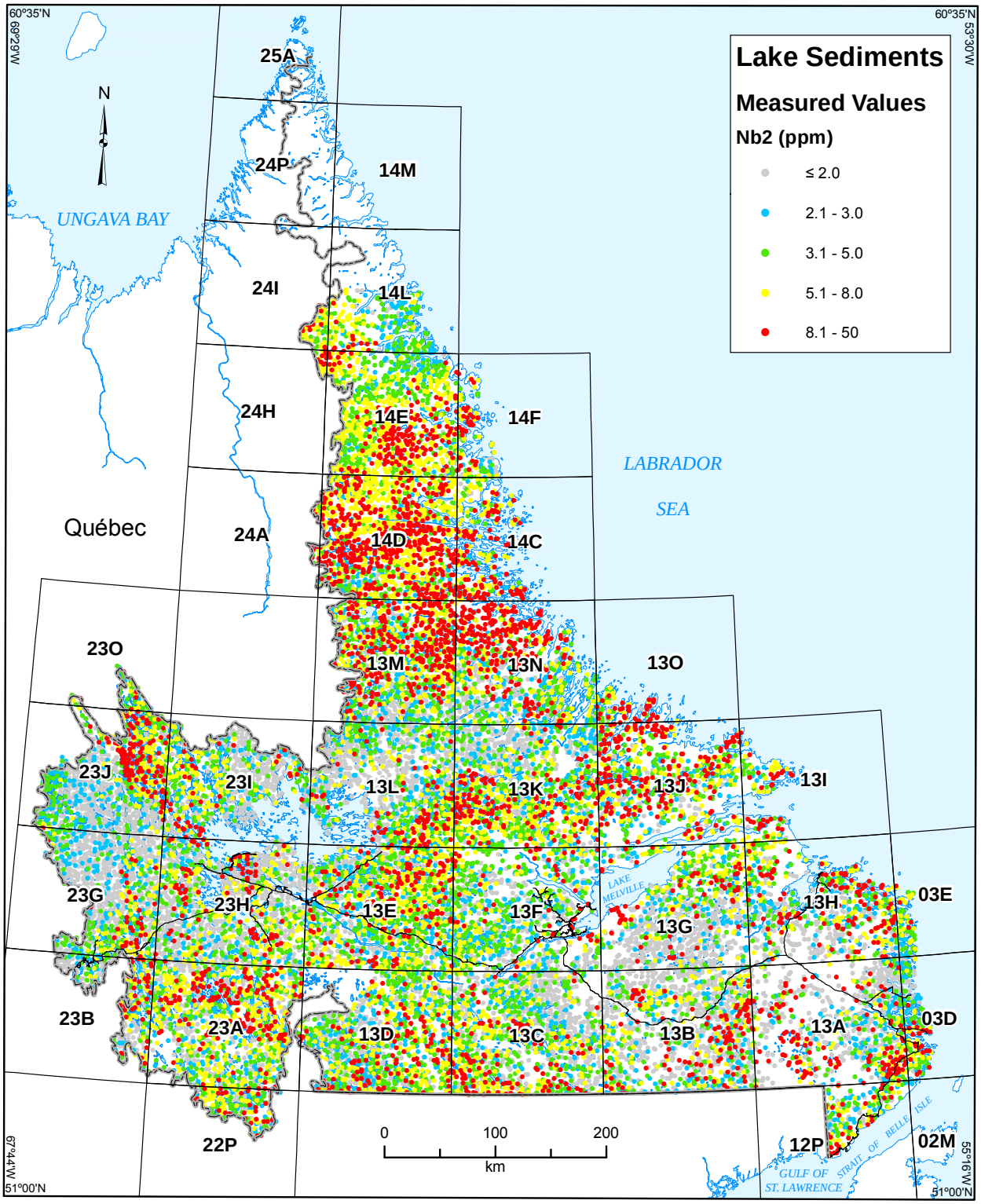


**Figure C5a.** *Measured values of Nb2 in lake sediment, Labrador.*

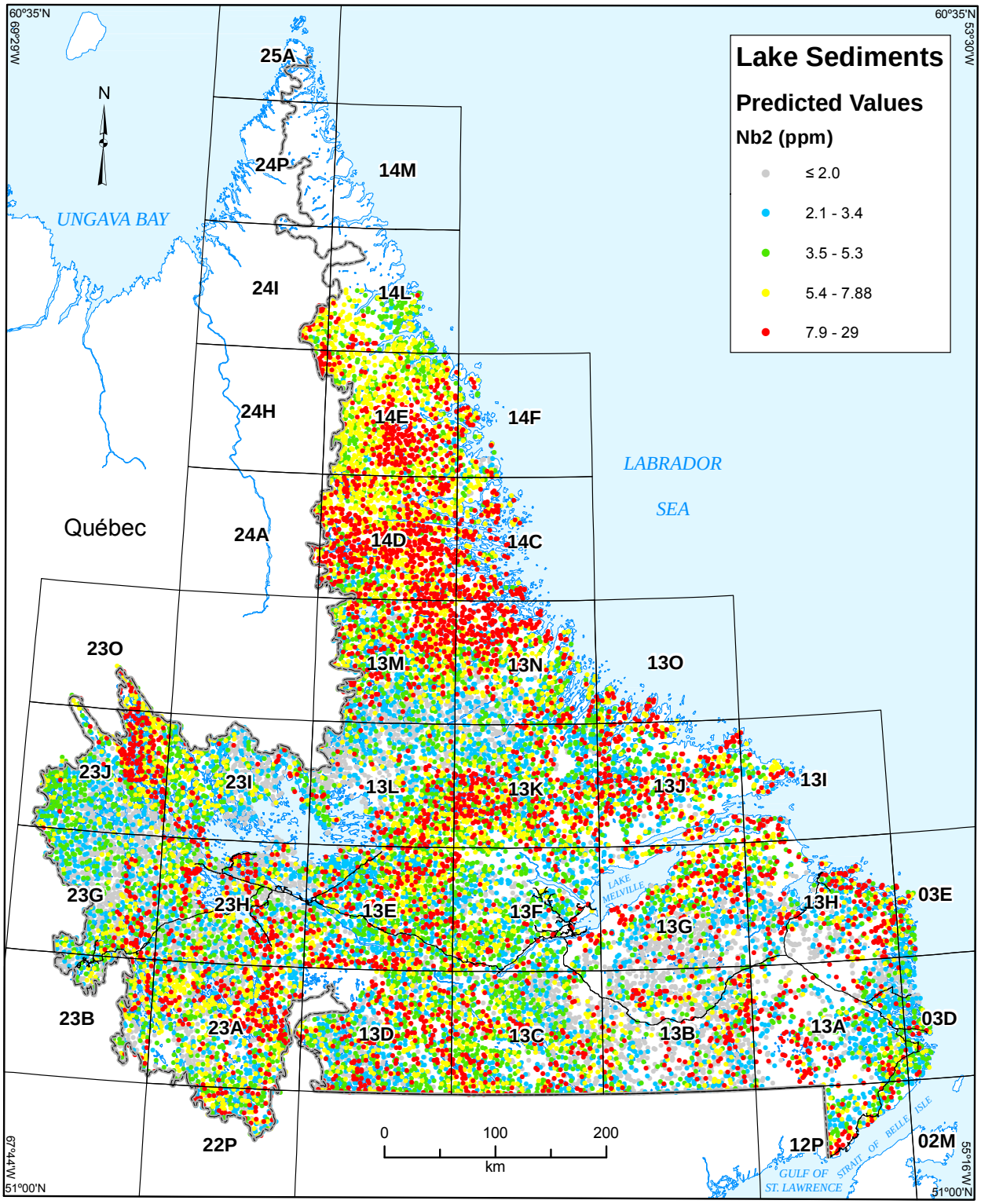


**Figure C5b.** *Multiple regression-predicted values of Nb2 in lake sediment, Labrador.*

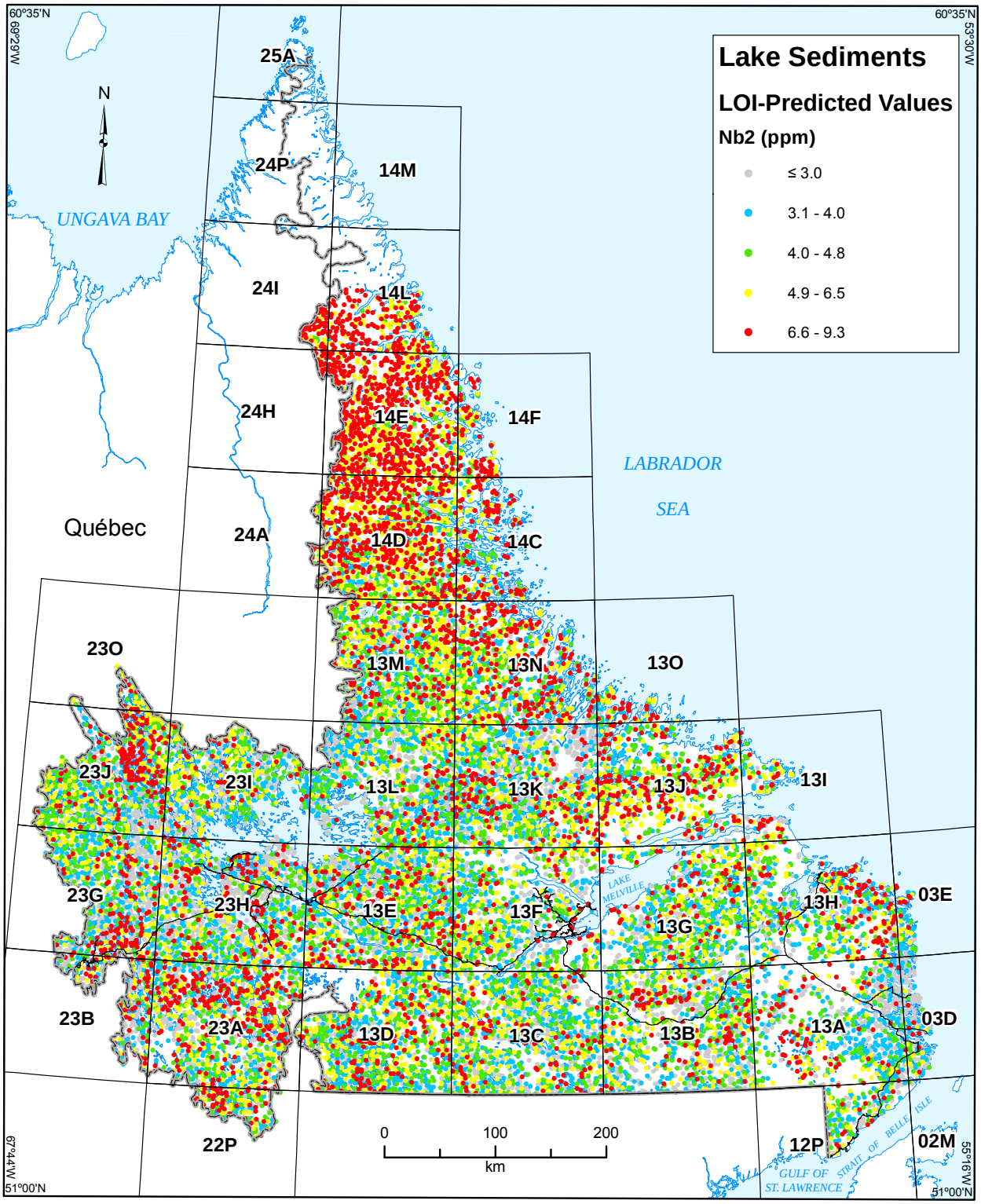


**Figure C5c.** *Simple regression-predicted values of Nb2 in lake sediment, Labrador.*

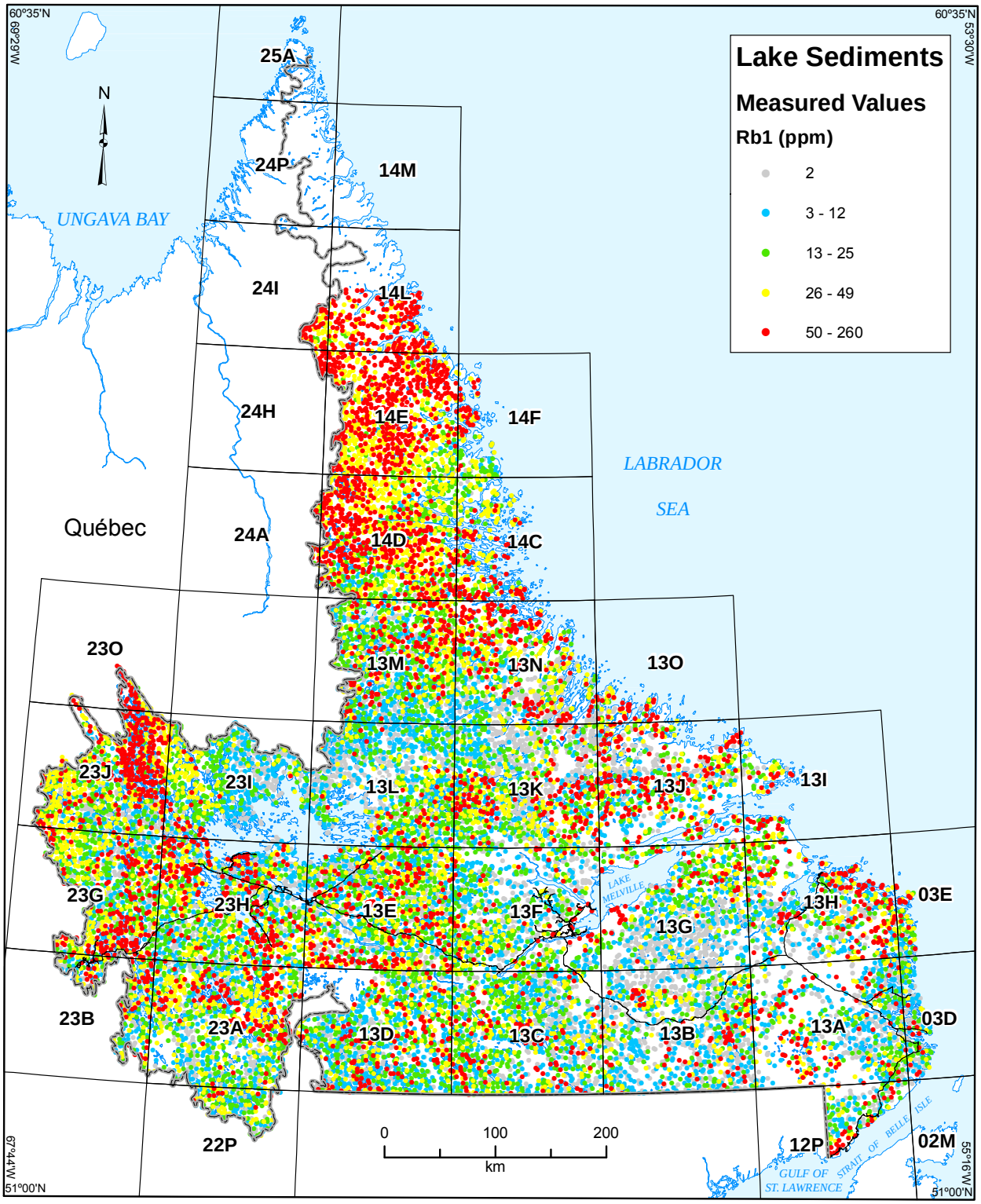


**Figure C6a.** *Measured values of Rb1 in lake sediment, Labrador.*

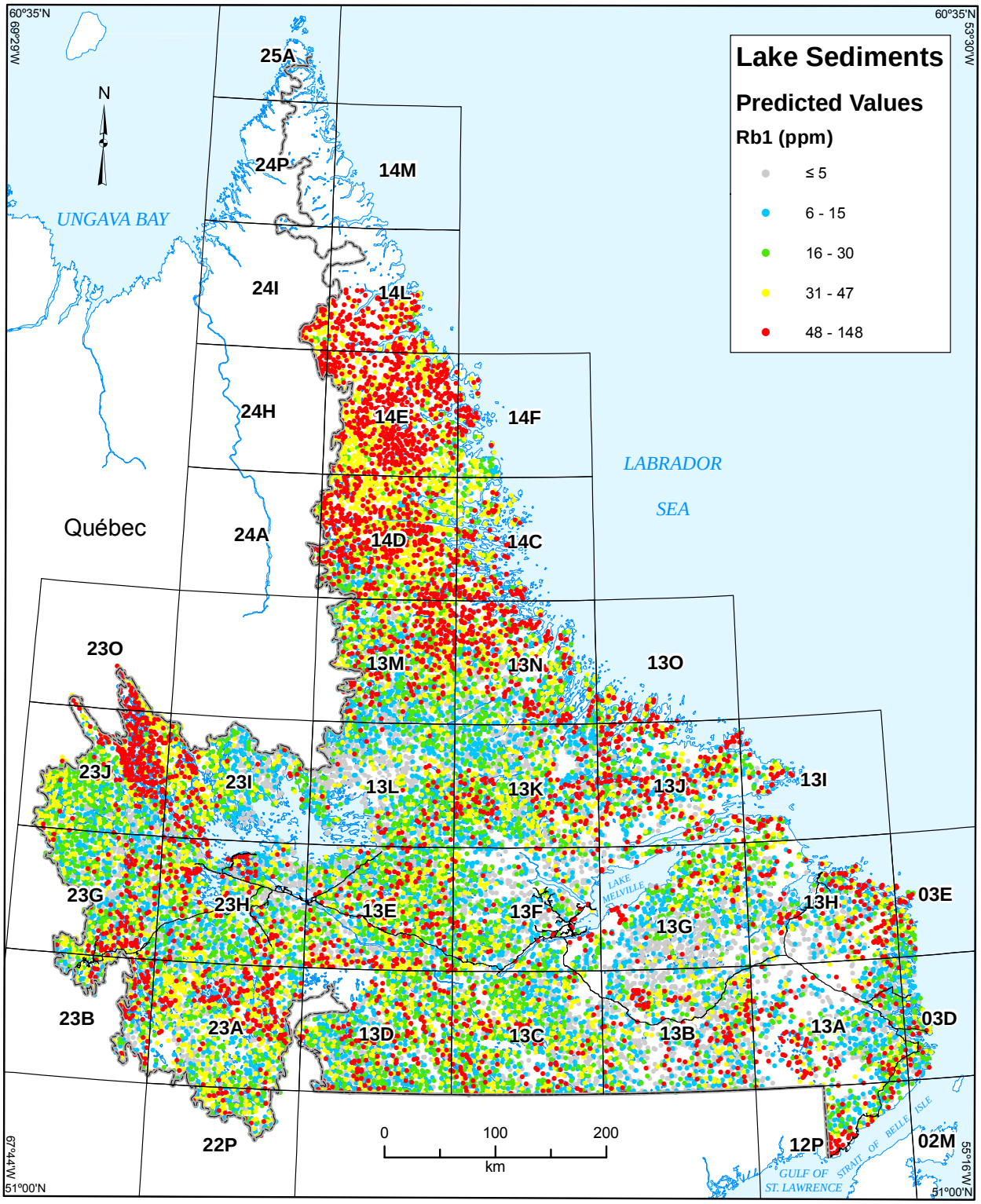


**Figure C6b.** *Multiple regression-predicted values of Rb1 in lake sediment, Labrador.*

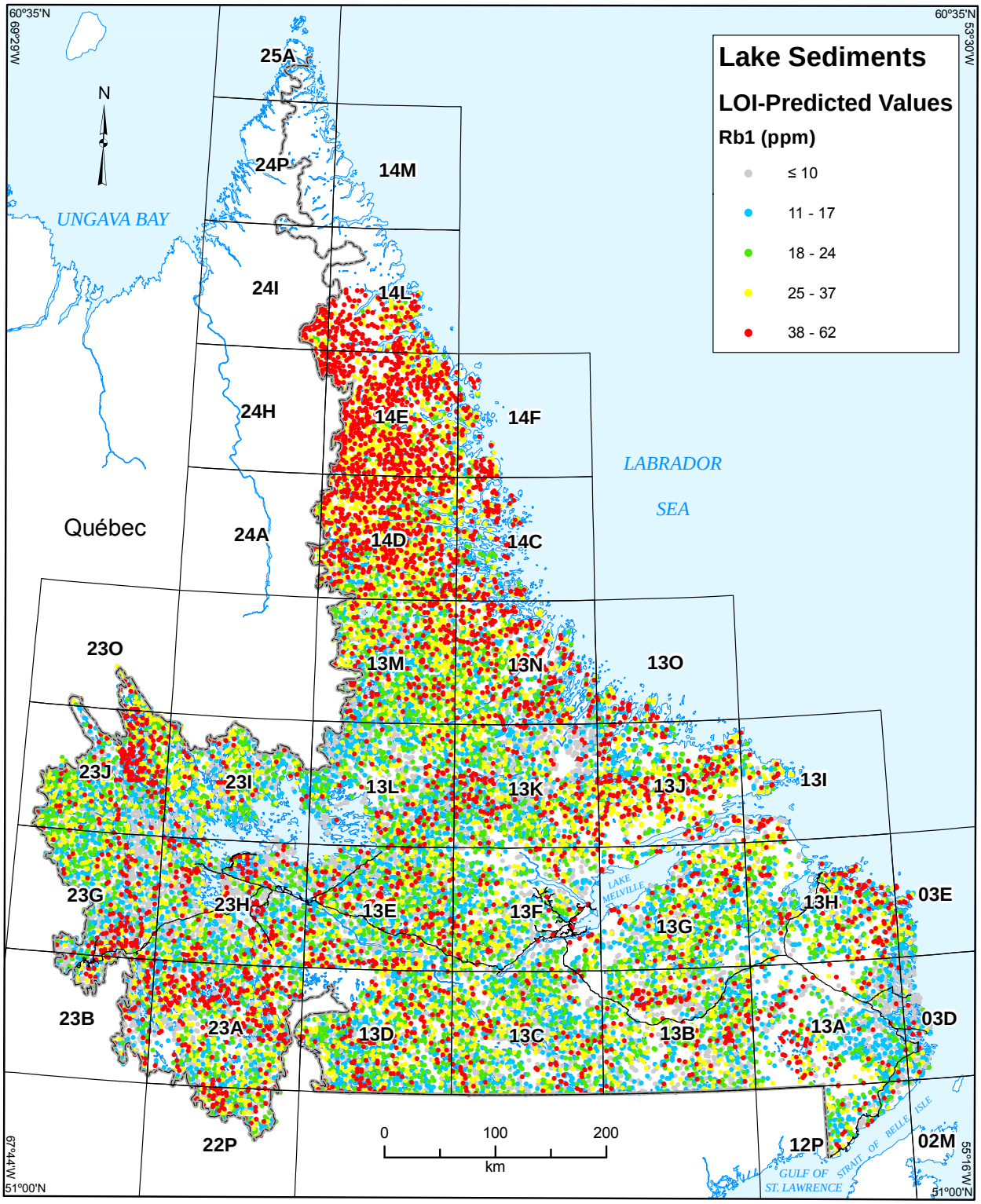


**Figure C6c.** *Simple regression-predicted values of Rb1 in lake sediment, Labrador.*

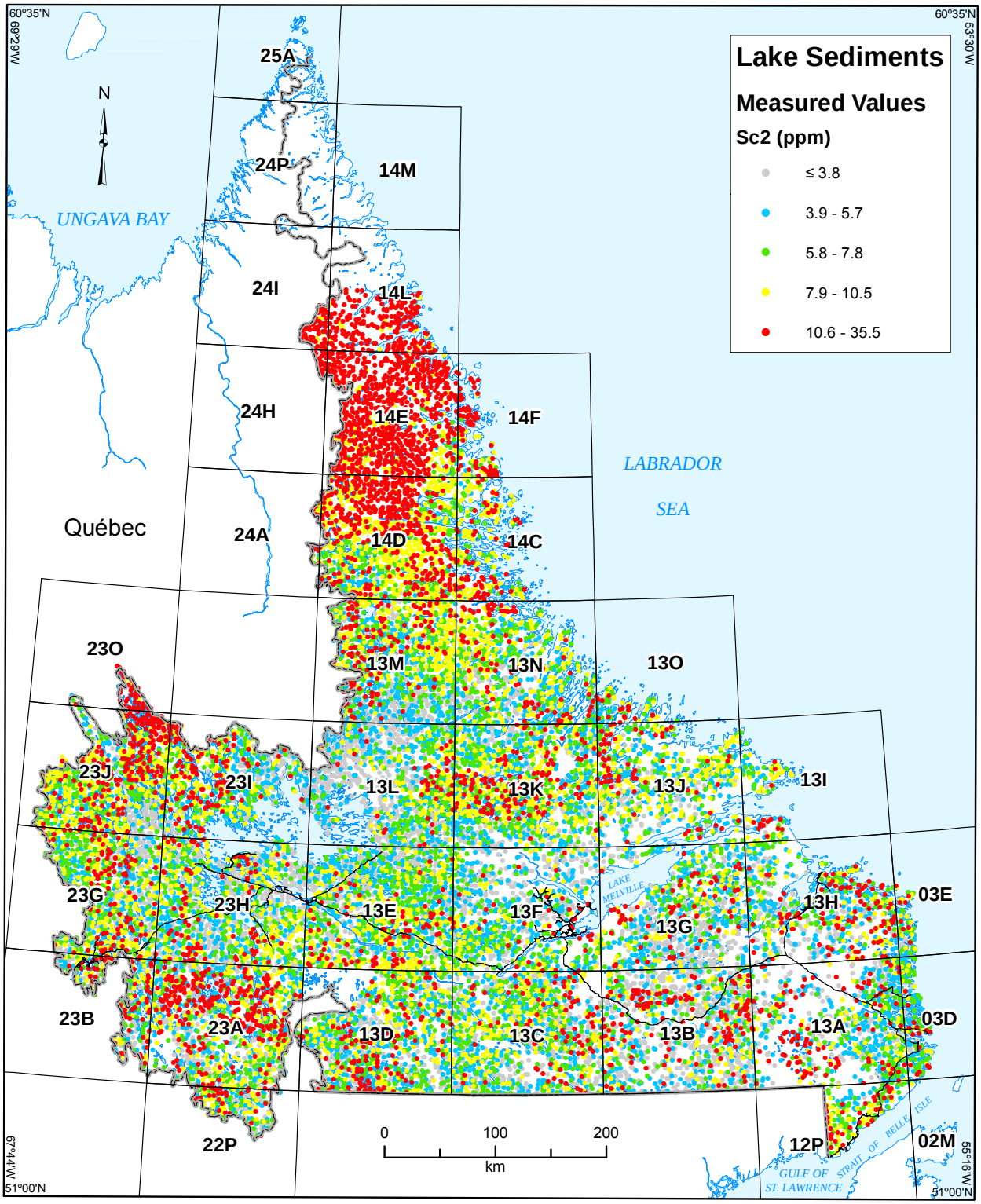


**Figure C7a.** *Measured values of Sc2 in lake sediment, Labrador.*

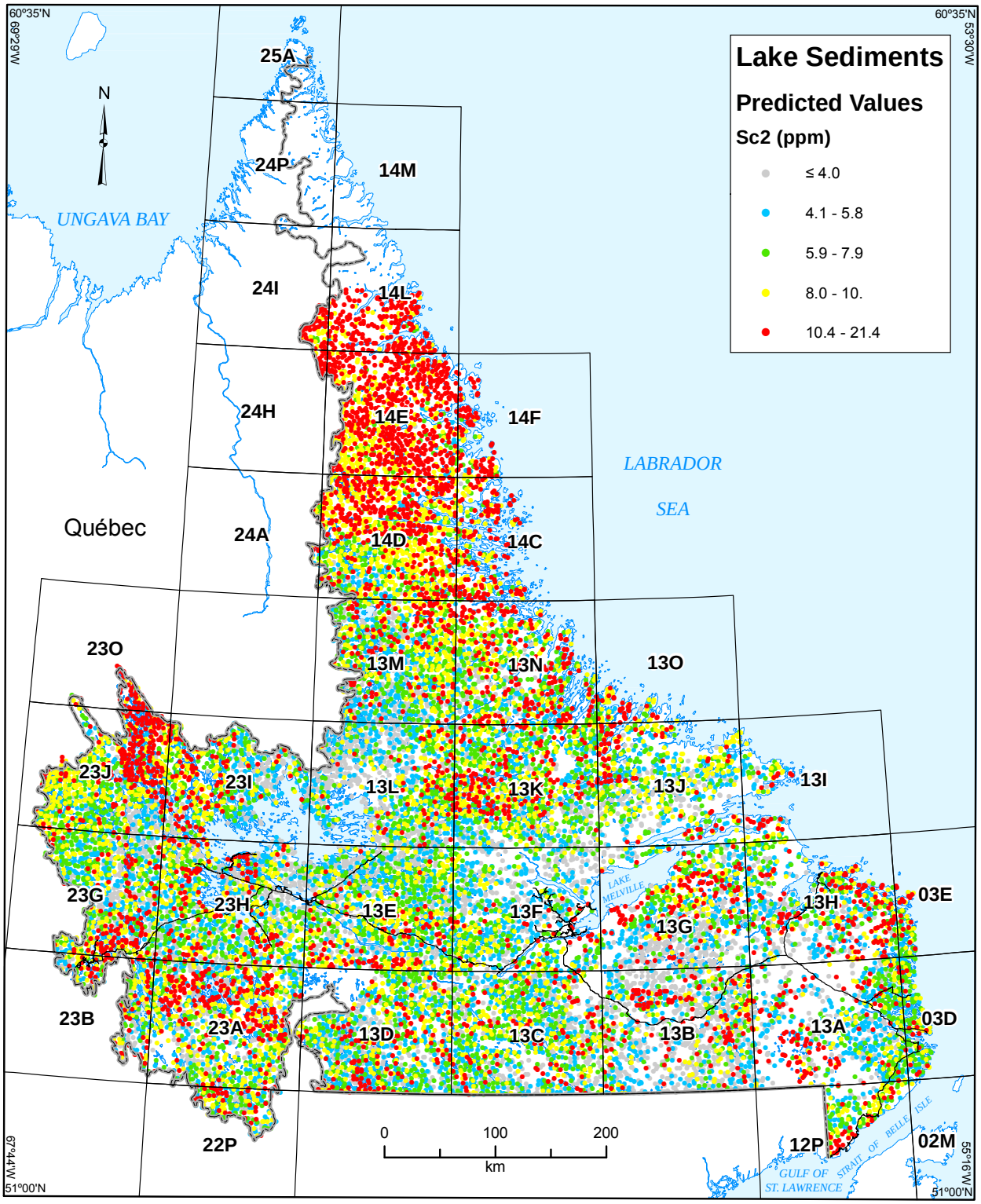


**Figure C7b.** *Multiple regression-predicted values of Sc2 in lake sediment, Labrador.*

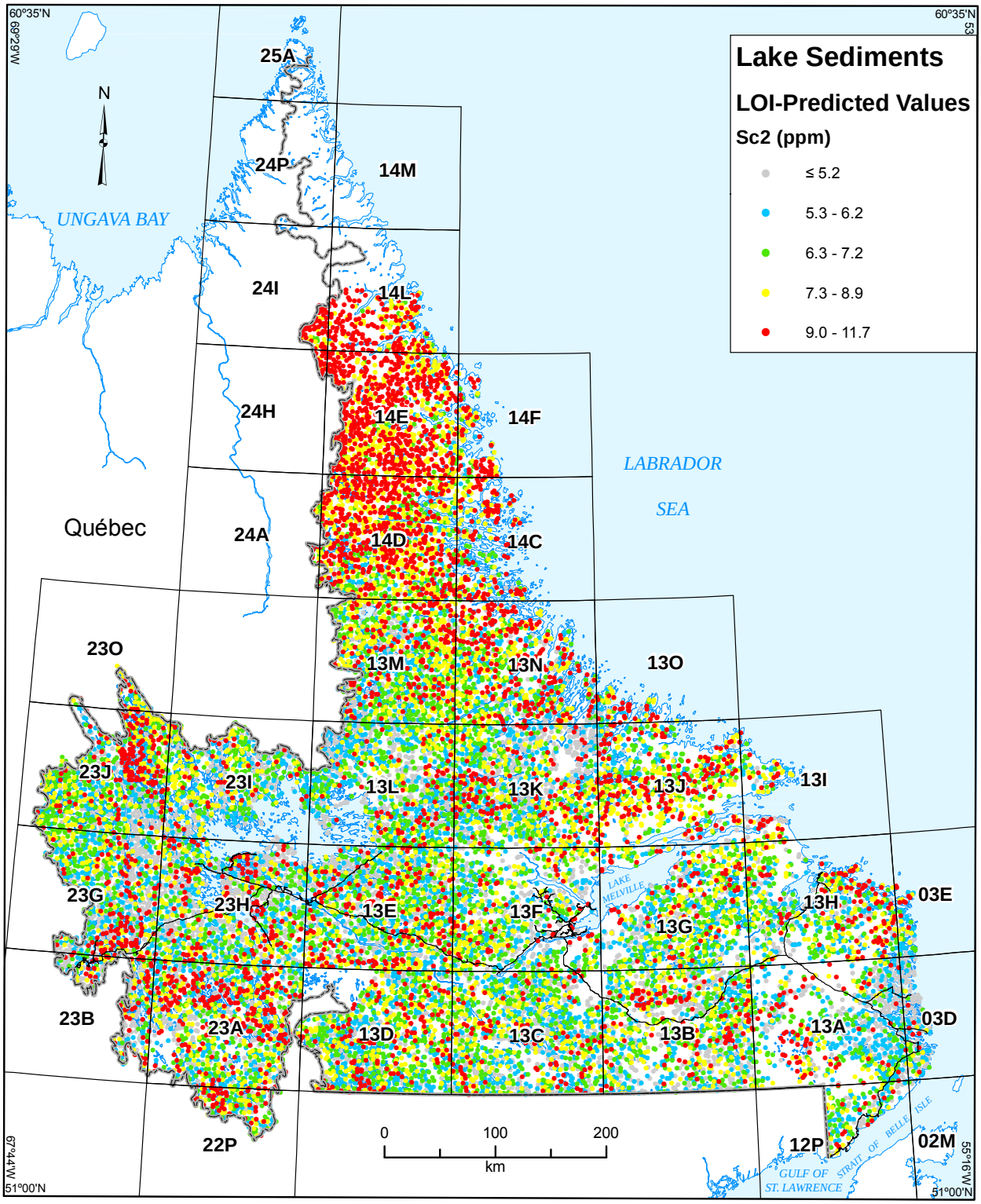


**Figure C7c.** *Simple regression-predicted values of Sc2 in lake sediment, Labrador.*

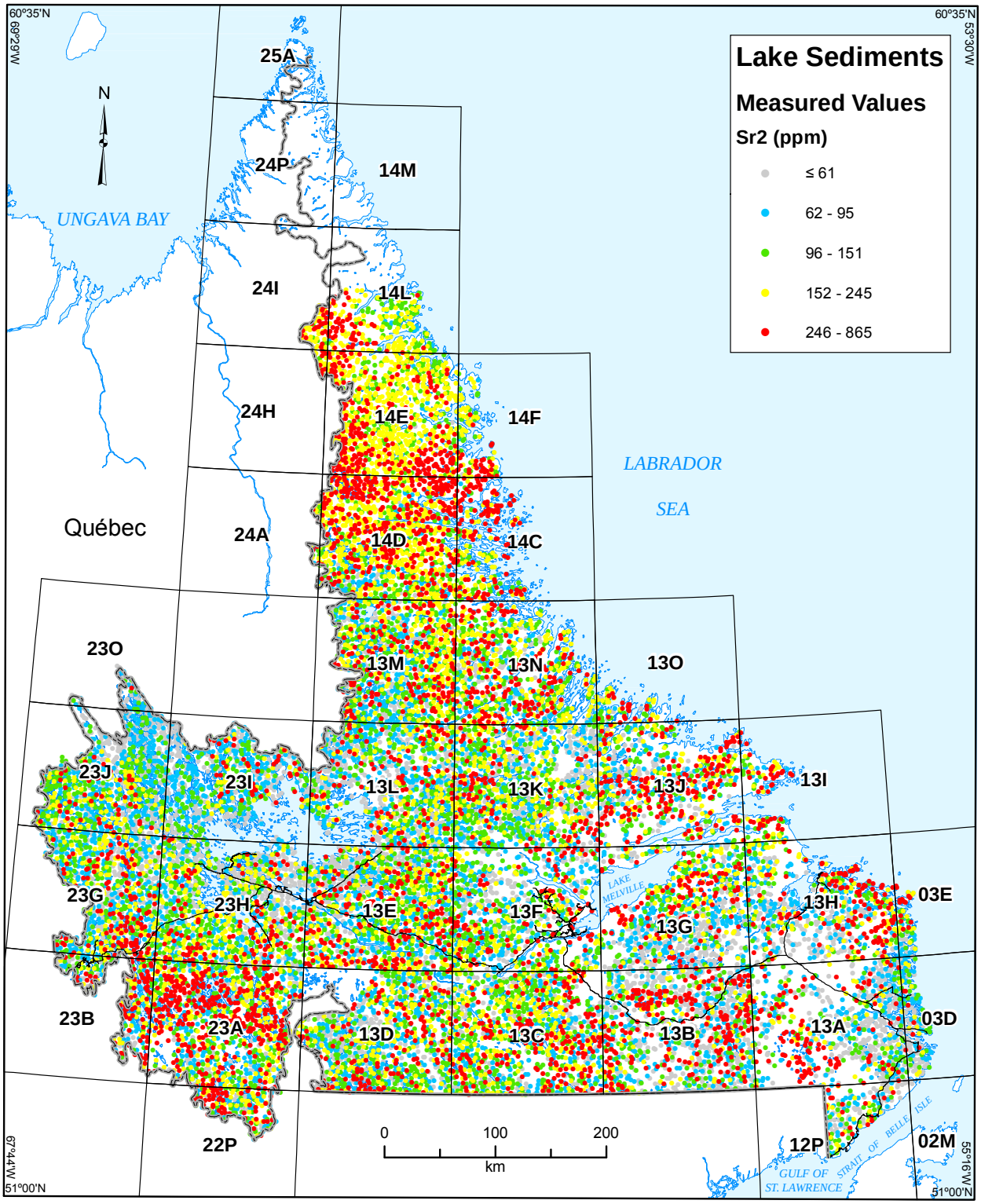


**Figure C8a.** *Measured values of Sr2 in lake sediment, Labrador.*

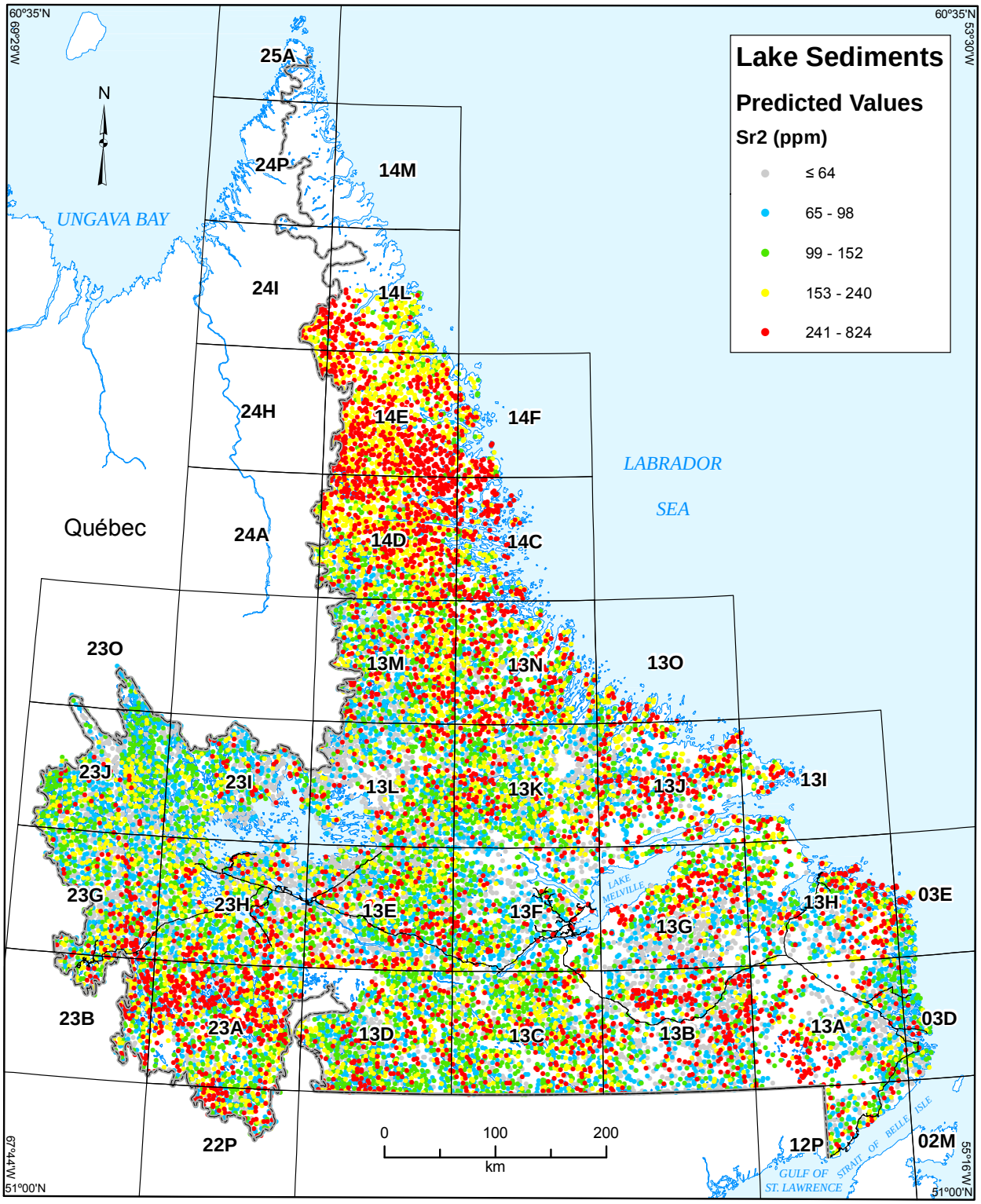


**Figure C8b.** *Multiple regression-predicted values of Sr2 in lake sediment, Labrador.*

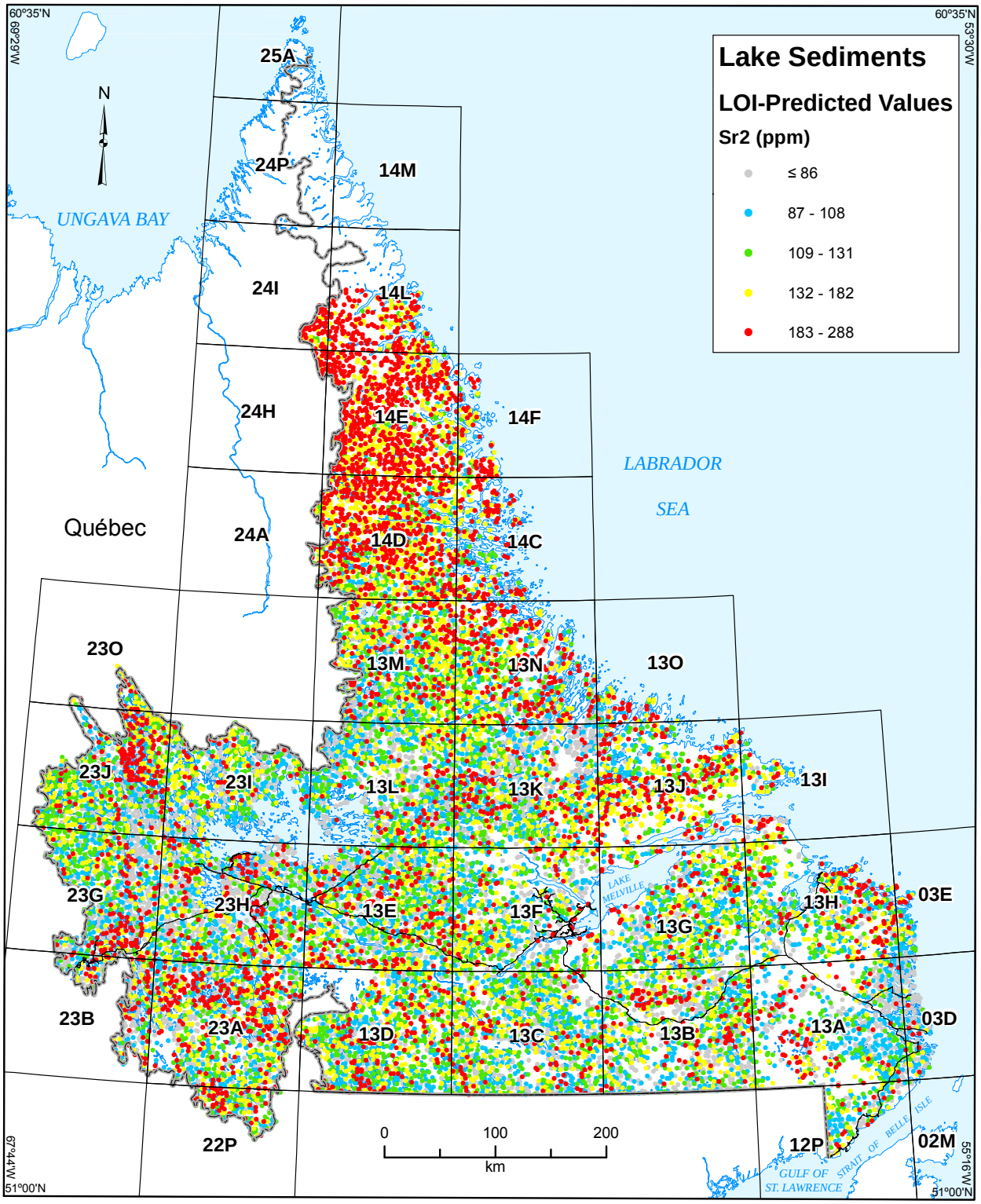


**Figure C8c.** *Simple regression-predicted values of Sr2 in lake sediment, Labrador.*